4-13-2011 12:00 AM

Investigation of Ash Deposition During Co-Firing Biomass/Peat with Coal in a Pilot-Scale Fluidized-Bed Reactor

Yuanyuan Shao, *The University of Western Ontario*

Supervisor: Prof. Jesse Zhu, *The University of Western Ontario*
Joint Supervisor: Prof. Charles (Chunbao) Xu, *The University of Western Ontario*
A thesis submitted in partial fulfillment of the requirements for the Doctor of Philosophy degree in Chemical and Biochemical Engineering

INVESTIGATION OF ASH DEPOSITION DURING CO-FIRING BIOMASS/PEAT WITH COAL IN A PILOT-SCALE FLUIDIZED-BED REACTOR

(Spine title: Investigation of Ash Deposition)
(Thesis format: Integrated-Article)

by

Yuanyuan Shao

Graduate Program in Chemical and Biochemical Engineering

A thesis submitted in partial fulfilment
of the requirements for the degree of
Doctor of Philosophy

Department of Chemical and Biochemical Engineering
Faculty of Engineering
School of Graduate and Postdoctoral Studies
The University of Western Ontario
London, Ontario, Canada

THE UNIVERSITY OF WESTERN ONTARIO
SCHOOL OF GRADUATE AND POSTDOCTORAL STUDIES

CERTIFICATE OF EXAMINATION

Supervisors	Examiners
Dr. Jesse Zhu	Dr. Chuangzhi Wu (External)
Dr. Charles Xu	Dr. Anthony Straatman (University)
	Dr. Shahzad Barghi (Program)
	Dr. Cedric Briens (Program)

The thesis by

Yuanyuan Shao

entitled:

Investigation of Ash Deposition during Co-firing Biomass/Peat and Coal in a Pilot-Scale Fluidized-Bed Reactor

is accepted in partial fulfillment of the
requirements for the degree of
Doctor of Philosophy

Date_____ _____
Chair of the Thesis Examination Board

ABSTRACT

Biomass, a promising alternative to fossil fuels, has been applied widely for energy generation by co-firing technology in recent year particularly in the EU countries. In this thesis, a key issue of biomass co-firing technology - ash deposition in combustion, co-combustion and gasification, was comprehensively investigated in a pilot-scale bubbling fluidized bed reactor. A custom-designed, air-cooled probe was installed in the freeboard zone of the reactor to simulate the heat-transfer surface and collect ash deposits from the process. A local lignite coal, a woody biomass (white pine), and a Canadian peat were involved in the tests. The main varying operating parameters investigated in this study included: blending ratio, air/fuel ratio, moisture content and sulphur addition for the combustion/combustion tests; equivalence ratio, bed materials and fuel types for the gasification tests.

A new parameter, "relative deposition rate" (RD_A) was proposed in this study to evaluate the relative deposition tendencies of biomass fuels and biomass-coal mixed fuels against the coal as the base fuel for co-firing. As expected, co-firing of the lignite and the wood pellets (with a much lower ash-content than the lignite) resulted in a decreased superficial rate of ash deposition. However, co-firing of woody biomass and lignite coal did not significantly increase the ash deposition tendency in terms of the values of RD_A, and more interestingly, co-firing of the fuel blend of 50% lignite-50% white pine pellets produced a lower RD_A. Co-combustion of three-fuel blend at 20%lignite-40%peat-40%pine resulted in the lowest deposition rate and the least deposition tendency among all the combustion tests with various mixed fuels or individual fuels.

Another new and interesting discovery of this study was that fluidized-bed combustion of an individual fuel or a fuel blend with a higher moisture content produced not only a more uniform temperature profile along the fluidized-bed column but also a reduced ash deposition rate. A higher chlorine concentration in the feed would generally result in a higher tendency of ash deposition. Adding sulfur into the fuel of coal or peat could effectively decrease the chloride deposition in the ash deposits via sulphation. The sulphur addition could also reduce the ash deposition rate for the combustion of lignite, while it slightly increased the ash deposition rate for the peat fuel.

In air-blown gasification of a woody biomass and a Canadian peat, the experimental results demonstrated that among the four bed materials (olivine, limestone, iron ore, and dolomite), the use of olivine resulted in the lowest ash deposition rate. The superb performance of olivine in retarding ash deposition could be accounted for by its outstanding thermal stability and mechanical strength. The other three bed materials, in particular limestone, were fragile during the fluidized bed gasification, and the fractured fines from the bed materials were found to deposit along with the fuel-ash on the heat transfer surface, leading to higher ash deposition rates.

Finally, mathematical models parameterized with interactions between fuel chlorine, alkali and ash particles were developed to analyze the ash and chlorine deposition behavior based on the experimental data from co-firing peat with lignite coal. The developed equations in this study can not only describe the dependence of the deposition rate and the ash chlorine content on the fraction of peat, but can also determine suitable range of the peat fraction for smooth operations, which would be useful for co-firing other fuel blends.

Keywords: Ash deposition, Co-firing; Co-combustion; Air-blown gasification; White pine; Peat; Lignite; Bubbling fluidized bed; Blending ratio; Moisture content; Air/fuel ratio; Sulphur addition; Equivalence ratio; Bed material; Chlorine.

CO-AUTHORSHIP

Title: Ash deposition in co-firing biomass and coal

Authors: Shao, Y.; Xu, C.; Zhu, J.; Preto, F.; Wang, J.; Tourigny, G.; Badour, C.; Li, H.

All portions of the experimental work were jointly undertaken by Yuanyuan Shao (PhD candidate) and Chadi Badour (M.Sc. student from Lakehead University) in CanmetENERGY, Ottawa, Ontario, Canada under the guidance of Dr. Jesse Zhu, Dr. Charles (Chunbao) Xu, Dr. Fernando Preto, and Dr. Jingsheng Wang. Yuanyuan Shao, in consultation with Dr. Jesse Zhu and Dr. Charles Xu, proposed the general idea. Yuanyuan Shao, co-operated with Chadi Badour and Guy Tourigny, performed majority of the experiments and carried out initial data analysis. All drafts of this manuscript were written by Yuanyuan Shao. Modifications were carried out under the close supervision of Dr. Charles Xu and Dr. Jesse Zhu. Dr. Jingsheng Wang and Guy Tourigny provided many valuable comments. A revised version was published in *Energy Fuels*; **24**(9):4681-4688.

Title: Ash and chlorine deposition in co-combustion of lignite and a chlorine-rich peat

Authors: Shao, Y.; Xu, C.; Zhu, J.; Preto, F.; Wang, J.; Tourigny, G.; Badour, C.; Li, H.

All portions of the experimental work were jointly undertaken by Yuanyuan Shao (PhD candidate) and Chadi Badour (M.Sc. student from Lakehead University) in CanmetENERGY, Ottawa, Ontario, Canada under the guidance of Dr. Jesse Zhu, Dr. Charles (Chunbao) Xu, Dr. Fernando Preto, and Dr. Jingsheng Wang. Yuanyuan Shao, in consultation with Dr. Jesse Zhu and Dr. Charles Xu, proposed the general idea. Yuanyuan Shao, co-operated with Chadi Badour and Guy Tourigny, performed majority

of the experiments and carried out initial data analysis. All drafts of this manuscript were written by Yuanyuan Shao. Modifications were carried out under the close supervision of Dr. Charles Xu and Dr. Jesse Zhu. Dr. Jingsheng Wang and Guy Tourigny provided many valuable comments. The final version was submitted to *Fuel* in January 2011.

Title: Ash deposition in co-firing three-fuel blends consisting of woody biomass, peat and lignite

Authors: Shao, Y.; Xu, C.; Zhu, J.; Preto, F.; Wang, J.; Hanning Li; Badour, C.

All portions of the experimental work were jointly undertaken by Yuanyuan Shao (PhD candidate) and Chadi Badour (M.Sc. student from Lakehead University) in CanmetENERGY, Ottawa, Ontario, Canada under the guidance of Dr. Jesse Zhu, Dr. Charles (Chunbao) Xu, Dr. Fernando Preto, and Dr. Jingsheng Wang. Yuanyuan Shao, in consultation with Dr. Jesse Zhu and Dr. Charles Xu, proposed the general idea. Yuanyuan Shao, co-operated with Chadi Badour and Guy Tourigny, performed majority of the experiments and carried out initial data analysis. All drafts of this manuscript were written by Yuanyuan Shao. Modifications were carried out under the close supervision of Dr. Charles Xu and Dr. Jesse Zhu. Dr. Jingsheng Wang and Guy Tourigny provided many valuable comments. The final version was submitted to *Energy Fuels* in February 2011.

Title: Ash deposition in air-blown gasification of peat and woody biomass

Authors: Shao, Y.; Xu, C.; Zhu, J.; Preto, F.; Wang, J.; Hurley, S.

All portions of the experimental work were jointly undertaken by Yuanyuan Shao (PhD candidate) and Scott Hurley (M.Sc. student from Lakehead University) in

CanmetENERGY, Ottawa, Ontario, Canada under the guidance of Dr. Jesse Zhu, Dr. Charles (Chunbao) Xu, Dr. Fernando Preto, and Dr. Jingsheng Wang. Yuanyuan Shao, in consultation with Dr. Jesse Zhu and Dr. Charles Xu, proposed the general idea. Yuanyuan Shao, co-operated with Scott Hurley, performed majority of the experiments and carried out initial data analysis. All drafts of this manuscript were written by Yuanyuan Shao. The final version will be submitted to *Biomass & Bioenergy*.

Title: A modelling study of ash deposition behaviour for co-firing peat with lignite

Authors: Shao, Y.; Wang, J.; Xu, C.; Zhu, J.; Preto, F.; Tourigny, G.; Badour, C.; Li, H

All the modelling work was carried out by Yuanyuan Shao under the guidance of Dr. Jingsheng Wang. All drafts of this manuscript were written by Yuanyuan Shao and Dr. Jingsheng Wang. Modifications were carried out under the close supervision of Dr. Charles Xu and Dr. Jesse Zhu. The final version has been accepted by *Applied Energy* for publication in February 2011.

DEDICATION

This work is dedicated to my parents and my daughter (Ashlyn Shao Zhang).

献词

此文谨献给我的父母和我的女儿 (张澜馨)。

ACKNOWLEDGEMENTS

I would like to express my deepest gratitude and sincere appreciation to Dr. Jesse Zhu and Dr. Charles Xu. This thesis would have been inconceivable without their guidance and continuous support. Dr. Zhu and Dr. Xu have helped me in each possible way: participating in planning of the experiments, revising/proofreading the thesis chapters and publications which improved the quality of the work both scientifically and editorially, and offering financial support. Additionally, Dr. Zhu always provides invaluable suggestions to ensure my studies in a smooth progress and in the right direction. Dr. Xu's patient and effective supervision and encouragement promoted my research capability, and my scientific and technical writing skills.

I deeply acknowledge Dr. Fernando Preto and Dr. Jingsheng Wang for mentoring me during the co-combustion/gasification tests in CanmetENERGY, Natural Resources Canada, Ottawa.

I would like to convey special thanks to CanmetENERGEY, Natural Resources Canada, Ottawa for providing the experimental setup and assisting on conducting the experiments. Much appreciation is extended to Guy Tourigny, Dave Wambolt, Benjamin Bronson, Dan Walsh, Bart Young, Chadi Badour, and Scott Hurley for their participation and assistance in the experiments.

Many thanks are given to Dr. Chuangzhi Wu, Dr. Anthony Straatman, Dr. Cedric Briens, and Dr. Shahzad Barghi for kindly serving on my thesis examination committee, and reviewing my thesis.

I am very grateful for the financial support from the Ontario Ministry of Energy,

Ontario Centres of Excellence, Nature Sciences and Engineering Research Council of Canada (NSERC), through the Atikokan Bioenergy Research Center (ABRC) program and the Discovery Grants awarded to J. Zhu and C. Xu. Ontario Power Generation and Peat Resources Limited are also gratefully acknowledged for supplying and donating the lignite and peat fuels for the tests.

Special thanks go to Hui Zhang, Yingliang Ma, Patrycja Galka, Jianzhang Wen, Michael Zhu, George Zhang, Lisa Desalaiz, Qing Mu, Yong Liu, Sayem Mozumder, Jing Xu, Sophia He, Amir Seyedmehdi, Mehran Andalib, Maozhan Qi, Ahmed Alassuity, Ming Li, Long Sang, Ahmed Eldyasti, Jingsi Yang, Pegah Saremi Rad, Jing Fu, Chengxiu Wang, Abbas Dadashi, Wen Shi, Rezwana Yeasmin, Liqiang Zhang, Danni Bao, Hezhou Ye for their help, advice and friendship.

Finally, I would like to express my appreciation to all faculty members in the Department of Chemical and Biochemical Engineering at Western for any help and encouragement.

TABLE OF CONTENTS

LIST OF TABLES

LIST OF FIGURES

LIST OF ABBREVIATIONS AND SYMBOLS

A/F	Air/fuel ratio
ASTM	the American society for testing and materials
BFB	Bubbling fluidized bed
CFB	Circulating fluidized bed
CL	Crushed lignite
D_A	Absolute ash deposition rate, g m^{-2} h^{-1}
db	Dry base
DOE	United State Department of Energy
EDX	Energy dispersive X-ray spectrometry
FBC	Fluidized bed combustor
FC	Fixed carbon
FTIR	Fourier transform infrared spectroscopy
HHV	High heating value, MJ/kg
IC	Ion chromatography
ICP-AES	Inductively coupled plasma-atomic emission spectrometry
IEA	International Energy Agency
OD	Outer diameter, mm
OPG	Ontario Power Generation
PAH	Poly-aromatic-hydrocarbons
PFC	Pulverized fuel combustor
PP	Peat pellet
RD_A	Relative ash deposition rate, g m^{-2} h^{-1}
SEM	Scanning electron microscopy
SI	Slagging index
USDA	United States Department of Agriculture
VM	Volatile matter
WPP	White pine pellet
XRD	X-ray powder diffraction
XRF	X-ray fluorescence

CHAPTER 1. **INTRODUCTION**

1.1. Availability and application of biomass as an energy source

The worldwide increased concerns over declining non-renewable fossil resources, energy security, climate change and sustainability of economy have intensified the search for alternatives to fossil resources for both energy and chemical production. In response for the increased concerns, Ontario of Canada has regulation in place to phase out the coal-fired power plants by 2014 due to the growing concerns over the environmental emissions (SO_2, mercury, and greenhouse gases). This, however, means that more than 6000 MW power currently produced from coal must be displaced by other types of energy or generated with alternative clean or renewable energy sources.

Biomass such as wood and woodwaste, forestry residues (limbs, bark, tree tops), energy crops and agricultural residues (wheat/rice straw and corn waste) is promising because it represents an immense renewable and hence sustainable energy source. About 14% of the world's primary energy supplies are achieved by biomass combustion or co-combustion (McGowan, 1991; Hall *et al.*, 1992). According to a report from International Energy Agency (IEA), a medium sized community with approximately 30,000 houses can be supplied with enough electricity by a 30MW power station fuelled by the biomass produced from 11,250 ha of plantations in the Northern Hemisphere (IEA, 2002) Additionally, IEA believes that during this century, the potential exists for biomass resources to meet 50% of world energy demands by developing currently-used and new technologies.

In Canada, bio-energy provides about 10% of energy, mainly in the pulp/paper industry. The pulp and paper industry and the sawmill industry are the largest users of bio-energy in Canada, amounted to 513×10^{15} J, or equivalent to 16.2 billion m^3 of natural gas, and supplying 50% of their own energy needs. Although 70% of the sawmill residues are utilized as energy, the remaining 30% (more than 5 million bone-dried tons per annum) is not utilized in Canada (Groves, 1998). In addition, the potential agricultural residues in Canada are estimated at 29.3 Mt oven dried biomass per year, among which 17.8 Mt oven dried could be available for energy and chemical production, provided that appropriate technologies were developed (Wood and Layzell, 2003). The potential of biomass resources for energy and chemical production in USA is 1.3 billion tonnes per year. As suggested in a report by the U.S. DOE/USDA, biomass could supply 5% of the nation's power by 2030 which is equivalent to 3% of current petroleum consumption. Moreover, in the continental U.S. some 55 million acres have been identified as available and having high potential for production of energy crops (i.e. switchgrass, polar, eucalyptus, and other species) (Fernholz, 2009).

On the other hand, peat is being accepted as a slowly renewable natural resource and as a promising clean substitute fuel for electricity generation, after the publication of a report from the Ministry of Trade and Industry of Finaland in 2000 (Crill *et al.*, 2000). Peat is a soft organic material accumulation of partially decayed vegetation matter together with deposited minerals from wetlands (Sopo, 2004). Peat fuel has many environmental and economic benefits. For example, peat contains a high carbon content (>17% by weight) and low sulfur content (only 10% as in coal), as well as virtually no mercury and low ash content (Hupa, 2005; Orjala and Ingalsuo, 1999). Peat fuel has

energy values equivalent to coal, but its price is lower than that of fossil fuels and is competitive with other biofuels. Moreover, when peat is co-fired with coal, minor engineering retrofit is needed for combustor system.

The world has rich peat resources and the global peat production was about 11.90 million tons in 2009 (IEA, 2010). The large peatlands of North American are in the continental areas of Alaska and Canada (Vitt *et al.*, 2000). It is estimated that Canada contains the largest area of peatlands, some 40% of the world's total peatlands, about 170 million hectares, potentially supporting 335.4 billion tons dry peat (Monenco, 1981). Northern Ontario of Canada has a potential of 8.8 million dry tons per year of fuel peat to generate 3200MW of electrical power (Peat Ltd, 2010). Using peat for energy production can be traced to before World War II (Sopo, 2004). As the first country adopting an energy peat development program (Sopo, 2004), Finland has the world's most advanced peat fuel industry, where peat supports its power plants ranging in size from 20-550 MW with a total output of over 7,000 MW (Telford, 2009). Dried peat has been one of the traditional fuels in places where the peat is of high quality and easily accessible, such as Ireland, which has seven peat-fired generation stations supporting one-third of Ireland's electric power (Bott, 2010). In Russia, more than 6000MW electric power (over 6% of Canada's electrical generation) is peat fired and about 4.5 million ton of peat are produced annually for home heating (Bott, 2010). In North America, using peat fuel for home heating are increasing in popularity, and Northern Canada has small scale district energy and heating systems in remote communities (Peat Ltd, 2010).

1.2. Biomass ash characteristics

Biomass ash characteristics play an important role in biomass-fired or co-fired boiler

design, because they would affect fly ash deposition behaviors during combustion (Fryda *et al.*, 2010, Chao et al., 2008, Hansen *et al.*, 2000). Severe ash deposition would lead to fouling, corrosion and de-fluidization (for fluidized bed combustors) (Baxter *et al.*, 1998; Skrifvars *et al.*, 1997). In most solid fuels, the primary components of ash are the inorganic species including the inherent inorganic materials and the extraneous inorganic materials. The inherent inorganic materials are generally in combination with oxygen-containing functional group within the organic structure of the biomass fuel to form cations or chelates. And, the extraneous inorganic materials refer to those additives such as common soil and other contaminates during geological processes, or during harvesting, handling and processing of the fuels/biofuels. The inherent inorganic materials are homogeneously dispersed in the fuel and are much mobile than extraneous inorganic materials and, thus are readily volatile in burning char (Obernberger *et al.*, 1999). As such, the inherent inorganic materials are mainly responsible for ash deposition in combustion.

The inherent inorganic materials in biomass fuels can be water soluble (in free ionic forms), associated to organic matters or present as minerals/precipitated species (amorphous or crystalline pure compound). It was found that the form of the inherent inorganic materials in biomass fuels could affect the ash behavior during combustion/co-combustion of the biomass. In old-age fuels such as high rank coals, for example, ash-forming elements are present as minerals. In relatively young-age fuels such as biomass, up to half of the ash-forming elements can be organically associated or present as easily soluble salts or as minerals (Veijonen *et al.*, 2003). Theis *et al.* (2006) reported the ash deposition behaviors from three sorts of feedstock, straw, peat and bark, with different

chemical fractionation. The ash-forming matters of straw consisted of a large part of soluble compounds which are perhaps easily volatilized under combustion conditions and presented highest fouling propensity. On the contrary, peat contains a significant amount of insoluble silicate minerals which might lead to less fouling tendency compared with straw.

Table 1-1 clearly lists the major inherent inorganic species found in the higher plants in most biomass materials, classified according to the form of the inherent inorganic materials in biomass, i.e., "water soluble", "organically associated" and "precipitated" forms (van Loo and Koppejan, 2008). As shown in the Table 1-1, the inorganic materials in biomass are mainly in the form water soluble inorganic salts, and principally as the oxides**,** nitrates, sulphates, chlorides, phosphates. This water-soluble form of the inherent inorganic materials in biomass would lead to a high mobility of alkali materials.

Compared with the most abundant alkali (sodium) metal in coal ash, potassium is the major alkali element of concern for biomass fuels (Table 1-2). Most biomass materials such as herbaceous species, younger tissues of woody species, nut hulls and shells, as well as some annual biomass contain > 1% and up to 34% K_2O for Alfalfa (Baxter *et al.*, 1998). Chlorine is another significant component in biomass fuels, playing an important role in ash deposition and corrosion. For example, straw invariably contains a substantial amount of chlorine along with potassium, usually at levels greater than 0.2 wt% and up to 3 wt% dry weight (Jenkins, 1989). Additionally, some biomass fuels contain substantial amounts of silica, e.g., the silica content in rice straw is typically 10 wt% of dry biomass weight (or 75.2 wt% of the total ash), and up to 20 wt% of dry biomass weight in rice hull is silica.

Table 1-1 Speciation of inorganic materials in higher plants (van Loo and Koppejan, 2008)

Element	Compound	Formula	Share of the element
Class 1– water soluble (free ionic form)			
Na	Sodium nitrate, chloride	$NaNO_3$, NaCl	>90%
K	Potassium nitrate, chloride	KNO_3, KCl	>90%
Ca	Calcium nitrate, chloride, phosphate	$Ca(NO_3)_2$, $CaCl_2$,$Ca_3(PO_4)_2$	20-60%
Mg	Magnesium nitrate, chloride, phosphate	$Mg(NO_3)_2$, $MgCl_2$,$Ca_3(PO_4)_2$	60-90%
Si	Silicon hydroxide	$Si(OH)_4$	<5%
S	Sulphate ion	SO_4^{2-}	>90%[1]
P	Phosphate ion	PO_4^{3-}	>80%[1]
Cl	Chloride ion	Cl^-	>90%[1]
Class 2 – organically associated (covalent or ionic boding with tissue)			
Ca	Calcium pectate	macromolecule	0.8-2.6%
Mg	Chlorophyll, magnesium pectate	$C_{55}H_{72}MgN_4O_5$, macromolecule-	8-35%
Mn	Various organic structures	Mn^{2+}, Mn^{3+}, Mn^{4+}	>90%[1]
Fe	Organic complex, organic sulphates	Fe^{3+}, Fe^{2+}	>80%[1]
S	Sulpholipids, amino acids, proteins	SO_4^{2-}, S	–
P	Nucleic acids	P_4^{3-}	–
Class 3 – precipitated (amorphous or crystalline pure compound)			
Ca	Calcium oxalate	$CaC_2O_4 \cdot nH_2O$	30-85%
Fe	Phytoferritin	$(FeO{\bullet}OH)_8$ $(FeO{\bullet}OPO_3H_2)$	Up to 50% [2]
P	Phytates	Ca-Mg-K-salt of $C_6H_6[OPO(OH)_2]_6$	Up to 50-86%[3]
Si	Phytolite	$SiO_2 \cdot nH_2O$	–

[1] no quantities have been reported, the value quoted indicates only that the speciation is the dominant for the specific element;
[2] in leaf tissue;
[3] in seeds.

Table 1-2 Chemical composition of agricultural wastes ash in wt% dry base (Bryers, 1996)

	SiO_2	Fe_2O_3	MgO	CaO	ZnO	K_2O	Na_2O	SO_3	P_2O_5	Total
Bean straw (I)	29.20	2.70	0.90	4.67	0.03	22.34	0.52	4.70	2.29	68.05
Safflower	20.46	1.20	6.10	10.84	0.03	30.01	0.91	8.36	3.64	81.65
Rice hulls	94.60	0.03	0.02	0.25	0.00	2.40	0.135	2.24	0.46	100.12
Alfalfa	7.96	0.51	2.87	11.20	0.125	33.97	3.64	4.64	10.46	75.46
Cotton gin trash	23.20	1.93	2.87	7.18	0.187	13.00	1.59	4.24	10.00	64.20
Barley straw	44.70	2.60	4.84	3.22	0.125	8.01	5.25	1.80	11.56	81.11
Corn stalks	50.70	3.14	3.08	3.90	0.95	10.30	0.53	11.08	10.00	93.68
Rice straw	75.20	0.58	0.83	0.72	0.00	11.90	0.28	1.51	8.87	99.89
Bean straw (II)	32.70	3.93	3.65	6.30	0.15	25.30	0.82	2.28	7.30	82.43
Wood chips	8.30	10.00	6.22	18.61	0.193	11.80	1.32	9.00	6.87	71.61
Corn fodder	55.30	2.40	3.32	1.05	0.087	9.59	0.73	3.48	2.98	78.95
Paper pellets	57.20	4.29	0.83	0.15	0.31	1.85	5.09	4.00	4.46	78.19
Almond shell	22.60	3.77	2.49	12.27	0.05	14.14	5.08	8.00	5.50	73.90
Corn cobs	40.30	4.06	2.49	1.27	0.22	2.04	1.19	8.74	6.87	85.53
Manzanita chips	5.97	2.86	4.94	24.49	0.25	10.96	2.85	6.74	8.20	67.16
Tree pruning	9.95	1.94	8.29	19.87	0.06	12.66	1.48	19.72	4.96	85.93
Walnut shell	13.60	2.44	3.65	7.00	0.44	21.50	1.08	8.48	4.58	62.92
Olive pits	10.50	2.20	3.48	25.89	0.12	3.13	7.60	17.20	7.56	77.74
Almond shells	18.60	3.83	1.99	16.00	0.23	14.70	5.86	17.48	7.79	86.48
Corn stalks	71.70	7.10	2.70	0.46	0.02	10.28	0.33	2.20	0.66	95.45
Cotton stalks	33.00	2.80	6.05	3.56	0.07	21.40	1.374	6.55	6.40	83.57

1.3. Challenges with fly ash deposition in a combustor/boiler

As mentioned in the last section, biomass usually contains high-alkali-level inorganic matters which are mostly in mobile forms at elevated temperatures (Baxter, 1993). As a result, ash deposition poses great challenges for almost all combustors/boilers when firing or co-firing biomass materials and coal, particularly when co-firing coal with some herbaceous materials like straw and wheat straw (van Loo and Koppejan, 2008; Jenkins *et al.*, 1998; Robinson *et al.*, 2002; Wieck-Hansen *et al.*, 2000 and Robinson *et al.*, 1998). The ash deposition amount and the appearance of the deposited ash on a test probe during co-firing of are illustrated in Figure 1-1 (Robinson *et al.*, 2002).

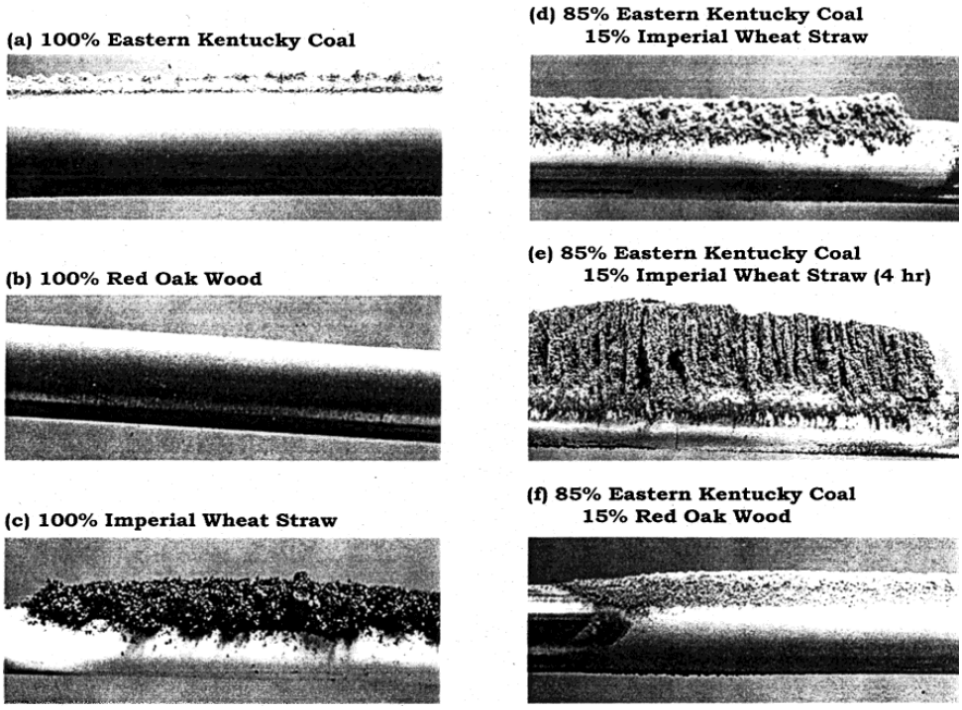

Figure 1-1 Pictures of deposits formed while firing unblended fuel (a, b, c) and co-firing blends (d, e, f) (Robinson *et al.*, 2002)

As clearly shown in the illustrations, the combustion of the coal and the red oak wood both led to less severe ash deposition and the deposited ashes were fine particles, while a more severe deposition of coarse ash was observed when firing wheat straw. Co-firing

the coal with either the two biomass materials led to increased ash deposition, compared with the combustion of the coal alone.

Some major negative impacts of increased ash deposition rates by co-firing on the combustion system efficiency and operation may be summarized as follows:

(1) Decreased the combustor utilizing efficiency. The increased ash deposition rates as well as the changed properties of the ash deposits (with decreased melting temperatures) would lead to agglomeration of the ash particles in the combustor and would eventually cause de-fluidization of a fluidized bed combustor, which would hence result in greatly reduced combustor utilizing efficiency. Moreover, the deposition of fused or partially fused ash deposits on the heat exchanger surfaces will retard the boiler heat transfer, leading to a decline in the combustor efficiency and capacity too.

(2) Damaged combustor equipment. Ash deposits may grow to the extent that the flue gas flow through the boiler is restricted, often by bridging across the steam tubes and tube bundles. This could cause mechanical damage of the combustor components and boiler equipment, and more importantly the ash deposits are associated with corrosion at high temperatures. Even for large pulverized fuel furnaces, the ash deposition on burner component and divergent surfaces could result in interference with burner light-up and operation. Again, the accumulation and subsequent shedding of large ash deposits on upper furnace and the steam tubes surfaces could restrict gas flow and thus damage the components of the combustion system.

(3) Maintenance problems. Severe deposits, for example on steam tubes, in hoppers

and on grates (for grate boilers), in quantities unmanageable by the facility, would require premature shut down for maintenance. Moreover, the build-up of accumulations of ash deposits on heat transfer surfaces also leads to increased furnace and chamber exit gas temperatures and reduced boiler efficiency. As such, unplanned outages for off-load cleaning are required for removing the ash deposits.

1.4. Objectives

In 2007, the Ontario government funded a research program, Atikokan Bioenergy Research Centre (ABRC) Program, to investigate biomass supply chains and utilization technologies for large-scale use of biomass energy in the province. As a part of this program, the main objectives of this PhD research project were to investigate the combustion/co-combustion/gasification performance of woody biomass (wood pellets and sawdust), peat (pellets and crushed peat) and lignite in a pilot-scale bubbling fluidized bed combustor, particularly the ash deposition behaviours, and the possible interactions between ashes from different types of feedstocks. The specific objectives of this project are as follows:

(1) investigate the ash deposition behaviours during co-combustion of a woody biomass and lignite coal in a fluidized bed;

(2) investigate the ash deposition behaviours during co-combustion of peat and lignite coal in a fluidized bed;

(3) investigate the ash deposition behaviours during co-combustion of fuel blends of biomass, peat and lignite in a fluidized bed;

(4) investigate the ash deposition behaviours during fluidized-bed air-blown gasification of a woody biomass and peat;

This research includes both experimental work (pilot-scale tests on direct/indirect co-firing of biomass/peat and lignite with a fluidized bed reactor) to study the possible interactions between ashes from biomass/peat and lignite, and some modelling studies based on the experimental data obtained from the co-firing tests. The combustion/co-combustion and gasification experiments were carried out at CanmetENERGY, Natural Resources Canada in Ottawa, on pilot-scale fluidized bed reactor. Due to the complexity of the facility and operating procedures (it took more than 12 hours to complete one run of experiment), limited numbers of the tests were planned and performed, as shown in Appendix A1 and Appendix A2. In addition to the experimental studies, extended simulation was conducted to examine and to solidify the experimental data. For example, a model based on the interactions of chlorine, which was high in some fuels like peat, with alkali species or alkaline earth metals was developed to describe ash deposition behaviours during co-combustion of peat and coal.

1.5. Thesis structure

This thesis follows the integrated-article format and includes three major parts. In the first part, Chapter 1 is a brief introduction to availability and application of biomass as an energy source, biomass ash characteristics, and ash-related problems in a combustor/gasifier, as well as the objectives and structure of this thesis. Chapter 2 provides an overview of current research efforts and a comprehensive literature review of biomass co-firing technologies and ash-related researches. This literature review helps in

understanding the mechanisms and chemistry of fly ash deposition, and the strategies/approaches/technologies to reduce ash deposition and corrosion in co-firing.

The second part of this thesis presents the experimental apparatus and methods, experimental results and discussion and key conclusions from the combustion/co-combustion and gasification tests in a pilot-scale fluidized bed reactor. Detailed experimental setup and procedures were described in Chapter 3. Chapters 4-6 presents the ash deposition behaviours during co-combustion of two-fuel blends of a woody biomass and lignite, two-fuel blends of a Canadian peat and lignite, and three-fuel bends of white pine, peat and lignite, respectively. Experimental results of biomass/peat gasification are discussed in Chapter 7. These Chapters also recount in detail the experimental setup, materials, operating conditions and methodologies.

The third part (Chapter 8) of this thesis presents a mathematical modelling study of ash deposition for co-firing peat with lignite. The developed model would be useful for the control and optimization of ash deposition in co-firing a variety of fuel blends. Finally, a brief summary of conclusions and recommendations for future work is given in Chapter 9.

1.6. References

Baxter, L.L.; Miles, T.R.; Miles Jr., T.R.; Jenkins, B.M.; Milne, T.; Dayton, D.; Bryers, R.W.; Oden, L.L. (1998). The behavior of inorganic material in biomass-fired power boilers: field and laboratory experiences. *Fuel Processing Technology*; **54**(1-3):47-78.

Baxter, L.L (1993). Ash deposition during biomass and coal combustion: A mechanistic approach. *Biomass and Bioenergy*; **4**(2): 85-102.

Bott, R.D. (2001). Peat. *2010 Historica Foundation of Canada*. The Canadian Encyclopedia (TCE). *http://www.thecanadianencyclopedia.com/index.cfm?PgNm=TCE&Params=A1ARTA006177* (accessed on June 2010).

Bryant, G.W. (1995). Treatments and additives to control deposition of ash resulting from combustion of Victorian brown coals. *PhD Thesis*, University of Newcastle.

Bryers, R.W. (1996). Fireside slagging, fouling, and high-temperature corrosion of heat-transfer surface due to impurities in steam-raising fuels. *Progress in Energy and Combustion Science*; **22**(1):29-120.

Crill, P., Hargreaves, K. and Korhola., A. (2000). The role of peat in Finnish greenhouse gas balances. *Ministry of Trade and Industry*. Helsinki, Finland.

Fernholz, K. (2009). Energy from woody biomass: a review of harvesting guidelines and a discussion of related challenges. Divetail Partners, Inc. *http://www.dovetailinc.org/files/DovetailBioGuides0709.pdf* (accessed on October 2009).

Fryda, L.; Sobrino, C.; Cieplik, C.; van de Kamp, W.L. (2010). Study on ash deposition under oxyfuel combustion of coal/biomass blends. *Fuel*; **89**: 1889-1902.

Groves, K.(1998). Unpublished Report for the Pulp and Paper Associate of Canada.

Hall, D.O.; Rosillo-Calle, F.; de Groot, P. (1992). Biomass energy lessons from case studies in developing countries. *Energy Policy*; 62-73.

Hansen, L.A.; Nielsen, H.P.; Frandsen, F.J.; Dam-Johansen, K.; Hørlyck, S.; Karlsson, A. (2000). Influence of deposit formation on corrosion at a straw-fired boiler. *Fuel Processing Technology*; **64**(1-3):189-209.

Hupa, M. (2005). Interaction of fuels in co-firing in FBC. *Fuel*; **84**:1312–1319.

International Energy Agency (IEA) (2010). *Part IV of Coal information* (2010 edition). International Energy Agency. ISBN: 978-92-64-08421-6 (PDF); 978-92-64-08420-9 (print).

International Energy Agency (IEA) (2002). Sustainable production of woody biomass for energy. *A position paper. ExCo2002:03*. *http://www.ieabioenergy.com/library/157_PositionPaperSustainableProductionofWoodyBiomassforEnergy.pdf* (accessed on January 2008).

Jenkins, B.M.; Baxter, L.L.; Miles Jr, T.R.; Miles, T.R. (1998). Combustion properties of biomass. *Fuel Processing Technology*; **54**:17-46.

Jenkins, B.M. (1989). Physical properties of biomass. In: Kitani, O. and Hall, C. (Eds), *Biomass Handbook*, New York: Gordon and Breach.

McGowan, F. (1991). Controlling the greenhouse effect: the role of renewables. *Energy Policy*; 111-118.

Monenco Ontario Ltd. (1981). Evaluation of the potential of peat in Ontario. *Ontario Ministry of Natural Re-sources Occasional Paper 7*.

Obernberger, I.; Dahl, J.; Brunner, T. (1999). Formation, composition and particle size

distribution of fly ashes from biomass combustion plants. *The 4th Biomass Conference of the Americas*, August 29-September 2, 1999, Oakland, CA. Oxford UK: Elsevier Science Ltd., pp.1377-1385.

Orjala, M.; Ingalsuo, R. (1999). *5th International Conference on Technologies and Combustion for a Clean Environment*; **12**(15):685-689.

Peat Resources Ltd. Peat Fuel. *http://www.peatresources.com/peat_fuel.htm* (accessed on November 2010).

Robinson, A.L., Junker, H., Baxter, L.L. (2002). Pilot-scale investigation of the influence of coal-biomass co-firing on ash deposition. *Energy Fuels*; **16**(2):343-355.

Robinson, A.L.; Junker, H.; Buckley, S.G.; Sclippa, G.; Baxter, L.L. (1998). Interactions between coal and biomass when cofiring. *Symposium (International) on Combustion*; **27**(1):1351-1359.

Skrifvars, B.J.; Backman, R.; Hupa, M.; Sfiris, G.; Åbyhammar, T.; Lyngfelt, A. (1997). Ash behavior in a CFB boiler during combustion of coal, peat or wood. *Fuel*; **77**(1/2):65-70.

Sopo, R. (2004). Peat as an energy resource. International Peat Society (IPS). Finland. *http://www.peatsociety.org/index.php?id=33* (accessed on November 2010).

Telford P.G. (2009). Peat Fuel - A Sustainable Bioenergy Resource. *IASTED International Conference Environmental Management and Engineering (EME 2009)*, July 7-8, 2009, Banff, Canada, pp 6-10.

Theis, M., Skrifvars, B.J., Zevenhoven, M., Hupa, M. and Tran, H. (2006), Fouling tendency of ash resulting from burning mixtures of biofuels. Part 2: Deposit chemistry. *Fuel*; **85**(14-15):1992-2001.

van Loo, S.; Koppejan, J (2008), Co-Combustion. In van Loo, S and Koppejan, J (Eds.): *The handbook of biomass combustion and co-firing* (Chapter 7: 203-45). London, UK: Earthscan.

Veijonen, K.; Vainikka, P.; Järvinen and Alakangas, E. (2003), Biomass co-firing: An efficient way to reduce greenhouse gas emissions. *European Bioenergy Networks*, *http://eubionet.vtt.fi.* (accessed on February 2008).

Vitt, D.H.; Halsey, L.A.; Bauer, I.E. and Campbell. C. (2000). Spatial and temporal trends in carbon storage of peatlands of continental western Canada through the Holocene. *Can. J. Earth Sci.*; **37**(5):683–693.

Wieck-Hansen, K.; Overgaard, P.; Larsen, O.H. (2000). Co-firing coal and straw in a 150 MWe power boiler experiences. *Biomass and Bioenergy*; **19**(6):395-409.

Wood, S., Layzell D.B. (2003). *BIOCAP Canada Foundation*, *www.biocap.ca/images/pdfs/BIOCAP_Biomass_Inventory.pdf* (accessed on February 2008).

CHAPTER 2. LITERATURE REVIEW

2.1. Co-firing technologies

Co-firing technology has proven to be a cost-effective technology to achieve the goal of increasing use of biomass-to-energy processes for power generation, thereby significantly reducing greenhouse gas emissions. The great majority of biomass co-firing worldwide is carried out in large pulverized coal power boilers. Depending on the manner of utilization of biomass in pulverized coal-fired power plants, co-firing processes can be generally classified into three categories: (1) biomass is simply blended with coal and then introduced into the boiler (Direct co-firing); (2) the biomass feedstock is combusted in a separated boiler to produce steam which, in turn, is utilized within the coal plant steam (Parallel co-firing); and (3) biomass is gasified before the subsequent co-firing process (Indirect co-firing).

Co-firing of biomass and coal is promising due to its potential in reduction of emissions of greenhouse gases and other toxic gases such as SO_x and maybe NO_x (McIlveen-Wright *et al.*, 2007; Armesto *et al.*, 2003; Tsai *et al.*, 2002; Demirbaş, 2003; Demirbaş, 2005; Baxter, 2005). The example of environmental impacts of co-firing in power generation applications (vs. 100% coal) can be shown in Table 2-1 (FEMP 2004). A decrease in fuel bound sulfur and nitrogen results in the reduction of the corresponding gaseous sulfur dioxide (SO_2) (almost zero for most biomass) and nitrogen oxides (NO_x) formation (Sami *et al.*, 2001). The reduction in SO_x emissions is not only ascribed to the lower sulfur content in the biomass feedstock, but also due to the retention of sulfur by alkali/alkaline earth elements present in the biomass (Demirbaş, 2005; Ericsson, 2007). Unlike the SO_x emission, the level of NO_x emission in co-firing is not monotonous. For

instance, Tsai *et al.* (2002) observed reduced NO_x emission in co-firing, and it was attributed to the high moisture content in biomass, which lowered the combustion temperature and consequently resulted in lower NO_x emissions. In contrast, an increased amount of N_2O was obtained in a bubbling fluidized combustor when co-firing coal and food cake, a high moisture waste material from the olive oil industry (Armesto *et al.*, 2003).

Table 2-1 Example environmental impacts of co-firing in power generation applications (vs. 100% coal) (FEMP 2004)

Boiler type	Plant size (MW)	Co-firing ratio	Reduced coal use (tones/yr)	Biomass used (tones/yr)[1]	Annual CO_2 reduction (tones/yr)[2]	Annual SO_2 reduction (tones/yr)
Stoker (low cost)	15	20%	10,125	16,453	27,843	466
Stoker (high cost)	15	20%	10,125	16,453	27,843	466
Fluidized bed	15	15%	7,578	12,314	20,839	349
Pulverized coal	100	3%	7,429	12,072	20,430	342
Pulverized coal	100	15%	37,146	60,362	102,151	1,709

[1] Depending on the source of biomass, "biomass used" could be avoided landfilled material.
[2] Carbon reduction may further be calculated from the CO_2 reduction.

The remarkable advantages of biomass co-combustion as discussed above have broadened the applications of biomass co-firing technology in the energy production fields. Co-firing has been commonly used in the USA, Finland, Denmark, Germany, Austria, Spain, and Sweden, The Netherlands, Poland and a number of other countries (van Loo and Koppejan 2008a). To date, more than 150 coal-fired power plants (mainly 50-700MWe) in the world have adopted or tested co-firing of coals with woody biomass or waste materials (IEA, 2007). Biomass systems can also be used for village-power applications in the 10–250 kW scale, for larger scale municipal electricity and heating applications (Bain *et al.*, 1998), for industrial application such as hog-fuel boilers and

black-liquor recovery boilers, and for agricultural applications such as electricity and steam generation in the sugar cane industry (Turn *et al.*, 2006), and for utility-scale electricity generation on the 150 MW scale (Hansen *et al.*, 1998). A variety of biomass including woodwaste, forestry/ agricultural residues and by-products, as well as herbaceous and energy crops materials have been co-combusted with essentially all types of commercially significant solid fossil fuels (e.g. lignites, sub-bituminous coals, bituminous coals, anthracites, and petroleum coke, etc.) at a co-firing ratio up to 15% (McIlveen-Wright *et al.*, 2007; Armesto *et al.*, 2003; Tsai *et al.*, 2002; Laursen and Grace, 2002; Ericsson, 2007). Owing to their wide range of applicability to a diverse set of needs, biomass-based power generating systems are so far the only non-hydro renewable source of electricity that can be used for base-load electricity generation.

Co-firing has been successfully demonstrated in almost all types of coal boiler including pulverized fuel combustor (PFC), fixed bed and fluidized beds combustors, as well as grate boilers (Winslow *et al.,* 1996; FEMP, 2004). For example, a very large-scale biomass co-firing plant, the Alholmens Kraft Combined Heat and Power plant in Pietarsaari (Finland), has been in operation since 2001. This plant employs a circulating fluidized bed (CFB) boiler and has electricity output of 240 MW_e (Veijonen *et al.*, 2003). Although fluidized bed combustors, bubbling fluidized beds (BFB) and circulating fluidized bed (CFB) are advantageous in terms of the fuel flexibility, being able to handle different types of fuels, solid, semi-solid, or liquid fuels, PFC is the most common technology used for co-firing biomass with coal. This is because less modification in equipment is required for co-firing biomass and coal in an existing large PFC. There has been rapid progress over the past decade in development of the co-firing of biomass

materials in pulverized coal-fired boiler plants worldwide, particularly in Europe, North America and Australia (van Loo and Koppejan, 2008b). According to the report by Baxter and Koppejan (2004), worldwide approximately 41.5% of 135 coal-fired power plants that have experienced co-firing biomass use PFC boilers. However, biomass co-firing in PFCs is limited due to both technical and non-technical problems. For example, co-firing ratio of biomass in most PFC boilers is no more than 10-15% on a thermal input basis due to the issues of increased ash deposition or accelerated corrosion rates for the boiler components. On the other hand, grate boilers have been traditionally used for solid fuel combustion on a relatively small-to-medium scale (15 kW up to 150 MW). On grate boilers, co-firing of recycled fuels, packaging derived fuels, refuse derived fuels, recovered fuels and plastics with wood fuels or other by-products of forest industry was practiced (Kupka *et al.*, 2008). Co-firing of recycled fuels in small power plants is relatively less challenging as the steam temperature is usually lower than 400°C and there is no risk of high-temperature corrosion. Nevertheless, special attention must be paid to flue gas cleaning. For biomass firing on grate boilers, the following key issues need to be addressed: homogeneity of the feedstock (particle size), proper sizing of the combustion chamber and efficient mixing of feedstock with the combustion air.

In contrast to those direct co-firing technology in either BFB, CFB, PFC or grate boilers, gasification may be regarded as an indirect co-combustion technology, enabling to use larger proportions of biomass or waste materials in PFCs, natural gas boilers and gas turbines (Overgaard *et al.*, 2005; Morehouse and Detwiler, 2009). From the concept of indirect co-firing, solid biomass is gasified in a separate gasification unit and the product gas is subsequently burned in a boiler together with pulverised coal or natural

gas. For indirect co-firing, as biomass is gasified before the subsequent co-firing process, it is particularly useful for ash management as it separates ash from biomass and coals, alleviating concerns in the utilization of the coal-based fly ash for cement industries (Tillman, 2000). The major challenge for the indirect co-firing however lies in product gas quality (containing alkali metals and tars), in particular when gas turbines are used. The major technical obstacle for commercialization of biomass gasification is related to the formation of tar, a highly variable mixture of condensable aromatic hydrocarbons (single ring to 5-ring aromatic compounds) along with other oxygen-containing hydrocarbons and complex poly-aromatic-hydrocarbons (PAH). Generally, an air/steam gasification process produces tar at approximately 20 g per Nm^3 of flue gas (McKendry, 2002). In an air-blown fluidized bed gasifier, typical tar contents in producer gas were reported between 0.5 and 100 g/m^3 (Han and Kim, 2008; Asadullah *et al.*, 2003; Lopamudra *et al.*, 2003). For many applications, with the exception of direct and immediate syngas combustion for heat or electricity production, these tar levels must be reduced, often to below 50 mg/Nm^3 (Han and Kim, 2008). Tars can have significant negative effects on gasification with respects to efficiency and operation. Specifically, the production of tars instead of combustible gases represents a decrease in gasification efficiency, and condensation and deposition of tars at temperatures below 350 °C can lead to fouling and potential blockage of downstream equipment and piping (Lopamudra *et al.*, 2003). For many applications, thus cleaning of the syngas by filtration or wet scrubbing to remove tar and alkali metals is needed, while this will increase the investment costs. This problem could be better addressed by developing the in-furnace tar control technology or the hot gas cleanup technology. For example, addition of nickel

and noble metal catalysts (such as Ru, Pt, and Rh) into a gasifier were found to be highly effective for reducing tar formation and improving the quality of syngas (Abu El-Rub *et al.*, 2004). Commercial nickel-based steam reforming catalysts were found to be very active for removal of tarry hydrocarbons at a hot state to produce hydrogen-rich syngas by catalytic reforming/cracking (Baker *et al.*, 1987; Anzar *et al.*, 1998; Bangala *et al.*, 1998), while the major issues for these nickel-based catalysts are that they could be deactivated readily by coke deposition. More research on catalytic biomass gasification for in-furnace tar abatement or hot-gas cleanup is thus critically needed in order to commercialize the indirect co-firing technologies.

Although co-firing technologies have been well developed and relatively widely applied in industries worldwide, co-firing processes are not yet completely understood and it is still challenging to increase the biomass co-firing ration to >20% (Zheng and Koziński, 2000). Due to the inferior properties of biomass (e.g., higher moisture contents, low bulk densities, etc.), direct co-firing processes are normally limited to low co-firing ratios. The major technical challenges associated with co-firing biomass fuels are summarized as follows: (1) firing high-alkali herbaceous biomass fuels such as switchgrass (containing potassium or sodium) would lead to increased slagging and fouling on boiler surfaces; (2) chlorine compounds in volatile ash would result in corrosion of heat transfer surfaces inside the boiler; (3) biomass materials are generally moist and strongly hydrophilic as well as non-friable, which would pose difficulties in fuel preparation, storage, and delivery; (4) Depending on the quality of the biomass feedstock, co-firing might result in a reduced thermal efficiency and an increased emission (NO_x); (5) economic utilization of the fly ash from co-firing biomass and coal

shall be explored. It herewith shall be noted that the fly ashes from biomass co-firing processes are currently unacceptable for cement manufacture since they do not conform to the ASTM standards. Clearly the key challenges for direct co-firing processes are related to fly ash behaviors (deposition, fouling and corrosion, etc.), the following sections will thus focus on approaches used in fly ash-related researches, chemistry and mechanisms of ash deposition during co-firing biomass and coal, and technologies for reducing ash deposition.

2.2. Ash deposition monitoring and analysis of ash deposits

The mostly commonly applied technique for ash-related researchers involves using air-cooled steel probes as the simulation of superheater tubes or heat exchangers, and collecting the ash deposits during co-firing/combustion biomass to monitor ash deposition as well as to analysis of ash deposits. At least one K-type thermocouple is usually embedded into the outside of a deposition probe wall to detect surface temperature. The surface temperature of deposition probe can thus be controlled to some extends via adjusting the flow rate of cooling air depending on flue gas temperature and the probe properties (i.e. size, metal conductivity). In most of deposit-related studies, the surface temperature of ash deposition probes was controlled at a metal temperature in boiler, typically 500-600°C (Xu *et al.*, 2010; Theis *et al.*, 2006a-c; Skrifvars *et al.*, 2005; Skrifvars *et al.*, 2004; Aho and Silvennoinen, 2004). On the other hand, ash deposit sampling was performed at a superheater zone in a small boiler furnace or multiple locations in a large scale unit using the air-cooled deposition probes. Generally, after an operation period during a biomass co-firing/combustion test, the sampling probe(s) was/were carefully removed from the combustion system. Ash deposits were then

brushed off from the probe surfaces to be weighed and to be analyzed. In some lab-scale experiments, on-line weight measurements have been achieved by connecting a balance to the probe (Hupa, 2005). Moreover, some researchers added some detachable rings (Skrifvars *et al.*, 2005; Skrifvars *et al.*, 2004) or coupons (Jenkins *et al.*, 2008; Liu *et al.*, 2000) on the probe surface to collect deposits instead of a permanent metal surface. Deposit samples collected from these single-used rings/coupons were directly sent to do laboratory analyses, which minimized the contaminant during brushing off or inter-contaminant of each different test.

After collection, ash deposits obtained from biomass co-firing/combustion can be characterized by many laboratory techniques including inductively coupled plasma-atomic emission spectrometry (ICP-AES), X-ray fluorescence (XRF), X-ray diffraction (XRD), scanning electron microscopy (SEM) with energy dispersive X-ray spectrometry (EDX), and ion chromatography (IC). ICP-AES, XRF and SEM-EDX have been developed and applied to detect ten major elements present in fuel ash and deposits such as SiO_2, Al_2O_3, Fe_2O_3, CaO, MgO, TiO_2, Na_2O, K_2O, P_2O_5 and SO_3 (Gogebakan *et al.*, 2009; Aho *et al.*, 2008; Ninomiya *et al.*, 2004; Skrifvars *et al.*, 2004; Robinson *et al.*, 2002; Liu *et al.*, 2000; Jenkins *et al.*, 2008). The elemental concentrations are conventionally expressed as oxides, in their highest oxidation states, which reflect the principal inorganic. Furthermore, SEM is a particularly powerful analytical technique for the examination of the microstructure of ashes and deposits (Wigley *et al.*, 2007; Frandsen, 2005; Strifvars *et al.*, 2005). XRD is commonly used for the identification of the major crystalline phases in deposits (Gogebakan *et al.*, 2009; Xiong *et al.*, 2008; Vamvuka and Zografos, 2004). Because of high chlorine contents in most of biomass, IC

has been developed as a practice method to determine chlorine and sulphur concentration in deposits (Aho *et al.*, 2008; Theis *et al.*, 2006b).

Combining with abovementioned technologies, ash-related researches have been focused on (1) the studies of the mechanisms of ash deposition, slagging/fouling, and high temperature corrosion; and (2) the development of technologies for reducing ash-related issues during biomass co-firing/combustion. The detailed literature reviews about these two focuses are separately demonstrated in the following sections.

2.3. Mechanisms and chemistry of fly ash deposition

As mentioned in the last section, researchers have looked into the mechanisms involved in the formation (Aho *et al.*, 2008; Theis *et al.* 2006a-c; Andersen and Wattenfall, 2002; Kupka *et al.*, 2008), slagging/fouling (Skrifvars *et al.*, 2005) and corrosion (Neilsen *et al.*, 2000b) of the ash deposits during co-firing biomass and coal. During combustion/co-firing, ash is formed from the fuel-bound inorganic materials through a combination of complex chemical and physical processes. After undergoing a systematic physical process including fragmentation, shedding, and coalescence during char burnout, the extraneous inorganic materials may be converted to the volatile compounds (such as KCl or KOH) or non-volatile ash compounds that remain inside and on the surface of the char depending on the temperature and chemical composition of the particles. Depending on the density and size of the residual ash particles, the combustion technology, operating conditions and the flue gas velocity, a fraction of the non-volatile ash compounds will also be entrained with the flue gas and form the coarse part of fly ash with a large particle size (typically greater than 5μm, Figure 2-1a), while the rest will remain in the furnace and form bottom ash (Obernberger *et al.*, 1999).

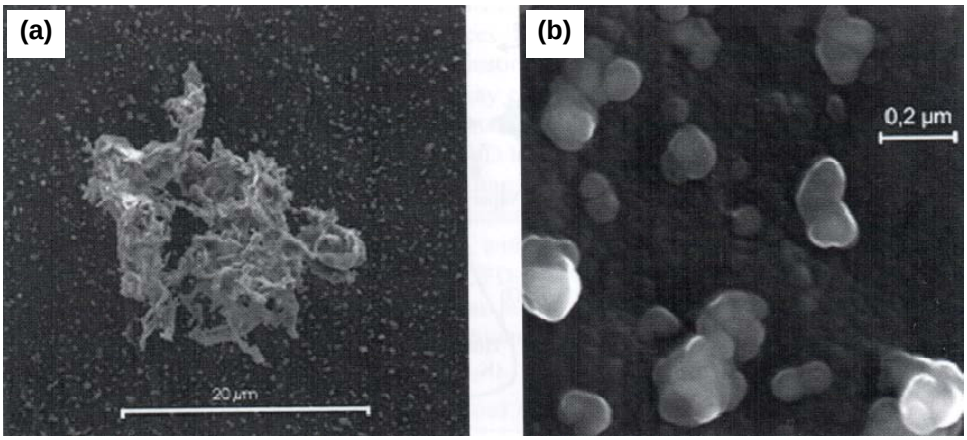

Figure 2-1 SEM-EDX images of coarse fly ash (a) and aerosol particles (b) from wood combustion in a grate furnace (Obernberger *et al.*, 1999)

Similarly, the inherent inorganic species may undergo several transformations including chemical and physical reactions during combustion/co-firing. Very small primary particles (about 5-10 nm) are formed by vaporization of the volatile species and subsequent nucleation in the boundary layer first, then they grow by coagulation, agglomeration and condensation in the flue gas. These particles are the basic fine fly ashes with a particle size of <1 µm as shown in Figure 2-1b. When the flue gas at high temperature containing many coarse and fine particles contacts the relatively cool heat transfer surface, coarse ash particles (typically greater than 10µm) (Stokes number is greater than 1) would cause inertial impaction, a dominant process responsible for the high temperature slag formation. Then, heterogeneous condensation between the pre-existing ash particles and the vapors of volatilized compounds in the flue gas will occur on the heat transfer surfaces. If the concentration of inorganic vapors in the flue gas and the cooling rate in the heat exchanger are both high, a local supersaturation of salts, e.g. Na_2SO_4, K_2SO_4, or KCl, could occur and cause formation of new particles by nucleation (Baxter *et al.*, 1998; Obernberger *et al.*, 1999). With the example of potassium, the major and most mobile/volatile alkali in the biomass fuels during combustion, vaporized K may

be present mainly as gaseous KCl or KOH in the flue gas at a high temperature > 800°C, as shown in Figure 2-2 (Baxter *et al.*, 1998). As the gas temperature decreases, the chloride and hydroxide are converted to sulphate by homogenous gas-phase reactions (a highly exothermic reaction, thus thermodynamically favorable at lower temperatures), as shown below.

$$KCl + SO_2 + 0.5\ O_2 + H_2O \rightarrow K_2SO_4 + 2\ HCl \quad \Delta H^o = -646.5\ kJ/mol \tag{2-1}$$

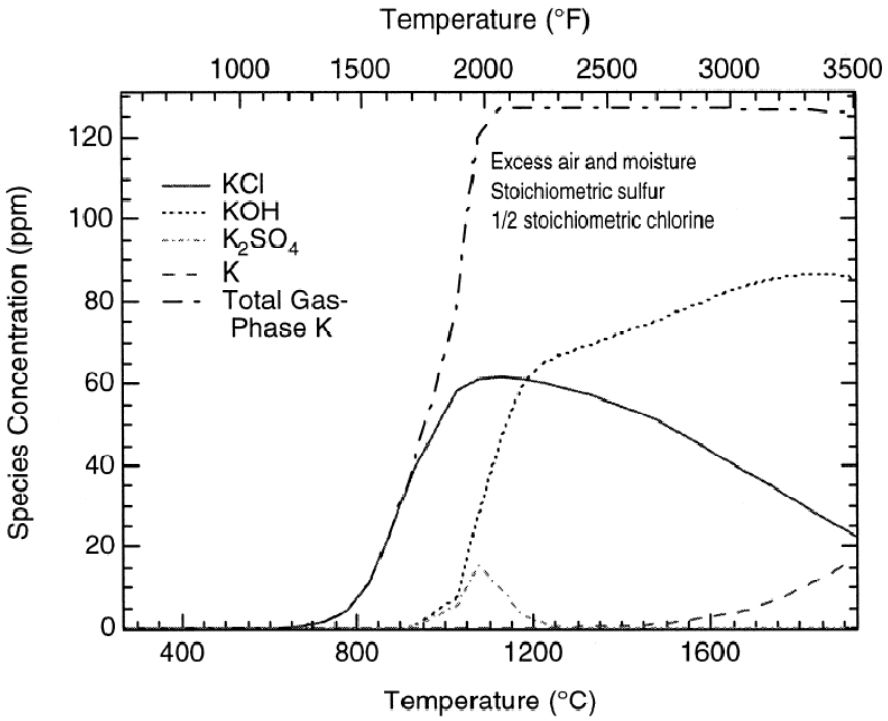

Figure 2-2 Equilibrium species concentrations for the major potassium-containing, gas-phase species present under typical biomass combustion conditions (Baxter *et al.*, 1998)

K_2SO_4 has a very low vapor pressure and becomes highly supersaturated as soon as it is formed, forming high numbers of new primary particles by homogenous nucleation. However, according to gas phase kinetic considerations, the equilibrium conversion to K_2SO_4 may not always be possible, i.e., only a part of the K in vapour phase is converted to K_2SO_4 (Christensen, 1995). The remaining part of the gaseous potassium may nucleate

either to KCl or K_2CO_3. As time proceeds in the flue gas, solid KCl or K_2CO_3 on the particles may undergo heterogeneous reactions with SO_2 (g) and form solid K_2SO_4.

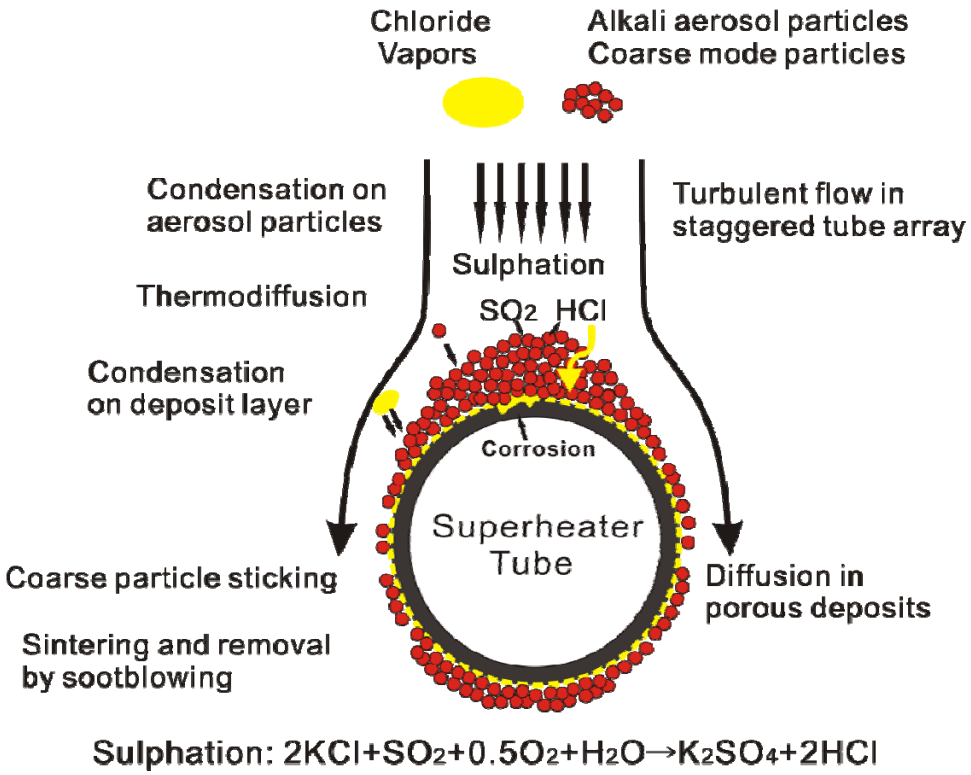

Figure 2-3 Schematic of mechanisms of ash formation and deposition on a superheater tube surface (modified from Veijonen *et al.*, 2003)

Generally there are four main mechanisms for ash deposition on heat transfer surfaces, including inertial impaction, condensation of vaporized inorganic compounds, thermophoresis and chemical reactions, as illustrated in Figure 2-3 (Veijonen *et al.*, 2003). The condensation of volatile inorganic species is the principle mechanism for the formation of convective pass fouling, e.g., on the heat transfer surfaces in a co-fired boiler, in particular when biomass fuels containing high levels of volatile species. In addition to condensation of vaporized inorganic compounds and inertial impaction, at the initial stage of the deposition when the local temperature gradients are at a maximum,

very small, sub-micron ash particles could be transported to cooled surface driven by the local gas temperature gradients regardless inertial impaction. This process is called thermophoresis. Such chemical reactions as oxidation, sulphation and chlorination processes would occur within the deposit layer and between gaseous and solid compounds under the combustion conditions (Theis *et al.* 2006b; Skrifvars *et al.*, 2004; Veijonen *et al.*, 2003; Robinson *et al.*, 2002). For example, silica in combination with alkali and alkaline earth metals especially with the readily volatilized forms of potassium present in biomass can lead to the formation of low melting point compounds which readily slag and foul at normal biomass boiler furnace temperatures (800-900°C) (Veijonen *et al.*, 2003, Baxter *et al.*, 1998). The produced alkali silicates and/or mixed alkali and/or calcium chlorides/sulfates tend to deposit on the reactor wall or the heat-exchanger surface causing fouling/corrosion with a low fusion temperature (typically < 700ºC) (Baxter, 1993).

2.4. Technologies for reducing ash deposition and corrosion in co-firing

As discussed before, firing or co-firing high-alkali (K/Na) herbaceous biomass fuels such as switchgrass and wheat straw would lead to severe problems of slagging and fouling on boiler surfaces, and the chlorine compounds in volatile ash would result in corrosion of heat transfer surfaces inside the boiler. Various technologies for reducing ash deposition as well as corrosion have been studied. These include (1) addition of so-called combustion additives such as sulphur or SO_2 and SiO_2 (Arvelakis *et al.*, 2005; Overgaard *et al.*, 2005; Aho and Silvennoinen, 2004; Andersson and Vattenfall, 2002), (2) pretreatment of the feedstocks to reduce the alkali metals (Jensen *et al.*, 2001a-b), (3) co-firing bio-fuels with low fouling-tendency fuels (Theis *et al.*, 2006a), and (4)

modification of the boiler (e.g. modification of the re-heater and super-heater in order to allow for larger spacing, more soot-blowing and a decrease in the live steam temperature to less than 500°C, etc) (Overgaard *et al.*, 2005). Details of some ash-deposition tackling technologies as mentioned above are provided below.

Anderson and Vattenfall (2002) demonstrated that it was effective for reducing ash deposition to spray a solution of ammonium sulfate (as an additive) into the flue gas from the combustor. Moreover, addition of Al was found to be effective for decreasing the ash deposition and thus reducing the fouling/slagging propensity. Al addition at 0.19% of the coal on dry basis resulted in reduced formation of Ca-Mg silicates by about 50% and the ash deposits were non-sticky ash particles. Another effective measure for preventing ash deposition is co-firing bio-fuels with low fouling-tendency fuels (Theis *et al.*, 2006a). That is replacing a part of biomass materials with a high fouling propensity with some bio-fuels with either low ash contents or a lower fouling propensity. The effectiveness of the above measure may be explained using the two reactions, i.e., the sulphation (Eq. 2-1) and the alkali capture reaction by aluminum silicates (Eq. 2-2).

$$Al_2O_3 \cdot 2SiO_2 + 2KCl + H_2O \rightarrow K_2O \cdot Al_2O_3 \cdot 2SiO_2 + 2HCl \qquad (2\text{-}2)$$

An excess of S in the flue gas could facilitate the sulphation of alkali chlorides and make the ash less sticky as well as increase melting point of the deposits, then preventing the slagging/fouling of heat transfer surface (Skrifvars *et al.*, 2004; Robinson *et al.*, 2002). Therefore, the sulphur-to-chlorine atomic ratio(S/Cl) in the feed stock was adopted as a useful indicator for the deposition and corrosion propensity of chlorine -containing ash, and it was suggested that if the S/Cl ratio of fuel is less than two, there is a high risk of superheater corrosion in combustion (Skrifvars *et al.*, 2004; Robinson *et al.*, 2002). If the

S/Cl ratio is at least four, the fuel blend could be regarded as non-corrosive (Veijonen *et al.,* 2003), while Theis *et al.* (2006b) recently reported the deposition could not be reduced unless the ratio reached at or above 6.7 due to the presence of Ca compounds that captured sulfur and thus restrained the sulphation.

Vuthaluru (1992) examined the effect of fuel pre-treatment methods for reducing ash deposition in combustion of Victorian brown coals. According to Vuthaluru (1992), the solid fuel was washed with either water or aqueous Al-lactate solution, or the solid fuel was just impregnated with Al-lactate solution. These experiments indicated that fuel-washing with water or Al-lactate reduced the condensable salts and subsequently fouling propensity. The addition of Al resulted in less sticky ash particles and lacey skeletal structure of deposits (Vuthaluru *et al.*, 1998). This study also suggested that addition of kaolin or alumina at 2–3 wt% of coal could alleviate the fouling and slagging problems during the combustion of Victorian brown coals. Bryant (1995) further showed that hydrothermal treatment of a brown coal could decrease its sodium content by up to 80%. The ash deposition experiments indicated that combustion of hydrothermally treated coal decreased fouling propensity of the brown coal by more than 50%.

2.5. Summary

Co-firing technology has been comprehensively developed in almost all types of coal boilers using a variety of biomass and essentially all ranks of coal. However, the co-firing level (blending ratio of the bio-fuel in the combustor feed) is normally limited to be less than 20 per cent on a thermal basis. Some problems with increased ash deposition or with accelerated corrosion rates of PFC boiler components have been reported. The ash-related problems become more apparent when co-firing biomass with coal in smaller

boilers or at higher blending ratios, as well as when co-firing fast-growing biomass materials and residues from fertilized crops. BFB/CFB combustors may be more advantageous for being employed for co-firing biomass and coal as they can achieve a higher level of co-firing and have higher fuel flexibility compared with PFC boilers.

Extensive researches have been reported on the behaviors and mechanisms of ash deposition during biomass co-firing, and on the development of some technologies for reducing ash deposition as well as corrosion. However, more studies are needed to investigate the interaction between ashes from different types of fuels, and the ash/chlorine deposition behaviors of peat fuels (abundant in Canada) during combustion/co-combustion/gasification, as well as cost-effective measures to alleviate/retard the ash-related problems (slagging, fouling, and corrosion) in a co-firing process.

2.6. References

Abu El-Rub, Z.; BramerBrem E.A.G.; Brem, G. (2004). Review of Catalysts for Tar Elimination in Biomass Gasification Processes. *Industrial and Engineering Chemistry Research*; **43**(22):6911-6919.

Aho, M.; Gil, A.; Taipale, R.; Vainikka, P.; Vesala, H. (2008). A pilot-scale fireside deposit study of co-firing Cynara with two coals in a fluidised bed. *Fuel*; **87**(1):58-69.

Aho, M.; Silvennoinen, J. (2004). Preventing chlorine deposition on heat transfer surfaces with aluminium–silicon rich biomass residue and additive. *Fuel*; **83**:1299-1305.

Andersson, C; Vattenfall, A.B. (2002). A method for operating a heat-producing plant for burning chlorine-containing fuels. Patent Number: WO 02059526.

Anzar, M.P.; Caballero, M.A.; Gil, J.; Martin, J.A.; Corella, J. (1998). Commercial steam reforming catalysts to improve biomass gasification with steam-oxygen mixtures. 2. Catalytic tar removal. *Industrial and Engineering Chemistry Research*; **37**(7):2668-2680.

Armesto, L.; Bahillo, A.; Cabanillas, A.; Veijonen, K.; Otero, J.; Plumed, A.; Salvador, L. (2003). Co-combustion of coal and olive oil industry residues in fluidized bed. *Fuel*; **82**:993-1000.

Arvelakis, S.; Gehrmann, H.; Beckmann, M.; Koukios, EG. (2005). Preliminary results on the ash behaviour of peach stones during fluidized bed gasification: evaluation of fractionation and leaching as pre-treatments. *Biomass and Bioenergy*; **28**:331-338.

Asadullah, M.; Miyazawa, T.; Kunimori K. (2003). Catalyst development for the gasification of biomass in the dual-bed gasifier. *Applied Catalysis A: General*;

255(2):169–180.

Baker, E.G.; Mudge, L.K., Brown, M.D. (1987). Steam gasification of biomass with nickel secondary catalysts. *Industrial and Engineering Chemistry Research*; **26**(7):1335-1339.

Bangala, D.N.; Abatzoglou, N.; Chornet, E. (1998). Steam reforming of naphthalene on Ni–Cr/Al_2O_3 catalysts doped with MgO, TiO_2, and La_2O_3. *AIChE J.*; **44**(4):927-936.

Baxter, L. (2005). Biomass-coal co-combustion: Opportunity for affordable renewable energy. *Fuel*; **84**(10):1295-1302.

Baxter, L; Koppejan, J (2004). Co-combustion of biomass and coal. *Euroheat and Power*; **1**:34-39.

Baxter, L.L.; Miles, T.R.; Miles Jr., T.R.; Jenkins, B.M.; Milne, T.; Dayton, D.; Bryers, R.W.; Oden, L.L. (1998). The behavior of inorganic material in biomass-fired power boilers: field and laboratory experiences. *Fuel Processing Technology*; **54**(1-3):47-78.

Baxter, L.L (1993). Ash deposition during biomass and coal combustion: A mechanistic approach. *Biomass and Bioenergy*; **4**(2):85-102.

Bryant, G.W. (1995). Treatments and additives to control deposition of ash resulting from combustion of Victorian brown coals. *PhD Thesis*, University of Newcastle.

Christensen, K.A. (1995), The formation of submicron particles from the combustion of straw, *PhD thesis*, Department of Chemical Engineering, Technical University of Denmark.

Demirbaş, A. (2003). Sustainable cofiring of biomass with coal. *Energy Conversion and Management*; **44**(9):1465-1479.

Demirbaş, A. (2005). Biomass co-firing for boilers associated with environmental

impacts. Energy Sources; **27**(14):1385-1396.

Ericsson, K. (2007). Co-firing-A strategy for bioenergy in Poland? *Energy*; **32**(10):1838-1847.

FEMP (Federal energy management program) (2004). Biomass co-firing in coal-fired boilers. Federal Technology Alert, DOE/EE-0288.

Frandsen, F.J. (2005). Utilizing biomass and waste for power production – a decade of contributing to the understanding, interpretation and analysis of deposits and corrosion products. *Fuel*; **84**:1277-1294.

Gogebakan, Z.; Gogebakan, Y.; Selçuk, N.; Selçuk, E. (2009). Investigation of ash deposition in a pilot-scale fluidized bed combustor co-firing biomass with lignite. *Bioresource Technology*; **100**(2):1033-1036.

Han, J.; Kim, H. (2008). The reduction and control technology of tar during biomass gasification/pyrolysis: An overview. *Renewable and Sustainable Energy Reviews*; **12**(2):397-416.

Hansen, P.F.B.; Andersen, K.H.; Wieck-Hansen, K.; Overgaard, P.; Rasmussen, I.; Frandsen, F.J.; Hansen, L.A.; Dam-Johansen, K. (1998). Co-firing straw and coal in a 150-MWe utility boiler: In situ measurements. *Fuel Processing Technology*; **54**(1-3):207-225.

Hupa, M. (2005). Interaction of fuels in co-firing in FBC. *Fuel*; **84**:1312–1319.

International Energy Agency (IEA) (2007). Bioenergy project development & biomass supply. *http://www.iea.org/textbase/nppdf/free/2007/biomass.pdf* (accessed on February 2009).

Jenkins, B.M.; Thy, P.; Turn, S.Q.; Blevins, L.G.; Baxter, L.L. and Jakeway, L.A.;

Williams, R.B.; Blunk, S.L.; Yore, M.W.; Wu, B.C.; Lesher, C.E. Composition and microstructure of ash deposits from co-firing biomass and coal. *http://www.google.ca/#sclient=psy&hl=en&site=&source=hp&q=composition+and+microstructure+of+ash+deposits+from+co-firing+biomass+and+coal&btnG=Google+Search&aq=&aqi=&aql=&oq=&gs_rfai=&pbx=1&fp=f995bf2ea2a12dc1* (accessed on March 2008)

Jensen, P.A.; Sander, B.; Dam-Johansen, K. (2001a). Pretreatment of straw for power production by pyrolysis and char wash. *Biomass and Bioenergy*; **20**(6):431-446.

Jensen, P.A.; Sander, B.; Dam-Johansen, K. (2001b). Removal of K and Cl by leaching of straw char. *Biomass and Bioenergy*; **20**(6):447-457.

Kupka, T.; Mancini, M.; Irmer, M.; Weber, R. (2008). Investigation of ash deposit formation during co-firing of coal with sewage sludge, saw-dust and refuse derived fuel. *Fuel*; **87**(12):2824-2837.

Laursen, K.; Grace, J.R. (2002). Some implications of co-combustion of biomass and coal in a fluidized bed boiler. *Fuel Processing Technology*; **76**(2):77-89.

Liu, K.; Xie, W.; Li, D.; Pan, W.P.; Riley, J.T.; Riga, A. (2000). The effect of chlorine and sulfur on the composition of ash deposits in a fluidized bed combustion system. *Energy Fuels*; **14**:963-972.

Lopamudra, D.; Ptasinski, K.J.; Janssen, F.J.J.G. (2003). A review of the primary measures for tar elimination in biomass gasification processes. *Biomass and Bioenergy*; **24**(2):125–140.

McIlveen-Wright, D.R.; Huang, Y.; Rezvani, S.; Wang, Y. (2007). A technical and environmental analysis of co-combustion of coal and biomass in fluidised bed

technologies. *Fuel*; **86**(14): 2032-2042.

McKendry, P. (2002). Energy production from biomass (part 1): overview of biomass *Bioresource Technology*; **83**(1):37–46.

Morehouse, J.H.; Detwiler, K.W. (2009). Assessment of a biomass gasification co-generation plant based on the UCS's "principles for bioenergy development". The 2nd International Conference on Energy Sustainability, August 10-14, 2008, Jacksonvill, USA. vol.**1**:399-404.

Nielsen, H.; Frandsen, F.; Dam-Johansen, K.; Baxter, L. (2000). The implications of chlorine-associated corrosion on the operation of biomass-fired boilers. *Process in Energy and Combustion Science*; **26**(3):283-298.

Ninomiya, Y.; Zhang, L.; Sakano, T.; Kanaoka, C.; Masui, M. (2004). Transformation of mineral and emission of particulate matters during co-combustion of coal with sewage sludge. *Fuel*; **83**(6):751-764.

Obernberger, I.; Dahl, J.; Brunner, T. (1999). Formation, composition and particle size distribution of fly ashes from biomass combustion plants. *The 4th Biomass Conference of the Americas*, August 29-September 2, 1999, Oakland, CA. Oxford UK: Elsevier Science Ltd., pp.1377-1385.

Overgaard, P.; Larsen, E.; Friborg, K.; Hille, T.; Jensen, P.A.; Knudsen, S. (2005). Full-scale tests on co-firing of straw in a natural gas-fired boiler. *http://www.dongenergy.com/SiteCollectionDocuments/NEW%20Corporate/PDF/Engineering/42.pdf.* (accessed on February 2008).

Robinson, A.L.; Junker, H.; Baxter, L.L. (2002). Pilot-scale investigation of the influence of coal-biomass co-firing on ash deposition. *Energy Fuels*; **16**(2): 343-355.

Sami, M.; Annamalai, K.; Wooldridge, M. (2001). Co-firing of coal and biomass fuel blends. *Progress in Energy and Combustion Science*; **27**(2):171-214.

Skrifvars, B.J.; Yrjas, P.; Laurén, T.; Kinni, J.; Tran, H.; Hupa, M. (2005). The fouling behavior of rice husk ash in fluidized-bed combustion. 2. Pilot-scale and full-scale measurements. *Energy Fuels*; **19**:1512–1519.

Skrifvars, B.J.; Laurén, T.; Hupa, M.; Korbee, R.; Ljung, P. (2004). Ash behaviour in a pulverized wood fired boiler – a case study. *Fuel*; **83**:1371–1379.

Theis, M.; Skrifvars, B.J.; Hupa, M.; Tran, H. (2006a). Fouling tendency of ash resulting from burning mixtures of biofuels. Part 1: Deposition rates. *Fuel*; **85**(7-8):1125-1130.

Theis, M.; Skrifvars, B.J.; Zevenhoven, M.; Hupa, M.; Tran, H. (2006b), Fouling tendency of ash resulting from burning mixtures of biofuels. Part 2: Deposit chemistry. *Fuel*; **85**(14-15):1992-2001.

Theis, M.; Skrifvars, B.J.; Zevenhoven, M.; Hupa, M.; Tran, H. (2006c). Fouling tendency of ash resulting from burning mixtures of biofuels. Part 3: Influence of probe surface temperature. *Fuel*; **85**(14-15):2002-2011.

Tillman, D.A. (2000). Biomass cofiring: the technology, the experience, the combustion consequences. *Biomass Bioenergy*; **19**:365-384.

Tsai, M.Y; Wu, K.T; Huang, C.C.; Lee, H.T. (2002). Co-firing of paper mill sludge and coal in an industrial circulating fluidized bed boiler. *Waste Management*; **22**(4):439-442.

Turn, S.Q.; Jenkins, B.M.; Jakeway, L.A.; Blevins, L.G.; Williams, R.B.; Rubenstein, G.; Kinoshita, C.M. (2006). Test results from sugar cane bagasse and high fiber cane co-fired with fossil fuels. *Biomass and Bioenergy*; **30**(6):565-574.

Vamvuka, D.; Zografos, D. (2004). Predicting the behaviour of ash from agricultural wastes during combustion. *Fuel*; **83**(14-15):2051-2057.

van Loo, S.; Koppejan, J (2008a), Combustion technologies for industrial and district heating systems. In van Loo, S. and Koppejan, J (eds.): *The handbook of biomass combustion and co-firing* (Chapter 5: 134-54). London, UK: Earthscan.

van Loo, S.; Koppejan, J (2008b), Co-Combustion. In van Loo, S and Koppejan, J (Eds.): *The handbook of biomass combustion and co-firing* (Chapter 7: 203-45). London, UK: Earthscan.

Veijonen, K.; Vainikka, P.; Järvinen and Alakangas, E. (2003), Biomass co-firing: An efficient way to reduce greenhouse gas emissions. *European Bioenergy Networks*, *http://eubionet.vtt.fi.* (accessed on February 2008).

Vuthaluru, H.B.; Vleeskens, J.M.; Wall, T.F. (1998). Reducing fouling from brown coals by sodium-binding additives. *Fuel Process Technology*; **55**:161–173.

Vuthaluru, H.B. (1992). Sodium/ash reactions during pulverized coal combustion treatments and additives to control deposition. *PhD Thesis*, University of Newcastle.

Wigley, F.; Williamson, J.; Malmgren, A.; Riley, G. (2007). Ash deposition at higher levels of coal replacement by biomass. *Fuel Processing Technology*; **88**(11-12):1148-1154.

Winslow, J.C.; Smouse, S.M.; Ekmann, J.M. (1996). Co-firing of coal and waste. *Report IEACR/90*. London: IEA Coal Research.

Xiong, S.J.; Burvall, J.; Örberg, H.; Kalen, G.; Thyrel, M.; Öhman, M.; Boström, D. (2008). Slagging characteristics during combustion of corn stovers with and without

kaolin and calcite. *Energy Fuels*; **22**:3465-3470.

Xu, X.G.; Li, S.Q.; Li, G.D.; Yao, Q. (2010). Effect of co-firing straw with two coals on the ash deposition behavior in a down-fired pulverized coal combustor. *Energy Fuels*; **24**:241-249.

Zheng, G.; Koziński, J.A. (2000). Thermal events occurring during the combustion of biomass residue. *Fuel*; **79**(2):181-192.

CHAPTER 3. EXPERIMENTAL SECTION

3.1. Materials and Preparation

Three fuels including lignite, white pine, and peat were used in this study, which were supplied by Ontario Power Generation, a local company in Southern Ontario and Peat Resources Limited, Canada, respectively. The white pine and the peat were received in the form of sawdust and pellet, respectively. Detailed proximate and ultimate analyses of these fuels and ash compositions are given in Table 3-1. Among these three fuels, the lignite coal has the highest ash content, 22 wt% dry base (db), and is characterized by its low ratio of volatile matters to fixed carbon, VM/FC ≈ 2.3. The white pine sawdust contains a low amount ash (0.4 wt% dry base) and is characterized by a high VM/FC (≈ 5.0). The white pine pellets (5 mm outer diameter (OD) and 40 mm length) were prepared from white pine sawdust using approximately 1 wt% of the binding agent Ameribond 2x (Ammonium Lignosulfonate), so that they contained higher ash and sulphur contents than that of sawdust. The peat fuel has a strikingly high chlorine content of 2008 μg/g db, a low amount ash (2 wt% db), and a VM/FC as same as lignite's. With regard to ash composition, the lignite ash is mainly composed of acidic oxides (SiO_2, Al_2O_3 and TiO_2), whereas the ash from the wood is enriched with basic oxides (CaO, MgO, K_2O, Na_2O and Fe_2O_3) and P_2O_5. The peat ash is balancing between acidic oxides and basic oxides.

Table 3-1 Proximate and ultimate analyses of the fuels and ash compositions

	Lignite	White Pine		Peat
		Sawdust	Pellet	
Moisture, wt% as received	30.0	38.0	5.3	35.8
HHV (MJ/ kg dry)	21.8	20.6	20.6	21.4
Proximate analysis, wt.% db				
Ash[1]	22.0	0.4	3.13	2.0
Volatile matters (VM)	54.0	84.5	80.75	68.6
Fixed carbon (FC)	24.0	15.1	16.12	29.4
Ultimate analysis, wt.% db				
Carbon	58.8	52.5	47.99	56.1
Hydrogen	4.2	6.3	6.25	5.7
Nitrogen	0.9	0.1	1.31	0.8
Sulphur	0.5	<0.1	0.58	0.2
Oxygen[2]	13.6	40.6	40.73	35.2
Chlorine[3], μg/g.	25	39.0	312	2008
Bromine[3], μg/g.	< 21	<29.0	203	153
Fluorine[3], μg/g	100	<29.0	<18	< 20
Dry ash analysis[4], wt.% db				
SiO_2	49.76	6.70	3.80	28.05
Al_2O_3	19.71	1.97	0.49	8.63
Fe_2O_3	3.82	1.46	0.58	5.56
TiO_2	0.86	0.09	<0.03	0.48
P_2O_5	0.30	3.52	23.13	1.31
CaO	9.91	31.10	23.36	12.65
MgO	2.11	4.34	6.86	17.72
SO_3	6.09	2.80	17.98	12.73
Na_2O	4.20	0.36	1.29	2.84
K_2O	1.04	15.45	16.46	1.14

[1] The ashing temperature was 750ºC for lignite and 500ºC for white pine;
[2]By difference; [3]By Pyrohydrolysis and IC; [4]By XRF of the ashes from the feedstocks.

Moreover, olivine, limestone, dolomite and iron ore were used as bed materials in the gasification tests. The sands of olivine, limestone, and dolomite were used as received at CanmetENERGY and were similar to relatively commonly-used materials in the market. The olivine sand mainly consists of MgO (42.5 wt%), SiO_2 (42 wt%), Fe_2O_3 (8.5 wt%), CaO (0.9 wt%), and Al_2O_3 (0.8 wt%). The major components of the dolomite are CaO (30.4 wt%) and MgO (21.7 wt%). The limestone is highly rich in CaO. In addition, limonite iron ore was obtained from the former Steep Rock Mine site in Atikokan, Ontario. Analysis of the material by XRD showed that the iron ore is composed mainly of iron oxides, in the form of goethite (FeOOH) and hematite (Fe_2O_3). From ICP-AES analysis of the iron oxide, the Fe content of material was measured at 42.2 wt%.

To prepare feedstock for the combustion tests, the received lignite was crushed and screened into particles (<4 mm) in the tests. The pellets of white pine and peat were used through all combustion/co-combustion tests. To investigate the effects of moisture content on the ash deposition behaviors in the combustion or co-combustion process, oven-dried fuels (to a moisture content of <5 wt%) were prepared by drying in air at 105°C for over 12 h. The actual moisture contents of each fuel was measured prior to each test, to determine the required fuel feeding rate (to maintain the same thermal input of 58.3 MJ/h in each combustion test).

On the other hand, for the gasification tests the white pine sawdust and the peat were used as fuels, while olivine, limestone, dolomite and iron ore were used as bed material as afore-mentioned. Because the white pine sawdust as received contained a relatively high moisture content (38 wt%), this material was simultaneously crushed to remove large particles (>10 mm) and dried to a moisture content approximately 15-20% using a

rotary dryer with a screening facility at CanmetENERGY, as pictured in Appendix B2. The pine sawdust was fed into the hopper where a crew feeder moved it to a chain crusher. Propane heated air was blown through the system to dry the material and send crushed particles to the collection barrel. The particle size and moisture content were controlled by the speed of the screw feeder and the chain crusher, as well as the blower-air temperature. In addition, due to poor fluidizability of the peat pellets and in order to obtain more representative results comparable to those from the pine sawdust, the peat pellets were crushed and sieved to 1-4 mm particle size using an electrical grinder. Due to of the partial loss of the fuel moisture during the crushing and further air drying processes, the crushed peat had a moisture content of around 25 wt% when they were applied to the gasification tests. The actual moisture content of the feedstock used was also measured prior to each test, to determine the fuel feeding rate for the gasification test. Additionally, The bed materials, olivine, limestone and dolomite, were crushed and sieved to ensure a uniform particle diameter (about 1 mm diameter), while the iron ore was crushed and sieved to a particle size of about 0.85 mm because of its greater particle density. All bed materials were calcined in air at >750 °C within the fluidized bed reactor during the warm-up combustion phase of each test using propane gas.

3.2. Co-Firing/Gasification Test Facility

The co-firing/gasification tests were conducted on a pilot-scale, fluidized bed reactor. The facility was operated in a bubbling fluidization regime. Figure 3-1 firstly presented an overview of the whole system. As illustrated in the Figure, the facility had a feeding capacity of up to 25 kg/h and equipped with a belt feeder combined with a rotary airlock

valve for stable fuel feeding by controlling the belt speed. From the main hoper, fuel/fuel blends are vibrated on to the belt feeder. The belt feeder sits on a scale, and feed rate is calculated using the fuel mass (on a dry basis), belt length and belt speed. The picture of the real fuel feeding system is presented in Appendix B1. The system was also coupled with a cyclone for fly ash collection, a tar sampling port, a water-cooled condenser for tar removal, and a flue gas sampling port. Furthermore, the flue gas was burned in an after-burner with propane gas and vented to the stack through an Induced Draft (ID) fan.

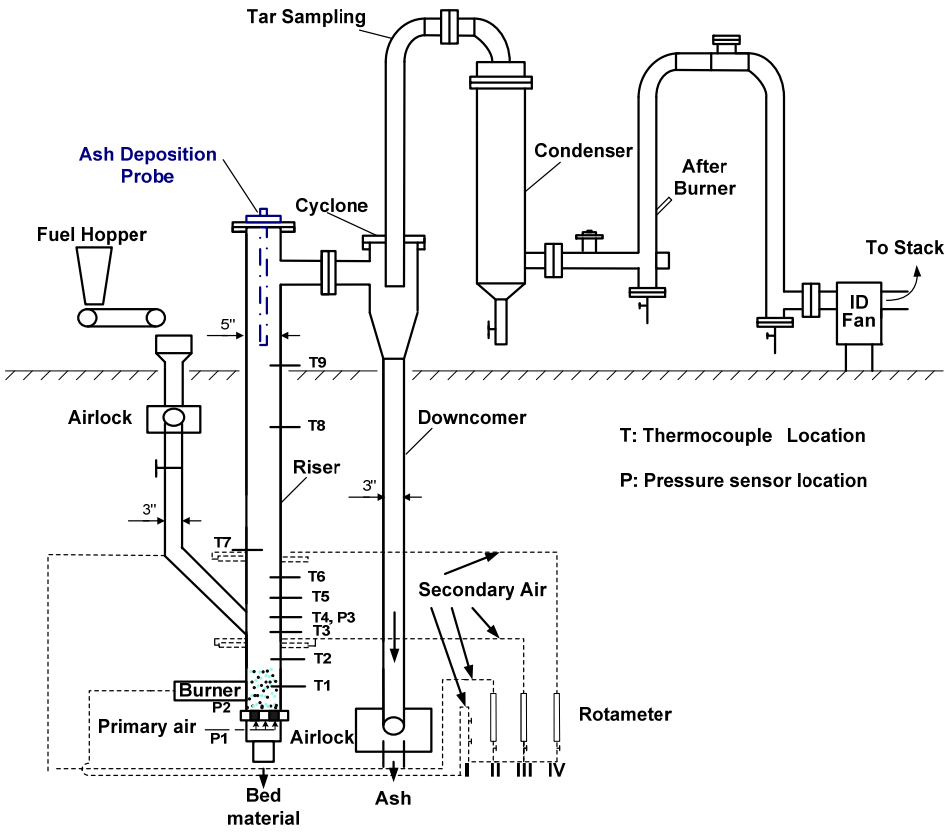

Figure 3-1 Schematic diagram of the fluidized-bed system at CanmetENERGY, Ottawa

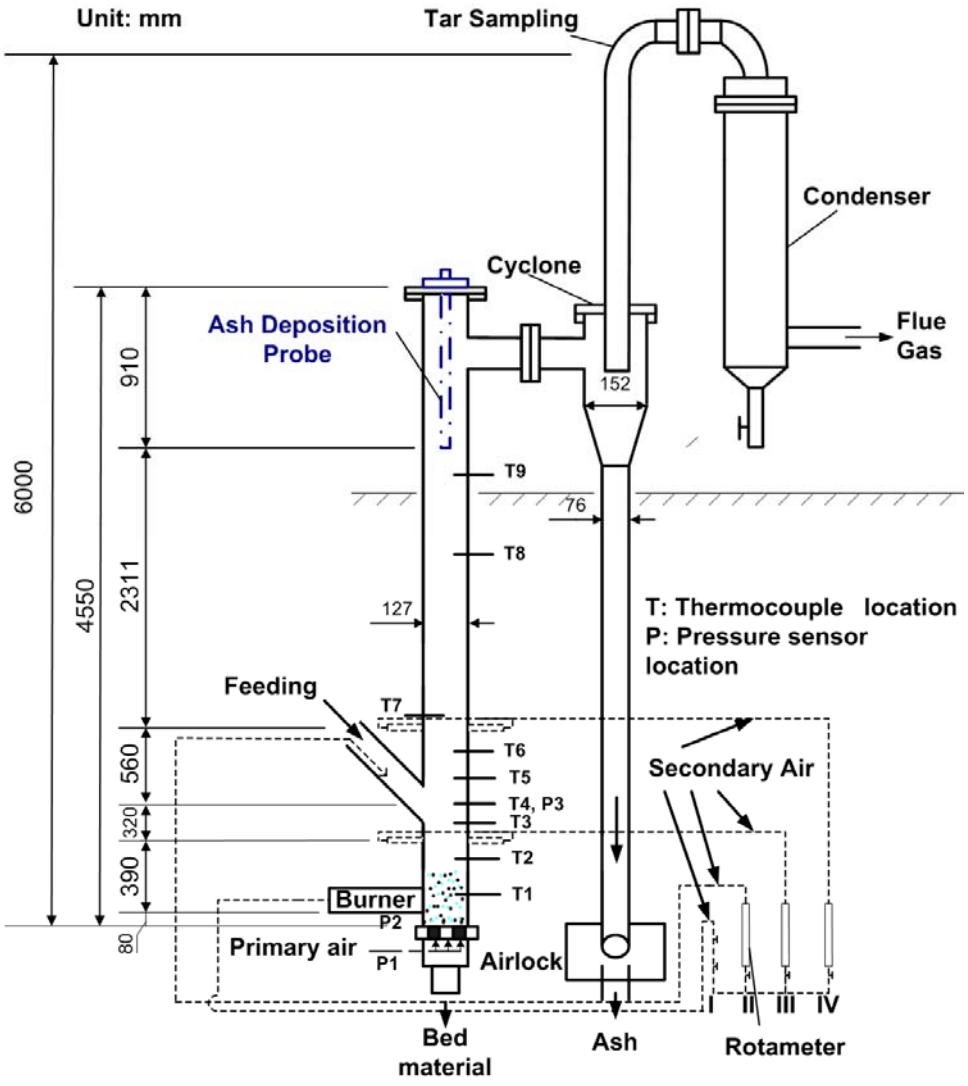

Figure 3-2 Enlarged diagram of the fluidized-bed reactor as a major part of the system at CanmetENERGY, Ottawa

The major parts of the unit were enlarged and shown in Figure 3-2 and were also pictured in Appendix B. The reactor is composed of a SS 316L riser (127-mm inner diameter and 4550 mm total height), and temperature sampling ports (T1-T9) as well as pressure sensors (P1-P3) at different heights on the riser column. Moreover, the unit was coupled with a primary air inlet and four secondary air inlets. The secondary air supplies were introduced through Line IV by two nozzles to the fluidized bed reactor at 560-mm above the center of the fuel feeding port. On-line measurement of the flue gas

compositions (CO, CO_2, O_2, NO_x, and SO_2) and the flue gas temperature were also performed.

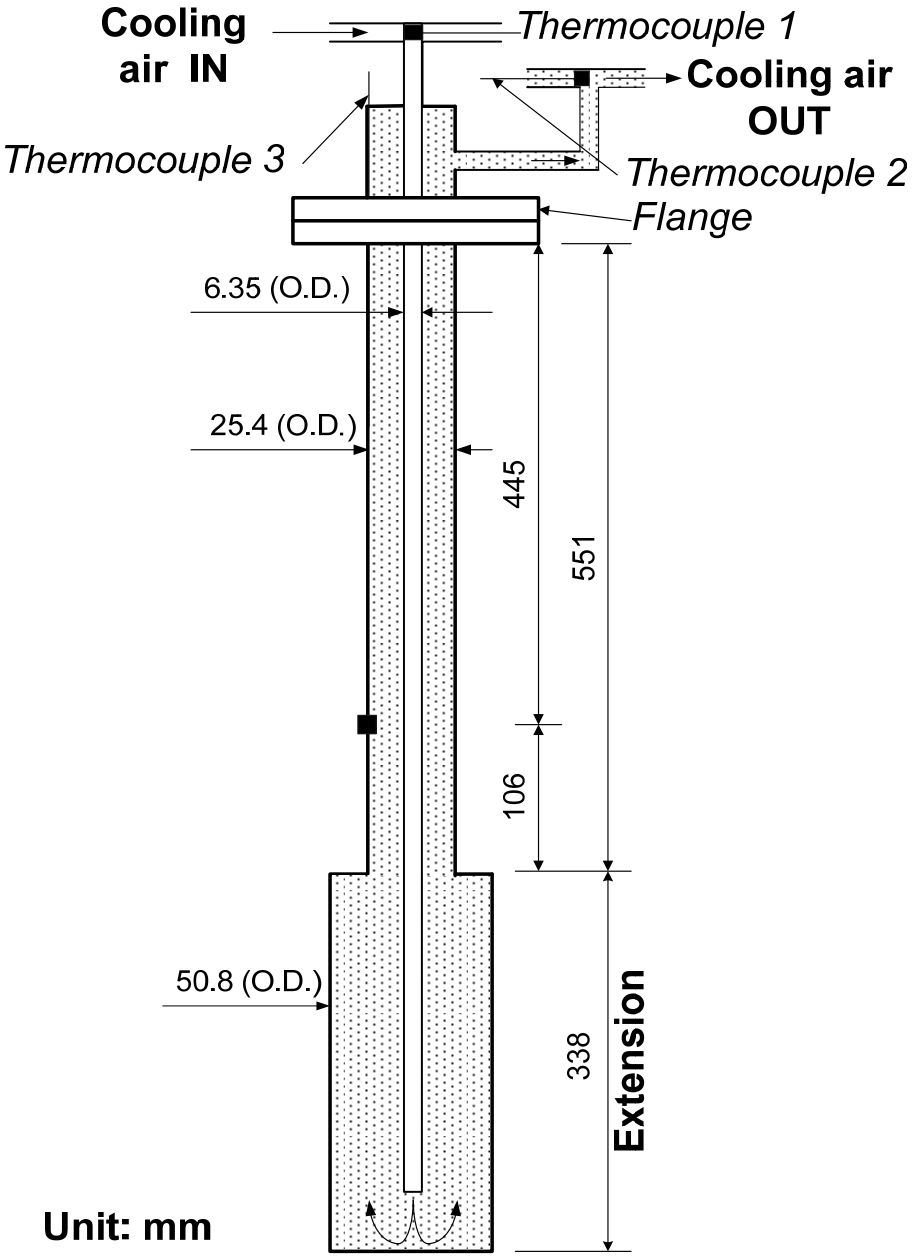

Figure 3-3 Schematic diagram of the ash deposition probe used in combustion tests

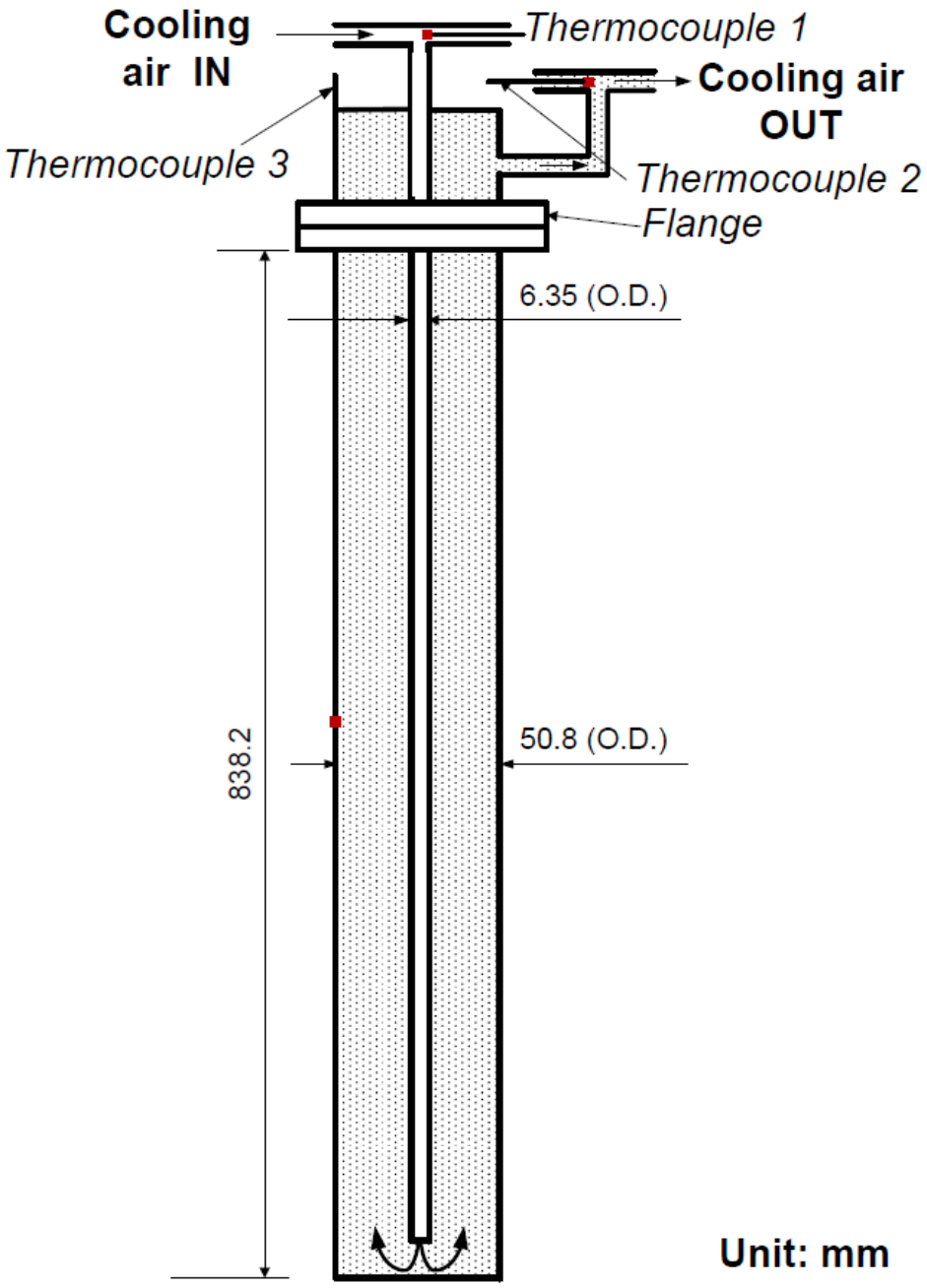

Figure 3-4 Schematic diagram of the ash deposition probe used in gasification tests

A custom-designed, air-cooled, ash-deposition probe was installed vertically in the freeboard region of the fluidized bed reactor using a flange. In the combustion tests, the probe, as depicted in Figure 3-3, was made of SS 316L and has the following dimensions: 610-mm long, 25.4-mm outer diameter with an extension of 338-mm long and 50.8-mm

outer diameter. The total effective length of the probe (for ash deposition inside the freeboard zone) was 889 mm (including 551-mm long 25.4-mm outer diameter pipe + 338-mm long 50.8-mm outer diameter extended pipe), and the total external surface area was calculated at 0.098 m². To obtain steady operation condition for all tests, the surface temperature of the probe was maintained at 430±10 °C by carefully adjusting the cooling-air flow rate.

Different from that was used for the combustion/co-combustion tests, the probe used in the gasification tests, also made of SS 316L, has different dimensions as depicted in Figure 3-4. The total effective length of the probe (for ash deposition inside the freeboard zone) was 838.2 mm, and the total external surface area was calculated to be 0.134 m^2. During the steady operation in all the tests, the surface temperature of the probe was maintained at 450±20 °C by carefully controlling the flow rate of the cooling air.

3.3. Combustion/Co-combustion Test Procedures

The experimental procedures mainly included three stages of operation, warm up, steady state operation and shut down operation, as described step-by-step as follows.

Warm Up:

Step 1: Span and zero analyzers, set up full-hopper fuels and a nice trail of sand on the belt feeder;

Step 2: Ignite using propane (if there was a run before the operating day, emptying cyclone bottom ash from the last run first);

Step 3: Warm up the reactor using a propane burner to a bed temperature of 400°C;

Step 4: Keep warming up of the bed (containing about 12-kg olivine sand) using the

propane burner and a little solid fuel;

Step 5: Once the solid fuel was fed into the reactor at the specified feeding rate, the temperatures of the unit might spike rapidly. Use the primary air, ID fan and feed rate to control temperature in the reactor;

Step 6: Turn of the propane gas fuel once the bed average temperature was consistently above 650 °C;

Steady-State Operation:

Step 7: Use the desired air flow rates when operating conditions attained a steady state (temperature profiles);

Step 8: Install ash deposition probe once the system operation reached a steady state;

Step 9: Connect the probe thermocouples with a computer, and connect the probe's cooling lines with an air supplied controlled with a rotameter;

Step 10: Start the data logging program to record the temperatures on the computer;

Step 11: Carefully adjust the cooling air flow rate to desired probe surface temperature, based on probe surface temperature readings;

Step 12: Take first set of two gas samples for GC-MS analysis right after the steady state was obtained;

Step 13: Particulate sampling, if required;

Step 14: Tar sampling, if required;

Step 15: Take another set of two gas samples for GC-MS analysis right before the system was shut down;

Shut Down Operation:

Step 16: Turn off the belt feeder. Wait one or two minutes to shut off the airlock after the feed was stopped;

Step 17: Decrease the primary air flow rate by 100 L/min and simultaneously increase the Nitrogen flow rate to 100 L/min. This would decrease the unit temperature while keeping the bed fluidized;

Step 18: Empty the sand in the fluidized bed unit to speed up the cooling of the unit, once the analyzer read the carbon dioxide concentrations below 0.5 vol.%;

Step 19: Increase the primary air flow rate up to 300 (L/min) and set the ID fan to a 50% capacity, to speed up the cooling of the unit;

Step 20: When the unit temperature was cooled down to room temperature, carefully remove the probe from the riser;

Step 21: Recover and weigh ash deposits from the probe surface;

Step 22: Collect the weigh the cyclone bottom ash.

3.4. Gasification Test Procedures

The gasification test procedures are similar to the above described combustion/co-combustion procedures, also comprising three stages of operation: warm up, steady state operation and shut down operation. It shall be noted that the system was firstly warmed up at a combustion mode at an air-to-fuel ratio (A/F) of 1.4 with a feed rate of about 8 kg/h of the fuel before the unit was switched to the gasification mode.

Warm-Up:

Step 1 through Step 6: Same as those for the combustion/co-combustion tests;

Step 7: Run the unit with an air/fuel ratio of 1.4 and a feeding rate of about 8kg/h until the average bed temperature was consistently above 750 °C;

Steady State Operation:

Step 8: Immediately change the fuel feeding rate and air flow rate to the desirable values as per the gasification equivalence ratio (ER) of 0.2~0.35;

Step 9: Monitor the gas analyzers for the H_2 and CO concentrations;

Step 10: Install ash deposition probe once the system operation reached a steady state;

Step 11: Connect the probe thermocouples with a computer, and connect the probe's cooling lines with an air supplied controlled with a rotameter;

Step 12: Start the data logging program to record the temperatures on the computer;

Step 13: Carefully adjust the cooling air flow rate to desired probe surface temperature, based on probe surface temperature readings;

Step 14: Take first set of two gas samples for GC-MS analysis right after the steady state was obtained;

Step 15: Particulate sampling, if required;

Step 16: Tar sampling;

Step 17: Take another set of two gas samples for GC-MS analysis right before the system was shut down;

Shut Down Operation:

Same as those for the combustion/co-combustion tests.

CHAPTER 4. ASH DEPOSITION IN CO-FIRING BIOMASS AND COAL

4.1. Introduction

Biomass (a carbon-neutral renewable energy source) from forestry and agriculture supplies about 14% of the world's primary energy (McGowan, 1991; Hall *et al.*, 1992). As estimated by the U.S. Department of Energy (DOE) /United States Department of Agriculture (USDA), biomass fuel could supply 5% for the nation's power by 2030, equivalent to 3% of the current petroleum consumption in the U.S. (Perlack *et al.*, 2008). Moreover, it has been identified that some 55 million acres of land in the continental U.S. would be available for energy crop planting (e.g., switchgrass, polar, eucalyptus, and other species) (Fernholz, 2009). Woody biomass can be a sustainable source of energy and an alternative to the depleted fossil fuels. According to International Energy Agency (IEA), woody crops can be produced for a yield of about 10-15 tons ha^{-1} yr^{-1} in the northern hemisphere. This would enable a medium sized community, approximately 30,000 houses, be supplied with enough electricity via a 30 MWe power station fueled by the biomass production from 11,250 ha of plantations (IEA, 2008). In Canada, bio-energy currently meets about 10% of the country's total energy demands, mainly for the pulp/paper industry. Additionally, IEA believes that biomass resources can potentially meet 50% of the world energy demands in the next century. In comparison to fossil fuels, biomass fuels are inferior with respect to their lower bulky energy densities, higher moisture contents and widely distributed resources. It is thus strategically important to develop cost-effective technologies for conversion of woody biomass to useful energy.

Co-firing (co-combustion) of biomass and coal has proven to be a cost-effective

technology to use bioenergy at a large scale while significantly reducing greenhouse gas, SO_2, and mercury emissions (U.S. EPA, 2008; Turn *et al.*, 2006). Co-firing has been widely demonstrated and implemented in Europe for power generation (in total over 100 units under demonstration or implementation), and this technology has been tested in North America (Baxter, 2005). To date, essentially all major types of biomass, such as forestry or agricultural wastes/residues and municipal solid wastes, in combination with essentially every rank of coal have been used in essentially every major type of coal boiler, such as pulverized-coal boilers, stoker/grate boilers and fluidized bed boilers (Gogebakan *et al.*, 2009; Glazer *et al.*, 2005; Hupa, 2005; Ferrer *et al.*, 2005; Wei *et al.*, 2002).

Although environmentally beneficial, co-firing of biomass and coal comes with several major challenges, specifically the difficulty in fuel handling, the possibly negative impacts on combustion efficiency and air emissions (e.g., particulate matters and NO_x), and the effects of co-firing on boiler operation with respect to slagging, fouling and corrosion because of high concentrations of alkali metals and chloride in some types of biomass fuels. The process of co-firing of biomass and coal for generation of power and heat, although appealing, is still challenging. The co-firing, the behaviors of ash deposition throughout the process are still not completely understood (Pronobis, 2006; Zhen and Koziński, 2000). Biomass-fired boilers usually experience ash-related problems, such as slagging/fouling and high-temperature corrosion on the heat transfer surfaces (Michelsen *et al.*, 1998). In particular, when firing/co-firing herbaceous biomass fuels (e.g. switchgrass and crop residues) that contain high contents of alkali metals and chlorine, the above ash-related problems are severe because the chlorine present in

biomass feedstocks facilitates the mobility of the alkali metals to form vapor-phase chloride ions/compounds at a high temperature (Baxter, 2005; Jenkins *et al.*, 1998; Jensen *et al.*, 1997; Bryers, 1996). The volatile chlorine compounds may deposit and result in corrosion of the heat transfer surfaces inside the boiler at high temperatures (Frandsen, 2005; Robinson *et al.*, 2002). As such, the steam temperature for a biomass unit is normally kept at <450°C to reduce the corrosion damage of the super-heater tubes. The low steam temperature, however, leads to a negative impact on the process economy (Nielsen *et al.*, 2000a; Michelsen *et al.*, 1998).

When silica absorbs alkali/alkaline earth metals in the fuel, silicates are formed and begin to melt or sinter at a temperature of 800-900ºC, which can take place in either the solid phase during the combustion or more commonly the vapor phase via fly ash (Baxter, 1993). The produced alkali silicates and mixed alkali and/or calcium chlorides/sulfates tend to deposit on the reactor wall or the heat-exchanger surface, causing fouling/corrosion with a low fusion temperature (typically < 700ºC). In the case of fluidized bed reactors, these low boiling point species would also cause sintering/de-fluidization of the bed materials (Arvelakis *et al.*, 2005). Additionally, although calcium sulfates ($CaSO_4$) have lower mobility and vapor pressure than those of K_2SO_4, they can still deposit on the reactor walls or on the heat exchange surfaces (Arvelakis *et al.*, 2005; Baxter *et al.*, 1998).

In recently years, there has seen growing interest in ash-related studies for co-firing. Employing various types of air-cooled ash deposition probes, researchers have looked into ash deposition mechanisms (Aho *et al.*, 2008; Kupka *et al.*, 2008; Theis *et al.*, 2006a-c; Andersen *et al.*, 2002), slagging/fouling (Skrifvars *et al.*, 2005) and corrosion

(Nielsen *et al.*, 2000b) of the ash deposits during co-firing of biomass and coal. Technologies to decrease ash deposition were also studied via various approaches, such as addition of combustion additives (e.g., sulphur or SO_2 and SiO_2) (Arvelakis *et al.*, 2005; Overgaard *et al.*, 2005; Aho and Silvennoinen, 2004; Andersson and Vattenfall, 2002), pretreatment of the biomass fuel to reduce alkali metals (Jensen *et al.*, 2001a-b), and modification of the boiler (e.g. modify the re-heater and super-heater to allow for larger spacing) (Overgaad *et al.*, 2005). However, there was not much research work reported on ash deposition tendencies of biomass fuels and the biomass-coal blended fuels against the base fuel (coal) during co-firing and how the operating parameters, such as blending ratio, moisture content, excess air percentage, etc., influence the ash deposition tendencies.

In comparison to other types of combustors (pulverized fuel or stoker boilers), fluidized bed combustion is an advantageous technology for combustion or co-combustion of a wide variety of fuels. It can achieve more uniform bed temperatures, a longer residence time of particles and a better quality of bed material mixing, and hence, a higher combustion efficiency. The main objective of this work was to investigate the ash deposition behaviors and tendencies of wood pellets and a Canadian lignite coal during co-firing on a pilot-scale bubbling fluidized-bed combustor and how the operating parameters affected the ash deposition tendencies. Employing a custom-designed, air-cooled probe installed on the freeboard zone of the fluidized bed combustor, effects of fuel type, fuel blending ratio (above 20% and up to 80% on a thermal basis), moisture content of the fuel and A/F, were studied on the ash deposition rate and compositions of the deposited ash.

4.2. Experimental

4.2.1. Material and Preparation

The lignite coal used in this study was supplied from Ontario Power Generation (OPG), and the white pine pellets (5 mm OD and 40 mm length) were supplied from a local company in Southern Ontario. The pellets, designated as "white pine pellets" (WPP) for short in this study, were prepared from white pine sawdust using approximately 1 wt% of the binding agent Ameribond 2x (Ammonium Lignosulfonate). Detailed proximate and ultimate analyses of these fuels and their ash compositions are given in Table 4-1. The lignite has an ash content of 22 wt% db and is characterized by its low ratio of VM/FC ≈ 2.3. The wood pellets contain a much lower amount ash (3.1 wt% db) and are characterized by a high VM/FC (≈ 5.0). With regard to ash composition, the lignite ash is mainly composed of acidic oxides (SiO_2, Al_2O_3 and TiO_2), whereas the ash from the wood pellets is enriched with basic oxides (CaO, MgO, K_2O, Na_2O and Fe_2O_3) and P_2O_5. As displayed in Table 3-1., the WPP fuel consists of a higher content of chlorine + bromine (515 μg/g) in the fuel and higher concentrations of P_2O_5 (23 wt% db) and SO_3 (18 wt% db) in the fuel ash, as compared to the lignite (<46 μg/g chlorine + bromine, 0.3 wt% db P_2O_5, and 6.1 wt% db SO_3).

To prepare coal feedstock for the combustion tests, the received lignite was crushed and screened into particles (<4 mm) and was designed as "crushed lignite" (CL) in this study. In most tests, both fuels (CL and WPP) were used either as received or after air-drying. To investigate the effects of moisture content on the ash deposition behaviours in the combustion or co-combustion process, oven-dried fuels (to a moisture content of <5 wt%) were prepared by drying in air at 105°C for over 12 h. The actual moisture contents

of each fuel was measured prior to each test, to determine the required fuel feeding rate (to maintain the same thermal input of 58.3 MJ/h in each combustion test).

Table 4-1 Proximate and ultimate analyses of the fuels and their ash compositions

	Lignite	White Pine Pellets
Moisture, wt% as received	30.0	5.3
HHV (MJ/ kg dry)	21.8	20.6
Proximate analysis, wt% db		
Ash[1]	22.0	3.1
Volatile matters (VM)	54.0	80.8
Fixed carbon (FC)	24.0	16.1
Ultimate analysis, wt% db		
Carbon	58.8	48.0
Hydrogen	4.2	6.3
Nitrogen	0.9	1.3
Sulphur	0.5	0.6
Oxygen[2]	13.6	40.7
Chlorine[3], μg/g.	25	312
Bromine[3], μg/g.	< 21	203
Fluorine[3], μg/g	100	<18
Dry ash analysis[4], wt% db		
SiO_2	49.8	3.8
Al_2O_3	19.7	0.5
Fe_2O_3	3.8	0.6
TiO_2	0.9	<0.1
P_2O_5	0.3	23.1
CaO	9.9	23.4
MgO	2.1	6.9
SO_3	6.1	18.0
Na_2O	4.2	1.3
K_2O	1.0	16.5

[1] The ashing temperature was 750ºC for lignite and 500ºC for white pine pellets;
[2] By difference; [3]By Pyrohydrolysis and IC; [4]By XRF of the fuel ashes.

4.2.2. Combustion Facility

The co-firing tests were conducted on a pilot-scale, fluidized bed combustor. The facility was operated in a bubbling fluidization mode, with a SS 316L column (127-mm inner diameter and 4550 mm total height), as illustrated in Figure 4-1.

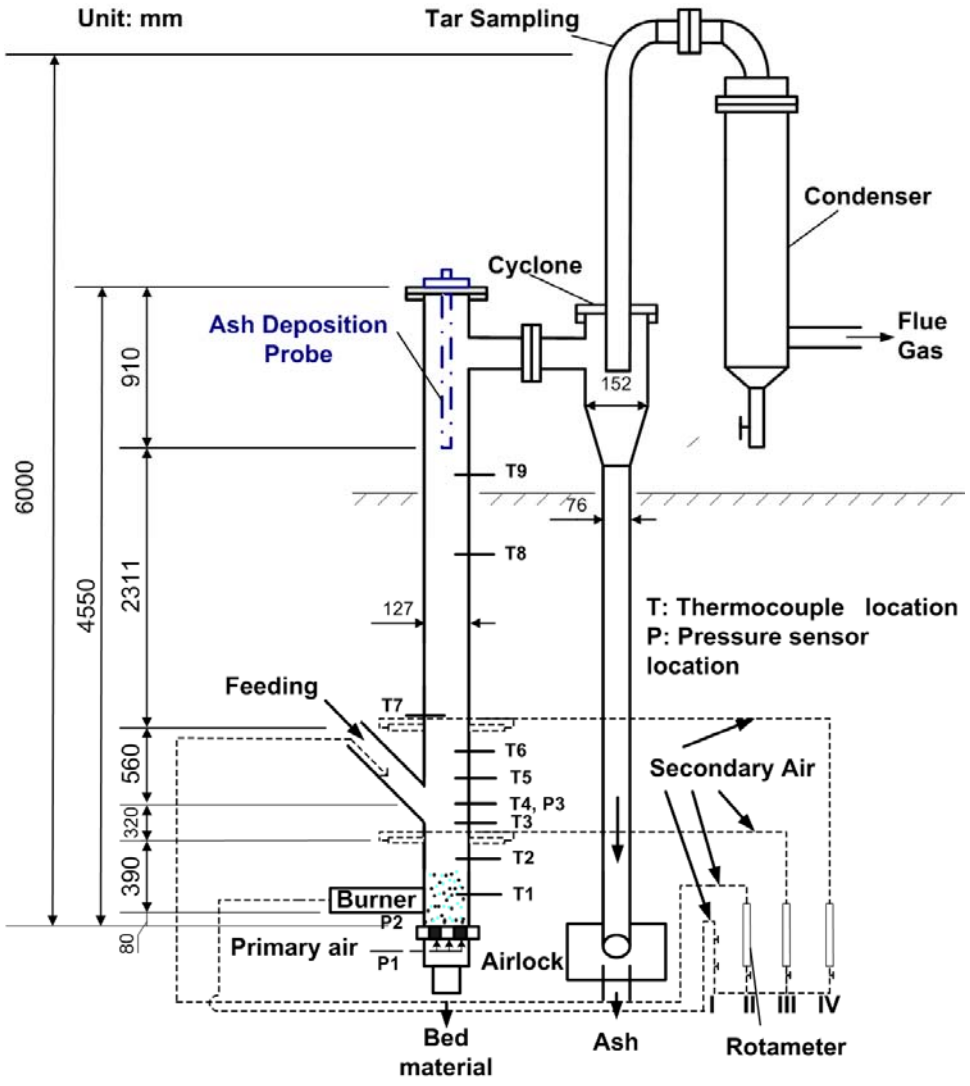

Figure 4-1 Schematic diagram of the fluidized-bed facility

The facility had a feeding capacity of up to 25 kg/h. It was equipped with a belt feeder for stable fuel feeding, a cyclone for fly ash collection, and a water-cooled condenser for tar

removal, as well as temperature sampling ports (T1-T9) at different heights on the riser column and the a flue gas sampling port. As shown in Figure 4-1, the unit was coupled with a primary air inlet and four secondary air inlets. The secondary air supplies were introduced through Line IV to the fluidized bed reactor at 560-mm above the center of the fuel feeding port. On-line measurement of the flue gas compositions (CO, CO_2, O_2, NO_x, and SO_2) and the flue gas temperature were performed.

A custom-designed, air-cooled, ash-deposition probe, as depicted in Figure 4-2. , was installed vertically in the freeboard region of the fluidized bed combustor using a flange. The probe was made of SS 316L and has the following dimensions: 610-mm long, 25.4-mm outer diameter with an extension of 338-mm long and 50.8-mm outer diameter. The total effective length of the probe (for ash deposition inside the freeboard zone) was 889 mm (including 551-mm long 25.4-mm outer diameter pipe + 338-mm long 50.8-mm outer diameter extended pipe), and the total external surface area was calculated at 0.098m². To obtain steady operation condition for all tests, the surface temperature of the probe was maintained at 430±10 ºC by carefully adjusting the cooling-air flow rate.

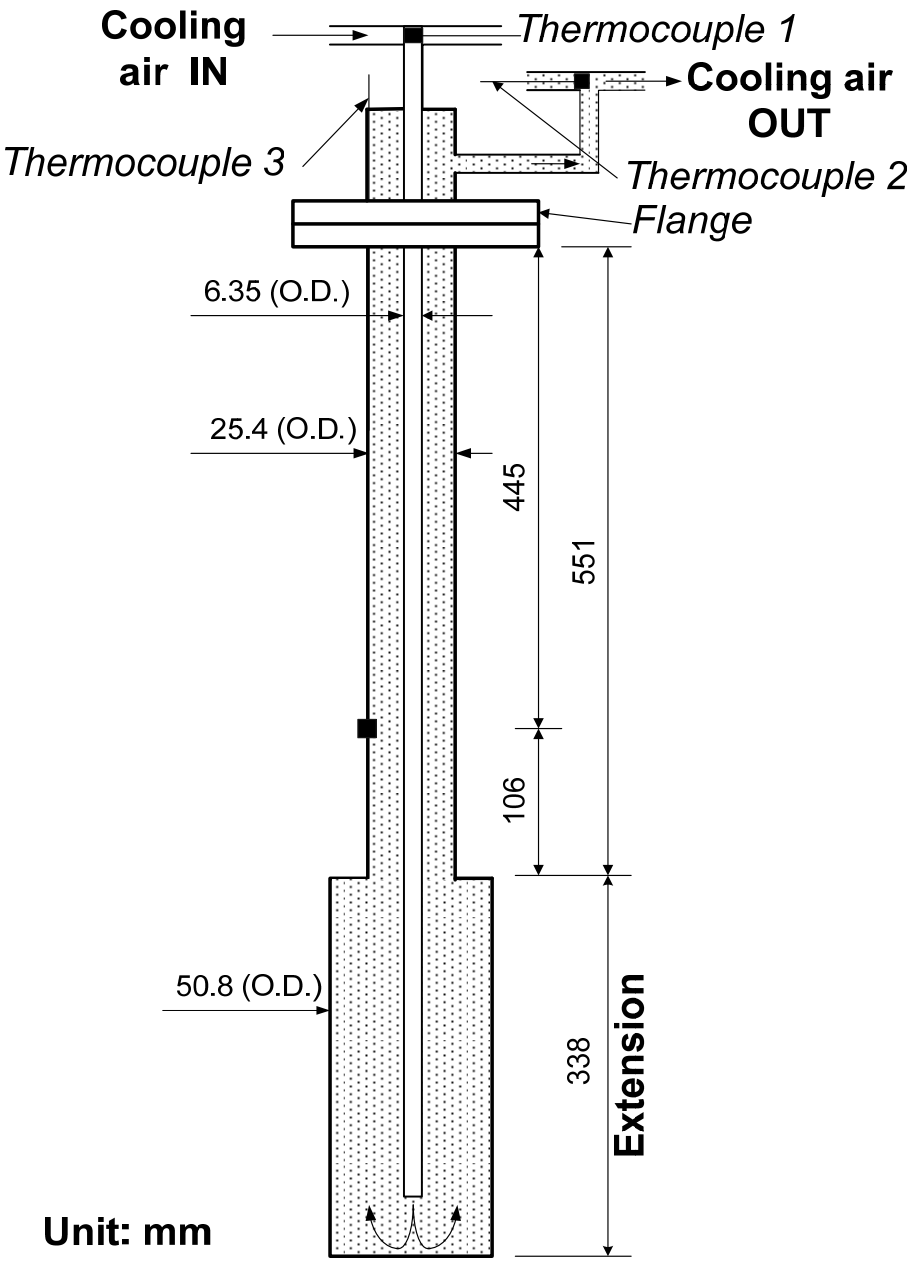

Figure 4-2 Schematic diagram of the ash deposition probe

4.2.3. Testing Methodologies and Parameters

A cleaned probe was installed vertically in the freeboard zone of the reactor as illustrated in Figure 4-1., right before the whole unit attained a steady state of operation. It shall however be noted that, in this study, because of the limited working space in the

freeboard and the difficulty associated with installing and removing the probe, it was installed vertically, instead of horizontally (cross to the flue gas flow), as was conventionally performed in many literature studies or in the real boiler operations. The reactor was loaded with 13 kg of olivine sand as the bed material and was heated up to above 600ºC via propane gas burners before introducing the solid fuels. For all the tests reported in this work, a constant heat input of 58.3 MJ/h was maintained and the excess air percentage was fixed at 40 or 60% (or an A/F of 1.4 or 1.6). Dependent upon the gross calorific value of the fuel used, the feed rate ranged from 3.1-3.8 kg/h on a dry basis, and the total air flow rate ranged between 360 and 400 L/min and between 420 and 460 L/min at an excess air percentage of 40 and 60%, respectively. At a steady state, the combustion temperatures (in the dense-phase zone of the fluidized bed) were typically in the range of 800-900°C, and the average flue gas temperatures in the freeboard and in the vicinity of the ash deposition probe were in the range of 650-700ºC. For each test, a relatively stable temperature profile along the bed height was obtained through adjusting the ratio of the secondary air to the primary air flow rate (while maintaining a total air flow rate at the value determined by the target excess air percentage). In a typical run, at least 3-4 h of steady-state operation was performed before cooling the reactor down to room temperature using nitrogen. For the combustion of 100% WPP (containing a low ash content), a longer steady-state operation for up to 7-8 hours was conducted in order to obtain enough fly-ash deposits (>1.0 g) to meet the requirement of the XRF analysis. Upon cooling the whole unit down to room temperature, the ash deposition probe was carefully removed from the freeboard and the deposited ash was completely collected for weighing to calculate the absolute ash deposition rate (D_A, g m^{-2} h^{-1}) and the relative ash

deposition rate (RD_A, g m^{-2} h^{-1}), respectively, as defined below:

$$D_A = \frac{\text{Mass of collected ash deposit (g)}}{\text{Surface area of the probe } (m^2) \times \text{Duration (h)}} \quad (4\text{-}1)$$

$$RD_A = D_A \times \frac{\text{Ash feeding rate of crushed lignite (g/h)}}{\text{Ash feeding rate of the fuel (g/h)}} \quad (4\text{-}2)$$

Here, the relative deposition rate (RD_A) was proposed as a new parameter to bring into account the fact that a biomass fuel has a much lower ash content (normally < 1-5 wt%) than coals (22 wt% for the lignite coal in this study). RD_A will thus be a more effective parameter to evaluate the deposition tendencies of different fuels in relation to the coal used for co-firing. The collected deposited ashes were submitted for various characterizations using SEM for morphology, IC for the chlorine contents, XRF for the chemical compositions in accordance to the American Society for Testing and Materials (ASTM) D4326 standard.

Reproducibility of the ash deposition rates in the combustion tests and reproducibility of the chemical compositions of the deposited ash were examined for some tests in this study. Because of the relatively large operating scale and the complexity of the fluidized-bed facilities used, it normally took 2-3 days to complete a successful combustion/co-combustion test (including fuel/facility preparation, operation, and after-run cleaning/maintenance). It is thus difficult to repeat all of the tests. In this work, repeated combustion tests were performed on the CL at A/F of 1.4 for 3 times. The relative standard deviation of the ash deposition rates for the three runs was within ±8.0%, and the maximum errors in the concentrations of major ash species were within ±7.0%.

4.3. Results and Discussion

A variety of combustion parameters were investigated in this work. These include types of fuel (CL and WPP), fuel blending ratios (0-100% on a thermal or heat-input basis), moisture contents (using fuels as received or after air-drying, and after oven drying), and A/Fs(1.4 and 1.6).

4.3.1. Compositions of Deposited Ash versus Flue Ash

Figure 4-3 displays a comparison of chemical compositions of the ash deposit on the probe and those of the fuel ash for the combustion tests of individual fuels of CL and WPP and a typical fuel blend of 50%CL-50%WPP. It should be noted that, in all ash deposits there was consistently an enrichment of Fe, which was likely due to the Fe-rich contaminants from the steel ash deposition probe (Theis *et al.*, 2006b).

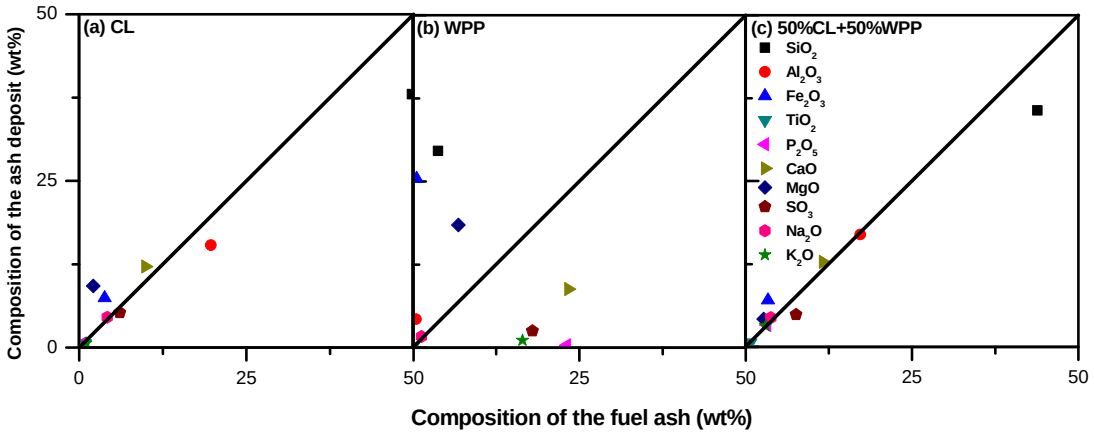

Figure 4-3 Chemical compositions of the fuel ash vs. chemical compositions of the ash deposits obtained in combustion of (a) CL, (b) WPP, and (c) the 50%CL-50%WPP fuel blend

As clearly displayed in panels a and c of Figures 4-3, for the combustion of 100% CL and the 50%CL-50%WPP fuel blend, the compositions of the deposited ash were very similar to those of the fuel ash. This result might be expected because, in a steady-state,

fluidized-bed operation at a high A/F (>1.4 in this study), the fluidizing gas could eventually entrain all the ash species to the freeboard zone, where the ash deposition occurred.

On the contrary, from the combustion of 100% WPP, the composition of the deposited ash significantly differed in some species from those of the fuel ash, as displayed in Figure 4-3b. The deposited ash was enriched with SiO_2 and MgO. The enrichment of magnesium silicate in the ash deposition was also confirmed by XRD)measurement and is in agreement with many literature research results, which demonstrated that Al, Si, and S were able to trap alkalis/alkalines (K, Ca, Mg etc.) to limit the formation of corrosive alkalichlorides (Overgaard *et al.*, 2005; Aho and Silvennoinen, 2004; Andersson and Vattenfall, 2002). Nevertheless, the deposited ash contained lower contents of Ca, S, K, and P elements, when compared to those in the fuel ash, differing from what was observed in some literature studies on co-firing (Aho *et al.*, 2008; Arvelakis *et al.*, 2005; Baxter *et al.*, 1998). The lower contents of Ca, S, K, and P elements in the deposited ash, as compared to those in the fuel ash, might be a result of the combination of the following factors: high contents of volatile matters (80 wt%) and chlorine (312 μg/g) of the wood pellets fuel, a high excess air percentage used in the fluidized bed reactor (40 % excess air), and the high bed temperatures during combustion (800-900°C) compared to 500ºC as the ashing temperature for the WPP fuel ash analysis. Upon rapidly heating the WPP fuel (containing 80 wt% volatile matters and 312 μg/g chlorine) to 800-900°C, the fuel would rapidly release VM and volatile vapors of Ca/K chloride, SO_3/SO_2 and P_2O_5. The rapidly released Ca, S, K, and P elements might not

have enough time to be deposited on the ash deposition probe but end up in the cyclone bottom fly ashes or in the flue gas because of the large air flow rate in the reactor system.

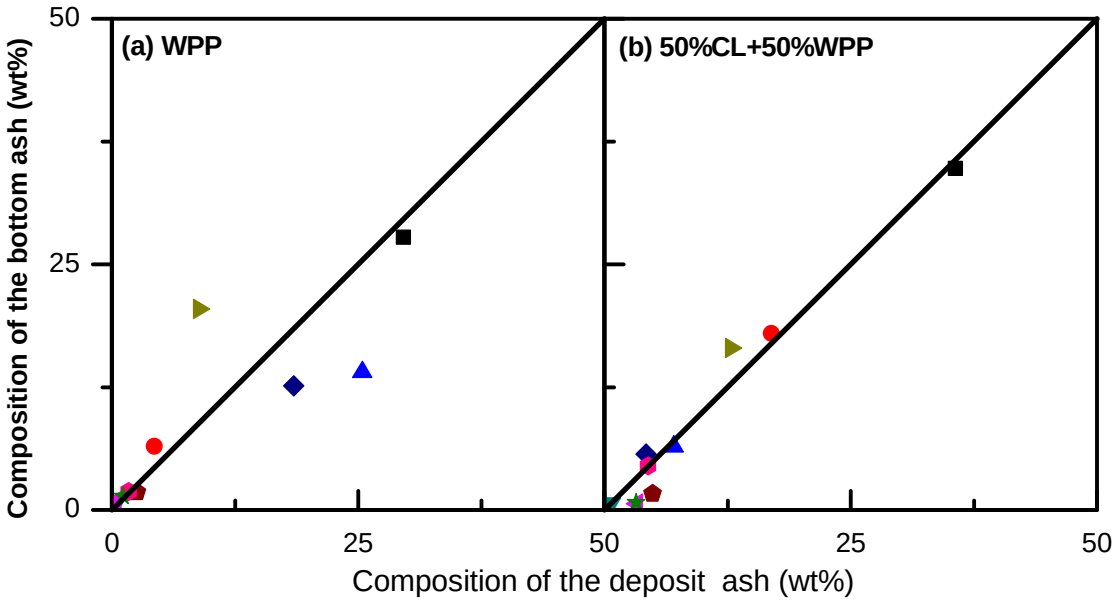

Figure 4-4 Chemical compositions of the ash deposits versus chemical compositions of the cyclone bottom fly ashes in combustion of (a) WPP, and (b) the 50%CL-50%WPP fuel blend

Figure 4-4 displays the compositions of the ash deposits against the compositions of the fly-ashes collected from the cyclone-bottom in the combustion of 100% WPP and the 50%CL-50%WPP fuel blend. The Ca content in the cyclone bottom fly ash is approximately twice that in the deposited ash on the probe, which can be evidence for the above explanation on the behavior of Ca deposition. In some previous studies reported by Molcan *et al.* (2009) and Baxter *et al.* (1996) for co-firing biomass and coal, the reduced content of SO_3 and the depletion of alkali species (i.e., K_2O) in the ash deposits were also observed, because of the loss of the highly mobile SO_3 and alkali chlorides in the gas phase.

The mechanisms of ash deposition on heat transfer surface are very complex, involving inertial impaction, condensation of vaporized inorganic compounds, thermodiffusion, and chemical reactions, etc. (Aho *et al.*, 2008; Kupka *et al.*, 2008; Baxter, 1993). The results in panels a and c of Figures 4.3 (for the combustion of 100% CL and co-firing of the 50% CL-50% WPP fuel blend) might suggest that the deposition of lignite ash was likely via the inertial impaction, leading to no significant difference between the compositions of the ash deposits and those of the fuel ash. The observation as shown in Figure 4-3b for the 100% WPP combustion, revealing the enrichment of Mg and Si in the deposited fly ash, might suggest condensation of vaporized inorganic compounds occurring along with chemical reactions (e.g., between the alkali/alkaline metals and silicate species) (Baxter *et al.*, 2009; Molcan *et al.*, 2009; Baxter, 1993).

4.3.2. Effects of Fuel Blending Ratio

Effects of fuel blending ratios (0 -100% WPP on a thermal or heat input basis) on ash deposition behaviors for co-firing WPP and CL were investigated at a constant excess air rate (i.e., 40%). The chemical compositions of the ash deposit samples are displayed in Figure 4-5. The obvious variation observed in the compositions of some major metal elements in the deposited ashes from the co-firing of WPP-CL blends implied the interactions between these fuel ashes during the co-combustion process. For instance, it was found that the contents of alkali/alkaline metals (K, Na, Ca) as well as Al_2O_3 and P_2O_5, were apparently enriched in the deposited ash under the co-combustion conditions. The similar phenomena of the interaction of the biomass and coal ashes during co-firing

were observed by many other researchers (Molcan *et al.*, 2009; Kupka *et al.*, 2008; Hansen *et al.*, 1999; Baxter *et al.*, 1998).

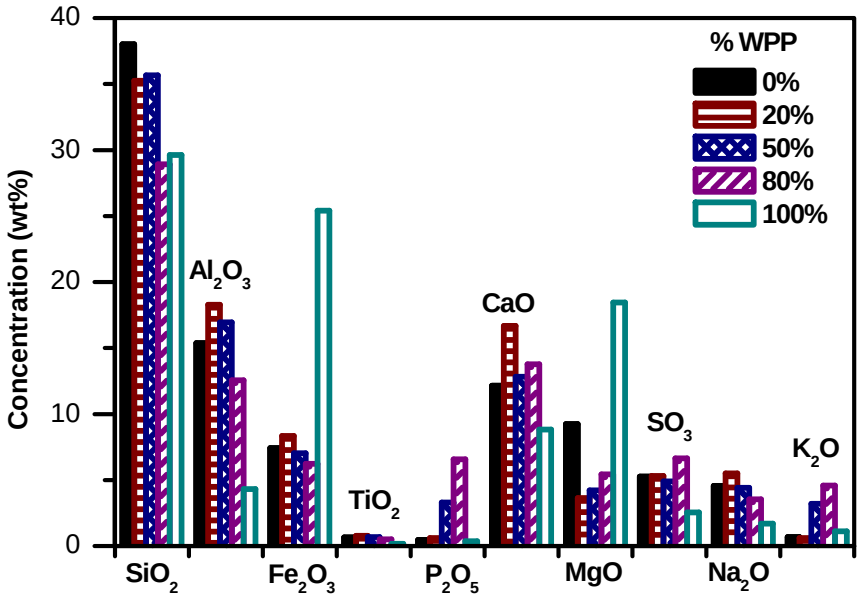

Figure 4-5 Chemical compositions of the deposited ashes from co-firing of the CL and WPP at various blending ratios

Figure 4-6 displays the absolute and relative ash deposition rates, D_A and RD_A, obtained during the co-combustion of WPP and CL at various blending ratios ranging from 0% WPP (or 100% CL) to 100% WPP. From the results of D_A, increasing the ratio of WPP in the WPP-CL blend fuel resulted in a decrease of the absolute ash deposition rates. However, this result is not a surprise because of the fact that wood pellets have a remarkably lower ash content (3.1 wt%) compared to 22 wt% ash for the lignite. Woody biomass as a fuel when co-fired with coal commonly produces relatively low rates of ash deposition on the heat transfer surface of the boiler because of its much lower ash content (Skrifvars, 1999). In co-firing of biomass and coal, a decrease in the absolute ash deposition rate can, however, be a result of different causes: (1) the significantly lower ash content in biomass than in the coal and (2) some interactions between the ash

elements from the component fuels in the fuel blends that suppresses the ash deposition. To distinguish between these two possible causes and to better evaluate the deposition tendency of mixture fuels in relation to that of the base fuel (i.e., 100% coal), it is more advantageous to compare the results of relative deposition rate (RD_A), as is also displayed in Figure 4-6.

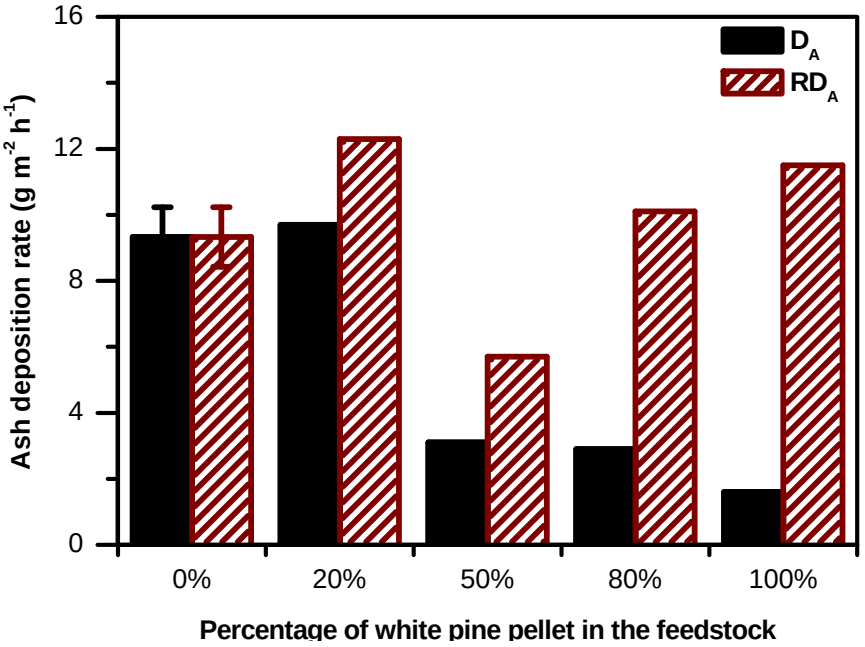

Figure 4-6 Ash deposition rates during co-firing of the CL and WPP at various blending ratios

From the Figure, combustion of 100% WPP had a slightly greater tendency of ash deposition (with a RD_A of 11 g m^{-2} h^{-1}) than that of 100% CL (with a RD_A of 9.4 g m^{-2} h^{-1}). This can be explained by the much higher contents of alkali and alkaline earth metals and halogens elements (Cl and Br) in the WPP, as shown previously in Table 4-1. Interestingly, co-firing of WPP and CL did not significantly increase the ash deposition tendency in terms of the values of RD_A, considering the unavoidable experimental error in the tests. Furthermore, co-firing of the 50%CL-50%WPP fuel blend produced a lower

RD_A, although the mechanism to account for this result is unclear thus far and more future studies will be needed.

4.3.3. Effects of Moisture

Pretreatment of feedstock using water washing proved to be an effective measure to reduce the amount of alkali metals and chlorine in the fuel and alleviate the fouling/slagging and corrosion problems in biomass co-firing boilers (Vamvuka *et al.*, 2008; Davidsson *et al.*, 2002; Arvelakis *et al.*, 2001; Jensen *et al.*, 2001a-b; Jenkins *et al.*, 1998; Knudsen *et al.*, 1998; Jenkins *et al.*, 1997). As a common practice, the washed fuels will undergo a dewatering and drying process, which is energy-intensive and costly. From an economical standpoint, the drying process shall be avoided if a fuel with relatively high moisture content could be used directly in the subsequent combustion/co-combustion processes. Moreover, many kinds of waste biomass feedstock, such as sawmill residues, crop residues, pulp/paper mill sludge, and municipal sewage sludge, contain a high content of moisture. From the available literature, there is thus far no research to elucidate the effects of fuel moisture content on the ash deposition behaviors in co-firing of biomass and coal on a fluidized-bed combustor. In this study, we performed the comparative tests with fuels as received (or after air drying) and after oven drying, to examine the influence of moisture content in the fuel or fuel blends. The ground lignite fuel as received contained a high moisture (30 wt%), while the wood pellets received had a relatively low moisture content (5.3 wt%), as shown in Table 4-1. After oven drying of the fuels at 105ºC for 12 hours, the moisture content of both fuels was ensured to be < 5 wt% for CL and < 2 wt% for WPP.

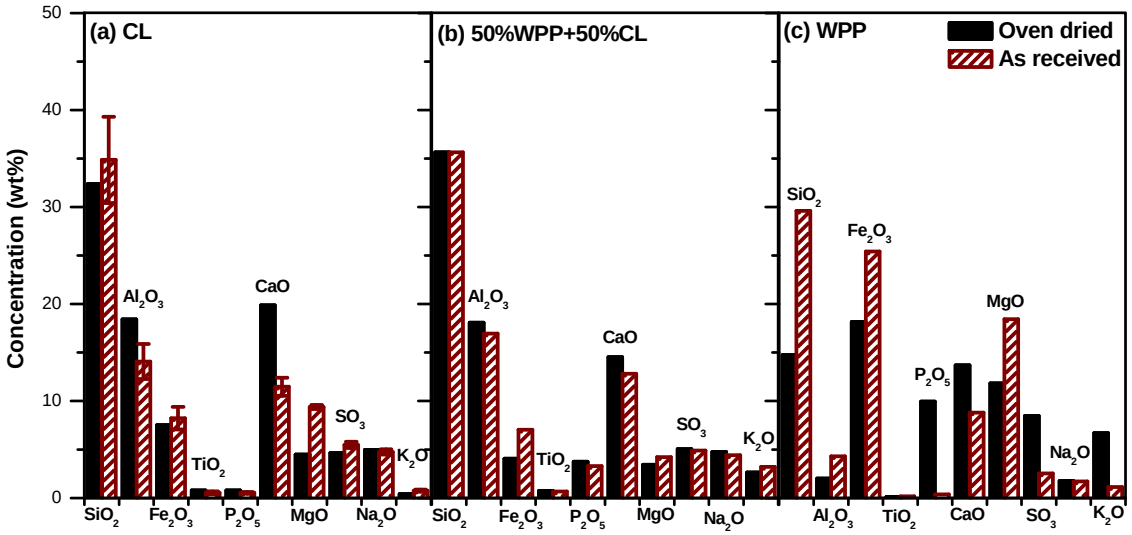

Figure 4-7 Effects of moisture contents on chemical compositions of the ash deposits during combustion of (a) 100% CL, (b) 50% WPP-50%CL, and (c) 100% WPP

The compositions of the ash deposits from the combustion runs with 100% CL, the 50% WPP-50% CL blend, and 100% WPP are presented in panels a, b, and c of Figure 4-7, respectively. For the combustion tests using 50% WPP-50% CL blend, the difference in moisture contents of the feed did not result in noticeable differences between the compositions of the ash deposits (Figure 4-7b). Combustion of the as-received CL or WPP led to enrichment of the SiO_2 and MgO but reduction of CaO and P_2O_5 in the ash deposits, as compared to that of the oven-dried feeds (panels a and c of Figures 4-7).

Figure 4-8 shows the effects of moisture contents on ash deposition rates for combustion of 100% CL, the 50% WPP-50% CL fuel blend, and 100% WPP. Another interesting finding of this study is that the absolute or the relative ash deposition rates with all fuels as received (of a higher moisture content) were consistently lower than those of the oven-dried fuels.

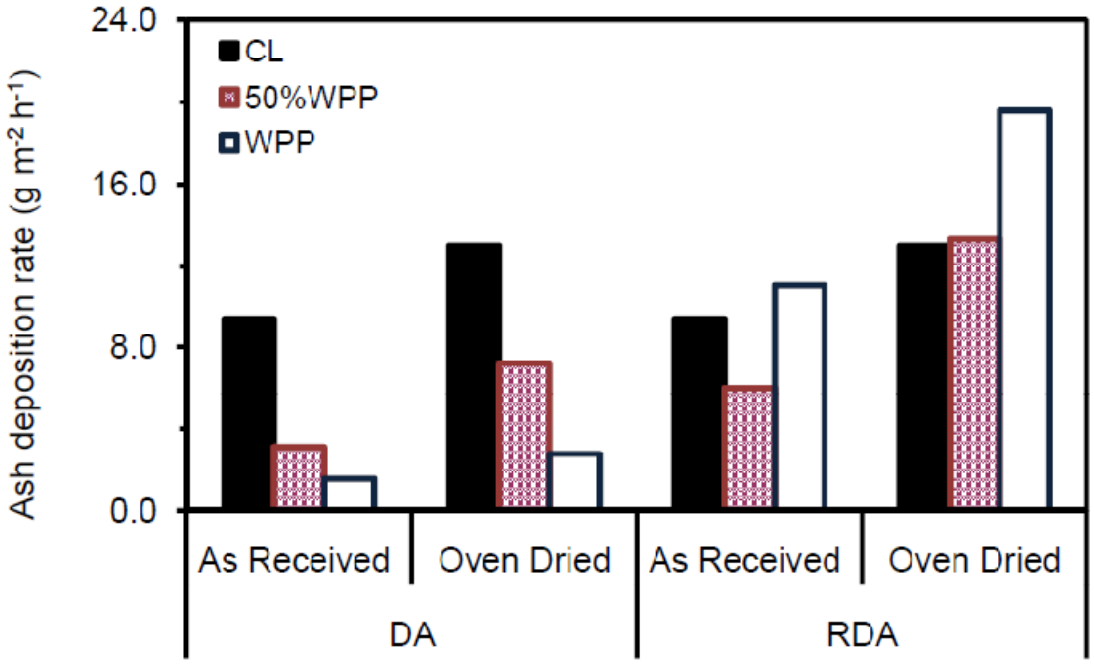

Figure 4-8 Effects of moisture contents on ash deposition rates for combustion of 100% CL, the 50% WPP-50% CL fuel blend, and 100% WPP

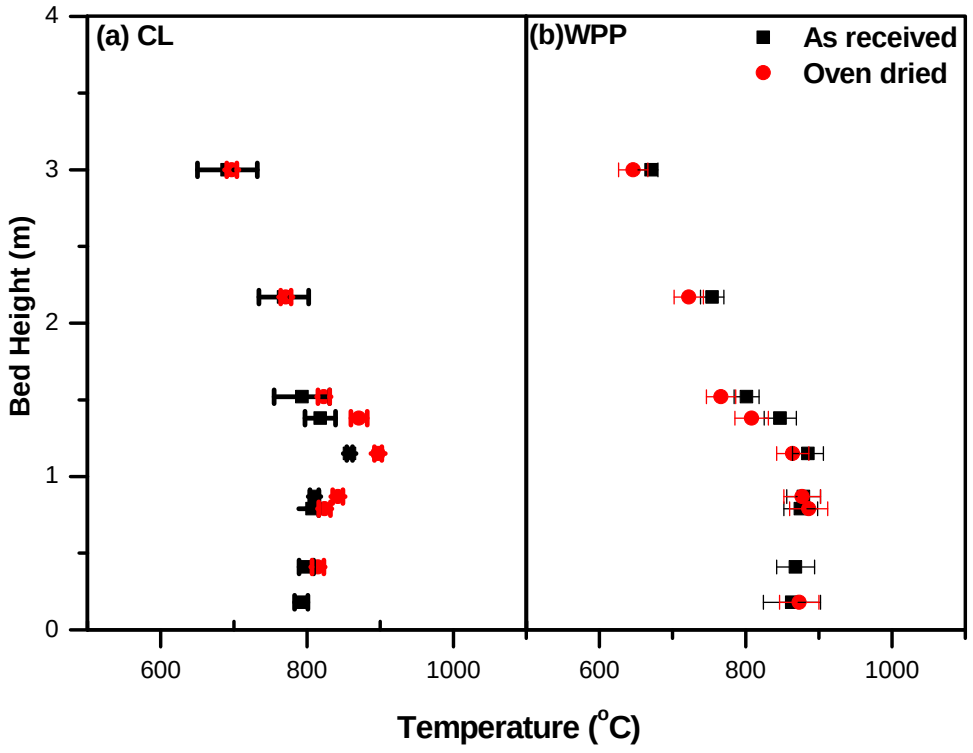

Figure 4-9 Temperature profiles of combustion or co-combustion of (a) 100% CL and (b) 100% WPP with different moisture contents

This suggests that the moisture content in the feed played positive roles in retarding the ash deposition during the combustion. The reduction in the ash deposition rates might be related to the presence of water. It shall be first noted that the presence of water did not lead to lower fluidized-bed combustion temperatures because all tests were carried out under a constant heat input. In fact, combustion of all as-received fuels consistently produced higher and more uniformly-distributed temperatures in the fluidized-bed combustor, as evidenced in Figure 4-9 for the temperature profiles from the combustion of 100% CL and 100% WPP fuels (both as received and oven-dried). The higher bed temperatures and more uniform temperature profiles may be attributed to the greater densities of the wet fuels compared to the oven-dried fuels, which increased the solid holdup in dense-phase zone of the fluidized bed reactor and, hence, improved the combustion efficiencies and the bed temperatures as well as the temperature distribution. The higher bed temperatures and more uniform temperature profiles could then increase the flue gas flow rate and, hence, reduce the contact time of the volatile vapor of Ca, K S, and P elements in the vicinity of the ash deposition probe, which would in turn reduce the ash deposition rates, as displayed in Figure 4-8. Alternately, the water vapor in the as-received fuels would be suddenly released along with the fuel volatile matter upon feeding the fuel to a hot bed at 800-900°C. This would greatly increase the flue gas flow rate, reduce the contact time of the volatile vapor of Ca, K, S, and P elements over the ash deposition probe, and hence, retard the ash deposition on the probe as well.

4.3.4. Effects of A/F

It has been demonstrated that A/F (or excess air percentage) has significant effects on

the co-combustion performance of fuels in fluidized beds (Atimtay and Kaynak, 2008; Gungor, 2008). The excess air percentage is this study was controlled by varying the flow rate of the secondary air while keeping the primary air flow rate as constant as possible.

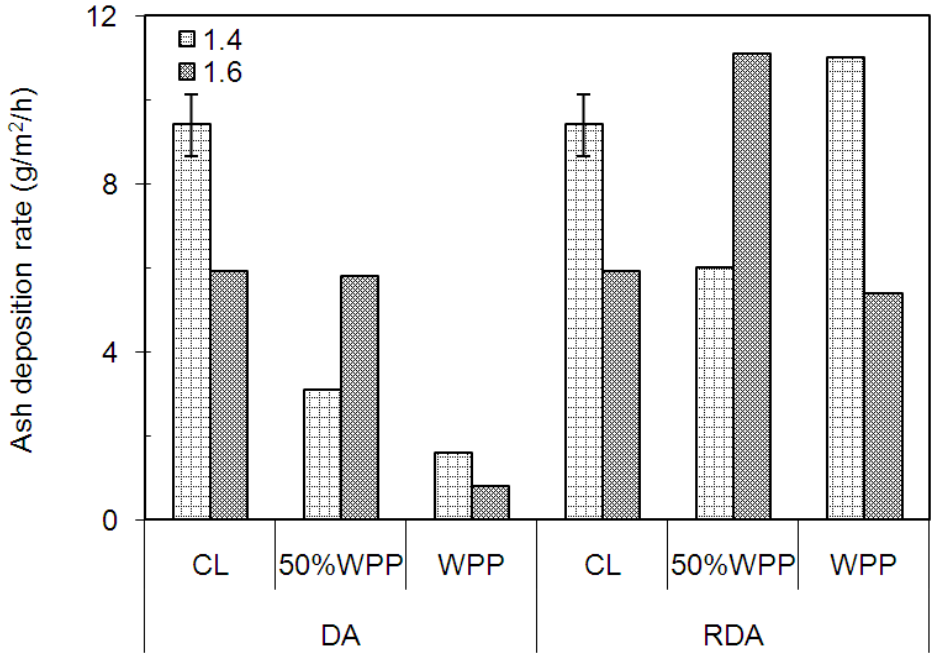

Figure 4-10 Effects of air-to-fuel ratio on ash deposition rates for combustion of 100% CL, 50% WPP-50% CL and 100% WPP

Figure 4-10 shows a comparison of D_A and RD_A for three typical fuels or fuel blends during the combustion at different A/Fs. Notably, except for the 50% WPP-50% CL blend, both D_A and RD_A values in the combustion of either 100% CL or 100% WPP decreased as A/F increased from 1.4 to 1.6, which may be explained by the decreased residence time of fly ash in the freeboard zone because of the increased gas velocity at a higher excess air percentage. However, for a fluidized-bed combustor, variation of excess air percentage would bring complicated influences to the combustion system, e.g., combustion efficiency, temperatures, temperature distribution profile (as will be discussed below), entrainment of particles of bed materials, fly ash, etc., all of which

could affect the ash deposition in the freeboard zone. It was observed that a variation of A/F had minimal effects on the chemical compositions of the ash deposits. For all tests with different fuels, the upper column temperatures were consistently lower at a higher excess air percentage, which is actually expected because of the increased flow rate of the secondary air. It was observed that, with 100% CL or 100% WPP fuel, a variation in A/F did not significantly affect the temperatures, as displayed in Figure 4-11.

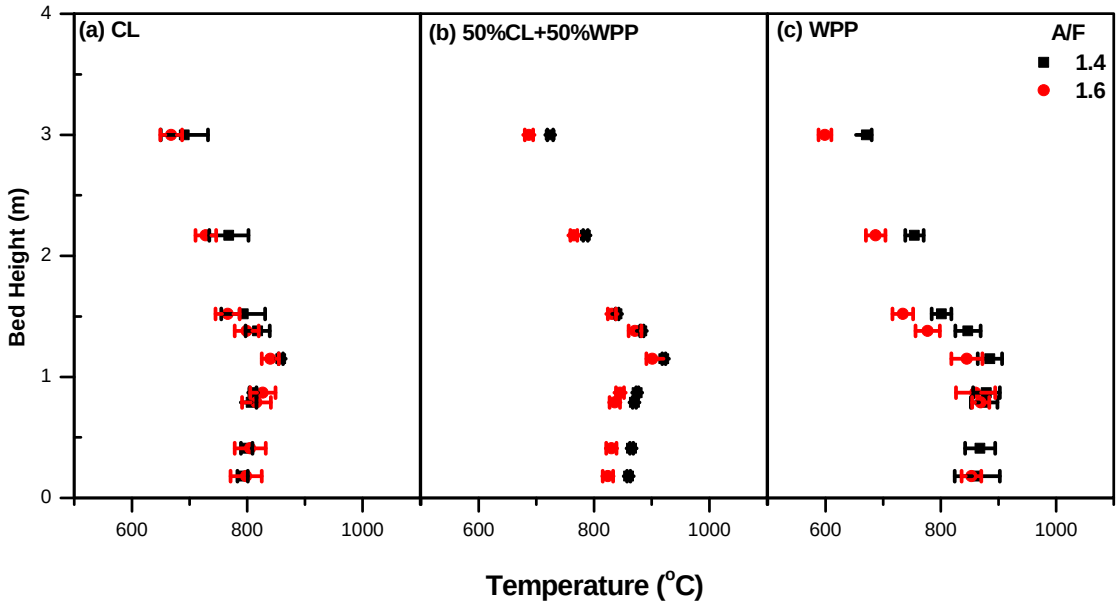

Figure 4-11 Temperature profiles from combustion of 100% CL (a), 50% WPP-50% CL (b) and 100% WPP (c) at different A/Fs

In contrast, in the tests with the 50% CL-50% WPP fuel blend, a higher A/F (=1.6) decreased the combustion zone temperatures by approximately 50°C. The reduction of the combustion zone temperatures could then retard the formation and sintering reactions of alkali/alkaline earth metals and silica during the combustion (Baxter 1993).

4.4. Conclusions

(1) Results from the co-firing tests of woody biomass and lignite suggest strong

interaction of chemical compositions in blended fuels. It was found that the contents of alkali/alkaline metals (K, Na, Ca) as well as Al_2O_3 and P_2O_5 were enriched in the deposited ash under the present fluidized-bed co-combustion conditions.

(2) A new parameter, i.e., the relative deposition rate (RD_A), was proposed to evaluate the deposition tendencies of biomass fuels and biomass-coal mixed fuels against the coal as the base fuel for co-firing. It was found that combustion of 100% WPP had a slightly greater tendency of ash deposition than that of 100% CL under the present fluidized-bed combustion conditions, because of the higher contents of alkali and alkaline earth metals and halogens elements (Cl and Br) in the WPP. Co-firing of WPP and CL did not significantly increase the ash deposition tendency in terms of the values of RD_A, and more interestingly, co-firing of the 50% CL-50% WPP fuel blend produced a lower RD_A.

(3) As another new and interesting finding, the moisture in the feed played a positive role in retarding the ash deposition for all the individual fuels and the fuel blends tested. The combustion of an all as-received fuels consistently produced lower deposition rates and higher and more uniformly distributed temperatures in the fluidized-bed combustor than those after oven drying. This could be explained by the decrease in the contact time of the volatile vapors of Ca, K S and P elements in the vicinity of the ash deposition probe, resulting from the release of water vapor during the combustion.

(4) A/F showed minimal influence in the chemical compositions of the deposited ashes, and the values of D_A and RD_A for the combustion of CL or WPP decreased at a higher A/F. This could be explained by a shorter residence time of fly ash in the freeboard zone at a higher excess air percentage.

4.5. References

Aho, M.; Gil, A.; Taipale, R.; Vainikka, P.; Vesala, H. (2008). A pilot-scale fireside deposit study of co-firing Cynara with two coals in a fluidised bed. *Fuel*; **87**(1):58-69.

Aho, M.; Silvennoinen, J. (2004). Preventing chlorine deposition on heat transfer surfaces with aluminium–silicon rich biomass residue and additive. *Fuel*; **83**:1299–1305.

Andersson, C.; Vattenfall, A.B. (2002). A method for operating a heat-producing plant for burning chlorine-containing fuels. *Patent Number: WO 02059526.*

Andersen, K.H.; Frsen, F.J.; Hansen, P.F.B.; Wieck-Hansen, K.; Rasmussen, I.; Overgaard, P.; Dam-Johansen, K. (2000). Deposit Formation in a 150 MWe Utility PF-Boiler during Co-combustion of Coal and Straw. *Biomass Bioenergy*; **19**(4):765-780.

Arvelakis, S.; Gehrmann, H.; Beckmann, M.; Koukios, E.G. (2005). Preliminary results on the ash behaviour of peach stones during fluidized bed gasification: evaluation of fractionation and leaching as pre-treatments. *Biomass and Bioenergy*; **28**:331-338.

Arvelakis, S.; Vourliotis, P.; Kakaras, E.; Koukios, E.G. (2001). Effect of leaching on the ash behavior of wheat straw and olive residue during fluidized bed combustion. *Biomass and Bioenergy*; **20**(6):459-470.

Atimtay, A.T.; Kaynak, B. (2008). Co-combustion of peach and apricot stone with coal in a bubbling fluidized bed. *Fuel Processing Technology*; **89**(2):183-197.

Baxter, L. (2005). Biomass-coal co-combustion: Opportunity for affordable renewable energy. *Fuel*; **84**(10):1295-1302.

Baxter, L.L.; Miles, T.R.; Miles Jr., T.R.; Jenkins, B.M.; Milne, T.; Dayton, D.; Bryers,

R.W.; Oden, L.L. (1998). The behavior of inorganic material in biomass-fired power boilers: field and laboratory experiences. *Fuel Processing Technology*; **54**(1-3):47-78.

Baxter, L.L.; Miles, T.R.; Miles, T.R.J.; Jenkins, B.M.; Dayton, D.C.; Milne, T.A.; Bryers, R.W.; Oden, L.L. (1996). Alkali deposits found in biomass boilers: The behavior of inorganic material in biomass-fired boilers-Field and laboratory experiences. *Rep#SAND96-8225, Vol. **II***, Sandia National Laboratories.

Baxter, L.L. (1993). Ash deposition during biomass and coal combustion: A mechanistic approach. *Biomass and Bioenergy*; **4**(2): 85-102.

Bryers, R.W. (1996). Fireside slagging, fouling, and high-temperature corrosion of heat-transfer surface due to impurities in steam-raising fuels. *Progress in Energy and Combustion Science*; **22**(1):29-120.

Davidsson, K.O.; Korsgren, J.G.; Pettersson, J.B.C.; Jäglid, U. (2002). The effects of fuel washing techniques on alkali release from biomass. *Fuel*; **81**:137–142.

Fernholz, K. (2009). Energy from woody biomass: a review of harvesting guidelines and a discussion of related challenges. Divetail Partners, Inc. *http://www.dovetailinc.org/files/DovetailBioGuides0709.pdf* (accessed on October 2009).

Ferrer, E.; Aho, M.; Silvennoinen, J.; Nurminen, R.V. (2005). Fluidized bed combustion of refuse-derived fuel in presence of protective coal ash. *Fuel Processing* Technology; **87**:33–44.

Frandsen, F.J. (2005). Utilizing biomass and waste for power production – a decade of contributing to the understanding, interpretation and analysis of deposits and corrosion products. *Fuel*; **84**:1277-1294.

Gogebakan, Z.; Gogebakan, Y.; Selçuk, N.; Selçuk, E. (2009). Investigation of ash deposition in a pilot-scale fluidized bed combustor co-firing biomass with lignite. *Bioresource Technology*; **100**(2):1033-1036.

Glazer, M.P.; Schürmann, H.; Monkhouse, P.; Jong, W.; Spliethoff, H. (2005). Co-combustion of coal with high alkali straw, measuring of gaseous alkali metals and sulfur emissions monitoring. In: *Proceedings of 8th International Conference on CFB*, in CD-ROM.

Grammelis, P.; Skodras, G.; Kakaras, E. (2006). Effects of biomass co-firing with coal on ash properties. Part I: Characterisation and PSD. *Fuel*; **85**(16): 2310-2315.

Gungor, A. (2008). Analysis of combustion efficiency in CFB coal combustors. *Fuel*; **87**(7):1083-1095.

Hall, D.O.; Rosillo-Calle, F.; de Groot, P. (1992). Biomass energy lessons from case studies in developing countries. *Energy Policy*; 62-73.

Hansen, L.A.; Frandsen, F.J.; Dam-Johansen, K.; Sorensen, H.S.; Skrifvars, B.J. (1999). Characterization of ashes and deposits from high-temperature coal-straw co-firing. *Energy and Fuels*;**13**(4):803-816.

Hupa, M. (2005). Interaction of fuels in co-firing in FBC. *Fuel*; **84**:1312–1319.

International Energy Agency (IEA) (2002). Sustainable production of woody biomass for energy. A position paper. ExCo2002:03. *http://www.ieabioenergy.com/library/157_PositionPaper-SustainableProductionofWoodyBiomassforEnergy.pdf* (accessed on January 2008).

Jenkins, B.M.; Baxter, L.L.; Miles Jr, T.R.; Miles, T.R. (1998). Combustion properties of biomass. *Fuel Processing Technology*; **54**:17-46.

Jenkins, B.M.; Bakker, R.R.; Wei, J.B. (1996). On the properties of washed straw. *Biomass and Bioenergy*; **10**(4):177-200.

Jensen, P.A.; Sander, B.; Dam-Johansen, K. (2001a). Pretreatment of straw for power production by pyrolysis and char wash. *Biomass and Bioenergy*; **20**(6):431-446.

Jensen, P.A.; Sander, B.; Dam-Johansen, K. (2001b). Removal of K and Cl by leaching of straw char. *Biomass and Bioenergy*; **20**(6):447-457.

Jensen, P. A.; Stenholm, M.; Hald, P. (1997). Deposition Investigation in Straw-Fired Boilers. *Energy Fuels*; **11**(5):1048-1055.

Kupka, T.; Mancini, M.; Irmer, M.; Weber, R. (2008). Investigation of ash deposit formation during co-firing of coal with sewage sludge, saw-dust and refuse derived fuel. *Fuel*; **87**(12):2824-2837.

Knudsen, N.O.; Jensen, P.A.; Sander, B.; Dam-Johansen, K. (1998). Possibilities and evaluation of straw pretreatment. Biomass for Energy and Industry. *Tenth European Conference and Technology Exhibition*. Wurzburg, Germany, pp.224.

McGowan, F. (1991). Controlling the greenhouse effect: the role of renewables. *Energy Policy*; 111-118.

Michelsen, H.P.; Frandsen, F.; Dam-Johansen, K.; Larsen, O.H. (1998). Deposition and high temperature corrosion in a 10 MW straw fired boiler. *Fuel Processing Technology*; **54**:95-108.

Molcan, P.; Lu, G.; Le Bris, T.; Yan, Y.; Taupin, B.; Caillat, S. (2009). Characterization of biomass and coal co-firing on a 3 MWth combustion test facility using flame imaging and gas/ash sampling techniques. *Fuel*; **88**:2328-2334.

Nielsen, H. P.; Baxter, L.L.; Sclippab, G.; Morey, C.; Frandsen, F.J.; Dam-Johansen, K.

(2000a). Deposition of potassium salts on heat transfer surfaces in straw-fired boilers: a pilot-scale study. *Fuel*; **79**(2):131-139.

Nielsen, H.; Frandsen, F.; Dam-Johansen, K.; Baxter, L. (2000b). The implications of chlorine-associated corrosion on the operation of biomass-fired boilers. *Process in Energy and Combustion Science*; **26**:283-298.

Overgaard, P.; Larsen, E.; Friborg, K.; Hille, T.; Jensen, P.A.; Knudsen, S. (2005). Full-scale tests on co-firing of straw in a natural gas-fired boiler. *http://www.dongenergy.com/SiteCollectionDocuments/NEW%20Corporate/PDF/Engineering/42.pdf* (accessed on February, 2008).

Perlack, R.; Wright, L.; Turhollow, A.; Graham, R.; Stokes, B.; Erbach, D. (2005). Biomass as Feedstock for a Bioenergy and Bioproducts Industry: The Technical Feasibility of a Billion-Ton Annual Supply. U.S. Department of Energy, Oak Ridge National Laboratory/U.S. Department of Agriculture. *http://www.eere.energy.gov/biomass/pdfs/final_billionton_vision_report2.pdf* (accessed on February 2008).

Pronobis, M. (2006). The influence of biomass co-combustion on boiler fouling and efficiency. *Fuel*; **85**(4):474-480.

Robinson, A.L.; Junker, H.; Baxter, L.L. (2002). Pilot-scale investigation of the influence of coal-biomass co-firing on ash deposition. *Energy Fuels*; **16**(2):343-355.

Shao, Y.; Xu, C.; Zhu, J.; Preto, F., Wang, J.; Tourigny, G.; Badour, C.; Li, H. (2010). Ash deposition during co-firing biomass and coal in a fluidized-bed combustor. *Energy Fuels*; **24**(9):4681-4688.

Skrifvars, B.J.; Yrjas, P.; Laurén, T.; Kinni, J.; Tran, H.; Hupa, M. (2005). The fouling

behavior of rice husk ash in fluidized-bed combustion. 2. Pilot-scale and full-scale measurements. *Energy Fuels*; **19**:1512–1519.

Skrifvars, B.J.; Laurén, T.; Hupa, M.; Korbee, R.; Ljung, P. (2004). Ash behaviour in a pulverized wood fired boiler – a case study. *Fuel*; **83**:1371–1379.

Theis, M.; Skrifvars, B.J.; Hupa, M.; Tran, H. (2006a). Fouling tendency of ash resulting from burning mixtures of biofuels. Part 1: Deposition rates. *Fuel*; **85**(7-8):1125-1130.

Theis, M.; Skrifvars, B.J.; Zevenhoven, M.; Hupa, M.; Tran, H. (2006b). Fouling tendency of ash resulting from burning mixtures of biofuels. Part 2: Deposit chemistry. *Fuel*; **85**(14-15):1992-2001.

Theis, M.; Skrifvars, B.J.; Zevenhoven, M.; Hupa, M.; Tran, H. (2006c). Fouling tendency of ash resulting from burning mixtures of biofuels. Part 3: Influence of probe surface temperature. *Fuel*; **85**(14-15):2002-2011.

Turn, S.Q.; Jenkins, B.M.; Jakeway, L.A.; Blevins, L.G.; Williams, R.B.; Rubenstein, G.; Kinoshita, C.M. (2006). Test results from sugar cane bagasse and high fiber cane co-fired with fossil fuels. *Biomass and Bioenergy*; **30**(6):565-574.

U.S Environmental Protection Agency (USEPA) (1990). 1990 Amendments to the Clean Air Act. *http://www.epa.gov/air/caa/* (accessed on January 2008).

Vamvuka, D.; Zografos, D.; Alevizos, G. (2008). Control methods for mitigating ash-related problems in fluidized beds. *Bioresour. Technol.*; **99:**3534–3544.

Wei, X.; Lopez, C.; von Puttkamer, T.; Schnell, U.; Unterberger, S.; Hein, K.R.G. (2002). Assessment of chlorine–alkali–mineral interactions during co-combustion of coal and straw. *Energy Fuels*; **16**:1095–1108.

Zheng, G.; Koziński J.A. (2000). Thermal events occurring during the combustion of biomass residue. *Fuel*; **79**(2):181-192.

CHAPTER 5. ASH AND CHLORINE DEPOSITION IN CO-FIRING LIGNITE AND A CHLORINE-RICH PEAT

5.1. Introduction

The declining resources and soaring prices of fossil fuels have intensified the interest and efforts worldwide in searching for alternative energy resources (particularly the carbon-neutral energy sources such as biomass) to substitute for oil and coal. Peat is a soft organic material accumulation of partially decayed vegetation matter together with deposited minerals from wetlands (Sopo, 2003). According to a report of the Finnish Ministry of Trade and Industry in 2000 (Crill *et al.*, 2000), peat was viewed as a slowly renewable natural resource. Compared with some low rank coal such as lignite, peat contains higher carbon contents, lower sulfur contents, and virtually no mercury (Orjala and Ingalsuo, 1999; Hupa, 2005). The world has rich peat resources and there are large peatlands in North American, particularly in the continental areas of Alaska and Canada (IEA, 2010; Vitt *et al.*, 2000). Canada contains the largest area of peatlands, approx. 170 million hectares or 40% of the world's total peatlands, with a potential to produce 335.4 billion tonnes dry peat (Monenco, 1981). In Northern Ontario alone, it can potentially supply fuel grade peat at 8.8 million dry tones per annum to fuel a 3200 MW power plant (Peat Ltd., 2010).

Peat fuel has an energy-content similar to lignite coal, which makes it a potential alternative fuel to coal for power generation in existing coal-fired boilers through co-firing. Minor engineering retrofit is needed for combustor system when co-firing peat and coal. Finland has the world's most advanced peat fuel industry, where peat is used for power generation at power plants ranging in size from 20 to 550 MW, contributing to a

total output of over 7000 MW (Telford, 2009). Similarly, Ireland has seven peat-fired generation stations supplying one-third of Ireland's electric power (Bott, 2010). In Russia, more than 6000MW electric power is produced from peat and about 4.5 million tonnes of peat is consumed annually for domestic heating (Bott, 2010). There are small scale district energy and heating systems operating in some remote communities of Northern Canada (Peat Ltd., 2010). Although peat as a fuel has found increasing applications as described above, there are still some issues that need to be addressed in combustion and co-firing, such as the ash-deposition and HCl emission problems.

Co-firing technologies have demonstrated to be one of the most cost-effective technologies to use renewable materials on a large scale and significantly reduce greenhouse gases and SO_2 emissions (U.S.EPA, 1990; Turn *et al.*, 2006). From Europe to North America, co-firing has been demonstrated and implemented in almost all major types of coal combustors including pulverized-coal combustor, stoker/grate combustors, and fluidized-bed combustors (Hupa, 2005; Baxter, 2005; Wei *et al.*, 2002; Gogebakan et al., 2009; Nielsen, 1995). For instance, for reducing total CO_2 emissions in Denmark, the Danish government has obliged the power utilities to apply a significant amount of biomass, mainly straw in new plants, dedicated to straw combustion and in existing pulverised coal-fired boilers through co-firing (Nielsen, 1995). It is more economically attractive to use biomass in the existing power plants by co-firing. However, ash related problems remain the long-standing challenges for co-firing coal and biomass or peat, in particular for agricultural residues such as cereal straws that contain high amounts of alkali/alkaline-earth metals (0.5–2 wt% potassium) and chlorine (up to 0.2–1 wt%). The chlorine and potassium elements are undesirable in power plant fuels when co-firing with

coal. On the one hand, they would lead to an increase in the amount of ash deposits on the surface of steam tubes, significantly decreasing the heat conduction coefficient of the tubes and reducing the overall thermal efficiency of the boiler. On the other hand, when firing/co-firing such kind of bio-fuels in a boiler, the chlorine-containing vapor along with other inorganic particles in the flue gas would condense and react further with metal on the heat exchanger surface, causing corrosion problem (Skrifvars *et al.*, 2002; Liu *et al.*, 2000a; Xie *et al.*, 1998; Baxter *et al.*, 1998; Nielsen *et al.*, 2000). Other potassium/chlorine-related problems include deactivation of SCR catalysts and inhibiting the use of fly ash for cement production (Hjalmarsson, 1990). The corrosion problems associated with chlorides deposits could be alleviated by addition sulfur through the following sulphation mechanism (Baxter, 2005).

$$2\mathrm{MeCl} + \mathrm{SO_2} + \frac{1}{2}\mathrm{O_2} + \mathrm{H_2O} \rightarrow \mathrm{Me_2SO_4} + 2\mathrm{HCl} \qquad (5\text{-}1)$$

where Me represents alkali metals such as Na or K.

However, in most of the co-firing power generation facilities demonstrated and implemented worldwide, biomass is utilized to substitute for coal at a relatively low substitution ratio, generally less than 20% on a thermal basis, in order to prevent from severe ash deposition and corrosion problems.

Compared to other co-combustion technologies, fluidized bed combustion (FBC) systems are advantageous for low grade fuels and diverse fuel blends. Some hazardous gases such as SO_x and HCl can be captured directly in the fluidized bed combustor by the addition of limestone. For a FBC, alkali chlorides (e.g. KCl, NaCl, $CaCl_2$) with lower melting points may lead to bed agglomeration in the furnace of the boiler (Skrifvars *et al.*, 2002). These chlorides are commonly regarded as important compounds governing

deposit formation and as aggressive materials causing problems of slagging/fouling (Baxter *et al.*, 1998) and high–temperature corrosion on heat-transfer surfaces (Nielsen *et al.*, 2000). In the presence of SO_2 in the flue gas at a high temperature, these chlorides could be sulphatised/oxidized into alkali sulphates via the above mentioned sulphation (Eq. 5-1), while releasing corrosive HCl. The chlorine-containing gases released during co-firing may directly cause the corrosion of high temperature superheater tubes (Nielsen *et al.*, 2000).

It is thus of great interest to investigate ash deposition behavior during combustion and co-firing of various fuels and fuel blends in a FBC system, especially for fuels containing a high amount of chlorine. Moreover, extensive ash-related research has been mainly done in Europe, which commonly used the only local biomasses. On the contrary, there are limited available ash-related studies based on the local bio-fuels in North American. In this research, a Canadian chlorine-rich peat was blended with lignite at various blending ratios and co-fired with a local lignite coal in a BFB combustor. The effects of moisture content of the fuels and sulfur addition on ash and chlorine deposition behaviors were also examined.

5.2. Experimental

5.2.1. Material and Preparation

The peat and lignite coal used in this study were from Western and Eastern Canada, respectively, and supplied by our industry partners. The proximate and ultimate analyses of these two fuels and ash compositions are given in Table 5-1.

Table 5-1 Proximate and ultimate analyses of the fuels and ash compositions

	Lignite	Peat
Moisture, wt% as received	30.0	35.8
HHV (MJ/ kg dry)	21.8	21.4
Proximate analysis, wt% db		
Ash[1]	22.0	2.0
Volatile matters (VM)	54.0	68.6
Fixed carbon (FC)	24.0	29.4
Ultimate analysis, wt% db		
Carbon	58.8	56.1
Hydrogen	4.2	5.7
Nitrogen	0.9	0.8
Sulphur	0.5	0.2
Oxygen[2]	13.6	35.2
Chlorine[3], μg/g.	25	2008
Bromine[3], μg/g.	< 21	153
Fluorine[3], μg/g	100	< 20
Dry ash analysis[4], wt% db		
SiO_2	49.76	28.05
Al_2O_3	19.71	8.63
Fe_2O_3	3.82	5.56
TiO_2	0.86	0.48
P_2O_5	0.30	1.31
CaO	9.91	12.65
MgO	2.11	17.72
SO_3	6.09	12.73
Na_2O	4.20	2.84
K_2O	1.04	1.14

[1] The ashing temperature was 750ºC for lignite and 500ºC for peat;
[2]By difference; [3] By Pyrohydrolysis and IC; [4] By XRF of the ashes from the feedstock.

The peat contains a strikingly high chlorine content of 2008 μg/g and high concentrations of alkaline-earth metals (Ca and Mg) in its ash. Lignite has a much higher ash content, i.e., 22 wt% on a dry basis, compared with the peat fuel (2 wt% db). With regard to ash composition, the lignite ash is rich in acidic oxides (SiO_2, Al_2O_3, and TiO_2), whereas the ash from the peat is balanced between acidic oxides and basic oxides (CaO, MgO, K_2O, Na_2O, and Fe_2O_3).

The peat was received in the form of pellets (10 mm diameter, 30 mm length), thus it was designated as "peat pellets" (PP) in this study. The lignite was crushed and screened into particles (<4 mm), designed as "crushed lignite" (CL), and the crushed lignite was used throughout the tests. Both feedstocks had a moisture content of 20-30 wt% as received. To investigate the effects of moisture content, oven dried fuels (to a moisture content of <5 wt%) were prepared by drying in the air at 105°C for over 12h. The actual moisture contents of all the fuels used were measured prior to each test in order to determine the feeding rate of the fuel or fuel blends and to ensure a constant heat input in all the combustion tests.

5.2.2. Combustion Facility

The combustion/co-combustion tests were performed with a pilot-scale bubbling fluidized bed combustor equipped with a belt feeder and a cyclone for fly ash collection (as illustrated in Figure 5-1) with a feeding capacity of up to 25 kg/h. It is also equipped with a water-cooled condenser for tar removal. Moreover, temperature measuring ports (T1-T9 in Figure 5-1) are located at different heights on the riser column and a flue gas sampling port is connected in the flue gas pipe for on-line measurement of reactor temperatures and flue gas compositions (CO, CO_2, and O_2). The combustion air was

supplied into the reactor through a primary air inlet and four secondary air inlets. A custom designed air-cooled probe made of SS 316L was installed in the freeboard region of the fluidized bed combustor.

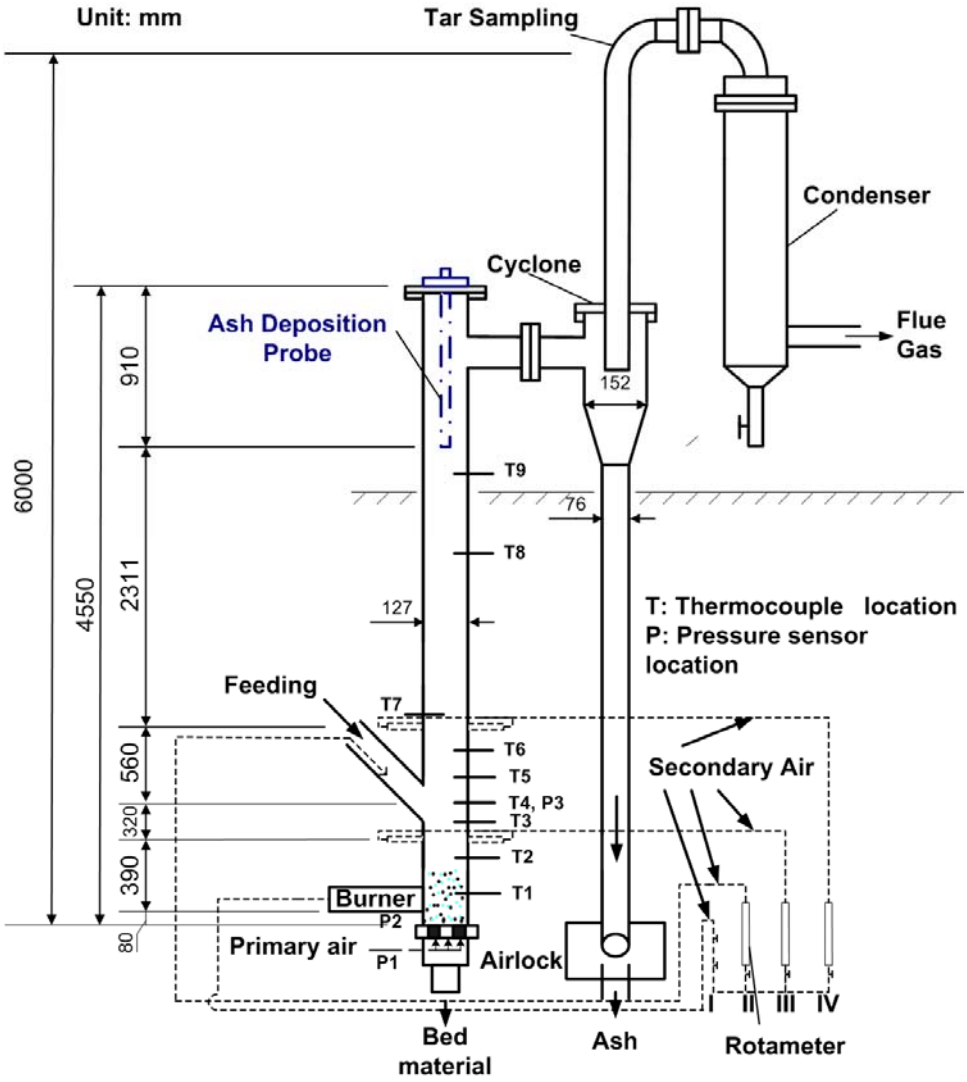

Figure 5-1 Schematic diagram of the fluidized-bed facility

The schematic and dimensions of the probe are displayed in Figure 5-2. The probe has an extension (2-inch OD) to increase the surface area, the total effective length of the probe (for ash deposition inside the freeboard zone) is 889 mm, and the total external surface area is ca. 0.098 m^2. It should be noted that the surface area of the up-facing

"stage" as shown in Figure 5-2 is exclusive on the calculation and so are extra ash deposits on the stage. During the steady operation in all the tests, the surface temperature of the probe was maintained at 430±10 ºC by carefully controlling the flow rate of the cooling air.

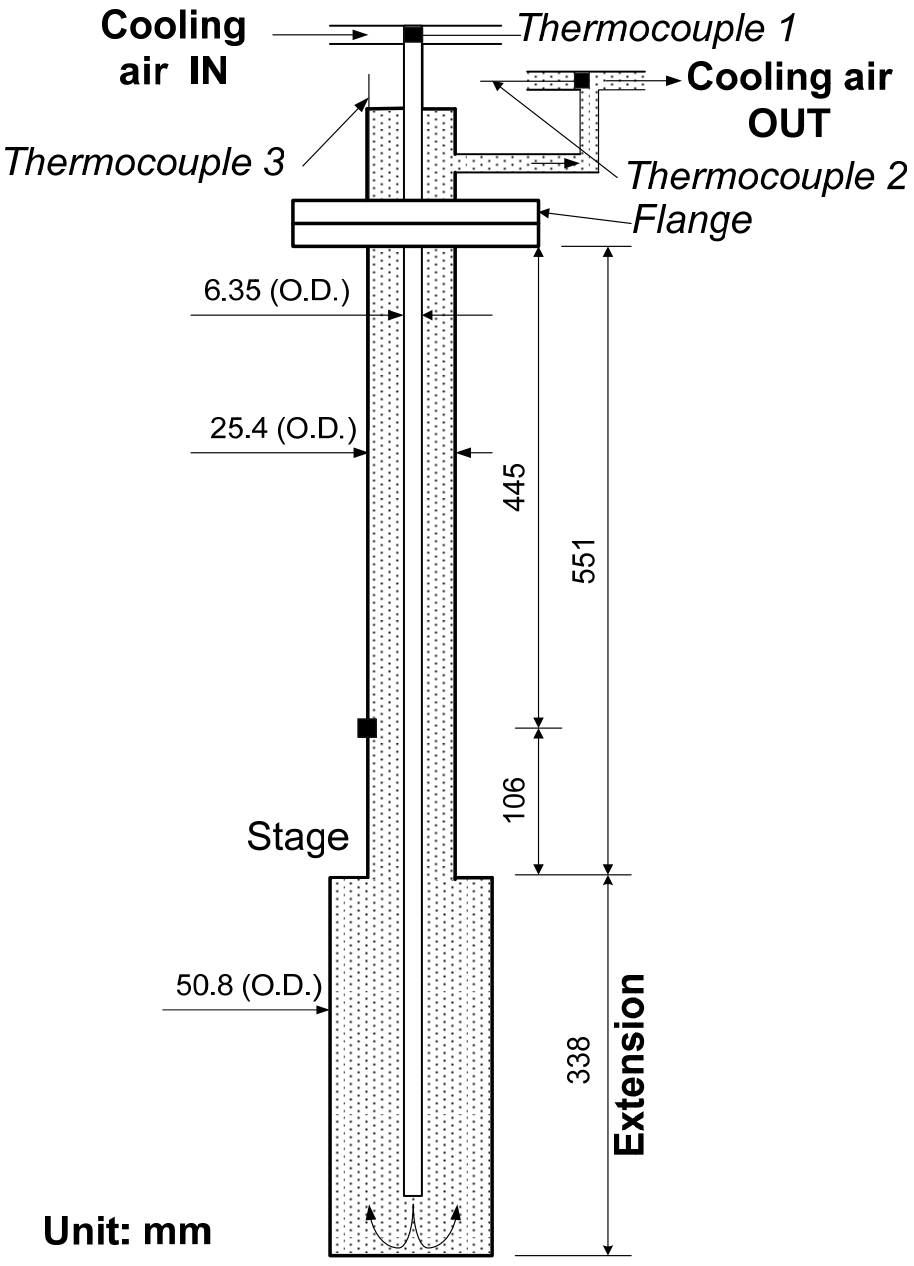

Figure 5-2 Schematic diagram of the ash deposition probe

5.2.3. Testing Methodologies and Parameters

A cleaned probe was installed in the freeboard zone of the reactor, right before the whole unit reached a steady state of operation. It should be noted that, however, in this study due to the limited working space in the freeboard and the difficulty associated with the probe installation and removal, that the probe was installed vertically using a flange on the reactor top, instead of horizontally (cross to the flue gas flow) as conventionally done in most of the literature work and in real boiler operations. The reactor was filled with 13 kg of olivine sand as bed materials in each test, and was heated up to above 600ºC using propane gas before introducing the solid fuels, i.e., CL-PP blends containing a PP portion ranging from 0% up to 100% on a thermal input basis with and without sulphur addition. For all the tests, a constant heat input of 58.3 MJ/h was used, and the fuel feed rates ranged from 3.1-3.8 kg/h on a dry basis depending on the heating values of the fuels. The total air flow rate was maintained at 360-400 L/min corresponding to an excess air ratio of 40% (or an A/F = 1.4). At a steady state, the combustion temperatures (in the combustion zone or the dense phase of the fluidized bed corresponding to the temperature sampling ports of T1-T5 in Figure 5-1) were in the range of 850-900°C. A relatively stable temperature profile along the bed height could be obtained through adjusting the secondary air and primary air ratios (while maintaining a constant total air flow rate). In this study, because of the introduction of the secondary air above the dense phase for combustion of volatiles and the inevitable heat loss along the reactor column, the average flue gas temperature in the vicinity of the ash deposition probe in the freeboard region was in the range of 600-700ºC. In a typical run, at least 3-4 hours of stable operation was performed before cooling the reactor down to room temperature

using nitrogen. When the whole unit was cooled to room temperature, the ash deposition probe was carefully removed from the freeboard and the deposited ash was completely recovered for weighing to calculate the accumulated absolute ash deposition rate (D_A, g m^{-2} h^{-1}) and the relative ash deposition rate (RD_A, g m^{-2} h^{-1}) as defined below, respectively:

$$D_A = \frac{\text{Mass of collected ash deposit (g)}}{\text{Surface area of the probe (m}^2\text{)} \times \text{Duration (h)}} \quad (5\text{-}2)$$

$$RD_A = D_A \times \frac{\text{Ash feeding rate of crushed lignite(g/h)}}{\text{Ash feeding rate of the fuel (g/h)}} \quad (5\text{-}3)$$

As was discussed in our previous study (Shao *et al.*, 2010), conclusions were difficult to be drawn based on the D_A results only, because the causes of a low ash deposition rate could be due to either a lower total ash content in the feed (e.g., 2 wt% ash content for the peat vs. 22 wt% ash content for the lignite) or the positive interaction (to suppress the ash deposition) between the ash elements from the component fuels in the fuel blends. A relative ash deposition rate (RD_A) was proposed and used in our previous study. The value of an RD_A was obtained from that of D_A by correction with the ash feeding rate of the base fuel (i.e., CL) in relation to the ash feeding rate of the co-firing fuel in the test. As such, comparison of RD_A values for the co-firing tests would help to rule out the effects of the total ash content in the feed on ash deposition. At the meantime, the value of an RD_A implies the deposition tendency of different co-firing fuels or fuel blends in relation to that of the base fuel (lignite coal) in combustion.

The collected deposited ashes were comprehensively characterized using various analytical techniques. For example, pyrohydrolysis was used to identify the total chlorine

contents. Ion chromatography was further applied to examine the soluble chlorine and sulfur contents. Moreover, mineralogical compositions and the crystallinity of the ash deposits were analyzed by XRD. The chemical compositions of fuel and deposited ashes were gotten via XRF analysis in accordance to the ASTM D4326 standard.

Because of the relatively large operating scale and the complexity of the fluidized bed facilities, it normally took 2-3 days to complete a successful combustion/co-combustion test (including fuel/facility preparation, operation, after-run cleaning/maintenance). Thus, reproducibility of the ash deposition rates and the chemical compositions of the deposited ash were examined only for some reference tests in this study. In this work, repeated combustion tests were performed on the 100% CL for three times, and on the 100% PP twice. The relative standard deviations of the ash deposition rates were within ±10.0%. The maximum relative errors in the ash concentrations (from XRF analysis) between the duplicate tests were within ±13.0%. These repeated data with error bars are shown in some of the Tables and Figures in the following sections.

5.3. Results and Discussion

The peat used in this research contained very high chlorine concentration (2008 μg/g db) compared to 25 μg/g db in the lignite used and 200-500 μg/g db in many commonly-used peats (Sloss, 1992). As discussed previously, chlorine along with alkali and alkaline earth metals plays an important role in the ash deposition during combustion/co-combustion of solid fuels. Thus, the chlorine deposition behavior will be taken into account in the discussion on ash deposition during co-combustion of CL and PP (as received or oven dried) at various blending ratios (0, 20, 50, 80 and 100%) with various wt. % of sulphur addition (0, 1 and 5 wt%).

5.3.1. Effects of Blending Ratio

Figure 5-3 shows changes of total chlorine concentration in the ash deposits and the relative ash deposition rates (RD_A) during co-firing of CL-PP blends at different blending ratios. Both total chlorine concentration in deposited ashes and the RD_A value consistently increase with the increasing ratio of PP in the CL-PP blends up to 80% on a thermal basis.

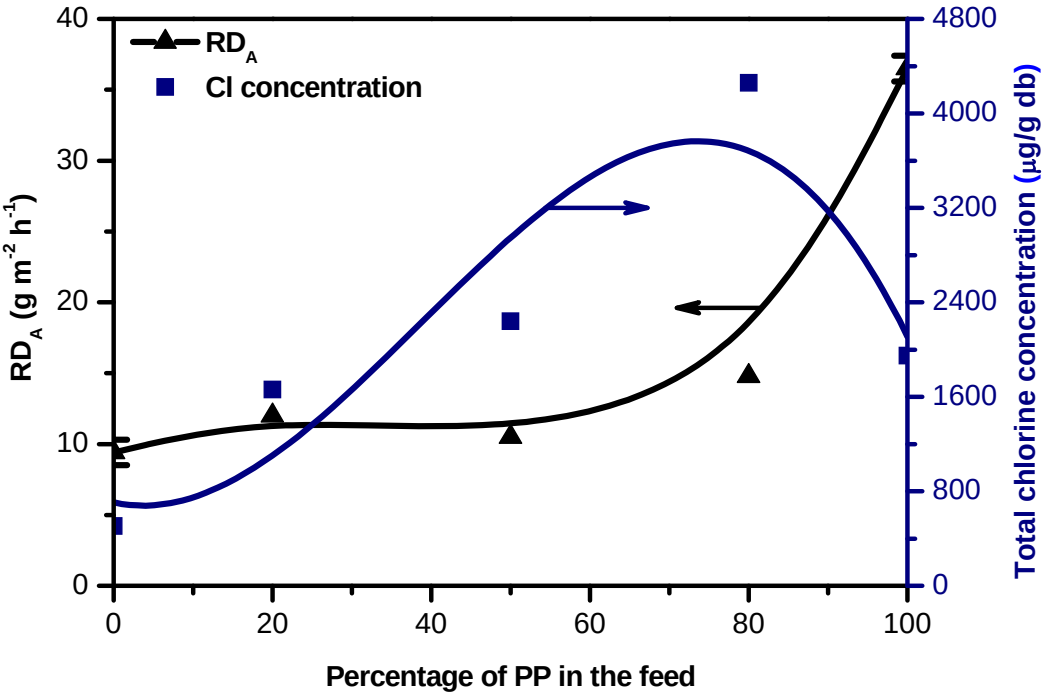

Figure 5-3 Comparison of RD_A and total chlorine concentration in the ash deposits obtained from co-firing of CL-PP fuel blends at different blending ratios

As the peat used in this research contains very high chlorine concentration (2008 μg/g db) compared to 25 μg/g db in the lignite used, this result could be explained by the increased reactions between the alkali/alkali-earth metals mainly from the lignite and the Cl-vapor mainly derived from peat (Kanters *et al.*, 1996; Banaee and Larson, 1993; Pan *et al.*, 1995). The deposited chlorides (such as NaCl, KCl, $CaCl_2$ and $MgCl_2$) usually

have relative low melting points (700-800°C) and would form a sticky layer on the heat transfer surface, leading to an increased ash deposition rate. As an interesting result displayed in Figure 5-3, the co-firing of the CL- PP blends with 50% PP produced the lowest RD_A, which was similarly observed in co-firing CL and white pine pellets in our previous study (Shao *et al.*, 2010). The lower rate of ash deposition might be a result from the formation of more minerals with high ash melting points by the interaction between the coal ash and the peat ash.

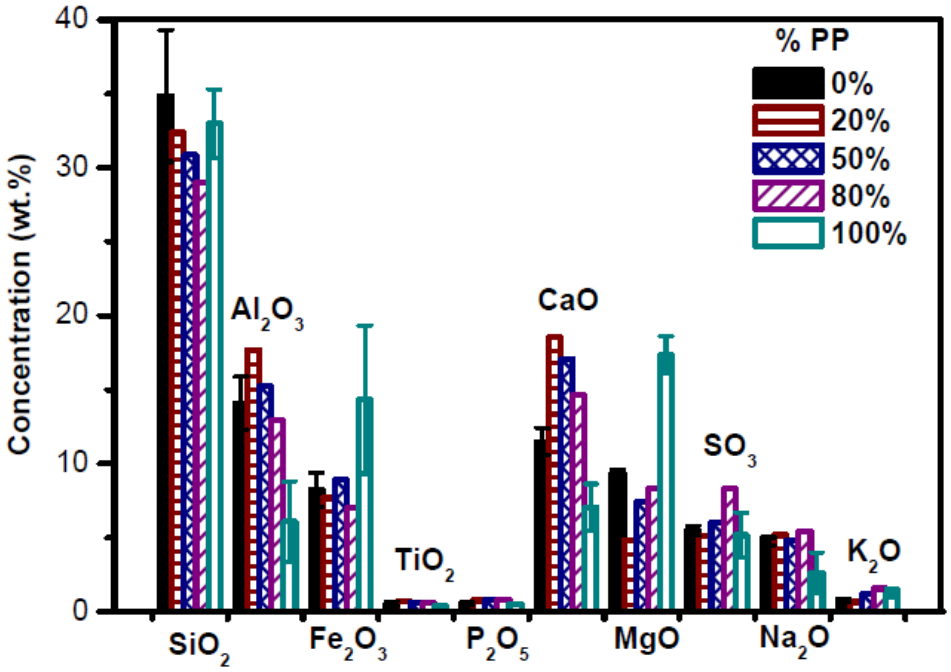

Figure 5-4 Chemical compositions determined by XRF analysis for the deposited ashes obtained from co-firing of CL and PP at various blending ratios

As demonstrated in Figure 5-4, PP blends with 50% PP contains high concentrations of Al_2O_3, CaO and SO_3. These minerals combined with MgO, Fe_2O_3 and SiO_2 could form compounds Anhydrite ($CaSO_4$) and Merwinite ($Ca_3Mg(SiO_4)_2$) and Brownmillerite ($Ca_2Al_2Fe_2O_5$), which have melting points of >1300-1400°C (Deer *et al.*, 1978; Schwartz, 1995; Lyon *et al.*, 1999; Hoch, 1993).

Table 5-2 Mineralogical compositions (wt %) determined by XRD measurement for the deposited ashes obtained from co-firing of CL and PP at various blending ratios

% PP	0%	20%	50%	80%	100%
Chemical Compound	Percentage of Chemical Compound (wt %)				
Anhydrite ($CaSO_4$)	4.1	9.2	8.6	3.3	2.9
Åkermanite ($Ca_2MgSi_2O_7$)	0.9	2.9	7.6	4.4	2.4
Forsterite (Mg_2SiO_4)	5.8	5.0	8.8	2.0	14.8
Hematitle (Fe_2O_3)	1.6	1.8	2.3	0.8	1.0
Lime (CaO)	0.3	0.9	1.3	0.2	0.4
Magnesium Oxide (MgO)	1.3	1.5	3.8	1.1	2.6
Quartz (SiO_2)	7.6	8.8	7.6	2.4	4.2
Tychite ($Na_6Mg_2(CO_3)_4(SO_4)$)	1.4	4.2	2.3	0.3	1.0
Brownmillerite ($Ca_2Al_2Fe_2O_5$)	1.6	2.2	1.8	0.6	
Anorthite ($CaAl_2Si_2O_8$)	1.5				3.0
Dolomite ($CaMg(CO_3)_2$)	0.9				
Goethite (FeO(OH))	1.5				
Magnesioferrite aluminian ($MgAl_{0.74}Fe_{1.26}O_4$)	1.1				
Magnesioferrite ($MgFe_2O_4$)		3.6	2.0	0.2	
Merwinite ($Ca_3Mg(SiO_4)_2$)		4.4	4.9	1.4	
Crystallinity (wt %)	**29.5**	**44.5**	**50.9**	**16.7**	**33.0**
Amorphous content (wt %)	**70.5**	**55.5**	**49.1**	**83.3**	**67.0**

The formation of the above listed high melting-point minerals was evidenced by the results of XRD measurements as provided in Table 5-2. The crystallinity of the deposited ash from the CL- PP blends with 50% PP is 51% which is much higher than that from the CL- PP blends with 20 or 80% PP. Here, the presence of a significantly high percentage of amorphous components in the deposited ashes was due to the relatively low operating temperature of the fluidized bed combustor (850- 900°C) (Xiong *et al.*, 2008). As such, the formation of more minerals with high ash melting points and high crystallinity may account for the lowest rate of ash deposition during co-firing of the CL- PP blends with 50% PP.

As shown in Figure 5-3, compared to co-firing of the CL- PP blends, combustion of 100% PP produced the highest RD_A but the total chlorine content in the deposited ash decreased markedly compared to that from the 20%CL-80%PP blend. The high value of RD_A from the combustion of 100% PP was likely due to the relatively higher contents of alkaline metals, particularly MgO, CaO and Fe_2O_3, in the peat fuel (Table 5-1). This would result in deposition of more minerals containing these metals and their derivative compounds such as Mg_2SiO_4, as evidenced by the XRF and XRD results shown in Figure 5-4 and Table 5-2, respectively. Moreover, the high content of Cl element in the peat fuel would also promote the deposition of the alkali/alkaline compounds as discussed previously. Xiong and co-workers (2008) detected simultaneously a high concentration of Mg_2SiO_4 in the ash and high slagging tendency of the ash in combustion of corn stover pellets. Silica can absorb alkali/alkaline earth metals in the fuel to form alkali silicates which easily deposit on the reactor wall or the heat-exchange surface via fly ash at a low fusion temperature (typically <700˚C) (Baxter, 1993). Although the melting points of pure calcium/magnesium oxide compounds (>2500°C) (Xie *et al.*, 1998) are high, the silicate minerals have much lower melting points (Lyon *et al.*, 1999; Hoch *et al.*, 1993).

The reason why the total chlorine content in the deposited ash from the combustion of 100% PP decreased markedly compared to that from the 20%CL-80%PP blend may be explained by the much lower ash content of the peat, 2 wt%, only approximately one tenth of that of the lignite fuel (22 wt%). Due to such low ash content in the peat fuel, the absolute amount of alkali/alkaline metals in the peat fuel is also much lower than the CL-PP blends, which would suppress the reactions between the alkali/alkali-earth metals and the Cl-vapor. Consequently, this would result in reduced capturing of the chlorine by the

alkali/alkali-earth metals, leading to lower deposited chlorides (such as NaCl, KCl, $CaCl_2$ and $MgCl_2$), and hence a decrease in total chlorine content in the deposited ash from the combustion of 100% PP, as shown in Figure 5-3.

5.3.2. Effects of Moisture Content in Fuels

Co-firing biomass such as cereal straws with coal in the existing power plants is economically attractive. However, the high chlorine and potassium content of straw may cause operating problems such as ash deposition, corrosion, and deactivation of SCR catalysts (Jensen *et al.*, 2001a; Jenkins *et al.*, 1996). Pretreatment processes have been investigated to remove chlorine and potassium from the biomass fuels before supplying them to the boiler for combustion/co-combustion. Typical pretreatment processes include thermal pretreatment (such as pyrolysis and gasification) and washing of biomass or bio-char (Jensen *et al.*, 2001a-b; Jenkins *et al.*, 1996; Knudsen *et al.*, 1998; Vamvuka *et al.*, 2008; Davidsson *et al.*, 2002; Arvelakis *et al.*, 2001). Depending on the drying processes employed after prewashing, the moisture contents of the feedstock would vary greatly. It is thus of great interest to investigate the effects of the moisture content of fuels on the ash and chlorine deposition in combustion/co-combustion.

In this study, to investigate the influence of moisture content in feedstock on ash and chlorine deposition, oven-dried fuels (to a moisture content of <5 wt%) were used comparatively with the as-received or air-dried fuels in the combustion/co-combustion experiments. Comparison of RD_A and total chlorine concentration in the deposits obtained from combustion of 100% CL, the 50% CL-50% PP, and 100% PP with different moisture contents is displayed in Figure 5-5.

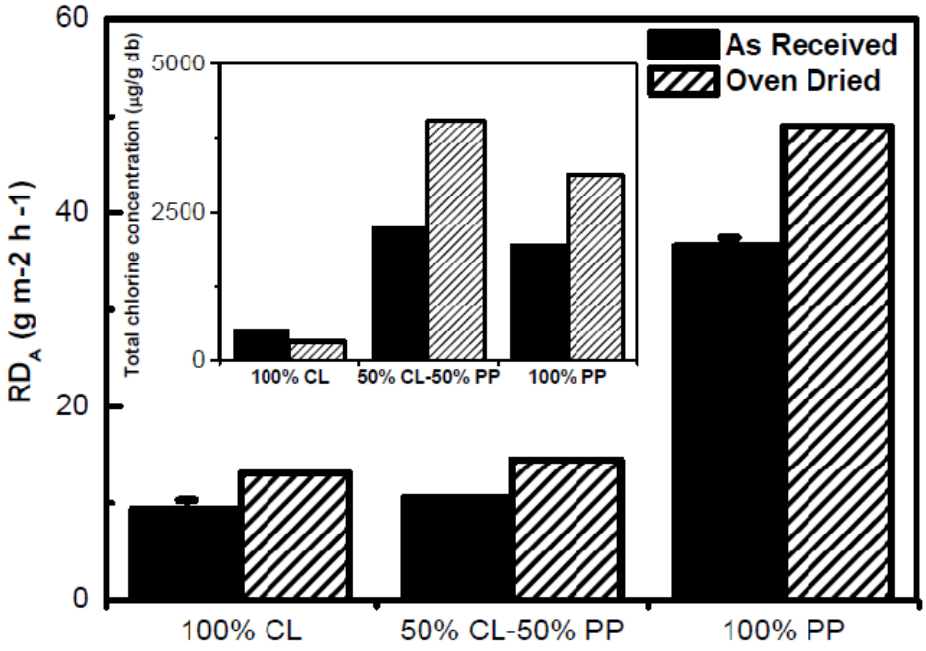

Figure 5-5 Comparison of RD_A and total chlorine concentration in the deposits obtained from combustion of 100% CL, the 50% CL-50% PP, and 100% PP with different moisture contents

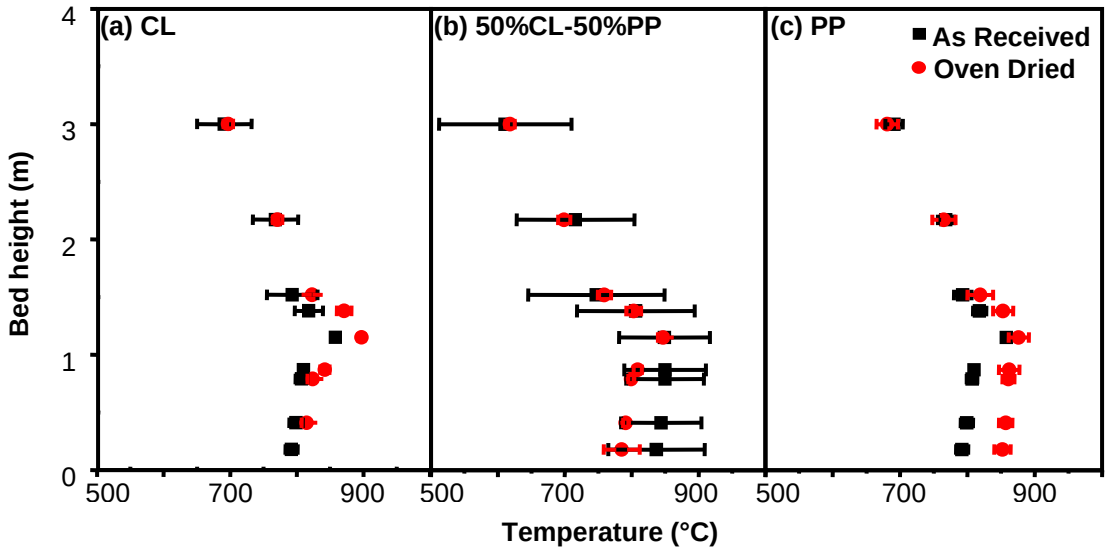

Figure 5-6 Temperature profiles of combustion or co-combustion of (a) 100% CL, (b) 50% CL-50% PP, and (c) 100% PP with different moisture contents

Interestingly, the experimental results indicated consistently a low RD_A and low chlorine in the ash deposits when burning relatively wet fuel/fuel blends. It should be

noted that excess water vapor did not affect fluidized-bed temperatures substantially because of the same heat input used in all tests, but combustions of the relatively wet fuels resulted in a more uniform temperature distribution profile within the combustion column as shown in Figure 5-6. This might be owing to the release of water vapor leading to increases in the flue gas flow rate, and to the greater densities of the wet fuels compared to the oven-dried fuels which increased the solid hold-up in the dense zone of the fluidized bed. The increase in the flue gas flow rate would lead to a shorter retention time of the volatile vapor containing fly ash elements of Cl, K/Na, Ca, and S inside the combustor. As a result, it reduced the contact time of these fly ash elements in the vicinity of the deposition probe, and would hence decrease the ash and chlorine deposition (as evidenced in Figure 5-5). In addition, the presence of water vapor may contribute to gasification of the volatile tarry vapor by steam reforming/gasification reaction which can be catalyzed by some ash-containing metals (Swierczynski *et al.*, 2007):

$$\text{Tar (or } C_xH_yO_z) + H_2O \rightarrow CO + CO_2 + H_2 \quad (5\text{-}4)$$

The reduction in tar formation and deposition might also play a positive role in decreasing the ash and chlorine deposition.

5.3.3. Effects of the Addition of Sulphur

Figure 5-7 compares the RD_A and total chlorine concentration in the ash deposits obtained from combustion of 100% CL and 100% PP with the addition of various amounts of sulphur. The figure clearly shows that the addition of sulphur to both fuels (CL and PP) led to consistent decline in the total chlorine content in the deposited ashes as the amount of sulphur addition increased from 0 to 5 wt%.

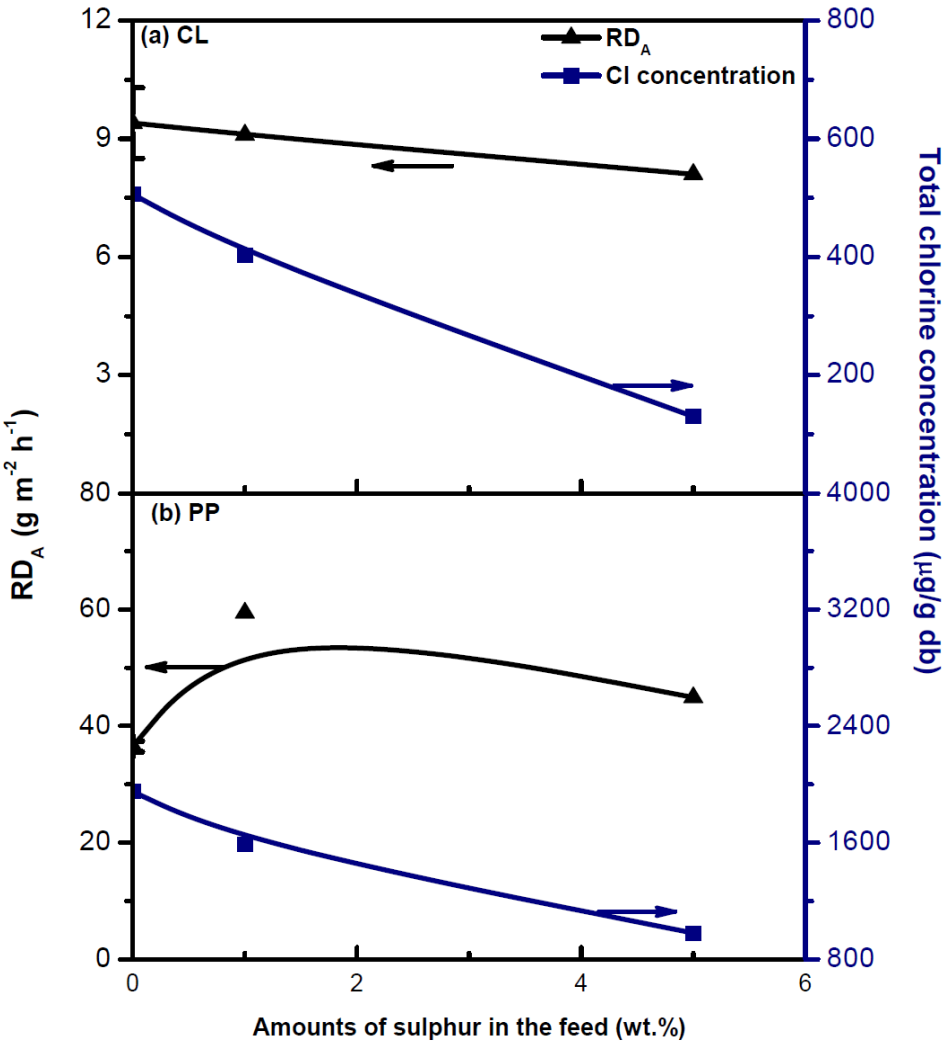

Figure 5-7 Comparison of *RD_A* and total chlorine concentration in the deposits obtained from combustion of (a) 100% CL and (b) 100% PP with addition of various amounts of sulphur

The decline in the chlorine deposition was accompanied by an increase in the sulfur contents (in the form of sulfide, sulfate or SO_3) in the corresponding deposits according to the XRF analysis (Figure 5-8). This result strongly suggests the occurrence of the sulphation (Eq.5-1) where the presence of SO_2 in the flue gas at a high temperature reacts with alkali chlorides to form alkali sulphates while releasing HCl into the flue gas and in turn reducing the chlorine concentration in the ash deposits.

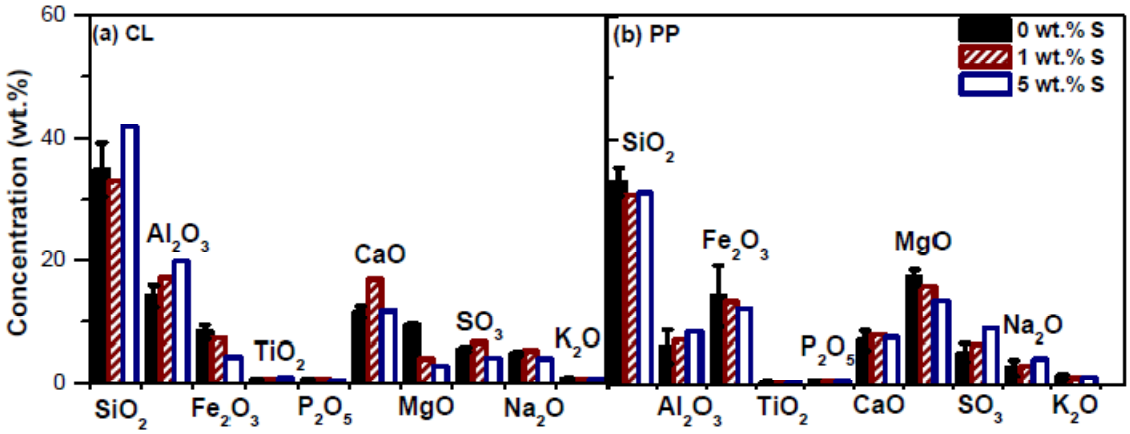

Figure 5-8 Chemical compositions of deposited ashes obtained from combustion of (a) 100% CL, and (b) 100% PP with varied sulfur additions

Table 5-3 presents the major crystalline mineralogical compositions of these ash deposits determined by XRD. Generally, the crystalline forms of S-containing compounds in the deposited ashes from the fuel with sulfur addition are $CaSO_4$ and $KHSO_4$ (Table 5-3), which might confirm the occurrence of sulphation. Besides sulphation, the low total chlorine contents in the deposits might also be a result from the formation of alkali aluminosilicates, represented by the reaction in Eq. 5-5. The formation of alkali aluminosilicates, such as *sodium aluminosilicate* ($Na_{1.65}Al_{1.65}Si_{0.35}O_4$), *Hauyne* ($Na_6Ca_2Al_6Si_6O_{24}(SO_4)_2$), *Albite* ($NaAlSi_3O_8$), and *Kalsilite* ($KAlSiO_4$), in the deposits from combustion of the sulphur-containing fuels was evidenced by the XRD measurement as listed in Table 5-3.

$$Al_2O_3 \cdot 2SiO_2 + 2MeCl + H_2O \rightarrow Me_2O \cdot Al_2O_3 \cdot 2SiO_2 + 2HCl \qquad (5\text{-}5)$$

As shown in Figure 5-7, the addition of sulphur to the lignite fuel decreased the ash deposition rate during combustion. This might be because of the reaction between SO_2 and the alkali/alkaline metal oxides from the lignite ash to form more stable sulphates (with higher boiling points), which would retard the fly ash deposition. In contrast, the

addition of sulfur to the peat fuel accelerated the ash deposition rate particularly when adding 1 wt% sulphur to the PP.

Table 5-3 Mineralogical compositions (wt %) of the deposited ashes obtained from combustion of CL and PP with the addition of sulphur

Fuel	CL			PP		
% Sulphur	0 wt %	1 wt %	5 wt %	0 wt %	1 wt %	5 wt %
Chemical Compound	Percentage of Chemical Compound (wt %)					
Åkermanite ($Ca_2MgSi_2O_7$)	0.9	7.7	5.6	2.4	3.6	2.0
Brownmillerite ($Ca_2Al_2Fe_2O_5$)	1.6	11.9	5.9		1.6	
Hematitle (Fe_2O_3)	1.6	6.0	1.8	1.0	1.7	1.6
Lime (CaO)	0.3	0.3	0.7	0.4	0.4	0.7
Periclasee (MgO)	1.3	4.0	3.3	2.6	2.8	1.4
Anhydrite ($CaSO_4$)	4.1	16.0		3.6	8.0	8.1
Dolomite ($CaMg(CO_3)_2$)	0.9	1.5			1.6	1.2
Magnesioferrite aluminian ($MgAl_{0.74}Fe_{1.26}O_4$)	1.1				3.2	1.3
Goethite (FeO(OH))	1.5					2.0
Anorthite ($CaAl_2Si_2O_8$)	1.5			3.0		1.6
Forsterite (Mg_2SiO_4)	5.8			14.8	16.2	11.5
Quartz (SiO_2)	7.6	17.9	23.8	4.2	10.9	5.8
Tychite ($Na_6Mg_2(CO_3)_4(SO_4)$)	1.4	2.5	1.9	1.0	1.0	
Mercallite ($KHSO_4$)		8.7	4.8		2.8	1.2
Sodium alumiosilicate ($Na_{1.65}Al_{1.65}Si_{0.35}O_4$)		3.9	9.1		2.4	
Calcite, magnesian ($Mg_{0.129}Ca_{0.871}CO_3$)		1.8	1.9		1.7	0.5
Hauyne ($Na_6Ca_2Al_6Si_6O_{24}(SO_4)_2$)		3.9	0.8			
Albite ($NaAlSi_3O_8$)					16.5	
Kyanite (Al_2SiO_5)						26.6
Kalsilite ($KAlSiO_4$)						2.4
Crystallinity (%)	**29.5**	**96.2**	**67.9**	**33.0**	**74.4**	**71.0**
Amorphous content (%)	**70.5**	**3.8**	**32.1**	**67.0**	**25.6**	**29.0**

With the peat fuel that contains a relatively low ash content (2 wt% db) but a high concentration of chorine, the above result might be explained by the sulphation (Eq. 5-1)

occurring on the heat transfer surface or within the reactor in the vapor phase. Via the sulphation, the compounds of alkali/alkaline metal chlorides (MeCl) would convert into sulphates with increased molecular weights; hence they increased the weight of the deposited ash on the probe. Furthermore, the addition of sulfur to PP seemed to promote the formation of alkali aluminosilicates such as *Albite* ($NaAlSi_3O_8$), and *Kalsilite* ($KAlSiO_4$), as evidenced by the XRD measurement (Table 5-3). Although alkali sulphates and alkali aluminosilicates have relatively higher melting points than alkali chlorides, ash deposition could be worse because the mixtures of these sulphates, alkali aluminosilicates and chlorides could lead to a lower the melting point compared to the pure components (Skrifvars *et al.*, 2002; Xie *et al.*, 1998).

5.3.4. The Fate of Fuel-containing Chlorine in FBC

The chlorine contents present in coal and biomass/peat include both inorganic chlorine and organic associated chlorine (Yudovich and Ketris, 2006). The inorganic chlorine is mainly present in the salts of alkali/alkali-earth chlorides and chlorine-bearing silicates, suphates and chlorides in pore moisture. Organic chlorine could be partially removed by pyrolysis of biomass in inert atmosphere up to 600°C (Jensen *et al.*, 2001b). Wei *et al.* (2009) and Raask (1985) reported that the gaseous HCl mainly from chlorine-containing organics started to evolve at about 200°C and completed at around 600°C, just before the vaporization inorganic Cl in the forms of NaCl and KCl, etc. In a fluidized bed combustor, Cl releases as vapors of HCl and NaCl/KCl into the flue gases. When the flue gas passes through the free board at a lower temperature, some HCl(g) may convert to Cl_2(g) via the Deacon reaction (Eq. 5-6). However, Cl_2(g) may be reduced by SO_2 back to HCl(g) via the reaction of Eq.5-7. Therefore, the concentrations of Cl_2 in the flue gas are

usually much less, one magnitude smaller (Wei *et al.*, 2009), than that of HCl/KCl/NaCl vapors in the flue gas during combustion/co-combustion.

$$2HCl + \frac{1}{2}O_2 \leftrightarrow H_2O + Cl_2 \quad (5\text{-}6)$$

$$Cl_2 + SO_2 + H_2O \leftrightarrow 2HCl + SO_3 \quad (5\text{-}7)$$

A part of KCl(g)/NaCl(g) may condense into fly ashes during the cooling process (Jensen *et al.*, 2000; Jensen *et al.*, 1998). Some of chlorides in fly ashes might deposit on a cold surface of the combustor wall or the heater exchange or the probe as used in this study, eventually, causing fouling, slagging, and high temperature corrosion in the combustor (Liu *et al.*, 2000; Hansen *et al.*, 1999). Unfortunately, the analyses for both HCl(g) and KCl (g)/NaCl (g) in flue gases require some specific methods and were difficult to perform in this study due to the lack of analytical equipments. One challenge for these analyses is that HCl/KCl/NaCl vapors would easily transform from gas phase to liquid/solid phases, although these vapors might be directly sampled into absorption solution at high temperatures (Liu *et al.*, 2000) and HCl (g) may be detected online by Fourier transform infrared spectroscopy (FTIR) (Wei *et al.*, 2009). In this study, no HCl was observed by GC-MS in all gas samples likely because HCl (g) transformed to HCl (l) in a gas sampling bag at a room temperature.

In this work, all bed materials were drained from the fluidized bed combustor after each run. After sieving, little amount of fines (< 10g) was found in the bed materials after combustion, and they mainly originated from the breakup of the bed materials added to the reactor (i.e., olivine sands). In each test, fly ash was collected from the cyclone bottom after cooling the system to room temperature. The collected cyclone bottom ash was weighed. Chemical compositions of some cyclone bottom ash samples were

analyzed by XRF to compare with those of the corresponding ash deposited on the probe, as plotted in Figure 5-9.

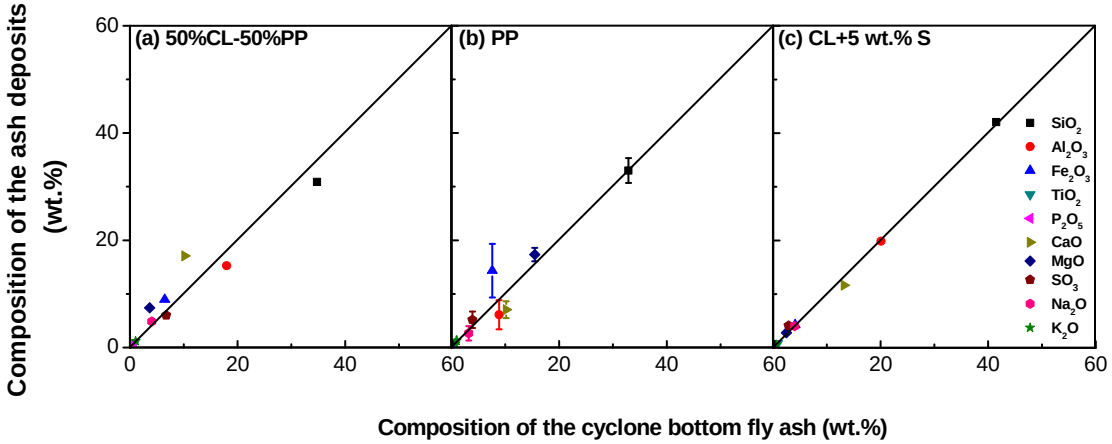

Figure 5-9 Chemical compositions of the cyclone bottom fly ashes versus chemical compositions of the ash deposits obtained from combustion of (a) the 50% CL-50% PP fuel blend, (b) 100% PP, and (c) 100% CL plus 5 wt% sulphur as received at A/F=1.4

From the Figure, one may find minimum differences of chemical compositions in the cyclone bottom ash and the deposited ash. As such, a total chlorine amount in the collected ash was then calculated by multiplying the total chlorine concentration in the ash deposits with the total weight of the fly ash collected from the cyclone. Compared to total chlorine contents fed in the system, it was observed that only a portion of chlorine was condensed in the fly ashes, depending on the type of fuel or fuel blend. In combustion of the lignite (a fuel with low Cl content and high ash content) at various operation conditions (with different amounts of sulphur addition and moisture contents) the portions of chlorine in the ashes ranged from 24% to 89% for each run. In contrast, combustion of the peat (a fuel with high Cl content and low ash content) the portions of chlorine in the ashes were less than 10%. Thus, fuels with higher ash content would facilitate capturing of the minerals and chlorine in the fly ashes (Xie *et al.*, 1998; Wei *et*

al., 2009). Most of Cl-containing vapours ended up in the flue gas, as similarly reported in some previous studies (Baxter *et al.*, 1998; Liu *et al.*, 2000b; Manninen *et al.*, 1997).

5.3.5. Slagging Index

As discussed previously, a relative ash deposition rate (RD_A) was proposed and used in our studies, and the value of an RD_A implies the deposition tendency of different co-firing fuels or fuel blends in relation to that of the base fuel (lignite coal) in combustion. To elucidate the tendency of different co-firing fuels, slagging index (SI, commonly defined as the base-to-acid ratio) was used by many previous co-firing studies (Jensen *et al.*, 1997). Similarly, in this study, SI, as defined below, was used to predict deposition/fouling tendencies.

$$SI = \frac{CaO + MgO + Na_2O + K_2O + Fe_2O_3 + P_2O_5}{SiO_2 + Al_2O_3 + TiO_2} \quad (5\text{-}8)$$

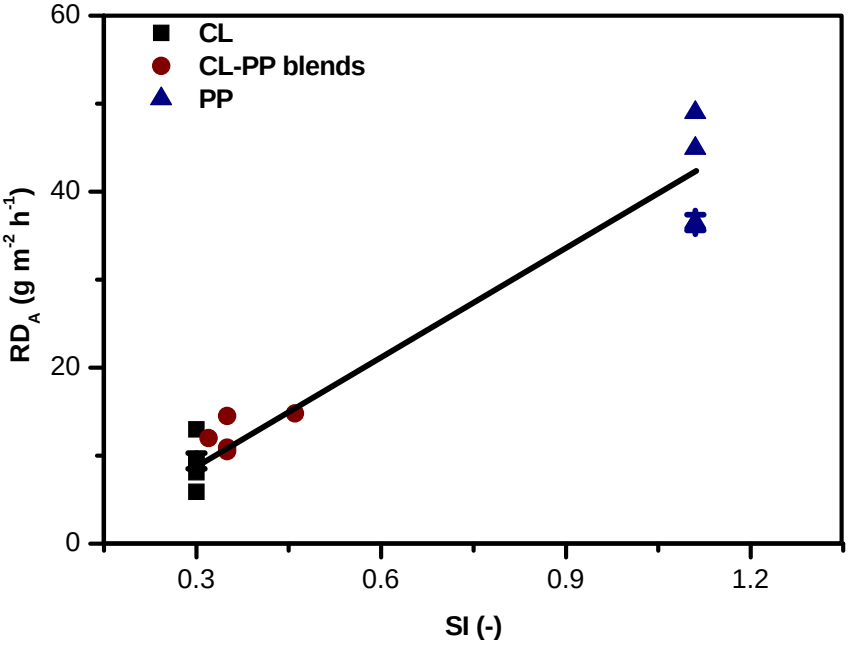

Figure 5-10 Relationships between RD_A and the SI index

RD_A values from all runs were plotted in Figure 5-10 as a function of the calculated SI from the ash compositions of the fuels as given in Table 5-1. The SI values are ranged from about 0.3 to 1.1 for all fuels (blends). An approximately linear relationship of RD_A vs. SI can be observed from Figure 5-10. This result is in agreement with many previous studies (Jensen *et al.*, 1997; Kupka *et al.*, 2008). However, as the SI index only takes into account the ash composition of raw fuels, it becomes less effective for predicting the ash deposition for the operations with the same fuels at different operating conditions (e.g., particle size and moisture content of the fuels, A/F ratio, and with sulphur addition, etc.). For instance, all combustion tests of 100% PP with the same SI value of 1.1 led to an RD_A value ranging from 30 to 50 g m^{-2} h^{-1} under different operating conditions, as displayed in Figure 5-10.

5.4. Conclusions

(1) The contents of chlorine element, alkali/alkaline earth metals and SiO_2 and Al_2O_3 of the feed played a key role in the ash deposition in combustion and co-combustion of lignite coal and a Canadian chlorine-rich peat in a bubbling fluidized bed combustor. A higher chlorine concentration in the feed would generally result in higher tendency of ash deposition. Combustion of 100% peat pellet showed a much higher tendency of ash deposition than combustion of the lignite alone.

(2) Co-firing of the lignite-peat blends with 50% peat resulted in the lowest relative ash deposition rate (RD_A).

(3) Combustion of relatively wet solid fuels produced a decreased RD_A value and reduced chlorine deposition.

(4) Adding sulphur into the fuel of coal or peat could effectively decrease the chloride deposition in the ash deposits, and reduce the ash deposition rate for the combustion of lignite. However addition of sulfur slightly increased the ash deposition rate for the peat fuel.

(5) Fuels with higher ash content would facilitate capturing of the minerals and chlorine in the fly ashes, but most of Cl-containing vapours ended up in the flue gas.

(6) The deposited Ca, Mg, Al and Si elements were present mostly in the forms of calcium and magnesium sulfates, aluminates and silicates that have relatively lower melting points.

5.5. References

Arvelakis, S.; Vourliotis, P.; Kakaras, E.; Koukios, EG. (2001). Effect of leaching on the ash behavior of wheat straw and olive residue during fluidized bed combustion. *Biomass and Bioenergy*; **20**(6):459-470.

Banaee, J.; Larson, R.A. (1993). Effects of additives on the formation of organic chlorine compounds during the combustion of a chlorine-containing polymer. *Waste Manage*; **13**:77-82.

Baxter, L. (2005). Biomass-coal co-combustion: Opportunity for affordable renewable energy. *Fuel*; **84**(10): 1295-1302.

Baxter, L.L.; Miles, T.R.; Miles Jr., T.R.; Jenkins, B.M.; Milne, T.; Dayton, D.; Bryers, R.W.; Oden, L.L. (1998). The behavior of inorganic material in biomass-fired power boilers: field and laboratory experiences. *Fuel Processing Technology*; **54**(1-3):47-78.

Baxter, L.L (1993). Ash deposition during biomass and coal combustion: A mechanistic approach. *Biomass and Bioenergy*; **4**(2):85-102.

Bott, R.D. (2001). Peat. *2010 Historica Foundation of Canada*. The Canadian Encyclopedia (TCE). *http://www.thecanadianencyclopedia.com/index.cfm?PgNm=TCE&Params=A1ARTA006177* (accessed on June 2010).

Crill, P.; Hargreaves, K.; Korhola, A. (2000). The role of peat in Finnish greenhouse gas balances. *Ministry of Trade and Industry*. Helsinki, Finland.

Davidsson, K.O.; Korsgren, J.G.; Pettersson, J.B.C.; Jäglid, U. (2002). The effects of fuel washing techniques on alkali release from biomass. *Fuel*; **81:**137–142.

Deer, W.A.; Howie, R.A.; Zussman, J. (1978). Disilicates and ring silicates-Melilite

group. *Rock-forming minerals*; **1B**: 256-314.

Gogebakan, Z.; Gogebakan, Y.; Selçuk, N.; Selçuk, E. (2009). Investigation of ash deposition in a pilot-scale fluidized bed combustor co-firing biomass with lignite. *Bioresource Technology*; **100**(2):1033-1036.

Hansen, L.A.; Frandsen, F.J.; Dam-Johansen, K.; Sorensen, H.S.; Skrifvars, B.-J. (1999). Characterization of ashes and deposits from high-temperature coal-straw co-firing. *Energy Fuels*; **13**(4):803-16.

Hjalmarsson A. (1990). NO_x control technologies for coal combustion. IEA Coal Research IEACR/24, 1990.

Hoch, M. (1993). Calculation of ternary, quaternary, and higher-order phase diagrams from binary diagrams and binary thermodynamic data. *Phase Equilibria*; **14**(6):710-717.

Hupa, M. (2005). Interaction of fuels in co-firing in FBC. *Fuel*; **84**:1312–1319.

International Energy Agency (IEA) (2010). *Part IV of Coal information* (2010 edition). International Energy Agency. ISBN: 978-92-64-08421-6 (PDF); 978-92-64-08420-9 (print).

Jenkins, B.M.; Bakker, R.R.; Wei, J.B. (1996). On the properties of washed straw. *Biomass and Bioenergy*; **10**(4):177-200.

Jensen, A.; Dam-Johansen, K.; Wójtowicz, M.A.; Serio, M.A. (1998). TG-FTIR Study of the influence of potassium chloride on wheat straw Pyrolysis. *Energy Fuels*;**12**:929-938.

Jensen, P.A.; Sander, B.; Dam-Johansen, K. (2001a). Pretreatment of straw for power production by pyrolysis and char wash. *Biomass and Bioenergy*; **20**(6):431-446.

Jensen, P.A.; Sander, B.; Dam-Johansen, K. (2001b). Removal of K and Cl by leaching of straw char. *Biomass and Bioenergy*; **20**(6):447-457.

Jensen, P.A.; Frandsen, F.J.; Dam-Johansen, K.; Sander, B. (2000). Experimental investigation of the transformation and release to gas phase of potassium and chlorine during straw Pyrolysis. *Energy Fuels*; **14**:1280-1285.

Jensen, P.A.; Stenholm, M.; Hald, P. (1997). Deposition Investigation in Straw-Fired Boilers. *Energy Fuels*; **11**(5):1048-1055.

Kanters, M.L.; Vannispen, R.; Louw, R.; Mulder, P. (1996). Chlorine input and chloro-phenol emission in the lab-scale combustion of municipal solid waste. *Environmental Science & Technology*; **30**:2121-2126.

Knudsen, N.O.; Jensen, P.A.; Sander, B.; Dam-Johansen, K. (1998). Possibilities and evaluation of straw pretreatment. Biomass for Energy and Industry. *Tenth European Conference and Technology Exhibition*, June 8-11, 1998**,** Wurzburg, Germany, pp.224.

Kupka, T.; Mancini, M.; Irmer, M.; Weber, R. (2008). Investigation of ash deposit formation during co-firing of coal with sewage sludge, saw-dust and refuse derived fuel. *Fuel*; **87**(12):2824-2837.

Liu, K.; Xie, W.; Li, D.; Pan, W.P.; Riley, J.T.; Riga, A. (2000a). The effect of chlorine and sulfur on the composition of ash deposits in a fluidized bed combustion system. *Energy Fuels*; **14**(5):963-972.

Liu, K.; Pan, W.P.; Riley, J.T. (2000b). A study of chlorine behavior in a simulated fluidized bed combustion system. *Fuel*; **79**(9):1115-1124.

Lyon, R.E.; Foden, A.J.; Balaguru, P.; Davidovits, J.; Davidovics, M. (1999). Properties

of geopolymer matrix-carbon fiber composites. *Geopolymere '99: Second international conference*, June 30-July 2, 1999, Saint-Quentin, France.

Manninen, H.; Peltola, K.; Ruuskanen, J. (1997). Co-combustion of refuse-derived and packaging-derived fuels (RDF and PDF) with conventional fuels. *Waste Management Research*; **15**(2):137-147.

Monenco Ontario Ltd. (1981). Evaluation of the potential of peat in Ontario. *Ontario Ministry of Natural Re-sources Occasional Paper 7*.

Nielsen, C. (1995). Utilization of straw and similar agricultural residues. *Biomass and Bioenergy*;**9**:315-323.

Nielsen, H.P.; Frandsen, F.; Dam-Johansen, K.; Baxter, L. (2000). The implications of chlorine-associated corrosion on the operation of biomass-fired boilers. *Process in Energy and Combustion Science*; **26**(3): 283-298.

Orjala, M.; Ingalsuo, R. (1999). Sulphur dioxide reduction in co-firing of peat and wood in fluidised bed boilers. *5th International Conference on Technologies and Combustion for a Clean Environment*; **12**(15): 685-689.

Pan, W.P.; Keene, J.; Li, H.; Gill, P.; Quattrochi, M. (1995). The fate of chlorine in coal combustion. *The eighth international conference on coal science*, September 10-15, 1995, Oviedo, Spain, pp. 815-818.

Peat Resources Ltd. (2010). Peat fuel. *http://www.peatresources.com/peat_fuel.htm* (accessed on November 2010).

Raask, E. (1985). Mineral impurities in coal combustion: behavior, problems, and remedial measures. Springer Verlag.

Schwartz, M.M. (1995). Braze filter melt and base material families. In: Brazing: for the

engineering technologist. First editor. London: Chapman&Hall.

Shao, Y.; Xu, C.; Zhu, J.; Preto, F., Wang, J.; Tourigny, G.; Badour, C.; Li, H. (2010). Ash deposition during co-firing biomass and coal in a fluidized-bed combustor. *Energy Fuels*; **24**(9):4681-4688.

Shao, Y.; Xu, C.; Zhu, J.; Preto, F., Wang, J.; Tourigny, G.; Badour, C.; Li, H. (2011). Ash and chlorine deposition during co-firing lignite and a chlorine-rich Canadian peat in a fluidized bed - effects of blending ratio, moisture content and sulfur addition. Submitted to *Fuel.*

Sloss, L.L. (1992). IEA Coal Res., London, IEACR/45.

Sopo, R. (2003). Peat campaign continues. *Peatlands International Magazine*; **2**:4.

Skrifvars, B.J.; Laurén, T.; Backman, R. and Hupa, M. (2002). The role of alkali sulphates and chlorides in post cyclone deposits from circulating fluidized bed boilers firing biomass and coal. In Gupta, R.P.; Wall, T.F.; Baxter, L. (Eds.): *Impact of Mineral Impurities in Solid Fuel Combustion* (Chapter IV: 525-539). *An engineering foundation conference on mineral matter in fuels*, November 2-7, 1997, Kona, Hawaii, USA.

Swierczynski, D.; Libs, S.; Courson, C.; Kiennemann, A. (2007). Steam reforming of tar from a biomass gasification process over Ni/olivine catalyst using toluene as a model compound. *Applied Catalysis B: Environmental*; **74**:211–222.

Telford, P.G. (2009). Peat fuel - a sustainable bioenergy resource. *IASTED International Conference Environmental Management and Engineering (EME 2009)*, July 7-8, 2009, Banff, Canada, pp 6-10.

Turn, S.Q.; Jenkins, B.M.; Jakeway, L.A.; Blevins, L.G.; Williams, R.B.; Rubenstein, G.;

Kinoshita, C.M. (2006). Test results from sugar cane bagasse and high fiber cane co-fired with fossil fuels. *Biomass and Bioenergy*; **30**(6):565-574.

United States Environmental Protection Agency (U.S. EPA) (1990). Clean Air Act. Washington, D.C.; *http://www.epa.gov/air/caa/*.(accessed on January 2008).

Vamvuka, D.; Zografos, D.; Alevizos, G. (2008). Control methods for mitigating ash-related problems in fluidized beds. *Bioresour. Technol.*; **99**:3534–3544.

Vitt, D.H.; Halsey, L.A.; Bauer, I.E. and Campbell. C. (2000). Spatial and temporal trends in carbon storage of peatlands of continental western Canada through the Holocene. *Can. J. Earth Sci.*; **37**(5):683–93.

Wei, X.; Wang, Y.; Liu, D.; Sheng, H.; Tian, W.; Xiao, Y. (2009). Release of sulfur and chlorine during cofiring RDF and coal in an internally circulating fluidized bed. *Energy Fuels*; **23**:1390-1397.

Wei, X.; Lopez, C.; von Puttkamer, T.; Schnell, U.; Unterberger, S.; Hein, K.R.G. (2002). Assessment of chlorine–alkali–mineral interactions during co-combustion of coal and straw. *Energy Fuels*; **16:**1095–1108.

Xie, Y.; Xie, W.; Pan, W.P.; Riga, A. (1998). A study of ash deposits on the exchange tubes using SDT/MS and XRD techniques. *Thermochimica Acta*; **324**:123-133.

Xiong, S.J.; Burvall, J.; Örberg, H.; Kalen, G.; Thyrel, M.; Öhman, M.; Boström, D. (2008). Slagging characteristics during combustion of corn stovers with and without kaolin and calcite. *Energy Fuels*; **22**:3465-3470.

Yudovich, U.; Ketris, M. (2006). Chlorine in coal: a review. *International Journal of Coal Geology*; **67**(1-2):127-144.

CHAPTER 6. ASH DEPOSITION IN CO-FIRING THREE-FUEL BLENDS CONSISTING OF WOODY BIOMASS, PEAT AND LIGNITE

6.1. Introduction

Due to the abundant resources (IEA, 2010; Fernholz, 2009), renewability and the environmental and economic benefits (Hupa, 2005), biomass and peat have become attractive alternatives for fossil fuels and have been widely utilized in many countries in Europe and North America, in particular Finland (Telford, 2009; Bott, 2010; Peat Ltd., 2010). Co-firing technology has been regarded as the most promising technology for applications of bio-energy for energy production on a large-scale, because co-firing of biomass or peat and coal can be employed in most existing coal-fired boilers with minimal capital costs for infrastructures. There are over 150 field demonstration and operation plants of biomass/coal co-firing in approximately 20 countries, involving different types of boilers (i.e. PFC, FBC, etc.) and various kinds of biomasses and coals (IEA, 2009). However, according to the industrial experiences and extensive studies concerning co-firing of coal and biomass (Armesto *et al.*, 2003; Sami *et al.*, 2002; Laursen and Grace; 2002; Leckner, 2006; Nevalainen *et al.*, 2007), the co-firing technology is associated with many challenges including fly ash deposition/fouling/corrosion, fuel preparation/storage/delivery, fly ash utilization, and possible low thermal efficiency and emissions. Among them, ash-related problems are the key issues and long-standing challenges resulting from different characteristics of biomass ash. For instance, biomasses commonly contain high amounts of water soluble inorganic salts which could be easily volatilized during combustion, leading to high mobility for alkali materials in the ash, and hence high fouling propensity

during the co-firing/combustion process (Theis *et al.*, 2006). For fluidized bed combustors, severe ash deposition would lead to fouling, corrosion and de-fluidization, which can decrease the combustor utilizing efficiency and may damage the combustor equipment as well as increase maintenance costs.

At a high temperature, alkali/alkaline metals and chorine contents in biomass fuels are highly active and may form vapor-phase chloride ions/compounds (Baxter, 2005). These chloride compounds commonly have low melting points, less than 800°C, and some of them like KCl is the most stable alkali species in the temperature range 800-1200°C (Baxter *et al.*, 1998). When the chlorides vapor is in contact with cool surfaces such as heat exchanger or heat transfer surfaces, they would easily deposit and form a sticky layer on the surfaces. Subsequently, more inorganic particles in fly ash will have high tendency of adhering to the particles in the existing layer (Nielsen *et al.*, 2000). The increased deposits on the surfaces will cause many problems including reduction of heat transfer efficiency, and fouling/slagging and corrosion, as afore-mentioned.

High-temperature corrosions caused by chlorides may be reduced through reactions between sulphur or silica/alumina and chlorides as shown in the following Eqs. 6-1 and 6-2 (Baxter, 2005; Overgaard *et al.*, 2005; Aho and Silvennoinen, 2004; Coda *et al.*, 2001), but completely removing the chlorine in the deposits is not likely possible due to the limited conditions of temperatures and availabilities of S/Si/Al in the combustion/co-combustion process.

$$2\mathrm{MeCl} + \mathrm{SO_2} + \frac{1}{2}\mathrm{O_2} + \mathrm{H_2O} \rightarrow \mathrm{Me_2SO_4} + 2\mathrm{HCl} \tag{6-1}$$

$$\mathrm{Al_2O_3 \cdot 2SiO_2} + 2\mathrm{MeCl} + \mathrm{H_2O} \rightarrow \mathrm{Me_2O \cdot Al_2O_3 \cdot 2SiO_2} + 2\mathrm{HCl} \tag{6-2}$$

where Me represents alkali metals such as Na or K.

However, the mixtures of chlorides and sulphates/silicates might form lower metling point compomds which may result in worse ash deposition (Skrifvars *et al.*, 2002; Xie *et al.*, 1998; Xu *et al.*, 2010; Shinata, 1987). As such, although the forming alkali-aluminum silicates reduces K/Na chlorides concentration in the combsution flue gas and hence inhibits their condenstion on the superheater surfaces, the formation of deposits with decreased melting temperatures would enhance the fly ash deposition via the inertial impact mechanism (Janz *et al.*, 1976). Therefore, the formation of sulphate, silica or alumina alkali compounds might not be an effective measure to decrease ash deposition rates in some co-firing operations.

As above discussed, ash deposition during co-combustion of fuel blends is a complex process, usually accompanied by complicated interactions between different fuel ashes. Extensive ash-related experimental studies have been focussed on co-firing a non-fouling fuel (e.g., coal) with a "problematic" biomass (e.g., a habecous biomass) (Coda *et al.*, 2001;Gogebakan *et al.*, 2009; Aho and Ferrer, 2005; Skrifvars *et al.*, 2005; Ninomiya *et al.*, 2004). The ash/chlorine deposition behaviors in co-firing of lignite and white pine pellets or peat pellets on a pilot-scale fluidized bed combustor were investigated by the authors' group (Shao *et al.*, 2010; Shao *et al.*, 2011), and some key results obtained from these studies are summarized below:

(1) The contents of Cl, K/Na, Ca/Mg, and Si/Al of the feed played a key role in the ash deposition in combustion and co-combustion of a lignite coal and a woody biomass or a chlorine-rich peat in a bubbling fluidized bed combustor.

(2) A higher chlorine concentration in the feed would generally result in higher tendency of ash deposition.

(3) Combustion of woody biomass or peat showed much higher tendency of ash deposition than combustion of the lignite coal.

(4) Co-firing of the lignite-peat or lignite-pine blends with 50% peat or 50% pine showed reduced ash deposition tendency.

To the best of our knowledge however, co-firing of three-fuel blends of coal, woody biomass and peat has not been studied previously. Co-firing more than two fuels can be easily employed in fluidized-bed combustion facilities. It is thus of great interest to investigate on the ash desposition behaviors for co-firing of the three-fuel blends in fluidized bed combustors. In this work, a woody biomass and a Canadian peat blended with a local coal at different blending ratios were co-fired in a pilot-scale BFB combustor. Using an air-cooled probe installed in the freeboard zone of the combustor to simulate a superheater surface, deposited ashes were collected from the co-firing tests to determine the ash deposition rates. Characteristics of the collected deposits were also comprehensively studied with IC, XRD, SEM and XRF.

6.2. Experimental

6.2.1. Material and Preparation

Three fuels including lignite, white pine, and peat were used in this study, which were supplied by or obtained from OPG, a sawmill in Southern Ontario and Peat Resources Limited, respectively. Detailed proximate and ultimate analyses of these fuels and their ash compositions are given in Table 6-1.

Table 6-1 Proximate and ultimate analyses of the fuels and ash compositions

	Lignite	White Pine Pellet	Peat
Moisture, wt% as received	30.0	5.3	35.8
HHV (MJ/ kg dry)	21.8	20.6	21.4
Proximate analysis, wt% db			
Ash[1]	22.0	3.13	2.0
Volatile matters (VM)	54.0	80.75	68.6
Fixed carbon (FC)	24.0	16.12	29.4
Ultimate analysis, wt% db			
Carbon	58.8	47.99	56.1
Hydrogen	4.2	6.25	5.7
Nitrogen	0.9	1.31	0.8
Sulphur	0.5	0.58	0.2
Oxygen[2]	13.6	40.73	35.2
Chlorine[3], μg/g.	25	312	2008
Bromine[3], μg/g.	< 21	203	153
Fluorine[3], μg/g	100	<18	< 20
Dry ash analysis[4], wt% db			
SiO_2	49.76	3.80	28.05
Al_2O_3	19.71	0.49	8.63
Fe_2O_3	3.82	0.58	5.56
TiO_2	0.86	<0.03	0.48
P_2O_5	0.30	23.13	1.31
CaO	9.91	23.36	12.65
MgO	2.11	6.86	17.72
SO_3	6.09	17.98	12.73
Na_2O	4.20	1.29	2.84
K_2O	1.04	16.46	1.14

[1] The ashing temperature was 750ºC for lignite and 500ºC for white pine;
[2]By difference; [3]By Pyrohydrolysis and IC; [4]By XRF of the ashes from the feedstocks.

Among these three fuels, the lignite coal has the highest ash content (22 wt% dry base) and is characterized by its low VM/FC ≈ 2.3. The white pine (pellets) contains a low amount ash (3.1 wt% dry base) and is characterized by a high VM/FC (≈ 5.0). The peat fuel has a strikingly high chlorine content of 2008 μg/g on a dry basis, a relatively lower amount of ash (2 wt% db), and a VM/FC ratio similar to that of the lignite. With regard to ash composition, the lignite ash is mainly composed of acidic oxides (SiO_2, Al_2O_3 and TiO_2), whereas the ash from the wood is enriched with basic oxides (CaO, MgO, K_2O, Na_2O and Fe_2O_3) and P_2O_5. The peat ash is balanced with acidic oxides and basic oxides.

To prepare coal feedstock for the combustion tests, the received lignite was crushed and screened into particles (<4 mm). The white pine pellets (5 mm outer diameter and 40 mm length) were prepared from white pine sawdust using approximately 1 wt% of the binding agent Ameribond 2x (Ammonium Lignosulfonate). The peat was received in the form of pellets (10 mm diameter, 20 mm length). Two mixtures of these three fuels at different blending ratios were used in the co-firing tests: the mixture of 25% white pine pellets and 25% peat pellets balanced by the crushed lignite, designated as FB1; and the mixture of 20% crushed lignite plus 40% white pine pellets and 40% peat pellets, denoted as FB2. All the fuel blending ratios were based on the heating value of each fuel. The actual moisture contents of each fuel was measured prior to each test, to determine the required fuel feeding rate (so as to maintain the same thermal input of 58.3 MJ/h in each combustion test). The three individual fuels, i.e., the crushed lignite, white pine pellets and peat pellets were denoted as CL, WPP and PP, respectively.

6.2.2. Combustion Facility

The co-firing tests were conducted on a pilot-scale fluidized bed combustor. The facility was a bubbling fluidized bed combustor with a feeding capacity of up to 25 kg/h, and was equipped with a belt feeder and a cyclone. A water-cooled condenser was also equipped to the facility for tar removal. Moreover, on-line measurements of temperature, pressure and flue gas compositions (CO, CO_2, and O_2) were performed. A custom designed air-cooled probe was installed vertically in the freeboard region of the fluidized bed combustor using a flange at the top. The probe made of SS 316L has the total effective length (for ash deposition inside the freeboard zone) of 889 mm and the total external surface area as calculated to be 0.098 m^2. More information about the combustion facility and the deposition probe can be found in our previous publication (Shao *et al.*, 2010; Shao *et al.*, 2011). During the steady operation in all the tests, the surface temperature of the probe was maintained at 430±10 ºC by carefully controlling the flow rate of the cooling air.

6.2.3. Testing Methodologies and Parameters

The reactor was filled with 13 kg of olivine sand as bed materials in each test. The reactor was pre-heated up to above 600ºC using propane gas before introducing the solid fuels. For all the tests reported in this work, a constant heat input of 58.3 MJ/h was used. Depending on the heating values of the fuels, the fuel feed rates ranged from 3.1-3.8 kg/h on a dry basis, and the total air flow rates were at 360-400 L/min for the operation at an excess air ratio of 40%. At the steady state, the combustion temperatures (in the combustion zone or the dense phase of the fluidized bed) were in the range of 800-900°C. A stable temperature profile along the bed height could be obtained through adjusting the

secondary air and primary air ratios (while maintaining a constant total air flow rate). A cleaned probe was installed in the freeboard zone of the reactor, right before the whole unit reached a steady state of operation. In the present study, because of the introduction of the secondary air above the dense phase of the fluidized bed and the inevitable heat loss along the reactor column, the average flue gas temperature in the freeboard and in the vicinity of the ash deposition probe was in the range of 650 - 700ºC. In a typical run, at least 3-4 hours of stable operation was performed before cooling down the reactor to room temperature using nitrogen. When the whole unit was cooled to room temperature, the ash deposition probe was carefully removed from the freeboard and the deposited ash was completely recovered. Figure 6-1 illustrate photos of the ash deposition probe (top) and the collected ash deposits (bottom) after the combustion tests of individual fuels of CL, WPP and PP, and the three-fuel blends of FB1 (25% WPP + 25% PP + 50% CL) and FB2 (40% WPP + 40% PP + 20% CL).

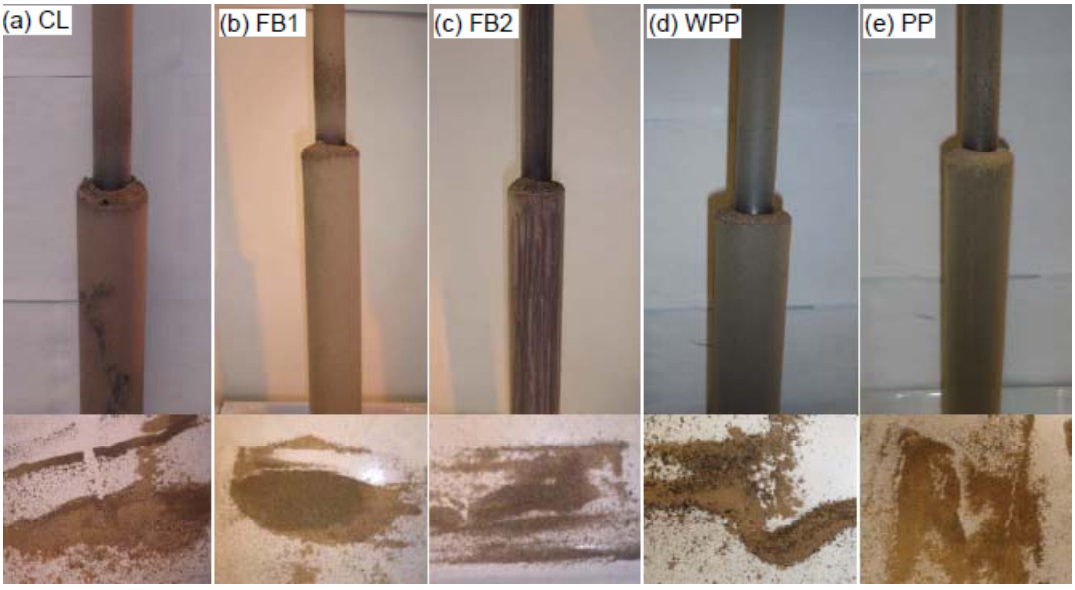

Figure 6-1 Photos of the ash deposition probe (up) and the collected deposit (down) right after the combustion tests of (a) 100% lignite and three-fuel blends (b) FB1 (25% WPP + 25% PP + 50% CL) and (c) FB2 (40% WPP + 40% PP + 20% CL), in comparison with those for (d) 100% WPP, and (e) 100% PP

The recovered ash from the probe was then weighed to calculate the absolute ash deposition rate (D_A, g m^{-2} h^{-1}) and the relative ash deposition rate (RD_A, g m^{-2} h^{-1}), respectively, as defined below:

$$D_A = \frac{\text{Mass of collected ash deposit (g)}}{\text{Surface area of the probe (m}^2\text{)} \times \text{Duration (h)}} \tag{6-3}$$

$$RD_A = D_A \times \frac{\text{Ash feeding rate of crushed lignite (g/h)}}{\text{Ash feeding rate of the fuel (g/h)}} \tag{6-4}$$

As was discussed in Chapters 4 and 5, conclusions were difficult to be drawn based on the D_A results only, because the causes of a low ash deposition rate could be due to either a lower total ash content in the feed (e.g., 2 wt% ash content for the peat vs. 22 wt% ash content for the lignite) or the positive interaction (to suppress the ash deposition) between the ash elements from the component fuels in the fuel blends. A relative ash deposition rate (RD_A) was proposed and used in our previous study. The value of an RD_A was obtained from that of D_A by correction with the ash feeding rate of the base fuel (i.e., CL) in relation to the ash feeding rate of the co-firing fuel in the test. As such, comparison of RD_A values for the co-firing tests would help to rule out the effects of the total ash content in the feed on ash deposition. At the meantime, the value of an RD_A implies the deposition tendency of different co-firing fuels or fuel blends in relation to that of the base fuel (the lignite coal) in combustion.

The collected deposited ashes were comprehensively characterized using various analytical techniques. For example, pyrohydrolysis was used to identify the total chlorine contents. Ion chromatography was further applied to examine the soluble chlorine and sulfur contents. Moreover, mineralogical compositions and the crystallinity of the ash

deposits were analyzed by XRD. Scanning electron microscope was adopted to examine the morphologies of the ash deposits. The chemical compositions of fuel ashes and the ash deposits on the probe were analyzed using XRF in accordance to the ASTM D4326 standard.

Because of the relatively large operating scale and the complexity of the fluidized bed facilities, it normally took 2-3 days to complete a successful combustion/co-combustion test (including fuel/facility preparation, operation, after-run cleaning/maintenance). Thus, reproducibility of the ash deposition rates and the chemical compositions of the deposited ash were examined only for some reference tests in this study. In this work, repeated combustion tests were performed on the 100% crushed lignite for three times and the 100% peat pellets for two times. The relative standard deviations of the ash deposition rates were within 10.0%. The maximum relative errors in the ash concentrations (from the XRF analysis) between the duplicate tests were within 13.0%. These repeated data with error bars are shown in some of the Tables and Figures in the following sections.

6.3. Results and Discussion

6.3.1. Compositions of ash deposits from co-firing of various fuel blends

Due to the difference in the ash compositions in the individual fuel, the ash compositions in the fuel blends varied with the blending ratio. The ash compositions in the fuel blends (FB1 and FB2) were calculated based on the blending ratio and the ash compositions in the individual fuel (Table 6-1) and are shown in Figure 6-2a.

Table 6-2 Mineralogical compositions (wt%) of the deposited ashes obtained from combustion of CL, FB1, and FB2

Fuel	CL	FB1	FB2	WPP	PP
Chemical Compound	Percentage of Chemical Compound (wt%)				
Anhydrite ($CaSO_4$)	4.1	12.7	5.8	4.0	3.6
Hematitle (Fe_2O_3)	1.6	3.7	1.8	2.0	1.0
Lime (CaO)	0.3	0.8	1.0	0.4	0.4
Magnesium Oxide (MgO)	1.3	1.8	0.8	0.5	2.6
Quartz (SiO_2)	7.6	8.2	10.3	2.7	4.2
Åkermanite ($Ca_2MgSi_2O_7$)	0.9	5.2	2.9		2.4
Tychite ($Na_6Mg_2(CO_3)_4(SO_4)$)	1.4	6.2	1.8		1.0
Brownmillerite ($Ca_2Al_2Fe_2O_5$)	1.6	3.5	2.0		
Anorthite ($CaAl_2Si_2O_8$)	1.5		4.1		3.0
Forsterite (Mg_2SiO_4)	5.8		4.7	6.4	14.8
Chromite ($FeCr_2O_4$)				1.8	
Dolomite ($CaMg(CO_3)_2$)	0.9				
Goethite (FeO(OH))	1.5				
Magnesioferrite aluminian ($MgAl_{0.74}Fe_{1.26}O_4$)	1.1				
Calcite ($CaCO_3$)		1.6	1.4		
Magnesium Chlorate Hydrate ($Mg(ClO_4)_2(H_2O)_6$)		3.1			
Hauyne ($Na_6Ca_2Al_6Si_6O_{24}(SO_4)_2$)		0.9			
Mercallite ($KHSO_4$)		0.9			
Sodium Calcium Sulfate Hydrate ($Na_2Ca_5(SO_4)_6{\cdot}3H_2O$)			12.6		
Crystallinity (wt %)	**29.5**	**48.5**	**49.1**	**17.7**	**33.0**
Amorphous content (wt %)	**70.5**	**51.5**	**50.9**	**82.3**	**67.0**

Note: FB1= 25% WPP + 25% PP + 50% CL; FB2= 40% WPP + 40% PP + 20% CL, all the portion is on a thermal basis.

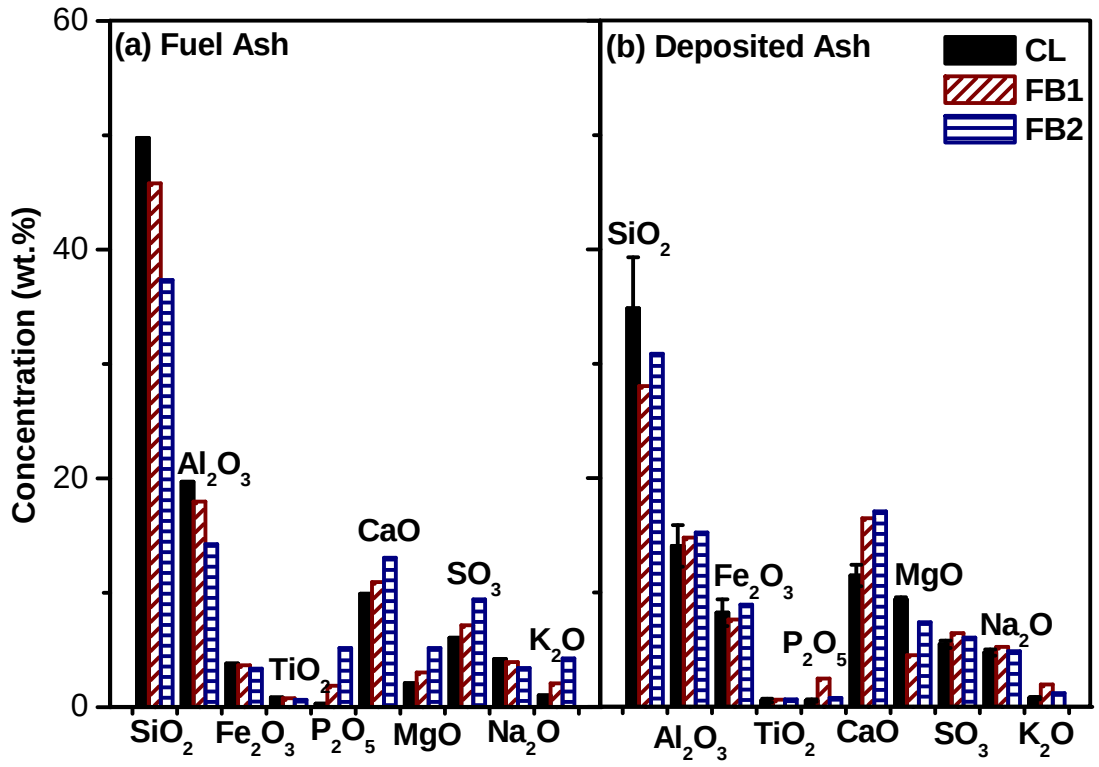

Figure 6-2 Chemical compositions of (a) fuel ash of CL, FB1, FB2, and (b) deposited ash obtained from combustion of 100% CL, three-fuel blends FB1 (25%WPP + 25% PP + 50% CL) and FB2 (40% WPP + 40% PP + 20% CL)

As discussed above, compared to the lignite coal, both fuels of WPP and PP contain low contents of Si and Al, and higher concentrations of P, Ca, Mg, S and K. With the addition of peat and white pine into the lignite coal, the fuel blends of FB1 and FB2 contain lower contents of Si and Al elements, but increased elements of P, Ca, Mg, S and K in their fuel ashes. Similar calculations also show that the two fuel blends of FB1 and FB2 contain higher total chlorine concentrations: 578 μg/g db for FB1 and 943 μg/g db for FB2, compared to 25 μg/g db for the lignite.

It would be interesting to examine the ash compositions in the deposited ashes from the co-firing tests, in order to elucidate the interactions between the fuel ashes during co-firing of the three-fuel blends. The analysis results for the deposited ash obtained from

the combustion of 100% CL, three-fuel blends FB1 (25%WPP + 25% PP + 50% CL) and FB2 (40% WPP + 40% PP + 20% CL) are displayed in Figure 6-2b. Generally, the ash deposits from the combustion of FB1 and FB2 were enriched with the elements of P, Ca, K and S, and were depleted in SiO_2, which are consistent with the original concentration of those elements in the fuel blends (Figure 6-2a). Interestingly, the ash deposits from the three-fuel blends were enriched in Al, while the Al concentrations in both flue blends were lower than that in the coal. Moreover, compared to that from FB1, the combustion of FB2 produced higher concentrations of Al, Si, Ca and Mg, and lower amounts of the elements of P and K. These results demonstrate that there were interactions between the fuel ashes during co-firing of the three-fuel blends, and these interactions would influence the ash deposition rates, which will be discussed in the following section.

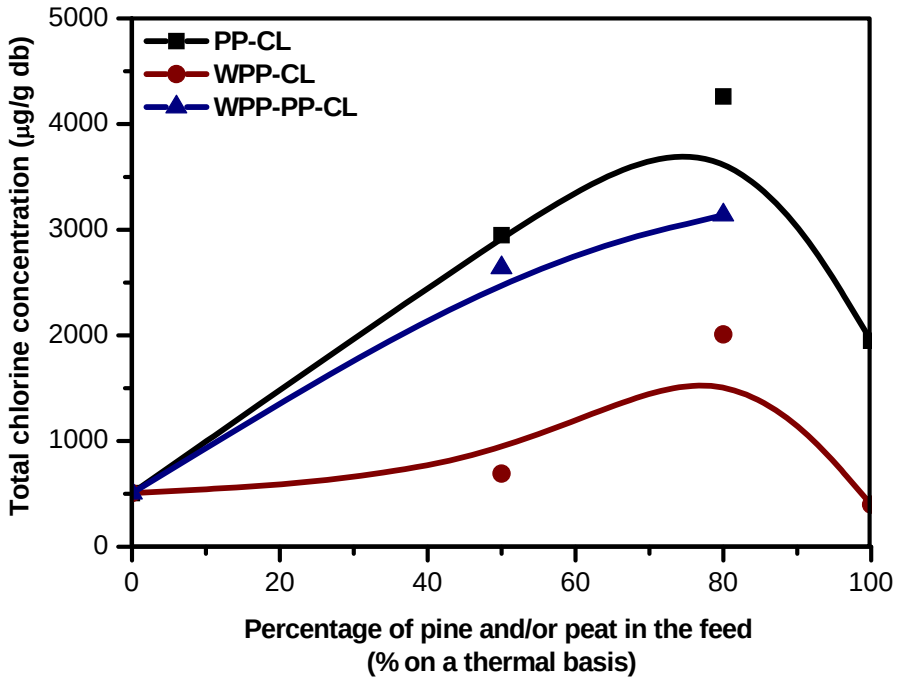

Figure 6-3 Total chlorine concentrations in the deposits obtained from the combustions of 100% CL and three-fuel blends FB1 (25% WPP + 25% PP + 50% CL) and FB2 (40% WPP + 40% PP + 20% CL), in comparison with those from combustion of 50% WPP + 50% CL, 50% PP + 50% CL, 80% WPP + 20% CL, 80% PP + 20% CL as well as 100% WPP, and 100% PP

Figure 6-3 shows the total chlorine concentrations in the deposits obtained from the combustions of 100% CL and the three-fuel blends FB1 (25% WPP + 25% PP + 50% CL) and FB2 (40% WPP + 40% PP + 20% CL), in comparison with those from combustion of 50% WPP + 50% CL, 50% PP + 50% CL, 80% WPP + 20% CL, 80% PP + 20% CL as well as 100% WPP, and 100% PP. As clearly shown in Figure 6-3, compared with combustion of individual fuel of either CL, PP or WPP, combustion of any fuel blends, regardless of two-fuel blends (i.e., WPP-CL or PP-CL) or three-fuel blends (WPP-PP-CL) produced an ash deposit with a much higher total Cl content. Some of these results, e.g., the addition of PP or WPP led to more Cl deposition from the combustion of the fuel blends than that from the CL, are not a surprise, as they were simply due to the higher Cl contents in the fuel blends. As the peat and white pine pellets used in this research contain a very high chlorine concentration (2008 μg/g db for PP and 312 μg/g db for WPP) compared to 25 μg/g db in the lignite used. However, the result that the combustion of any fuel blends produced more Cl deposition in the ash than combustion of the PP or WPP alone, needs some explanation. The increased Cl deposition from the combustion of fuel-blends might be explained by the increased reactions between the alkali/alkali-earth metals mainly from the lignite and the Cl-vapor mainly derived from the peat and white pine pellets (Kanters *et al.*, 1996; Banaee and Larson, 1993; Pan *et al.*, 1995). The markedly low chlorine concentrations in the deposits obtained from combustion of 100% WPP or 100% PP were likely due to the much lower ash content in the pine (3 wt%) and the peat (2 wt%) fuels, only about one tenth of that of the lignite fuel (22 wt%). Because of such low ash content in WPP and PP, the absolute amount of alkali/alkaline metals in the fuels are also much lower than the WPP/PP-CL

blends, which would suppress the reactions between the alkali/alkaline metals and the Cl-vapor. Consequently, combustion of 100% WPP or 100% PP led to lower chlorides (such as NaCl, KCl, $CaCl_2$ and $MgCl_2$) deposited on the probe surface.

6.3.2. Ash deposition rates from co-combustion of various fuel blends

Figure 6-4 shows the comparison of ash deposition rates for the combustion of individual fuels and various fuel blends. As clearly shown in Figure 6-4a, the absolute ash deposition rate (D_A) consistently decreased with increasing the blending ratios of WPP and/or PP. This may simply ascribe to the lower ash content in the white pine pellets (3.1 wt% db) or the peat pellets (2 wt% db) compared to that of the lignite coal (22 wt%). However, as mentioned previously, conclusions were difficult to be drawn based on the D_A results only, because the causes of a low ash deposition rate could be due to either a lower total ash content in the feed (e.g., 2 wt% ash content for the peat vs. 22 wt% ash content for the lignite) or the positive interaction (to suppress the ash deposition) between the ash elements from the component fuels in the fuel blends. A relative ash deposition rate (RD_A) was proposed (Eq. 6-4) and used in previous Chapters. The value of an RD_A was obtained from that of D_A by correction with the ash feeding rate of the base fuel (i.e., CL) in relation to the ash feeding rate of the co-firing fuel in the test. As such, comparison of RD_A values for the co-firing tests would help to rule out the effects of the total ash content in the feed on ash deposition. At the meantime, the value of an RD_A implies the deposition tendency of different co-firing fuels or fuel blends in relation to that of the base fuel (lignite coal) in combustion.

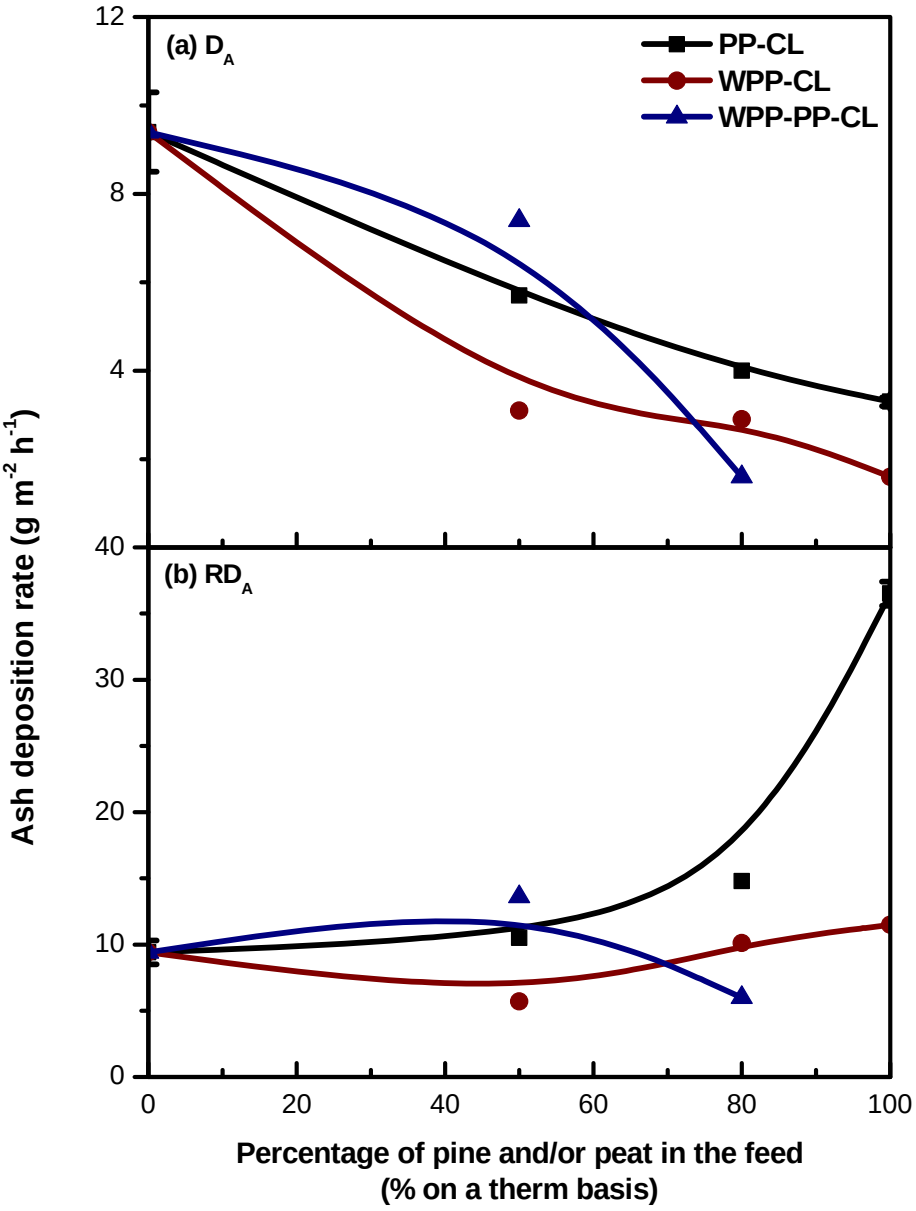

Figure 6-4 Comparison of absolute ash deposition rates D_A (a) and relative ash deposition rates RD_A (b) obtained from the combustions of 100% lignite and three-fuel blends FB1 (25% WPP + 25% PP + 50% CL) and FB2 (40% WPP + 40% PP + 20% CL), in comparison with those from combustion of 50% WPP + 50% CL, 50% PP + 50% CL, 80% WPP + 20% CL, 80% PP + 20% CL as well as 100% WPP, and 100% PP

As displayed in Figure 6-4b, the relative ash deposition rates from the individual fuel of WPP or PP and various fuel blends, except the 50%WPP-50%CL and 40%WPP-40%PP-20%CL blends, were higher than that of from the lignite coal. The high relative

ash deposition rates from the individual fuel of WPP or PP and various fuel blends may be explained by the higher Cl contents in these fuels (2008 μg/g db for PP and 312 μg/g db for WPP, compared to 25 μg/g db in the lignite used). The higher Cl content in the fuel could promote the reactions between the alkali/alkali-earth metals and the Cl-vapor to form alkali/alkali-earth metal chlorides (such as NaCl, KCl, $CaCl_2$ and $MgCl_2$) (Kanters *et al.*, 1996; Banaee and Larson, 1993; Pan *et al.*, 1995). This could be evidenced by the results as discussed earlier in Figure 6-3, where the total Cl compositions of the ash deposits from the individual fuel of WPP or PP and various fuel blends were higher than that from 100% CL. The deposited chlorides usually have relative low melting points (700-800°C) and would form a sticky layer on the heat transfer surface, leading to an increased relative ash deposition rate.

The ash deposition tendency for the three-fuel blends was found to be strongly dependent on the fuel blending ratio. Combustion of the three-fuel blend FB1, 25%WPP-25%PP-50%CL resulted in a much higher RD_A than combustion of any two-fuel blends of 50%WPP (or PP)-50%CL. More interestingly, combustion of the three-fuel blend FB2, 40%WPP-40%PP-20%CL, resulted in the lowest RD_A than combustion of any individual fuel and any fuel blends. This suggests that co-combustion of the three-fuel blends at a proper blending ratio could yield synergistic effects on suppressing the ash deposition tendency. It is thus of particular interest to discuss about the possible cause for the above mentioned result. As described earlier in Figure 6-2, compared to that from FB1, the combustion of FB2 produced higher concentrations of Al, Si, Ca and Mg, and lower amounts of the elements of P and K, likely resulting from the interactions between the fuel ashes during co-firing of the three-fuel blends. Furthermore, Table 6-2 provides

mineralogical compositions of the deposited ashes obtained from combustion of CL, WPP, PP and their blends (FB1 and FB2). As clearly observed from these XRD analytical results, the deposited ash from FB2 contains the highest concentrations of lime (CaO), quartz (SiO_2), *akermanite* ($Ca_2MgSi_2O_7$) and *anorthite* ($CaAl_2Si_2O_8$). It is thus believed that the Al and Si would trap alkali/alkaline (K/Na/Ca/Mg) to prevent from the formation of the lower-melting-point and corrosive alkali chlorides via the reaction of Eq. 6-2 (Overgaard *et al.*, 2005; Aho and Silvennoinen, 2004; Coda *et al.*, 2001), which could hence decrease the ash deposition tendency of the fly ash during the combustion of the three-fuel mixture (FB2). In addition, from Table 6-2, one may find that the deposited ash from FB2 has the highest crystallinity among those from all individual and blended fuels. Xiong and co-workers (2008) reported the presence of a significantly high percentage of amorphous components in the deposited ashes was due to the relatively low operating temperature of the fluidized bed combustor (800-900°C). On the other hand, compared with in FB1, more substitution of WPP and PP in FB2 resulted in much more volatile matters (VM) in the fuel mixture. In the devolatilization stage of the FB2 combustion, volatile P_2O_5, SO_3/SO_2 and the vapor of KCl might rapidly release from the fuel, resulting in a shorter contact time of these species with the ash deposition probe because of the relatively larger air flow rate in the reactor system and thus a reduced ash deposition tendency (Baxter *et al.*, 1998; Molcan *et al.*, 2009). In summary, the formation of minerals with a higher ash melting point and crystallinity, and the rapidly release of fly-ash species during the combustion of FB2 may account for its slow ash deposition.

6.3.3. Morphology of ash deposits from co-firing of three-fuel blends

The morphological differences between the ash deposits from the individual fuels (CL, WPP and PP) and the three-fuel blends can be viewed from Figure 6-6. The particle sizes of all ash deposits obtained from the tests are in a wide range of 10-200 μm. The formation of big fly ash particles suggested aggregation of fine (submicron) particles such as alkali chlorides and alkali aluminum silicates (Nielsen *et al.*, 2000; Xu *et al.*, 2010). The fine particles with relatively low melting points could play a role as "glue" for coarse particles to form bigger particles. Some big particles of wood cell wall-like structure can be observed in the ash deposit from the combustion of pure white pine pellets and pure peat pellets. They are likely the unburned carbon particles from the woody biomass or the peat fuel (Lind *et al.*, 2002), as confirmed by the magnified images of the particles (right side images of Figure 6-6d and Figure 6-6e). This result suggests that in combustion of WPP or PP some solids fines (of a lower density) from the WPP or PP fuel would be entrained to the freeboard zone of the fluidized bed reactor, and deposit on the probe as unburned carbon particles along with the fly ash.

Magnified SEM images of the ash deposits are presented in the right side of Figure 6-6. The deposited ash particles from combustion of pure lignite have a round/spherical shape with relatively dense structure. In contrast, the deposited ash particles from combustion of the woody biomass and the peat fuels have an irregular shape with relatively loose structure, which is consistent with observations by other researchers (Lind *et al.*, 2002; Jenkins *et al.*, 2002). The ash particles from co-firing of the three-fuel blends exhibit a round shape and porous structure, and the pore size seemed to be enlarged when increasing the share of pine and peat in the blended fuel mixtures (Figure 6-6c). The effects of fuel blending on the morphology of the ash deposits could be related to many factors such as devolatilization/combustion of the fuel blends and the interaction between the ash components from different fuels during the co-firing process. More research is needed in this regard.

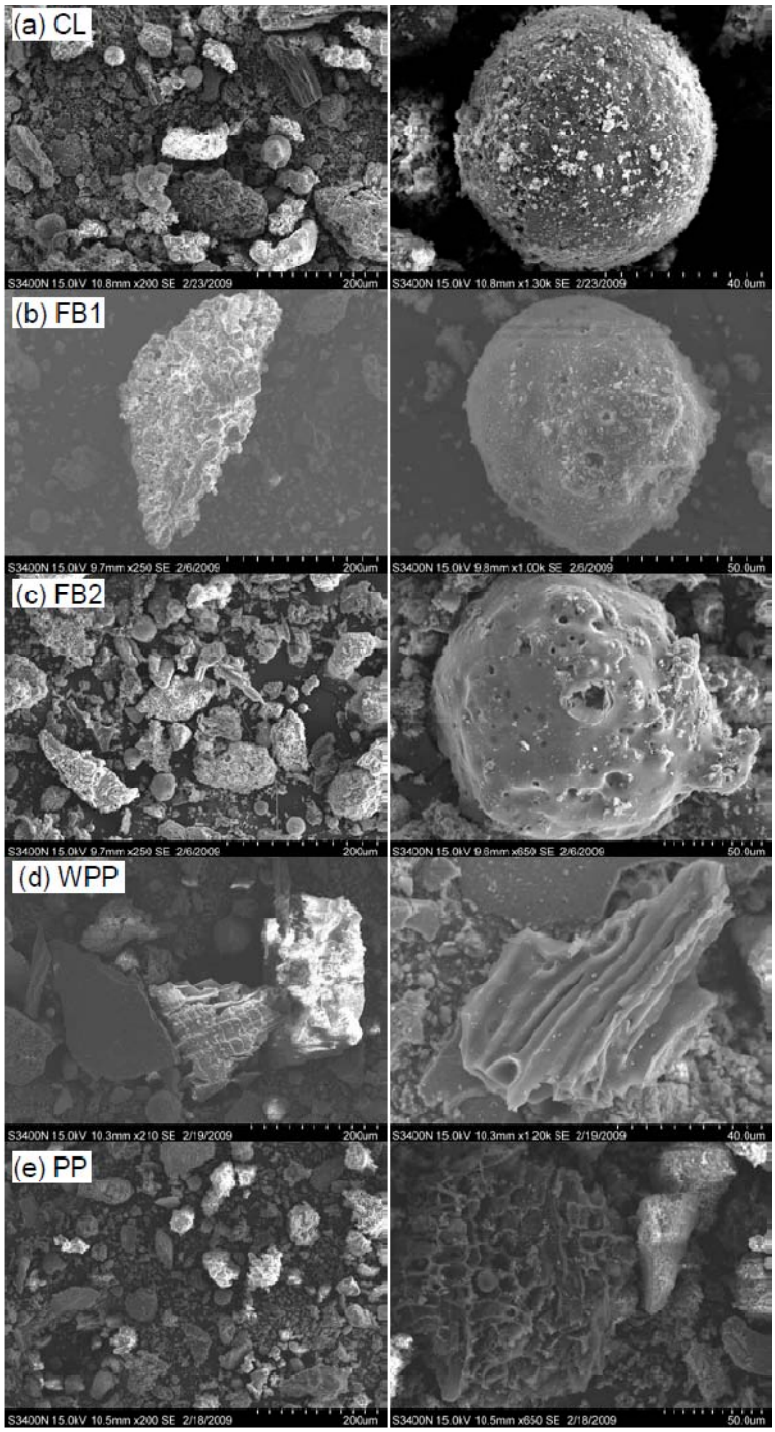

Figure 6-5 SEM morphological transformation of ash deposits in combustion of (a) 100% CL, (b) FB1 (25% WPP + 25% PP + 50% CL), and (c) FB2 (40% WPP + 40% PP + 20% CL) in comparison with those for (d) 100% WPP (d), and (e) 100% PP

6.4. Conclusions

(1) Generally, the ash deposits from the combustion of three-fuel blends consisting of crushed lignite coal (CL), white pine pellets (WPP) and peat pellets (PP) were enriched with the elements of Al, P, Ca, K and S. Compared to that from FB1 (25%WPP-25%PP-50%CL), the combustion of FB2 (40%WPP-40%PP-20%CL) produced higher concentrations of Al, Si, Ca and Mg, and lower amounts of the elements of P and K in the deposited ash.

(2) Compared with combustion of individual fuel of either CL, PP or WPP, combustion of any fuel blends regardless of two-fuel blends (i.e., WPP-CL or PP-CL) or three-fuel blends (WPP-PP-CL) produced an ash deposit with a higher total Cl content. The increased Cl deposition from the combustion of fuel-blends might be explained by the increased reactions between the alkali/alkali-earth metals mainly from the lignite and the Cl-vapor mainly derived from the peat and white pine pellets.

(3) Combustion of the three-fuel blend 40%WPP-40%PP-20%CL resulted in the lowest RD_A than combustion of any individual fuel and any fuel blends. This suggests that co-combustion of the three-fuel blends at a proper blending ratio could yield synergistic effects on suppressing the ash deposition tendency.

(4) The formation of minerals with a higher ash melting point and crystallinity such as lime (CaO), quartz (SiO_2), *akermanite* ($Ca_2MgSi_2O_7$) and *anorthite* ($CaAl_2Si_2O_8$), and the rapidly release of fly-ash species during the combustion of the three-fuel blend 40%WPP-40%PP-20%CL may account for the slow ash deposition in the combustion.

6.5. References

Aho, M.; Ferrer, E (2005). Importance of coal ash composition in protecting the boiler against chlorine deposition during combustion of chlorine-rich biomass. *Fuel*; **84**:201–212.

Aho, M.; Silvennoinen, J. (2004). Preventing chlorine deposition on heat transfer surfaces with aluminium–silicon rich biomass residue and additive. *Fuel*; **83**:1299-1305.

Armesto, L.; Bahillo, A.; Cabanillas, A.; Veijonen, K.; Otero, J.; Plumed, A.; Salvador, L. (2003). Co-combustion of coal and olive oil industry residues in fluidized bed. *Fuel*; **82**: 993-1000.

Banaee, J.; Larson, R.A. (1993). Effects of additives on the formation of organic chlorine compounds during the combustion of a chlorine-containing polymer. *Waste Manage*; **13**:77-82.

Baxter, L. (2005). Biomass-coal co-combustion: Opportunity for affordable renewable energy. *Fuel*; **84**(10): 1295-1302.

Baxter, L.L.; Miles, T.R.; Miles Jr., T.R.; Jenkins, B.M.; Milne, T.; Dayton, D.; Bryers, R.W.; Oden, L.L. (1998). The behavior of inorganic material in biomass-fired power boilers: field and laboratory experiences. *Fuel Processing Technology*; **54**(1-3):47-78.

Bott, R.D. (2010). Peat. *2010 Historica Foundation of Canada*. The Canadian Encyclopedia (TCE). *http://www.thecanadianencyclopedia.com/index.cfm?PgNm=TCE&Params=A1ARTA006177* (accessed on June 2010).

Coda, B.; Aho, M.; Berger, R.; Hein, K.R.G. (2001). Behavior of chlorine and enrichment of risky elements in bubbling fluidized bed combustion of biomass and

waste assisted by additives. *Energy Fuels*; **15**(3): 680-690.

Fernholz, K. (2009). Energy from woody biomass: a review of harvesting guidelines and a discussion of related challenges. Divetail Partners, Inc. *http://www.dovetailinc.org/files/DovetailBioGuides0709.pdf* (accessed on October 2009).

Gogebakan, Z.; Gogebakan, Y.; Selçuk, N.; Selçuk, E. (2009). Investigation of ash deposition in a pilot-scale fluidized bed combustor co-firing biomass with lignite. *Bioresource Technology*; **100**(2):1033-1036.

Hupa, M. (2005). Interaction of fuels in co-firing in FBC. *Fuel*; **84**:1312–1319.

International Energy Agency (IEA) (2010). *Part IV of Coal information* (2010 edition). International Energy Agency. ISBN: 978-92-64-08421-6 (PDF); 978-92-64-08420-9 (print).

International Energy Agency (IEA) (2007). Bioenergy project development & biomass supply. http://www.iea.org/textbase/nppdf/free/2007/biomass.pdf (accessed on February, 2009).

Janz, G.J.; Allen, G.B.; Downey Jr., J.R.; Tamkins, R.P.T. (1976). Eutectic data; safety, hazard, corrosion, melting points, compositions and bibliography. *Troy, NY: Molten Salts Data Center, Rensselaer Polytechnic Institute*, 1976.

Jenkins, B.M.; Thy, P.; Turn, S.Q.; Blevins, L.G.; Baxter, L.L. and Jakeway, L.A.; Williams, R.B.; Blunk, S.L.; Yore, M.W.; Wu, B.C.; Lesher, C.E. (2002). Composition and microstructure of ash deposits from co-firing biomass and coal. *http://www.google.ca/#sclient=psy&hl=en&site=&source=hp&q=composition+and+microstructure+of+ash+deposits+from+co-*

firing+biomass+and+coal&btnG=Google+Search&aq=&aqi=&aql=&oq=&gs_rfai=&pbx=1&fp=f995bf2ea2a12dc1 (Access on March 2008).

Kanters, M.L.; Vannispen, R.; Louw, R.; Mulder, P. (1996). Chlorine input and chlorophenol emission in the lab-scale combustion of municipal solid waste. *Environmental Science & Technology*, **30**:2121-2126.

Kazagic, A.; Smajevic, I. (2009). Synergy effects of co-firing wooden biomass with Bosnian coal. *Energy*; **34**:699-707.

Kupka, T.; Mancini, M.; Irmer, M.; Weber, R. (2008). Investigation of ash deposit formation during co-firing of coal with sewage sludge, saw-dust and refuse derived fuel. *Fuel*; **87**(12):2824-2837.

Laursen, K.; Grace, J.R. (2002). Some implications of co-combustion of biomass and coal in a fluidized bed boiler. *Fuel Processing Technology*; **76**(2):77-89.

Leckner, B. (2006). Possibilities and limitations of co-firing of biomass. In Proceeding of 1st Project Conference AGS, Stockholm, October 2006.

Lind, T.; Kauppinen, E.I.; Sfiris, G.; Nillson, K.; Maenhant, W.C. (2002). Fly ash deposition onto the convective heat exchangers during combustion of willow in a circulating fluidized bed boiler. In Gupta, R.P., Wall, T.F. and Baxter, L. (Eds.): Impact of mineral impurities in solid fuel combustion (Chapter 4: 541-53), US: Springer.

Molcan, P.; Lu, G.; Le Bris, T.; Yan, Y.; Taupin, B.; Caillat, S. (2009). Characterization of biomass and coal co-firing on a 3 MWth combustion test facility using flame imaging and gas/ash sampling techniques. *Fuel*; **88**:2328-2334.

Nevalainen, H.; Jegoroff, M.; Saastamoinen, J.; Tourunen, A.; Jantti, T.; Kettunen, A.;

Johnsson, F.; Niklasson, F. (2007). Firing of coal and biomass and their mixtures in 50kW and 12MW circulating fluidized beds-Phenomenon study and coparison of scales. *Fuel*; **86**(14): 2043-2051.

Nielsen, H.P.; Baxter, L.L.; Sclippab, G., Morey, C., Frandsen, F.J.; Dam-Johansen, K. (2000). Deposition of potassium salts on heat transfer surfaces in straw-fired boilers: a pilot-scale study. *Fuel*; **79**(2):131-139.

Ninomiya, Y.; Zhang, L.; Sakano, T.; Kanaoka, C.; Masui, M. (2004). Transformation of mineral and emission of particulate matters during co-combustion of coal with sewage sludge. *Fuel*; **83**(6):751-764.

Overgaard, P.; Larsen, E.; Friborg, K.; Hille, T.; Jensen, P.A.; Knudsen, S. (2005). Full-scale tests on co-firing of straw in a natural gas-fired boiler. *http://www.dongenergy.com/SiteCollectionDocuments/NEW%20Corporate/PDF/Engineering/42.pdf.* (accessed on February 2008).

Pan, W.P.; Keene, J.; Li, H.; Gill, P.; Quattrochi, M. (1995). The fate of chlorine in coal combustion. *The eighth international conference on coal science*, September 10-15, 1995, Oviedo, Spain, pp. 815-818.

Peat Resources Ltd. Peat fuel. *http://www.peatresources.com/peat_fuel.htm* (accessed on November 2010).

Sami, M.; Annamalai, K.; Wooldridge, M. (2002). Co-firing of coal and biomass fuel blends. *Progress in Energy and Combustion Science*; **27**(2): 171-214.

Shao, Y.; Xu, C.; Zhu, J.; Preto, F., Wang, J.; Tourigny, G.; Badour, C.; Li, H. (2010). Ash deposition during co-firing biomass and coal in a fluidized-bed combustor. *Energy Fuels*; **24**(9):4681-4688.

Shao, Y.; Xu, C.; Zhu, J.; Preto, F., Wang, J.; Tourigny, G.; Badour, C.; Li, H. (2011). Ash and chlorine deposition during co-firing lignite and a chlorine-rich Canadian peat in a fluidized bed - effects of blending ratio, moisture content and sulfur addition. Submitted to *Fuel.*

Shinata, Y. (1987). Accelerated oxidation rate of chromium induced by sodium chloride. *Oxidation of Metals*; **27**(5-6):315-332.

Skrifvars, B.J.; Yrjas, P.; Laurén, T.; Kinni, J.; Tran, H.; Hupa, M. (2005). The fouling behavior of rice husk ash in fluidized-bed combustion. 2. Pilot-scale and full-scale measurements. *Energy Fuels*; **19**:1512–1519.

Skrifvars, B.J.; Backman, R.; Hupa, M.; Sfiris, G.; Åbyhammar, T.; Lyngfelt, A. (1997). Ash behavior in a CFB boiler during combustion of coal, peat or wood. *Fuel*; **77**(1/2): 65-70.

Telford P.G. (2009). Peat fuel - a sustainable bioenergy resource. *IASTED International Conference Environmental Management and Engineering (EME 2009)*, July 7-8, 2009, Banff, Canada, pp 6-10.

Theis, M., Skrifvars, B.J., Zevenhoven, M., Hupa, M. and Tran, H. (2006), Fouling tendency of ash resulting from burning mixtures of biofuels. Part 2: Deposit chemistry. *Fuel*; **85**(14-15):1992-2001.

Xie, Y.; Xie, W.; Pan, W.P.; Riga, A. (1998). A study of ash deposits on the exchange tubes using SDT/MS and XRD techniques. *Thermochimica Acta*; **324**:123-133.

Xiong, S.J.; Burvall, J.; Örberg, H.; Kalen, G.; Thyrel, M.; Öhman, M.; Boström, D. (2008). Slagging characteristics during combustion of corn stovers with and without kaolin and calcite. *Energy Fuels*; **22**:3465-3470.

Xu, X.G.; Li, S.Q.; Li, G.D.; Yao, Q. (2010). Effect of co-firing straw with two coals on the ash deposition behavior in a down-fired pulverized coal combustor. *Energy Fuels*; **24**:241-249.

CHAPTER 7. ASH DEPOSITION IN AIR-BLOWN GASIFICATION OF PEAT AND WOODY BIOMASS

7.1. Introduction

Biomass as a renewable and carbon-neutral fuel with abundant resources (Fernholz, 2009; Wood and Layzell, 2003) has been widely utilized for heat and power generation via kinds of conversion processes such as direct combustion/co-combustion, prolysis and bio-conversions (McGowan, 1991; Hall *et al.*, 1992). Among all biomass conversion technologies, gasification is attractive because of its higher energy efficiency, larger biomass loading compared to combustion, reduced CO_2 emissions, and compact equipment with a smaller footprint (Overgaard *et al.*, 2005; Morehouse and Detwiler, 2009). Biomass gasification is a thermo-chemical conversion technology using gasification agents including air/oxygen, steam or CO_2 for converting biomass into low to medium Btu fuel gases (5-15 MJ/Nm^3). The gases produced during biomass gasification such as H_2, CO, CO_2, CH_4 and C_{2+} can be utilized directly as fuels for heat and electricity generation, or as feedstocks for productions of liquid fuels and chemicals (methanol, ethanol, dimethyl ether, and Fischer-Tropsch oils, etc.) (McKendry, 2002a).

However, biomass gasification technology still has some challenges, in particular the tar formation and the quality of the gas products. In biomass gasification, a highly variable mixture of condensable aromatic hydrocarbons (single ring to 5-ring aromatic compounds) along with other oxygen-containing hydrocarbons and complex PAH, so called tars, are produced (Lopamudra *et al.*, 2003). Generally, an air/steam gasification process produces tar at approximately 20 g per Nm^3 of the flue gas (McKendry, 2002b). In an air-blown fluidized bed gasifier, typical tar contents in

producer gas were reported between 0.5 and 100 g/m^3 (Han and Kim, 2008; Asadullah *et al.*, 2003; Lopamudra *et al.*, 2003). The production of tars instead of combustible gases decreases the gasification efficiency and the condensation and deposition of tars at temperatures below 350°C can lead to fouling and potential blockage of downstream equipment and piping (Lopamudra *et al.*, 2003).

On the other hand, biomass fuels, particularly some agricultural residues, usually contain high concentrations of inherent inorganic elements such as potassium, sodium, calcium, silicon, and phosphorus etc. (Bryers, 1996), which lead to an increased tendency of ash deposition, leading to fouling/slagging/corrosion problems (Björkman and Strömberg, 1997; Olsson *et al.*, 1997). Moreover, high chlorine contents were also found in some biomass to exacerbate the alkali metal emission from the ash above 500°C (Jensen *et al.*, 2000). The alkali/alkaline-containing vapors thus may react with other elements and partially condensed onto the reactor internal wall or some heat transfer surfaces (Michelsen *et al.*, 1998; Baxter *et al.*, 1998). Some of fly ash may also enter downstream equipments and damage gas turbine hardware as a result of alkali corrosion and/or deposition (Salo and Mojtahedi, 1998).

Using reactive bed materials in fluidized-bed gasifiers has been proved an effective and economical primary approach to reduce/remove tar during gasification (Devi *et al.*, 2003). Such reactive bed materials as natural olivine ($(Fe_xMg_{1-x})_2SiO_4$) (Pencho et al., 2008), calcined dolomite (CaO-MgO) (Gusta *et al.*, 2009), and calcined limestone (calcite) (Weimer *et al.*, 2008) were investigated and have been commonly used for in-bed tar control during biomass gasification. Many literature studies have been published concerning the effects of bed materials on the reduction of tar formation. However, there

is almost no reported study concerning the effects of bed materials and other operating parameters for fluidized bed gasification on ash deposition. Attrition and thermal instability of the bed materials are the major issues for use of such active bed materials in a fluidized bed reactor (Rapagnà *et al.*, 2000), which would affect the ash deposition behaviors during the gasification process.

In this study, the air-blown gasification tests were performed on a pilot-scale air-blown bubbling fluidized-bed gasifier using four different bed materials (olivine, limestone, dolomite, and iron ore) and at varying ER (0.20-0.35). An air-cooled probe was installed in the freeboard of the gasifier to simulate a surface of reactor wall, heat transfer surface or the surface of the downstream equipment/pipes. A typical woody biomass (i.e., white pine sawdust) and a Canadian peat were used for the gasification tests.

7.2. Experimental

7.2.1. Materials and Preparation

A woody biomass, white pine sawdust and a Canadian peat fuels were used in this study. They were supplied by a local sawmill in southern Ontario and obtained from Peat Resources Limited, respectively. The detailed proximate and ultimate analyses of these two fuels and their ash compositions are given in Table 7-1.

Table 7-1 Proximate and ultimate analyses of the fuels and ash compositions

	White Pine	Peat
Moisture, wt% as received	38.0	35.8
HHV (MJ/ kg dry)	20.6	21.4
Proximate analysis, wt% db		
Ash[1]	0.4	2.0
Volatile matters (VM)	84.5	68.6
Fixed carbon (FC)	15.1	29.4
Ultimate analysis, wt% db		
Carbon	52.5	56.1
Hydrogen	6.3	5.7
Nitrogen	0.1	0.8
Sulphur	<0.1	0.2
Oxygen[2]	40.6	35.2
Chlorine[3], μg/g db	39	2008
Bromine[3], μg/g db	< 29	153
Fluorine[3], μg/g db	< 29	< 20
Dry ash analysis[4], wt% db		
SiO_2	6.70	28.05
Al_2O_3	1.97	8.63
Fe_2O_3	1.46	5.56
TiO_2	0.09	0.48
P_2O_5	3.52	1.31
CaO	31.10	12.65
MgO	4.34	17.72
SO_3	2.80	12.73
Na_2O	0.36	2.84
K_2O	15.45	1.14

[1] The ashing temperature was 500ºC ;[2]By difference;
[3] By Pyrohydrolysis and IC; [4] By XRF of the ashes from the feedstock.

The white pine sawdust has extremely low ash content, i.e., 0.4 wt% on a dry basis, and is characterized by its high VM/FC≈5.6. The peat contains strikingly high chlorine content of 2008 μg/g and is characterized by its low VM/FC (≈2.3). With regard to ash composition, both the fuels contain high concentrations of alkaline-earth metals (Ca, Mg) in their ashes, but the white pine has higher alkali metals (K+Na) than the peat. The ash from the white pine is enriched with basic oxides (CaO, MgO, K_2O, Na_2O, and Fe_2O_3) and P_2O_5, while the peat is balanced between acidic oxides (SiO_2, Al_2O_3, and TiO_2) and basic oxides.

Olivine, limestone, dolomite and iron ore were used as bed materials in the gasification tests. The sands, olivine, limestone, and dolomite, were used as received from various commercial sources. The olivine sand used mainly consists of MgO (42.5 wt%), SiO_2 (42 wt%), Fe_2O_3 (8.5 wt%), CaO (0.9 wt%), and Al_2O_3 (0.8 wt%). The major components of the dolomite are CaO (30.4 wt%) and MgO (21.7 wt%). The limestone after calcination is mainly CaO. In addition, limonite iron ore was obtained from the former Steep Rock Mine site in Atikokan, Ontario. Analysis of the material by XRD showed that the iron ore is composed mainly of iron oxides, in the form of goethite (FeOOH) and hematite (Fe_2O_3). From ICP-AES analysis of the iron oxide, the Fe content of material was measured at 42.2 wt%.

As for the feedstock preparation for the tests, the white pine sawdust as received contained a relatively high moisture content (38 wt%). This material was sieved to remove large particles (>10 mm) and dried to a moisture content approximately 15-20% using a rotary dryer with a screening facility at CanmetENERGY. The peat was received in the form of pellet and a moisture content of approximately 36 wt%. Due to poor

fluidizability of the peat pellets and in order to obtain more representative results comparable to those from the pine sawdust, these pellets were crushed and sieved to 1-4 mm particle size using an electrical grinder. Due to the partial loss of the moisture of the feedstock during the crushing and further air drying, the crushed peat had a moisture content of around 25 wt% when they were applied to the gasification tests. The actual moisture content of the fuel used was measured prior to each test, to determine the fuel feeding rate for the gasification test. The bed materials, olivine, limestone and dolomite, were crushed and sieved to ensure a uniform particle diameter (about 1 mm diameter), while the iron ore was crushed and sieved to particles of a size of about 0.85 mm because of its higher particle density. All bed materials were in-situ calcined in air at >750 °C within the fluidized bed reactor during the warm-up combustion phase of each test using propane gas.

7.2.2. Gasification Facility

The gasification tests were conducted on a pilot-scale, air-blown fluidized bed gasifier, as schematically illustrated in Figure 7-1. The system is composed of a stainless steel cylindrical riser with a 127 mm inner diameter and 4.55 m in height. The facility was a bubbling fluidized bed reactor with a feeding capacity of up to 25 kg/h, and was equipped with a belt feeder combined with a rotary airlock valve and a cyclone for fly ash collection. A water-cooled condenser was also equipped to the facility for tar removal. Moreover, multiple temperature sampling ports (T1-T9 in Figure 7-1) were located at different heights on the riser column and a flue gas sampling port was connected in the flue gas pipe. The unit was coupled with a primary air inlet and four secondary air inlets. The major secondary air supply was introduced through line IV to the fluidized-bed

reactor at 560 mm above the center of the fuel feeding port. On-line measurement of flue gas compositions (H_2, CO, CO_2, O_2, CH_4, SO_2 and N_2) and flue gas temperature were performed. A custom designed air-cooled probe was installed vertically in the freeboard region of the fluidized bed combustor using a flange at the top.

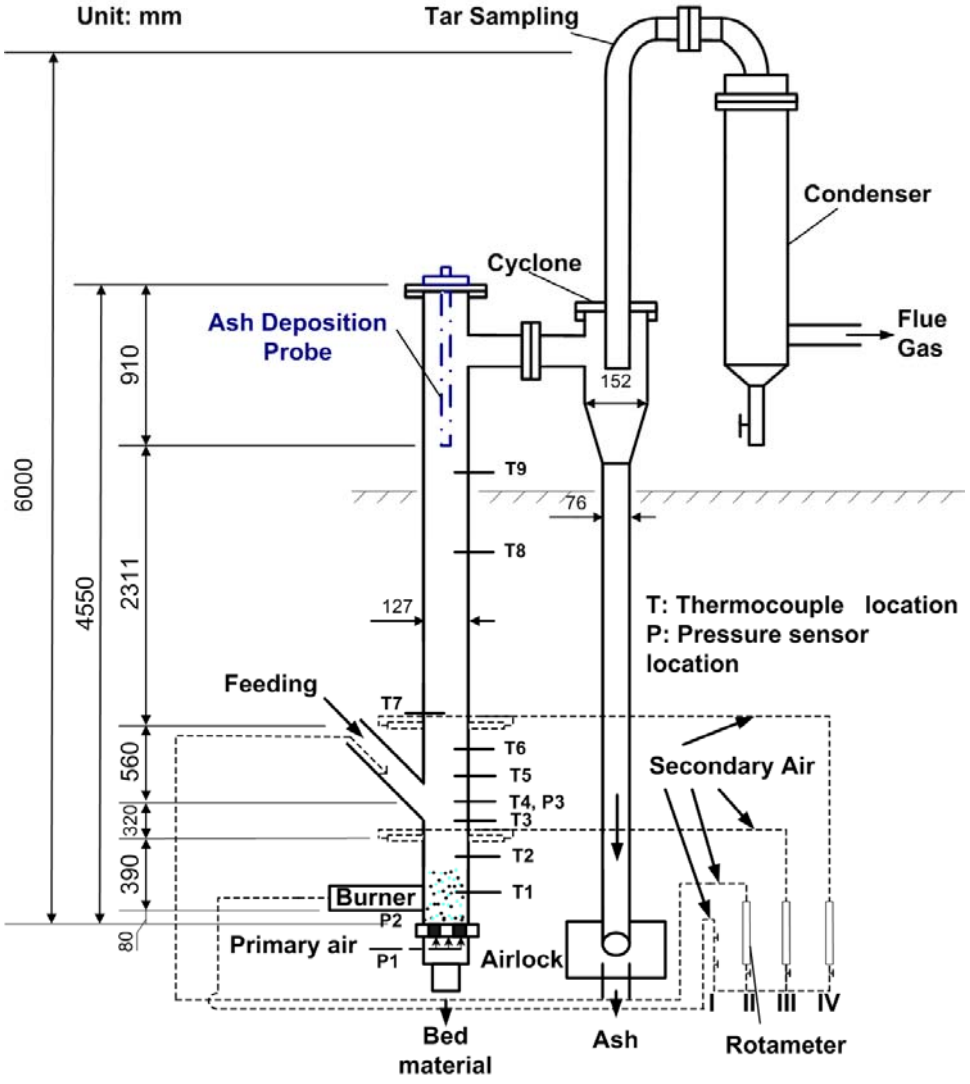

Figure 7-1 Schematic diagram of the fluidized bed facility

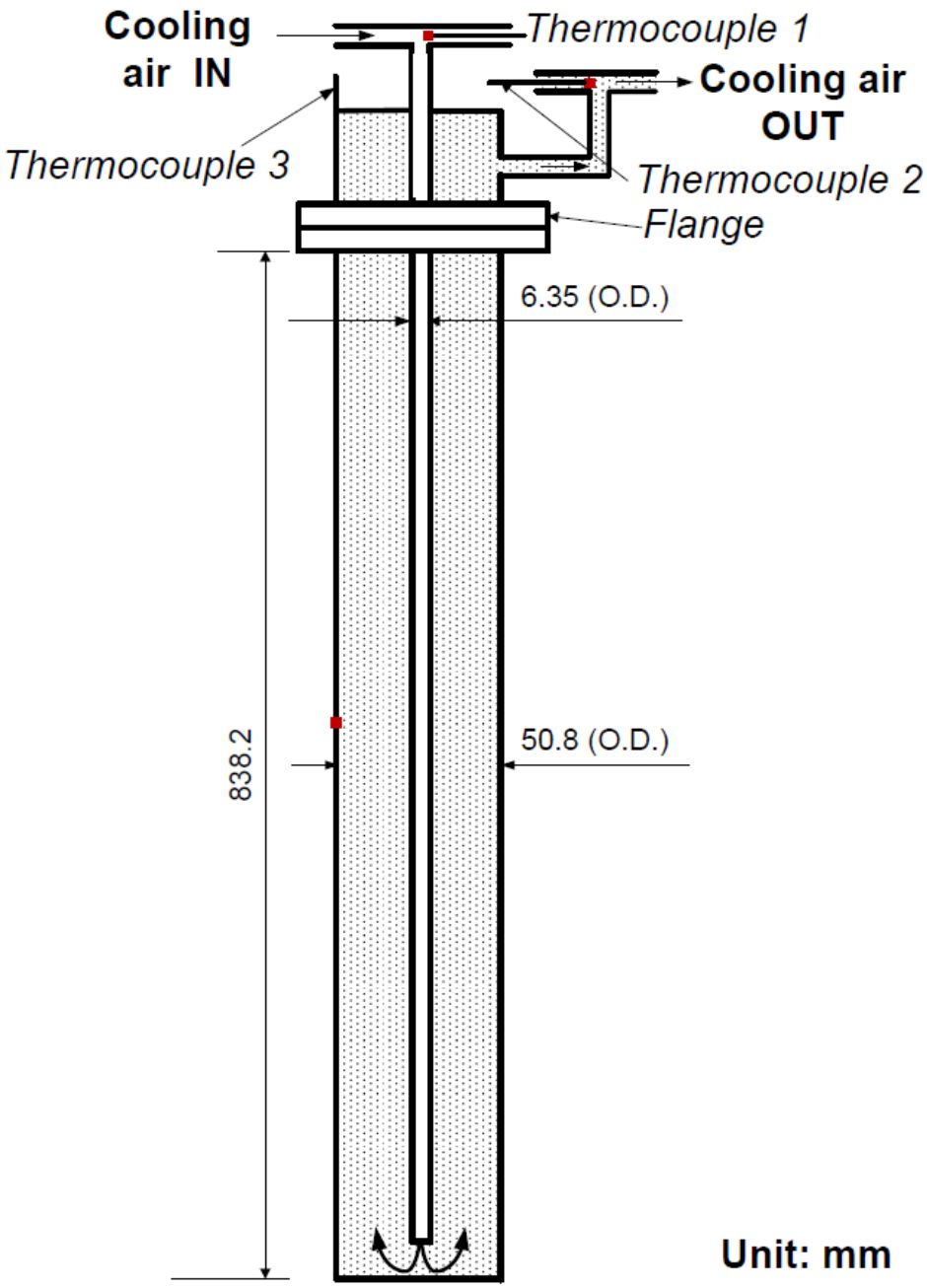

Figure 7-2 Schematic diagram of the ash deposition probe

The probe was made of SS 316L and has the dimensions as marked in Figure 7-2. The total effective length of the probe (for ash deposition inside the freeboard zone) was 838.2 mm, and the total external surface area was calculated to be 0.134 m^2. During the steady operation in all the tests, the surface temperature of the probe was maintained around 450 ºC by carefully controlling the flow rate of the cooling air.

7.2.3. Testing Methodologies and Parameters

The reactor was filled with 12-17 kg bed materials in each test, which was fluidized by the primary air (around 185 L/min) and was heated up to above 750ºC for 1-2 hours using propane gas before introducing the solid fuels. A combustion mode was initially performed at an air-to-fuel ratio of 1.4 with a feed rate of about 8 kg/h of the fuel to warm up the whole system before the unit was switched to gasification mode. When a relatively stable bed temperature profile was reached, the gasification mode was started by increasing feed rate to 10-25 kg/h and decreasing total air flow rate to around 300 L/min to match the desired equivalence ratio (ER). In oxygen/air-blown gasification, ER has been commonly used as an important operating parameter, defined as the ratio of oxygen content of air supply to oxygen required for complete combustion (Devi *et al.*, 2003).The value of ER has been observed to strongly influence the gas product compositions and gasification efficiency for air-blown biomass gasification (Kinoshita *et al.*, 1994; Narváez *et al.*, 1996). Usually, the ER is in a range from 0.2 to 0.4 for biomass gasification, to avoid incomplete gasification and excessive char formation at an excessively low ER (<0.2) as well as to prevent formation of incombustible gases like CO_2, and H_2O at an extremely high ER (>0.4) (Narváez *et al.*, 1996). Specific operational conditions for each gasification test can be found in Table 7-2. The gasification tests were performed with the four aforementioned bed materials (dolomite, olivine, limestone and iron ore) at varying ER from 0.20 to 0.35. By adjusting both fuel feeding rate and total air flow rate, the desired ER can be maintained. For instance, as shown in Table 7-2, an higher ER was usually achieved by decreasing the fuel feeding rate while keeping the total air flow rate controlled at around 290-300 L/min for most runs, However, in the tests with a same ER

for different bed materials, the fuel feeding rate was kept approximately the same on a thermal-input basis.

Table 7-2 Specific operation parameters for each run

Fuel	Bed Material	Equivalence Ratio (ER)	Feed Rate (kg/h)	Total Air Flow Rate (L/min)
Pine Sawdust	Dolomite	0.20	20.7	290
Pine Sawdust	Dolomite	0.25	16.6	290
Pine Sawdust	Dolomite	0.30	13.9	290
Pine Sawdust	Dolomite	0.35	12.0	292
Pine Sawdust	Dolomite	0.40	10.8	300
Pine Sawdust	Olivine	0.20	19.0	270
Pine Sawdust	Olivine	0.25	17.7	300
Pine Sawdust	Olivine	0.30	16.0	300
Pine Sawdust	Olivine	0.35	15.0	370
Pine Sawdust	Olivine	0.40	15.0	400
Pine Sawdust	Limestone	0.20	20.4	290
Pine Sawdust	Limestone	0.25	16.4	290
Pine Sawdust	Limestone	0.30	14.1	300
Pine Sawdust	Limestone	0.35	12.2	300
Pine Sawdust	Limestone	0.40	10.4	300
Pine Sawdust	Iron Ore	0.20	21.0	290
Pine Sawdust	Iron Ore	0.25	16.3	270
Pine Sawdust	Iron Ore	0.30	16.0	315
Pine Sawdust	Iron Ore	0.35	12.2	290
Pine Sawdust	Iron Ore	0.40	10.4	290
Crushed Peat	Olivine	0.20	17.4	290
Crushed Peat	Olivine	0.25	14.5	300
Crushed Peat	Olivine	0.30	12.0	300
Crushed Peat	Olivine	0.35	10.9	300

At the steady state, the gasification temperatures (in the dense phase of the fluidized bed) were maintained in the range of 700- 900°C (depending on the applied ER) by the partial combustion of the fuel without external heating. A stable temperature profile

along the bed height could be obtained through adjusting the secondary air and primary air ratios (while maintaining a constant total air flow rate). In this study, because the secondary air was introduced above the dense phase of the fluidized bed, the heat loss was inevitable along the reactor column. The average flue gas temperature in the freeboard and in the vicinity of the ash deposition probe was thus in a relatively wide range of 500-700ºC, a temperature that still prevented condensation of tar formed in the gasification process. Additionally, a significant loss of bed material due to physical attrition and thermal fragmentation was observed during some tests, so that additional bed materials had to be added to keep a constant bed level, which was monitored via three pressure sensors located at different heights of the bed as shown in Figure 7-1. In a typical run, at least 3-4 hours of stable operation was performed before cooling down the reactor to room temperature using nitrogen.

A cleaned probe was installed vertically in the freeboard zone of the reactor, right before the whole unit attained a steady state of operation of the gasification mode. When the whole unit was cooled to room temperature, the ash deposition probe was carefully removed from the freeboard and the deposited ash was completely recovered for weighing to calculate the ash deposition rate (D_A, g m^{-2} h^{-1}), as defined below:

$$D_A = \frac{\text{Mass of collected ash deposit (g)}}{\text{Surface area of the probe } (\text{m}^2) \times \text{Duration (h)}} \tag{7-1}$$

The collected deposited ashes were submitted for various characterizations by using XRF for chemical compositions in accordance to the ASTM D4326 standard and SEM in order to have a clear view regarding the effects of the different operations (i.e. bed materials and ER) on the morphology.

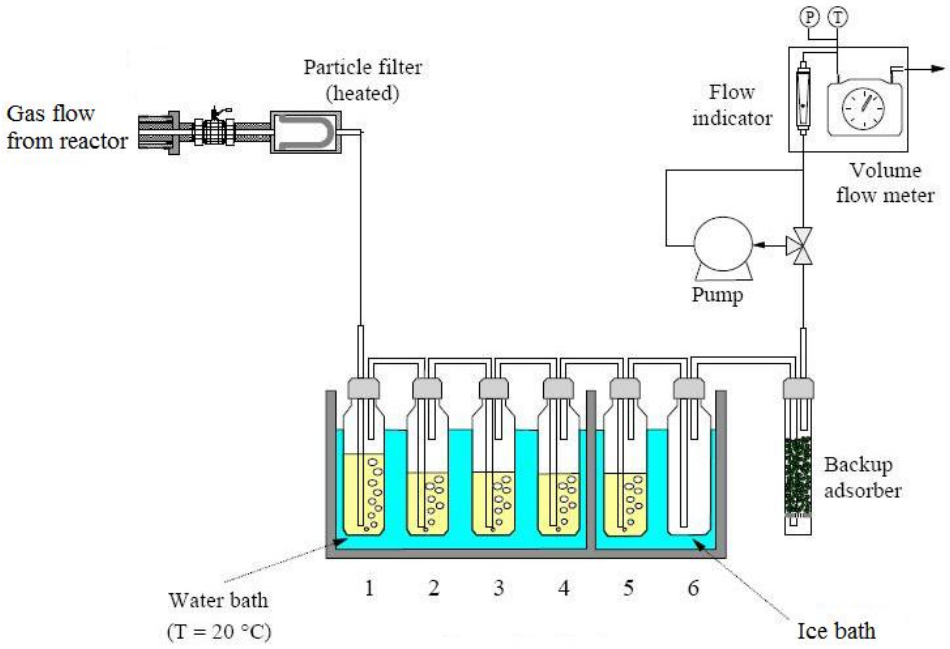

Figure 7-3 Schematic of the tar sampling system

Additionally, a non-iso-kinetic tar sampling system was used in this study, using a train of impingers containing an isopropanol solvent, as illustrated in Figure 7-3. Produced gas was drawn using a vacuum pump through a particulate filter into electrically heated lines (maintained at > 350°C to prevent the condensation of tars), the tar was condensed at the impinge train, and the incondensable product gas flowed through a wet-gas meter and vacuum pump before it was finally vented. The impinger system was composed of six solvent-containing vessels, three in a water bath (20°C) and three in an ethylene glycol bath at -10°C, plus a final droplet trap. Tar sampling was started after reaching steady state operation, and continued for 45-90 minutes. Total gas volume and smpling time were recorded with a wet gas meter. Following gasification, the solvent/tar mixture was collected. The impinger system and any piping below 350°C were washed with isopropanol, and the solvent/tar mixture filtered to remove any residual particulate matters. The isopropanol was evaporated at 50°C under reduced pressure with

a rotary evaporator, and the tars were weighed for calculation of the tar concentration in the producer gas.

Because of the relatively large operating scale and the complexity of the fluidized bed facilities, it normally took 2-3 days to complete a successful gasification test (including fuel/facility preparation, operation, after-run cleaning/maintenance). As such in this study duplicate tests were carried out only for the reference test (gasification of pine sawdust using limestone as the bed material at ER=0.3) to examine the reproducibility of the ash deposition rates. The relative standard deviations of the ash deposition rates were within 15.0%.

7.3. RESULTS AND DISCUSSION

7.3.1. Effects of bed materials on ash deposition

Figure 7-4 displays the ash deposition rates during the pine sawdust gasification with different bed materials at various ERs. The ash deposition rates generally remained nearly constant for all the bed materials for the ER ranging from 0.2 to 0.3. For example, when using olivine sand as the bed material, ash deposition rates did not significantly change with ER and were extremely low (< 1.0 g m^{-2} h^{-1}) with a small peak deposition rate (D_A=0.81 g m^{-2} h^{-1}) at ER=0.3. In the tests using iron ore as the bed materials, the ash deposition rates were fluctuated depending on the ER. In contrast, D_A in the tests with limestone bed materials constantly increased with increasing ER, in particular as the ER increased from 0.3 to 0.35 (as clearly indicated in Figure 7-4). For the whole range of ER tested (0.2 – 0.35), the ash deposition rates had the following sequence of order: iron ore > dolomite ≈ limestone > olivine. With the use of olivine, the lowest D_A values (<1 g m^{-2}

h^{-1}) were obtained for all ERs tested from 0.20 to 0.35. As such, the bed materials of olivine showed the best performance in suppressing the fly ash deposition during the gasification. In the contrast, at a higher ER (=0.35), the ash deposition rate for the gasification test using calcined limestone soared up to ~16.0 g m^{-2} h^{-1}.

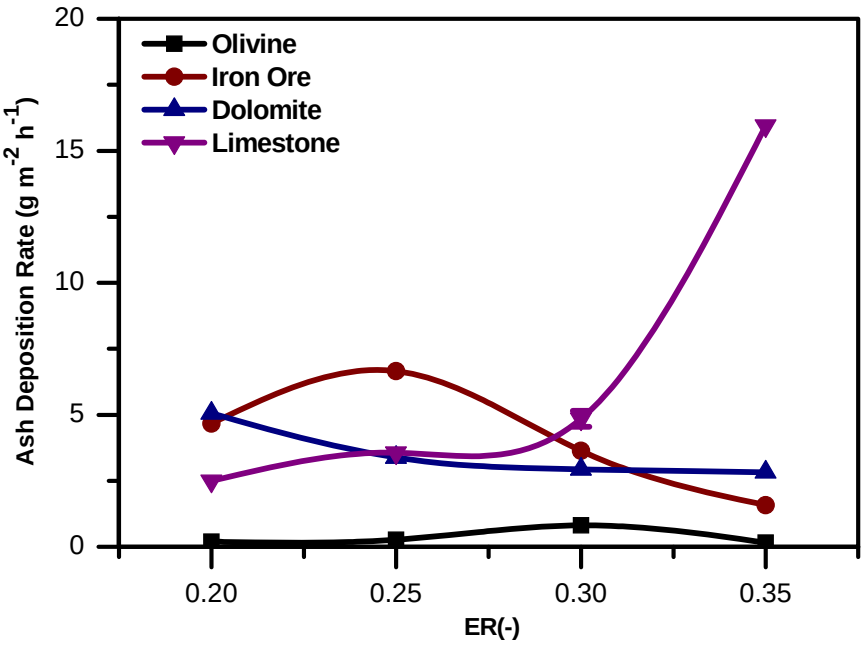

Figure 7-4 Ash deposition rate during pine sawdust gasification at varying ERs with different bed materials

It is worthy to be noted that the fly ash deposition behaviours for the gasification tests do not seem to be related to tar formation in the process. As shown in Figure 7-5, the tar formation in the gasification generally decreased with increasing the ER value, which could be accounted for by the more oxidizing atmosphere and more likely the higher temperatures in the fluidized bed reactor, as evidenced by the fluidized-bed column temperature profiles (Figure 7-6). A higher reactor temperature and the oxidizing atmosphere at a higher ER would destruct the tar vapour thermally and chemically, leading to a decrease in tar formation.

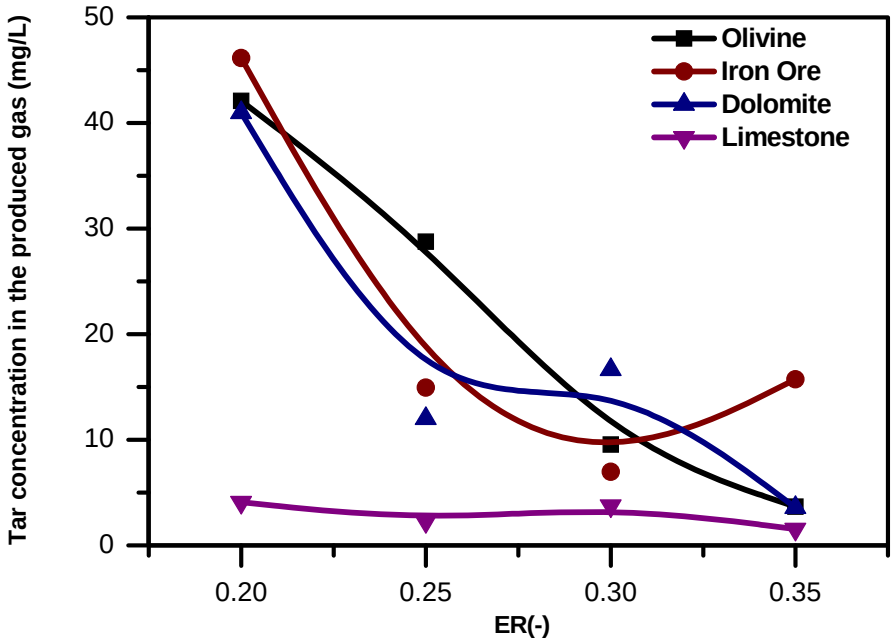

Figure 7-5 Tar formation from the pine sawdust gasification with different bed materials at various ERs (modified from Hurley *et al.*, 2009)

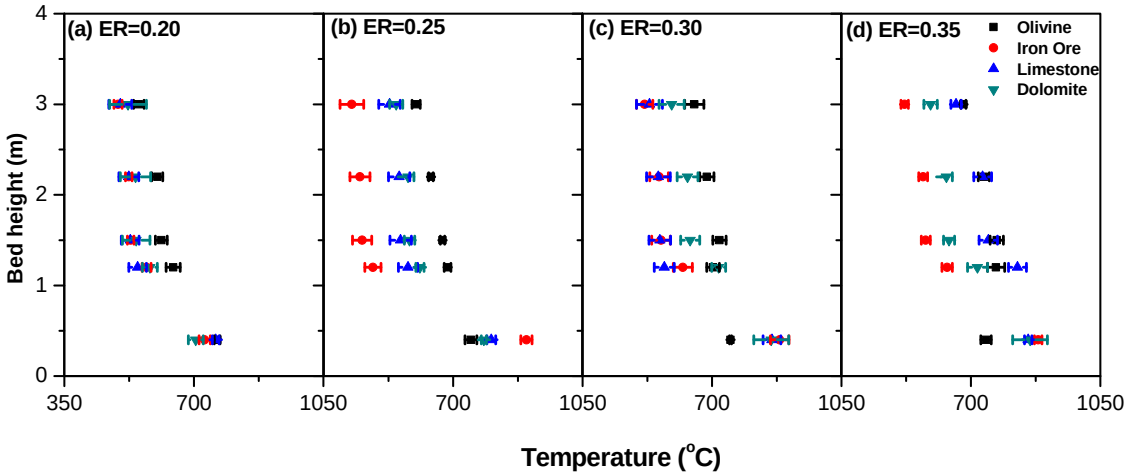

Figure 7-6 Comparisons of temperature profiles along the bed height during the pine sawdust gasification with different bed materials at (a) ER=0.20, (b) ER=0.25, (c) ER=0.30 and (d) ER=0.35.

From Figure 7-5, the tar formation the pine sawdust gasification with olivine was at a similar level as that with either the iron ore or dolomite bed material, but was much higher than that from the gasification test with limestone at all ERs, suggesting the highest activity of limestone for tar reduction. However, as displayed in Figure 7-4, the

fly ash deposition rate was the lowest with olivine and the highest with limestone, especially at ER>0.3. It is thus of a particular interest to discuss the possible causes for the superb performance of olivine, as well as the poor performance of limestone, in the fluidized bed biomass gasification with respect to fly ash deposition. Olivine in the tests showed outstanding mechanical strength with negligible formation of fines during the tests, which is consistent with the observation by other researchers (Rapagnà *et al.*, 2000).

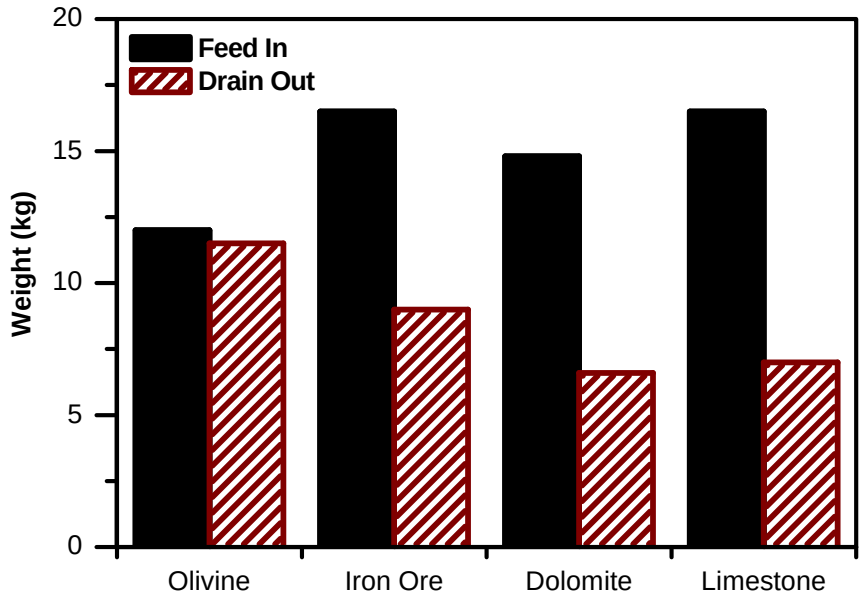

Figure 7-7 Comparison of attrition resistance of different bed materials during the fluidized-bed pine sawdust gasification at ER=0.30

The attrition resistance of different bed materials during the fluidized-bed pine sawdust gasification at ER=0.30 is compared in Figure 7-7. Negligible loss of the olivine bed materials was observed during the test. In contrast, the calcined limestone was found to be very fragile, producing a substantial amount of fines, leading to more than 50% loss of the bed materials during the test (as shown in Figure 7-7).

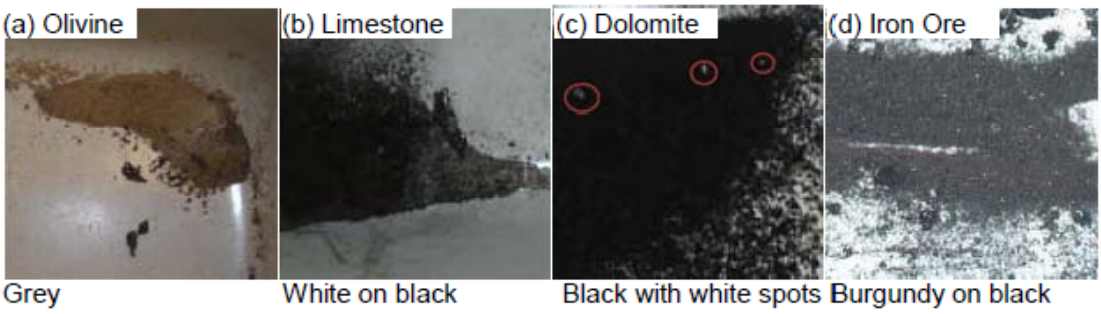

Figure 7-8 Appearance of deposited ash obtained from pine gasification tests performing at ER=0.3 with different bed materials (a) olivine, (b) limestone, (c) dolomite, and (d) iron ore

Visual comparison of deposits collected from the tests at the same ER (0.3) with these four bed materials was displayed in Figure 7-8. Different from the grey color deposits (originated from the fuel ash) collected from the test with olivine sand, fines originated from the respective bed materials were observable in the deposits collected from the tests using the other three bed materials. For example, as shown in Figure 7-8, particles of the burgundy color are present in the ash deposits from the test with iron ore, and white particles were observed in the deposits from the tests using dolomite and limestone. The loss of these three bed materials (i.e., limestone, or dolomite, or iron ore) was further confirmed by the XRF analysis of the collected cyclone bottom ashes. Figure 7-9 shows the chemical compositions (determined by XRF analysis) of the ash deposits collected from the pine sawdust gasification using olivine sand (Figure 7-9A) and limestone (Figure 7-9B) as the bed materials. It should be noted that significant losses on fusion were observed in the XRF analyses of the ash deposits (as shown in Figure 7-9A), which was likely due to the presence of the carbonaceous matters such as the char/unburned carbon or low boiling point alkali salts in the deposits.

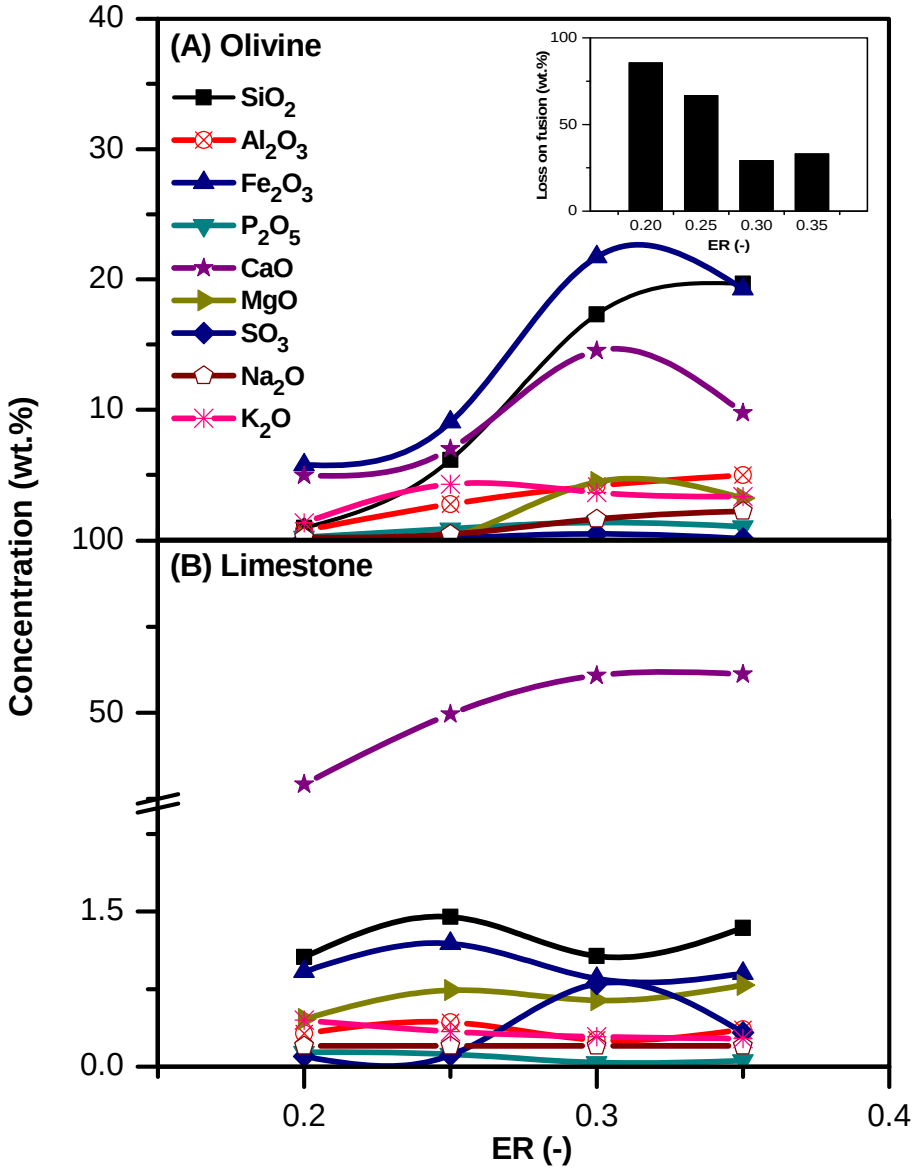

Figure 7-9 Chemical compositions of the ash deposits collected from the pine sawdust gasification using (A) olivine sand and (B) limestone as the bed materials.

Compared to the olivine tests, the deposits from the tests using limestone contained an extraordinary high content of CaO (>50 wt% of the deposits), originated in the limestone bed materials. The CaO in calcined limestone was known to be able to improve the formation of alkali/alkaline carbonates/sulphates/chlorides (Zevenhoven-Onderwater *et al.*, 2001), which have a relatively lower melting point (> 600 °C), and hence might

promote ash deposition as observed in Figure 7-4. Although fast ash deposition might also related to the chlorine deposition as discussed in our previous work (Shao *et al.*, 2011) and other literature work (Theis *et al.*, 2006; Aho *et al.*, 2004; Michelsen *et al.*, 1998), the ash deposit collected from each run in this study was unfortunately not enough for an analysis of chlorine contents in the deposits. Therefore, it can be concluded that the ash deposition behaviors during the pine gasification in a fluidized bed with various bed materials do not seem to be related to tar formation and their activities for biomass gasification and tar reduction, but are more likely related to their resistance to attrition during the fluidized bed tests.

7.3.2. Effects of different fuels on ash deposition

Figure 7-10 presents the comparison of ash deposition rates during gasification of the pine sawdust and crushed peat at various ERs but with the same bed materials (i.e., olivine sand). From the Figure, one may find that at all ERs tested (0.20 through 0.35), the ash deposition rates for peat gasification were consistently faster than those for the pine sawdust. For instance, the maximum deposition rate attained 5.5 g m^{-2} h^{-1}t for the peat gasification at an ER of 0.2, compared to only 0.8 g m^{-2} h^{-1} for the pine sawdust gasification at an ER of 0.3. The compositions of the ash deposits from each fuel are comparatively shown in Figure 7-11. Generally the deposited ashes from the peat gasification test contained higher concentrations of MgO and SO_3, but lower concentrations of K_2O and CaO. These composition distributions are actually in a good agreement with the fuel ash compositions as shown in Table 7-1.

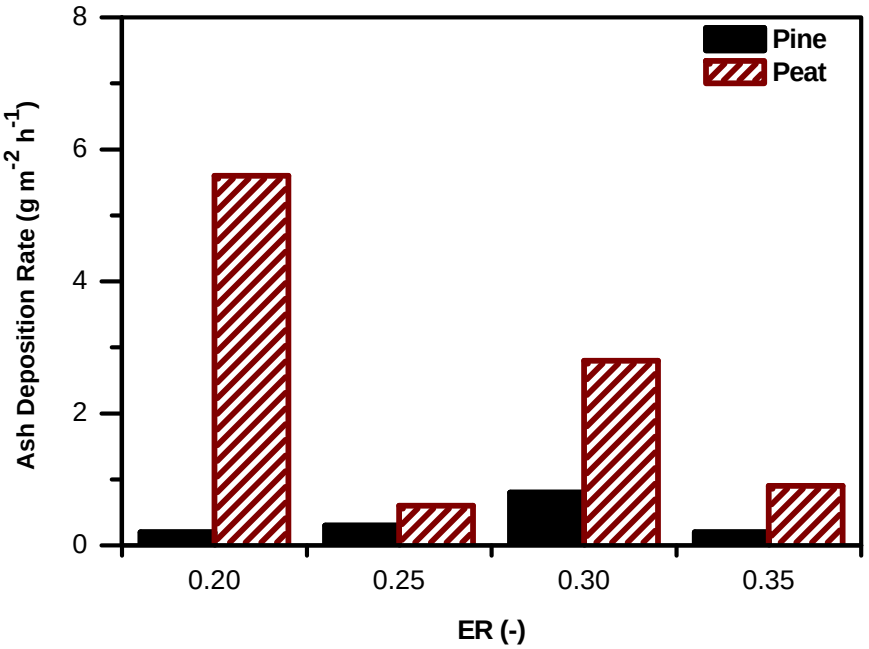

Figure 7-10 Comparisons of ash deposition rate during the gasification of pine sawdust and crushed peat at various ER and using olivine sand as the bed material

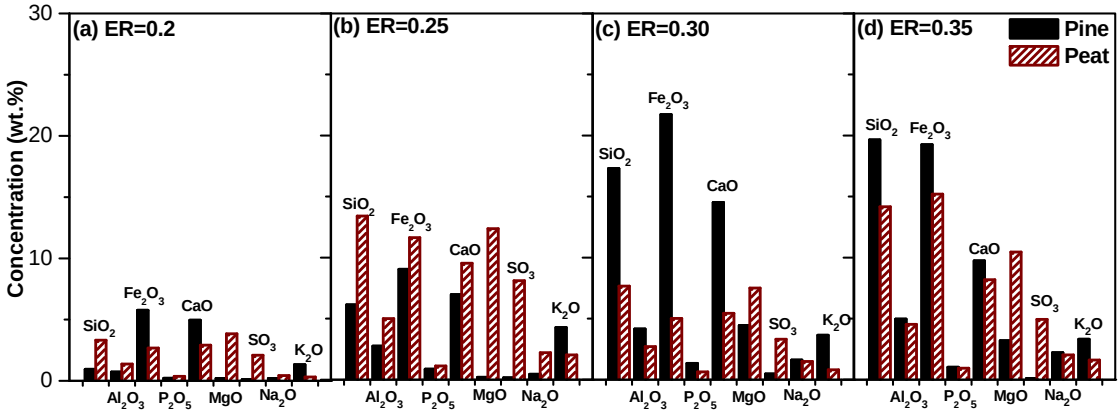

Figure 7-11 Comparisons of chemical compositions of the ash deposits collected from the gasification of pine sawdust and crushed peat using olivine sand as the bed material and at (a) ER=0.20, (b) ER=0.25, (c) ER=0.30, and (d) ER=0.35

At a low ER (0.2 or 0.25), the SiO_2 was founded to be at a significantly higher concentration in the ash deposits from the peat gasification than those from the pine sawdust gasification, which was also expected as the peat fuel ash contains a markedly higher SiO_2 (28.1 wt% for the crushed peat and 6.7 wt% for the pine sawdust). However, at a higher ER (0.3 or 0.35), the SiO_2 concentration in the ash deposits from the pine

sawdust gasification increased greatly, higher than that from the peat gasification. The enrichment of SiO_2 in the ash deposits from the pine sawdust might be due to the contamination from the olivine bed materials (containing 42 wt% SiO_2). Even though the olivine sand has superb thermal/mechanical stability, slight degradation of the bed materials to form fines did occur in the pine sawdust gasification process at a higher ER, as evidenced preciously in Figure 7-7.

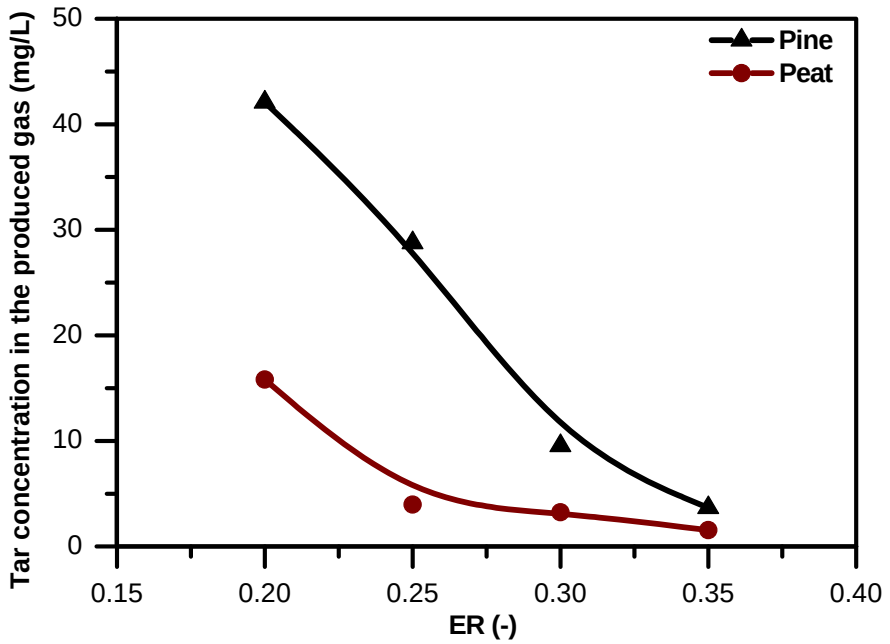

Figure 7-12 Comparison of tar formation during the gasification of pine sawdust and crushed peat at various ERs using olivine as the bed material (modified from Hurley *et al.*, 2009).

As described in the previous section, the ash deposition from the sawdust gasification using olivine was negligible due to the superb thermal and mechanical stability of the olivine sand, as well as the very low ash content of the sawdust (0.4 wt% db). With the same gasification conditions especially using the same bed materials, the difference in the ash deposition rates between the peat and pine sawdust fuel must result from the differences in fuel properties, in particular the volatile matters and fuel ash properties. As

mentioned previously, the pine sawdust has more volatile matters than the peat fuel, which would make the woody biomass more reactive in gasification, releasing more volatile vapour during the gasification process. The larger volatile vapour formation that entrained the fly ash species led to a shorter contact time between the fly ash and the ash deposition probe (Shao *et al.*, 2010), which could hence result in a lower ash deposition rate as shown in Figure 7-10. The formation of a larger volume of volatile matters from the sawdust gasification can be evidenced by its greater tar formation as clearly shown in Figure 7-12.

More importantly, the difference in the ash deposition rates between the peat and pine sawdust fuel might be explained by the big difference in the fuel ash content and compositions. As given previously in Table 7-1, the white pine sawdust has extremely low ash content, i.e., 0.4 wt% on a dry basis (db), while the peat contains 2 wt% ash and a strikingly high chlorine content of 2008 μg/g. The high ash content of the peat fuel might account for its faster ash deposition rates in the gasification process. Furthermore, the high chlorine content of the peat fuel was believed to play an important role in promoting the ash deposition. As similarly observed in our previous studies on co-firing biomass and/or peat with lignite coal in the same fluidized-bed facilities (Shao *et al.*, 2010, 2011a and 2011b), peat fuel with a high chlorine content exhibited much higher ash deposition tendency than other fuels with a lower Cl content.

7.4. CONCLUSIONS

(1) Among the four bed materials, the use of limestone led to the highest gasification efficiency (measured by the lowest tar formation), but also the highest ash deposition

rate, being ~ 16 $gm^{-2}h^{-1}$ in the gasification of pine sawdust at an equivalence ratio (ER) of 0.35.

(2) The use of olivine resulted in the lowest ash deposition rate < 1.0 $gm^{-2}h^{-1}$, and the superb performance of olivine in retarding ash deposition could be accounted for by its outstanding thermal stability and mechanical strength.

(3) The other three bed materials, in particular limestone, were fragile during the fluidized bed gasification, and the fractured fines from the bed materials were found to deposit along with the fuel-ash on the heat transfer surface, leading to higher ash deposition rates.

(4) The ash deposition rates for the peat gasification were much higher than those for the pine sawdust gasification. This might be explained by the big difference in the fuel ash content and compositions. Compared with the pine sawdust, the peat fuel used in this work contains much higher ash content (2 wt% ash) and strikingly higher chlorine content (2008 μg/g).

7.5. REFERENCES

Aho, M.; Silvennoinen, J. (2004). Preventing chlorine deposition on heat transfer surfaces with aluminium–silicon rich biomass residue and additive. *Fuel*; **83**:1299-1305.

Asadullah, M.; Miyazawa, T.; Kunimori K. (2003). Catalyst development for the gasification of biomass in the dual-bed gasifier. *Applied Catalysis A: General*; **255**(2):169–180.

Baxter, L.L.; Miles, T.R.; Miles Jr., T.R.; Jenkins, B.M.; Milne, T.; Dayton, D.; Bryers, R.W.; Oden, L.L. (1998). The behavior of inorganic material in biomass-fired power boilers: field and laboratory experiences. *Fuel Processing Technology*; **54**(1-3):47-78.

Björkman, E.; Strömberg, B. (1997). Release of chlorine from biomass at pyrolysis and gasification conditions. *Energy Fuels*; **11**:1026-32.

Bryers, R.W. (1996). Fireside slagging, fouling, and high-temperature corrosion of heat-transfer surface due to impurities in steam-raising fuels. *Progress in Energy and Combustion Science*; **22** (1):29-120.

Devi, L; Ptasinski, K.; Janssen, F. (2003). A review of the primary measures for tar elimination in biomass gasification processes. *Biomass and Bioenergy*; **24**: 125-140.

Fernholz, K. (2009). Energy from woody biomass: a review of harvesting guidelines and a discussion of related challenges. Divetail Partners, Inc. *http://www.dovetailinc.org/files/DovetailBioGuides0709.pdf* (accessed on October 2009).

Gusta, E.; Dalai, A.; Uddin, M.; Sasaoka, E. (2009). Catalytic decomposition of biomass tars with dolomites. *Energy Fuels*; **23**(4): 2264-2272.

Hall, D.O.; Rosillo-Calle, F.; de Groot, P. (1992). Biomass energy lessons from case

studies in developing countries. *Energy Policy*; 62-73.

Han, J., Kim, H. (2008). The reduction and control technology of tar during biomass gasification/pyrolysis: An overview. *Renewable and Sustainable Energy Reviews*; **12**(2):397-416.

Hurley, S.; Shao, Y., Preto, F., Tourigny, G., Li, H.; Xu, C. (2009). Catalytic gasification of biomass in a pilot-scale fluidized bed reactor. *Proceeding of the 2nd annual particle technology research centre conference*, July 9-10, 2009, London, Ontario, Canada.

Jensen, P.A.; Frandsen, F.J.; Dam-Johansen, K.; Sander, B. (2000). Experimental investigation of the transformation and release to gas phase of potassium and chlorine during straw Pyrolysis. *Energy Fuels*; **14**:1280-1285.

Kinoshita, C.M.; Wang, Y.; Zhou, J. (1994). Tar formation under different biomass gasification conditions. *Journal of Analytical and Applied Pyrolysis*; **29**(2):169-181.

Lopamudra, D.; Ptasinski, K.J.; Janssen, F.J.J.G. (2003). A review of the primary measures for tar elimination in biomass gasification processes. *Biomass and Bioenergy*; **24**(2):125–140.

McGowan, F. (1991). Controlling the greenhouse effect: the role of renewables. *Energy Policy*: 111-118.

McKendry, P. (2002a). Energy production from biomass (part 3): gasification technologies. *Bioresource Technology*; **83**(1):55–63.

McKendry, P. (2002b). Energy production from biomass (part 1): overview of biomass. *Bioresource Technology*; **83**(1):37–46.

Michelsen, H.P.; Frandsen, F.; Dam-Johansen, K.; Larsen, O.H. (1998). Deposition and high temperature corrosion in a 10 MW straw fired boiler. *Fuel Processing*

Technology; **54**:95-108.

Morehouse, J.H.; Detwiler, K.W. (2008). Assessment of a biomass gasification co-generation plant based on the UCS's "principles for bioenergy development". The 2nd International Conference on Energy Sustainability, August 10-14, 2008, Jacksonvill, USA. vol. **1**:399-404.

Narváez, I.; Orío, A.; Aznar, M.P.; Corella, J. (1996). Biomass gasification with air in an atmospheric bubbling fluidized bed. Effect of six operational variables on the quality of produced raw gas. *Industrial and Engineering Chemistry Research*; **35**(7):2110-2120.

Olsson, J.O.; Jäglid, U.; Pettersson, J.B.C.; Hald, P. (1997). Alkali metal emission during Pyrolysis of biomass. *Energy Fuels*; **11**:779-784.

Overgaard, P.; Larsen, E.; Friborg, K.; Hille, T.; Jensen, P.A.; Knudsen, S. (2005). Full-scale tests on co-firing of straw in a natural gas-fired boiler. *http://www.dongenergy.com/SiteCollectionDocuments/NEW%20Corporate/PDF/Engineering/42.pdf.* (accessed on February 2008).

Pencho, J.; Schildhauer, T.; Sturzenegger, M.; Biollaz, S.; Wokaun, A. (2008). Reactive bed materials for improved biomass gasification in a circulating fluidized bed reactor. *Chemical Engineering Science*; **63**(9):2465-2476.

Rapagnà, S.; Jand, N.; Kiennemann, A.; Foscolo, P.U. (2000). Steam-gasification of biomass in a fluidised-bed of olivine particles. *Biomass and Bioenergy*; **19**(3):187-197.

Salo, K.; Mojtahedi, W. (1998). Fate of alkali and trace metals in biomass gasification. *Biomass and Bioenergy*; **15**(3):263-267.

Shao, Y.; Xu, C.; Zhu, J.; Preto, F., Wang, J.; Tourigny, G.; Badour, C.; Li, H. (2010). Ash deposition during co-firing biomass and coal in a fluidized-bed combustor. *Energy Fuels*; **24**(9):4681-4688.

Shao, Y.; Xu, C.; Zhu, J.; Preto, F., Wang, J.; Tourigny, G.; Badour, C.; Li, H. (2011a). Ash and chlorine deposition during co-firing lignite and a chlorine-rich Canadian peat in a fluidized bed - effects of blending ratio, moisture content and sulfur addition. Submitted to *Fuel.*

Shao, Y.; Wang, J.; Xu, C.; Zhu, J.; Preto, F., Tourigny, G.; Badour, C.; Li, H. (2011b). An experimental and modeling study of ash deposition behavior for co-firing peat with lignite. *Applied Energy*; in press.

Theis, M.; Skrifvars, B.J.; Zevenhoven, M.; Hupa, M.; Tran, H. (2006). Fouling tendency of ash resulting from burning mixtures of biofuels. Part 3: Influence of probe surface temperature. *Fuel*; **85**(14-15): 2002-11.

Weimer, T.; Berger, R.; Hawthorne, C.; Abanades, J.C. (2008). Lime enhanced gasification of solid fuels: Examination of a process for simultaneous hydrogen production and CO_2 capture. *Fuel*; **87** (8-9): 1678-1686.

Wood, S., Layzell D.B. (2003). *BIOCAP Canada Foundation*, *www.biocap.ca/images/pdfs/BIOCAP_Biomass_Inventory.pdf* (accessed on February 2008).

Zevenhoven-Ondervater, M.; Backman, R.; Skrifvars, B.J.; Hupa, M. (2001). The ash chemistry influidized bed gasification of biomass fuels. Part I: predicting the chemistry of melting ashes and ash-bed material interaction. *Fuel*; **80**(10):1489-1502.

CHAPTER 8. A MODELING STUDY OF ASH DEPOSITION BEHAVIOUR FOR CO-FIRING PEAT WITH LIGNITE

8.1. Introduction

Coal-fired power plants are a major anthropogenic source of emissions of CO_2 and harmful pollutants such as SO_2, particulates and mercury. Co-combustion of coal and alternative fuels such as biomass in existing power plants can reduce the coal input and hence the emissions, and avoid high investment costs for new plants. However, co-combustion often causes operational problems, such as slagging, fouling and corrosion, due to deposition of ash which has relatively low fusion temperature and high chlorine and alkali metal content (Hein and Bemtgen, 1998; Heinzel *et al.*, 1998; McIlveen-Wright *et al.*, 2007; Lundmark *et al.*, 2007).

Canada has large fuel-grade peat resources, estimated to be 41% of the world's total (WEC, 2004; Biopact, 2004). Peat can be regarded as a slowly renewable biomass and carbon neutral fuel (Sudol, 2005; Theis *et al.*, 2006a), and has played an important role in energy production in a few countries including Finland, Ireland and Sweden. Co-firing peat can reduce CO_2 emission from existing coal-fired Canadian power plants. Besides, analytical tests show that peat deposits which can potentially fuel several existing Canadian power plants have low sulphur and ash content, and virtually no mercury (Biopact, 2004; Sudol, 2005). Accordingly, the co-firing can also reduce emissions of SO_2, particulates and mercury. However, peat may have similar combustion and ash deposition properties to many biomass species, and cause similar ash-related problems. For instance, it has been observed that peat could add to ash deposition when co-fired with bark (Theis et al., 2006a-c). To implement co-firing peat and coal for power

generation in existing power plants, it is critically important to assess the ash deposition issue.

In this study, we investigated ash deposition behaviour in co-firing a Canadian peat and a lignite coal on a pilot-scale fluidized bed combustor. Fluidized bed combustion is able to operate at relatively low temperature and burn high moisture fuels, and is considered to be a promising technology for direct/indirect co-firing of low-grade fuels (biomass or peat) and coal for power generation. The pilot-scale results are expected to provide important information and insights to enable reduction of ash-deposition related problems for full-scale implementation of co-firing peat in coal-fired power plants.

8.2. Experimental

8.2.1. Fuels

The lignite used in this study was provided by OP. The peat, provided by Peat Resources Ltd, was from Newfoundland, Canada. The proximate and ultimate analyses of these two fuels are given in Table 8-1, and the analyses for fuel ashes are given in Table 8-2. As can be seen, the peat has much lower ash content (2 wt% db) compared to the lignite (22 wt% db). The ultimate analysis and the higher heating values (HHV) of the peat are comparable to those of the lignite except for much higher chlorine content in the peat. The compositions of the ashes are generally similar, but the peat contains relatively lower contents of SiO_2 and Al_2O_3, and higher concentrations of CaO and MgO.

Table 8-1 Proximate and ultimate analyses of fuels

	Lignite	**Peat**
Moisture, wt% as received	30.0	35.8
HHV (MJ/ kg dry)	21.8	21.4
Proximate analysis, wt% db		
Ash	22.0	2.0
Volatile matters (VM)	54.0	68.6
Fixed carbon	24.0	29.4
Ultimate analysis, wt% db		
Carbon	58.8	56.1
Hydrogen	4.2	5.7
Nitrogen	0.9	0.8
Sulphur	0.5	0.2
Oxygen[1]	13.6	35.2
Chlorine[2], μg/g.	25	2010
Bromine[2], μg/g.	< 21	153
Fluorine[2], μg/g	100	< 20

[1]By difference ; [2] By pyrohydrolysis.

Table 8-2 Compositions of fuel ashes[1]

	Lignite	**Peat**
Dry ash analysis[2], wt% db		
SiO_2	49.76	28.05
Al_2O_3	19.71	8.63
Fe_2O_3	3.82	5.56
TiO_2	0.86	0.48
P_2O_5	0.30	1.31
CaO	9.91	12.65
MgO	2.11	17.72
SO_3	6.09	12.73
Na_2O	4.20	2.84
K_2O	1.04	1.14

[1]Ashing temperature 750°C for lignite and 500°C for peat;
[2]By XRF of the ashes from the feedstocks.

For the co-firing tests, the lignite was crushed and screened into particles below 4 mm. The peat was supplied in the form of pellets of 10 mm diameter and 30 mm long. Some of the peat pellets was further crushed into particles below 4 mm size. All the fuels were used either as received or air-dried, with a moisture content of 20-30 wt%. Prior to each test, the actual moisture content of each feedstock was accurately measured.

8.2.2. Test Facility

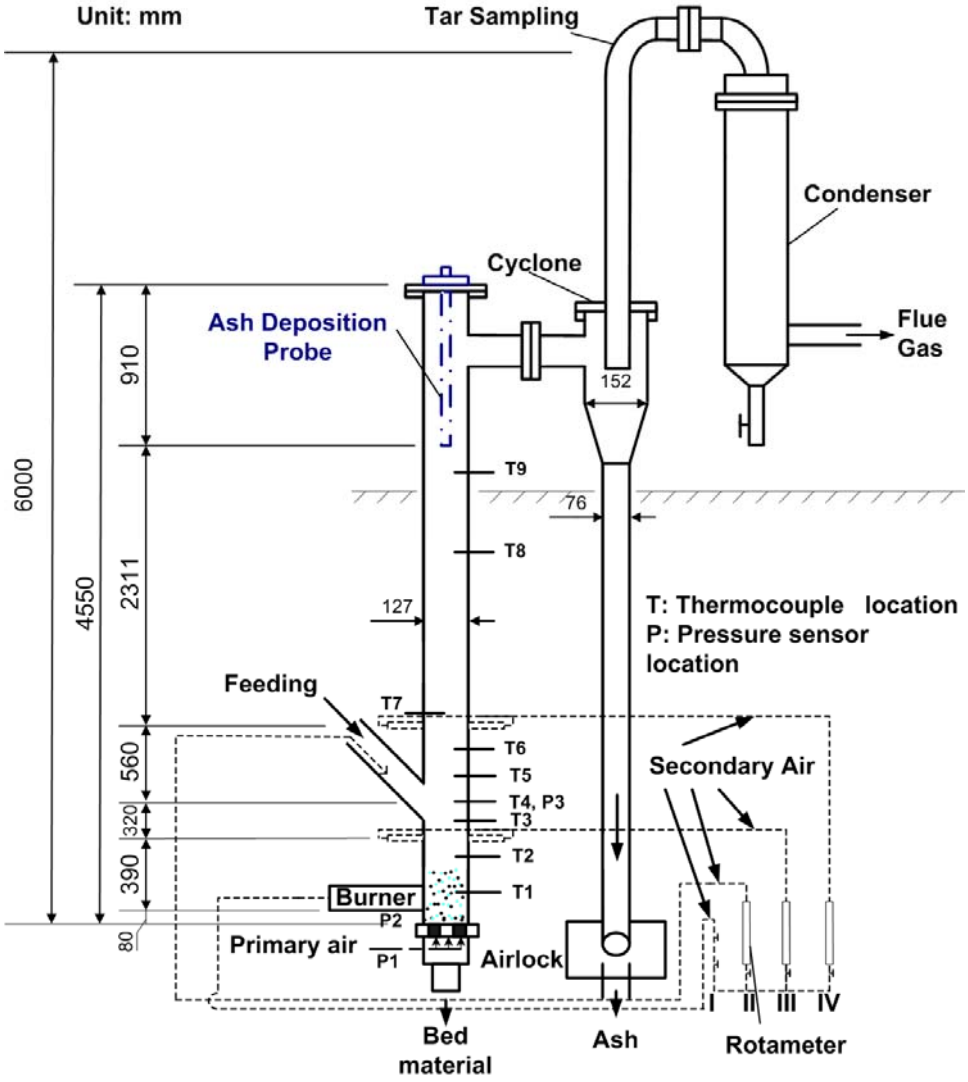

Figure 8-1 Schematic of the pilot fluidized bed combustor

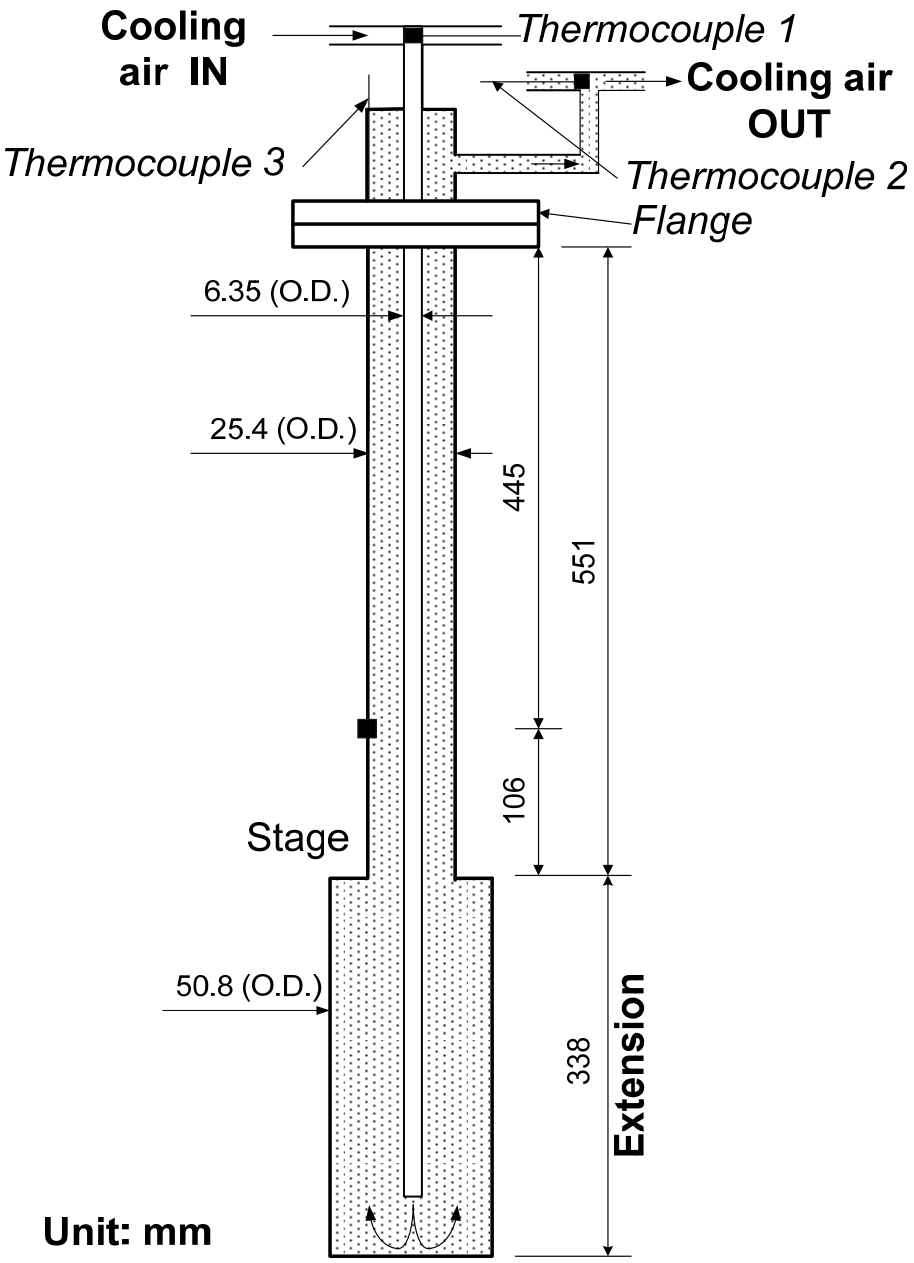

Figure 8-2 Schematic of the ash deposition probe

The co-firing tests were conducted with a pilot-scale fluidized bed combustor. The combustor, which is illustrated in Figure 8-1, is 4.55 m high with an inner diameter of 0.127 m. The feeding capacity is up to 25 kg/h. Thermocouples were installed at temperature measurement ports distributed throughout the combustor. Flue gas was sampled and analyzed online (infrared method for CO, CO_2 and SO_2; paramagnetic

method for O_2; chemiluminescence method for NO_x). Real-time temperature profiles along the combustor height and flue gas composition are monitored by a computer system.

The deposited ash was sampled with a specially designed air-cooled probe as illustrated in Figure 8-2. The probe has the following dimensions: 551 mm long and 25.4 mm OD with an extension of 338 mm long and 50.8mm OD. Due to the limitation in the equipment configuration, in this study the ash deposition probe was installed vertically in the freeboard region (which differs from the real boiler operations where the steam tubes are perpendicular to flue gas). During the steady operations the surface temperature of the probe was maintained at 430±10ºC.

8.2.3. Test procedure

For all tests, a synthetic olivine sand (with a standard formula $[Mg.Fe]_2SiO_4$ and a mean particle density 2.83) was used as the bed material. The combustor was preheated up to above 600 ºC using propane gas before introducing the solid fuels. Then peat was mixed with lignite in various proportions and fed to the combustor. In all cases the rate of heat input was kept at 58.3 MJ/h by controlling the feed rate (3.8 – 4.2 kg/h). By adjusting the secondary air and primary air ratios while maintaining a constant total air flow rate, a stable temperature profile along the bed height was attained. As shown in Figure 8-1, the unit was coupled with a primary air inlet and four secondary air inlets. The secondary air supply was introduced through Line IV to the fluidized bed reactor at 560-mm above the center of the fuel feeding port. The combustion tests were carried out at a constant air-to-fuel ratio of 1.4. The average flue gas temperature of the freeboard region was in the range of 650-700 ºC. In each test run, a stable period of about 3-4 hours

was operated.

After the tests the probe with ash deposits was carefully removed and the deposited ash was weighed to determine the rate of ash deposition. Tests for the reproducibility indicated that the relative standard error of the measured rates was below 8%. The deposited ash was also subjected to analyses by XRF for chemical composition (according to ASTM D4326 standard), by IC for soluble chlorine content, and by pyrohydrolysis for total chlorine content.

8.3. Results and discussion

8.3.1. Nonlinear dependence of ash deposition on the fraction of peat

The rate of ash deposition is shown in Figure 8-3 as a function of the fraction of the peat in the feed (on a thermal input basis).

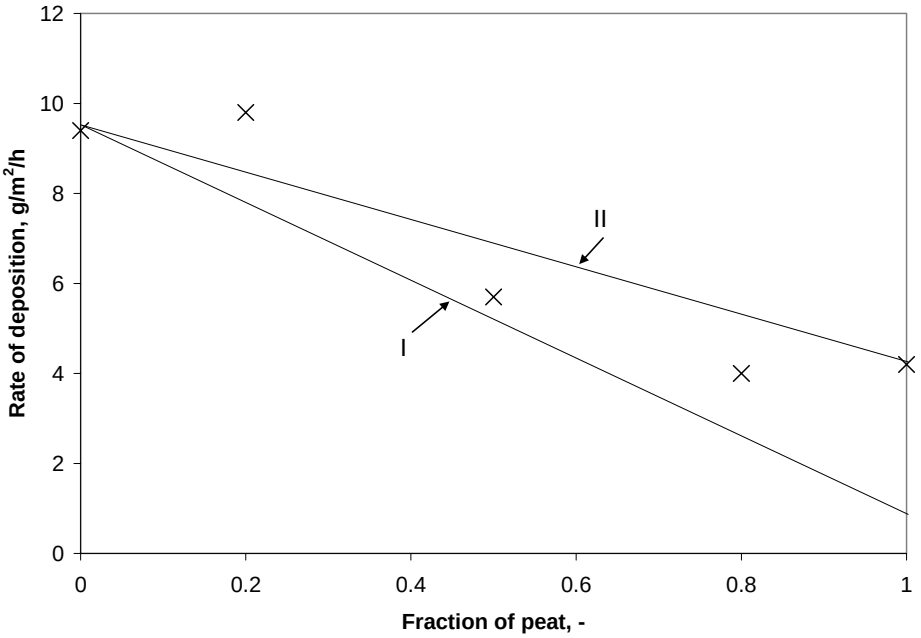

Figure 8-3 Ash deposition rate as a function of the fraction of peat in the blends The symbol represents measured deposition rate. Line I is the expected trend line based on the deposition rate of pure lignite and total ash contents in the blends. Line II is the expected trend line based on different but fraction-independent deposition rates of the two ash components.

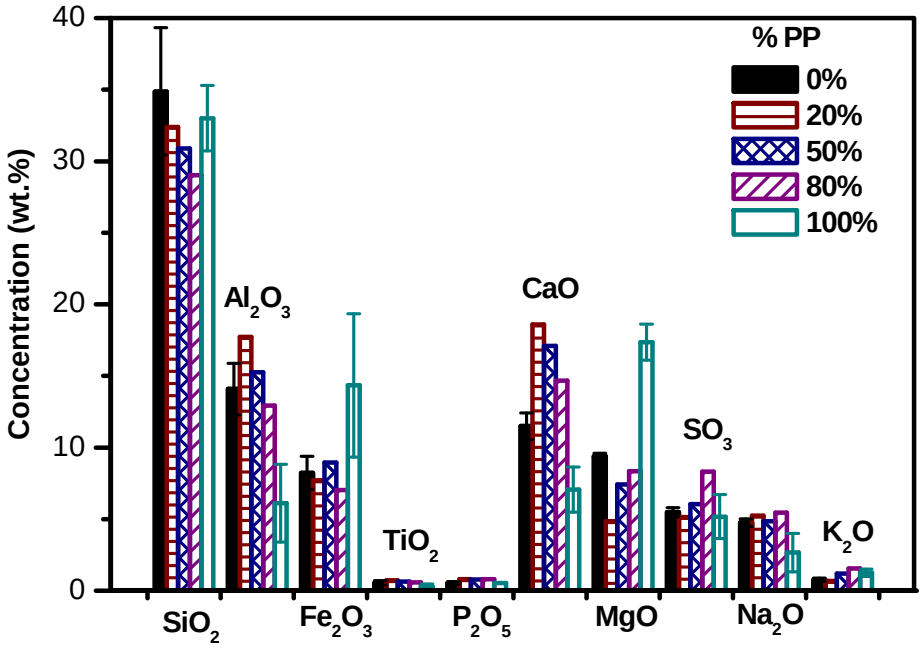

Figure 8-4 Chemical composition of the ash deposits

The chemical compositions of the ashes are shown in Figure 8-4. As a general trend, the ash deposition decreases with increasing peat fraction, which could be explained by the lower ash content of the peat compared to the lignite. However, the degree of the decrease in the deposition rate is significantly smaller than expected from the deposition rate of pure lignite and total ash contents of the blends. An analysis of the behaviour is given as follows.

The ash deposition rate is expected to depend on ash content of the feed, and the tendency of ash deposition. As a simple case we consider a linear dependence :

$$R = k_1 A_1 (1 - X) + k_2 A_2 X \tag{8-1}$$

where k_1, A_1, k_2 and A_2 denote the rate coefficients and ash contents for lignite and peat, respectively. X is the fraction of peat in the feed. If the ash from the peat has the same tendency of deposition as that of the ash from the lignite, i.e., $k_1 = k_2$, the rate would be represented by a straight line (line I in Figure 8-3) whose slope corresponds to peat-

fraction dependence of the total ash content of the feed. By contrast, the measured rates are consistently above this line and the deviation increases with increasing fraction of peat, suggesting higher deposition tendency of the ash from the peat. On the other hand, when $k_2 \neq k_1$ but the two coefficients are independent of the peat fraction, the rate would be represented by another straight line (line II in Figure 8-3) connecting the two points $X = 0$ (pure lignite) and $X = 1$ (pure peat). As is obvious from the figure, such a line does not give an adequate approximation. The deviation of the data from the straight line is too large to be ignored, and may only be accounted for by considering interactions of the ash components.

As has been noted earlier, the peat had remarkably high chlorine content than the lignite (2008 μg/g vs 25 μg/g). Chlorine is believed to facilitate the transport of alkali species from the bulk fuel to surfaces in burning biomass, and the liberation of the alkalis into the vapour/gas phase (Jenkins *et al.*, 1998; Nielsen *et al.*, 2000; Davidsson *et al.*, 2007). Deposition of alkali chlorides leads to formation of a sticky coating, which catches more ash (Baxter *et al.*, 1996; Davidsson *et al.*, 2008). The alkali chlorides can react with sulphur oxides to form sulphates and release the chlorine to the gas phase. In this way, chlorine plays a shuttle role to transport alkalis from the fuel to the deposition surface. Chlorine may also react with calcium to form $CaCl_2$ under fluidized bed conditions (Desroches-Ducarne *et al.*, 1998; Xie *et al.*, 2000; Aho and Silvennoinen, 2004). $CaCl_2$ would be prone to stick to deposition surfaces due to its low melting point (772°C), and be sulphated subsequently to form $CaSO_4$ and release the chlorine. The $CaSO_4$ could become a binder between ash particles on deposit surface (Miles *et al.*, 1996). The above mechanism would explain the XRF results for the chemical compositions of the deposited

ash shown in Figure 8-4, where K_2O, Na_2O and CaO in the deposited ash from combustion of the blends are significantly higher than those from combustion of the lignite or the peat alone.

The higher contents of K_2O, Na_2O and CaO may include K_2SO_4, Na_2SO_4 and $CaSO_4$ formed by deposited KCl, NaCl and $CaCl_2$ via reactions such as

$$2KCl + SO_2 + O_2 = K_2SO_4 + Cl_2 \qquad \Delta G^o = -113.7 \text{ kJ/mol}$$

$$2KCl + SO_2 + (1/2)O_2 + H_2O = K_2SO_4 + 2HCl \qquad \Delta G^o = -102.7 \text{ kJ/mol}$$

$$2NaCl + SO_2 + O_2 = Na_2SO_4 + Cl_2 \qquad \Delta G^o = -115.1 \text{ kJ/mol}$$

$$2NaCl + SO_2 + (1/2)O_2 + H_2O = Na_2SO_4 + 2HCl \qquad \Delta G^o = -134.7 \text{ kJ/mol}$$

$$CaCl_2 + SO_2 + O_2 = CaSO_4 + Cl_2 \qquad \Delta G^o = -180.1 \text{ kJ/mol}$$

$$CaCl_2 + SO_2 + (1/2)O_2 + H_2O = CaSO_4 + 2HCl \qquad \Delta G^o = -169.0 \text{ kJ/mol}$$

where ΔG° is the change of the standard Gibbs free energy at the temperature of the ash deposition probe. The ΔG° values suggest that the reactions, by which chlorine could be released and promote further deposition of ash, are quite plausible. The formation of the solid chlorides would be dependent on the contents of Cl and the alkali/alkaline metals of the fuel. Potassium has been regarded as the most problematic substance for ash deposition in combustion of biomass (Jenkins *et al.*, 1998; Nielsen *et al.*, 2000; Davidsson *et al.*, 2007), and fuels with high K and Cl values would result in higher concentrations of the gaseous alkalis (Glazer *et al.*, 2005; Coda *et al.*, 2001). However, in the present fuel blends the contents of calcium and sodium are significantly higher than the content of potassium (Table 8-2), and thus the contribution of calcium and sodium to the ash deposition could be quite important. For simplicity, we lump the K, Na and Ca contents together and relate this total metal content and Cl content to the rate coefficients

k_1 and k_2 in Eq. 8-1, using linear relationships:

$$k_1 = k_1^0(1+\alpha_1[Cl][Me]) \tag{8-2-1}$$

$$k_2 = k_2^0(1+\alpha_2[Cl][Me]) \tag{8-2-2}$$

with

$$[Cl] = [Cl]_1 + ([Cl]_2 - [Cl]_1)X \tag{8-2-3}$$

$$[Me] = [Me]_1 + ([Me]_2 - [Me]_1)X \tag{8-2-4}$$

where k_1^0 and k_2^0 are the coefficients for zero Cl or metal content instances, and may depend on physical properties such as particle size. This is suggested by the results of tests with smaller sized crushed peat, which showed smaller rate of deposition (by about 30%) compared to uncrushed peat. α_1 and α_2 in Eqs. 8-2-1 and 8-2-2 are coefficients for *Cl* and metal interactions for lignite and peat, respectively; [*Cl*] and [*Me*] denote total *Cl* and alkali/alkaline metal contents of the blend, respectively; $[Cl]_1$, $[Cl]_2$, $[Me]_1$ and $[Me]_2$ denote *Cl* and metal contents of the lignite and peat, which can be obtained from fuel analysis (Tables 8-1 and 8-2). Here for simplicity we ignore the difference of chlorine and the metals in the lignite and the peat, which may have different reactivities (Baxter *et al.*, 1996; Dayton *et al.*, 1999). With the above relations, Eq. 8-1 becomes

$$\begin{aligned} R = {} & k_1^0 A_1 \{1+\alpha_1[[Cl]_1 + ([Cl]_2 - [Cl]_1)X][[Me]_1 + ([Me]_2 - [Me]_1)X]\}(1-X) \\ & + k_2^0 A_2 \{1+\alpha_2[[Cl]_1 + ([Cl]_2 - [Cl]_1)X][[Me]_1 + ([Me]_2 - [Me]_1)X]\}X \end{aligned} \tag{8-3}$$

when firing lignite along ($X = 0$), we obtain from Eq. 8-3

$$R_0 = k_1^0 A_1(1+\alpha_1[Cl]_1[Me]_1) \tag{8-4}$$

With this expression, Eq. 8-3 can be normalized into a dimensionless form

$$\frac{R}{R_0} = \frac{1 + \beta_1(1+\psi_1 X)(1+\psi_2 X) + \delta[1+\lambda(1+\psi_1 X)(1+\psi_2 X)]X}{1+\beta_1} \tag{8-5}$$

where $\beta_1 = \alpha_1[Cl]_1[Me]_1$, $\psi_1 = ([Cl]_2/[Cl]_1 - 1)$, $\psi_2 = ([Me]_2/[Me]_1 - 1)$,

$\delta = (A_2 k_2^0 / A_1 k_1^0 - 1)$, and $\lambda = (A_2\alpha_2 k_2^0 - A_1\alpha_1 k_1^0)[Cl]_1[Me]_1/(A_2 k_2^0 - A_1 k_1^0)$

are dimensional parameters. In Figure 8-5 calculated deposition rate in terms of Eq. 8-5 is shown as a function of *X*, which represents the measured peat-fraction dependence fairly well.

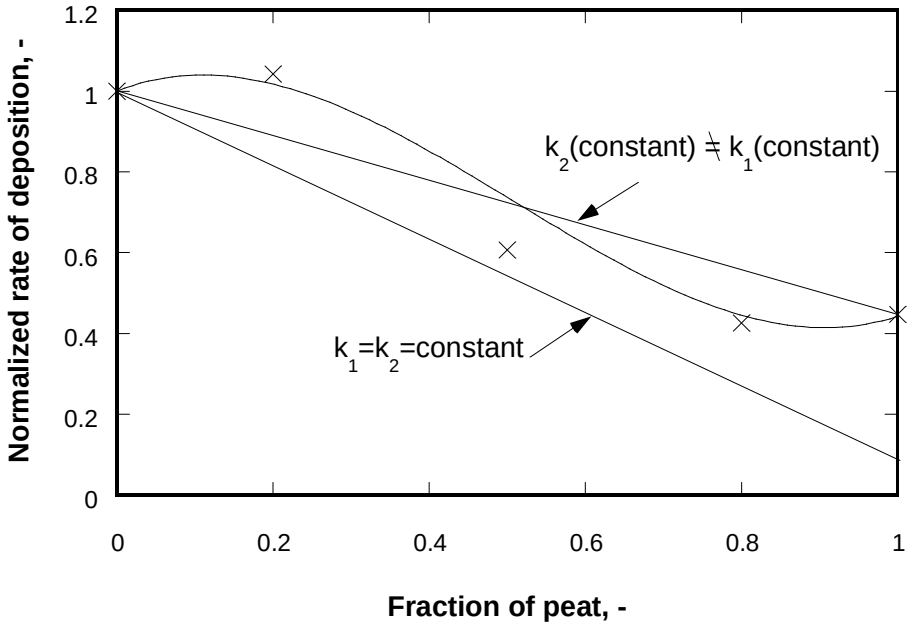

Figure 8-5 Normalized ash deposition rate as a function of the fraction of peat
The curve represents the description by Eq. 8-5, with β_1 = 0.015, δ = -0.39 and λ = 0.09. The values of ψ_1 and ψ_2 were determined from fuel analyses (Tables 8-1 and 8-2) as 79.4 and -0.9, respectively.

It is interesting to see that Eq. 8-5 could also describe ash deposition data of other peat blends. In Figure 8-6 the equation is applied to reported data (Theis *et al.*, 2006c) for co-firing peat with bark and straw, respectively. For these reported data only potassium is considered for the effect of the metals since the potassium content in the blends is quite

high. The blend-ratio dependence of the deposition rate in the two cases shown in Figure 8-6 is very different from that of the peat/lignite system of Figure 8-5, yet the equation reasonably follows the trends over a large part of the fraction ranges.

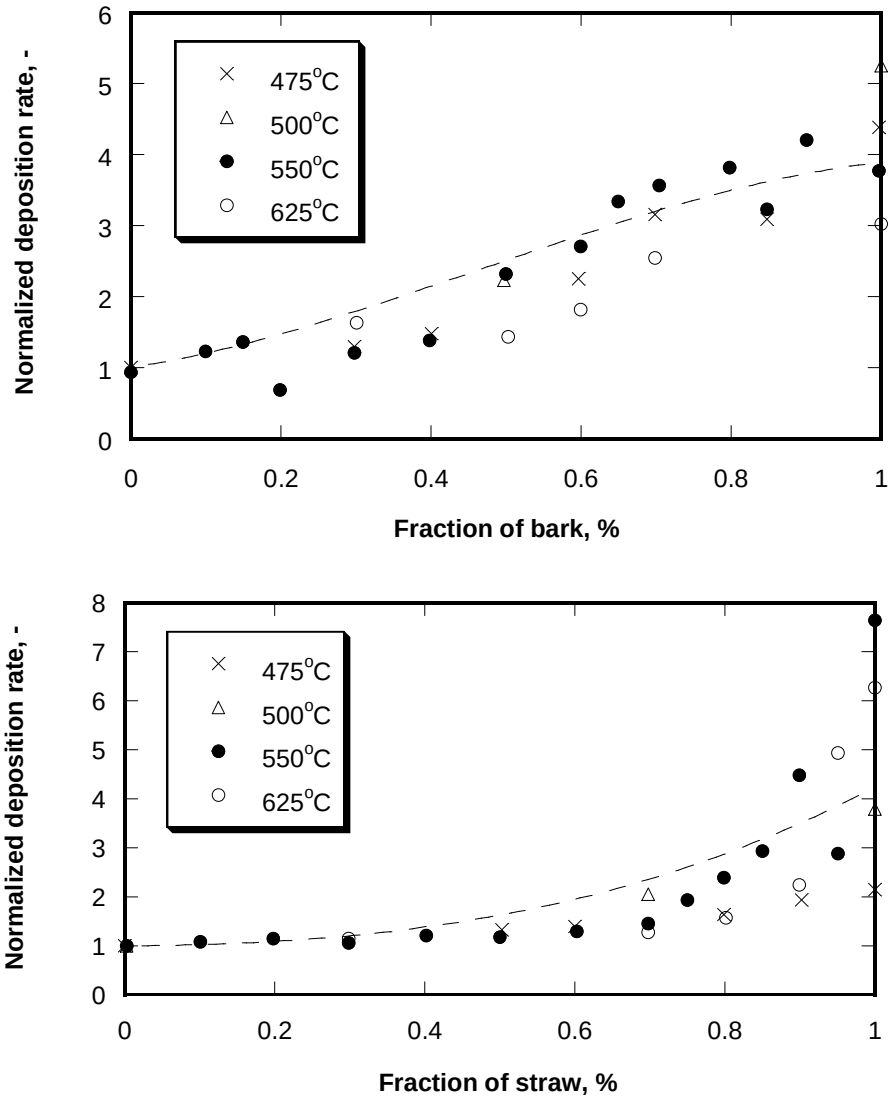

Figure 8-6 Application of Eq. 8-5 for reported ash deposition rate (Theis *et al.*, 2006c) in co-firing peat with bark (upper) and co-firing peat with straw (lower). For peat/bark β_1 = 0.14, δ = 0.09 and λ = -0.9. For peat/straw β_1 = 0.001, δ = 0.003 and λ = 16.

It can also be seen that, although the interactions discussed above resulted in higher-than-expected ash deposition rate, the total amount of ash deposit decreased substantially with increasing peat fraction. This gives the potential of reducing the cost related to ash

deposition in the boiler, from decreased soot blowing and cleaning cycles. However, the higher chlorine content of the peat may result in corrosive ash deposits harmful to boiler tubes and internals, as will be discussed in the following section.

8.3.2. Chlorine content in ash deposits

As has been discussed, the high chlorine content in peat would be a negative factor for co-firing peat and coal due to its promoting effects on ash deposition. Furthermore, as well known, fuel-bound chlorine evolves and deposits on boiler tubes and internals would cause severe corrosion problems (Nielsen *et al.*, 2000; Aho and Silvennoinen, 2004; Miles *et al.*, 1996; Salmenoja *et al.*, 1996). It is thus of high interest to analyze the chlorine contents of the ash deposits, and to examine the effects of co-firing lignite and the high-chlorine peat on chlorine deposition on heat-transfer surfaces inside a combustor.

Figure 8-7 shows chlorine contents of the ash deposits determined by pyrohydrolysis and IC, respectively. The two sets of data show similar trends: the chlorine content of the blends was higher than both that of the lignite and of the peat, with a maximum of chlorine content at about 80% peat fraction. This behaviour could not be explained from the feed chlorine content alone, which should increase linearly with increasing fraction of the high-chlorine peat. As we have attributed the ash deposition behaviour to interactions involving chlorine and the alkali/alkaline earth metals, we believe that metals in the feed have played a role in chlorine deposition. As can be understood from the data of Tables 8-1 and 8-2, the content of chlorine in the blends increases with the fraction of peat, whereas the content of the alkali/alkaline earth metals decreases with the fraction of peat.

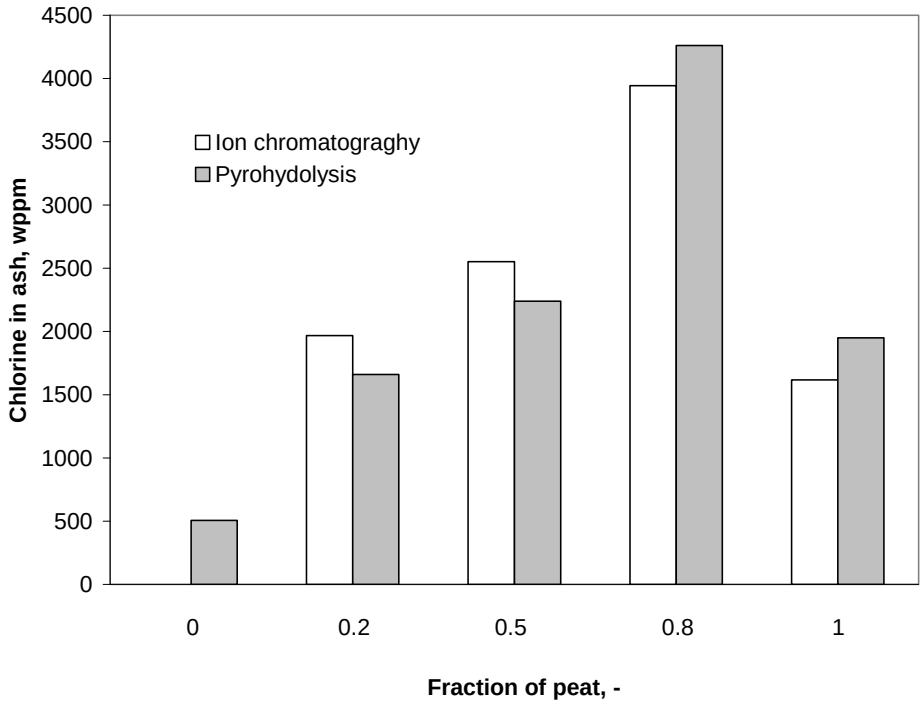

Figure 8-7 Chlorine content in deposited ash as a function of the fraction of peat in the blends

In consequence, the formation of the metal chlorides, which would have higher deposition tendency than other chlorine compounds, could be limited by the metals at higher peat fractions. The rate of the formation of the chlorides may be related to [Cl][Me], the product of the two contents in the blends.

In Figure 8-8 the product expressed as $[Cl][Me]/[Me]_1$ is given as a function of the fraction of peat, where $[Me]_1$ is the content of the metals of the pure lignite. The quantity $[Cl][Me]/[Me]_1$ would reflect the relative tendency of chlorine deposition. A maximum is seen in this plot at about 60% peat fraction. This is a sign that the ash chlorine content is related to $[Cl][Me]/[Me]_1$, but the two maximums do not occur at the same peat fraction. However, the ash chlorine content is also dependent on the amount of ash. The maximum of the ash chlorine content would appear at a higher peat fraction because the ash deposit decreases with peat fraction.

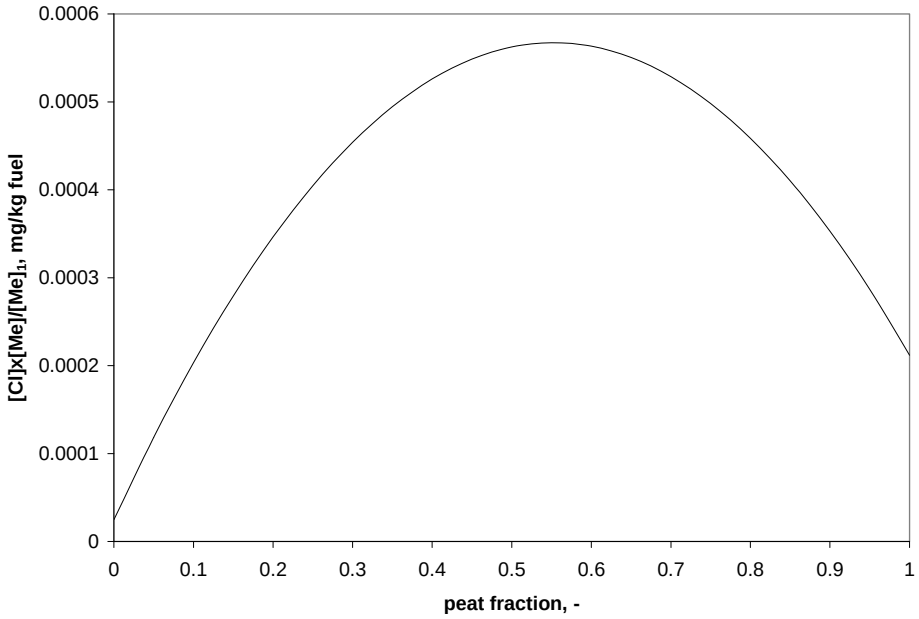

Figure 8-8 Chlorine deposition tendency (in terms of [Cl][Me]/[Me]$_1$) as a function of blend ratio

We therefore compare the peat-fraction dependence of the measured ash chlorine content with the following equation

$$C_{Cl} = \frac{([Cl][Me]/[Me]_1)\gamma}{W_{ash}} \tag{8-6}$$

where C_{Cl} is the ash chlorine content; W_{ash} is the weight of ash deposit, whose dependence on the fraction of peat can be obtained from Eq. 8-5; γ is a parameter related to the ratio of deposited chlorine to total depositable chlorine.

Figure 8-9 shows that the predicted trend and position of the maximum in terms of Eq. 8-6 agree well with the measured results. It should be emphasized that in the above analysis we did not differentiate the activities of the metals in the lignite and the peat. Besides, we did not consider different affinities of the two ash components to the chlorine. In spite of the greatly simplified analyses, remarkable agreement with the observed ash chlorine content is obtained.

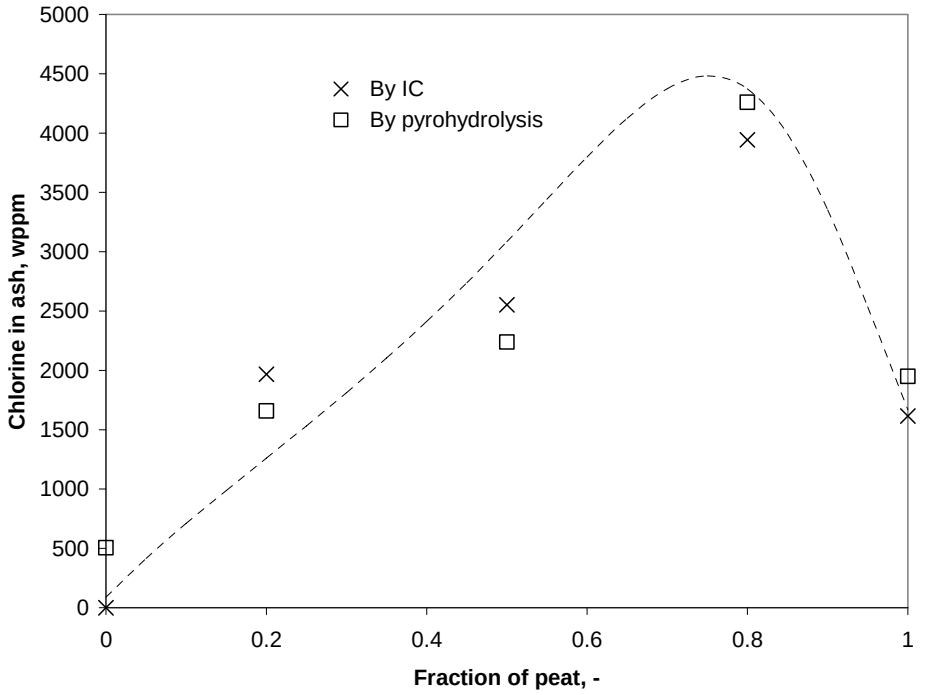

Figure 8-9 Comparison of Eq. 8-6 with measured dependence of ash chlorine content on blend ratio. The curve represents the description by Eq.8-6 with γ=0.8.

It can be inferred that the occurrence of the maximum ash chlorine content was due to the different dependence of *Cl* and metal contents on the blend ratio. If *Cl* and metal both increase or decrease with the blend ratio, a maximum would not occur. On the other hand, in co-firing fuels whose total *Cl* and metal contents change in opposite directions as the blend ratio varies, a maximum ash chlorine content may be observed between $X = 0$ and $X = 1$. In assessing chlorine deposition potentials for co-firing coal with various types of biomass fuels, a plot of [Cl] x [Me] against blend ratio may provide a quick estimate on whether a maximum of ash chlorine content would occur at a certain blend ratios.

As has been seen above, the total ash deposition decreases with peat fraction, the chlorine content increases with peat fraction and exhibits a maximum value of around 4000 wppm. Although this value is not particularly high – in firing straw the ash chlorine can be as high as 38 wt % (Nielsen *et al.*, 2000) - increased chlorine content means

increased corrosion potential. If the maximum value is close to the threshold chlorine level for corrosion of the existing boiler tubes, new tubes of higher corrosion-resistance would be necessary. On the other hand, if the blend ratio related to maximum ash chlorine is predictable from fuel chlorine and alkali contents, it can be avoided to reduce chlorine deposition. For instance, in the present lignite/peat blends, the maximum ash chlorine is predicted to occur at 80% peat fraction. In comparison with the predicted ash deposition rate (Figure 8-5), it could be seen that decreasing the peat fraction to about 50% would decrease ash chlorine content significantly yet achieve a relatively low ash deposition rate.

8.4. Conclusions

The ash deposition rate in co-firing the lignite and peat decreases with increasing fraction of the peat. This can lead to decreased ash cleaning and removal requirements. On the other hand, the chlorine content of the ash increases with the fraction of peat and exhibits a maximum. The dependence of the deposition rate and the ash chlorine content on the fraction of peat can be described by the equations developed in this work. Based on these equations, suitable range of the peat fraction can be determined for smooth operations. For instance, in the present blends a peat fraction around 50% would decrease the ash chlorine content significantly yet achieve a relatively low ash deposition rate.

8.5. References

Aho, M.; Silvennoinen, J. (2004). Preventing chlorine deposition on heat transfer surfaces with aluminium–silicon rich biomass residue and additive. *Fuel*; **83**:1299-1305.

Baxter, L.L.; Miles, T.R.; Jr. Miles T.R.; Jenkins, B.M.; Dayton, D.; Milne, T.; Bryers, R.W.; Oden, L.L. (1996). Alkali deposits found in biomass boilers - The Behavior of Inorganic Material in Biomass - Fired Power Boilers - Field and Laboratory Experiences. *Sandia National Laboratory*, Livermore, CA 1996.

Biopact (2004). Canadian researchers study co-firing of peat and biomass with coal. *http://news.mongabay.com/bioenergy/2007/12/canadian-researchers-study-co-firing-of.html* (accessed on May 2010).

Coda, B.; Aho, M.; Berger, R.; Hein, K.R.G. (2001). Behavior of chlorine and enrichment of risky elements in bubbling fluidized bed combustion of biomass and waste assisted by additives. *Energy Fuels*; **15**(3): 680-690.

Davidsson, K.O.; Åmand, L.E.; Steenari, B.M.; Elled, A.L.; Eskilsson, D.; Leckner, B. (2008). Countermeasures against alkali-related problems during combustion of biomass in a circulating fluidized bed boiler. *Chemical Engineering Science*; **63**:5314-5329.

Davidsson, K.O.; Åmand, L.E.; Leckner, B.; Kovacevik, B.; Svane, M., Hagström, M.; Pettersson, J.B.C.; Pettersson, J.; Asteman, H.; Svensson, J.E.; Johansson, L.G. (2007). Potassium, chlorine, and sulfur in ash, particles, deposits, and corrosion during wood combustion in a circulating fluidized-bed boiler. *Energy Fuels*; **21**:71-81.

Dayton, D.C.; Belle-Oudry, D.; Nordin, A. (1999). Effect of coal minerals on chlorine

and alkali metals released during biomass/coal cofiring. *Energy Fuels*; **13**:1203-11.

Desroches-Ducarne, E.; Marty, E.; Martin, G.; Delfosse, L.; Nordin, A. (1998). Effect of operating conditions on HCl emissions from municipal solid waste combustion in a laboratory-scale fluidized bed incinerator. *Environmental Engineering Science*; **15**: 279-289.

Glazer, M.P.; Khan, N.A.; de Jong, W.; Spliethoff, H.; Schürmann, H.; Monkhouse, P. (2005). Alkali metals in circulating fluidized bed combustion of biomass and coal: measurements and chemical equilibrium analysis. *Energy Fuels*; **19**:1889-1897.

Hein, K.R.G; Bemtgen, J.M. (1998). EU clean coal technology-co-combustion of coal and biomass. *Fuel Processing Technology*; **54**:159-169.

Heinzel, T.; Siegle, V.; Spliethoff, H.; Hein, K.R.G. (1998). Investigation of slagging in pulverized fuel co-combustion of biomass and coal at a pilot-scale test facility. *Fuel Processing Technology*; **54**: 109-125.

Jenkins, B.M.; Baxter, L.L.; Miles Jr, T.R.; Miles, T.R. (1998). Combustion properties of biomass. *Fuel Processing Technology*; **54**:17-46.

Lundmark, D.; Mueller, C.; Skrifvars, B.J.; Hupa, M (2007). Computational fluid dynamic modeling of combustion and ash deposition in a biomass-co-fired bubbling fluidized bed boiler. *Clean Air*; **8**:155-169.

McIlveen-Wright, D.R.; Huang, Y.; Rezvani, S.; Wang, Y. (2007). A technical and environmental analysis of co-combustion of coal and biomass in fluidised bed technologies. *Fuel*; **86**(14):2032-2042.

Miles, T.R.; Miles Jr., T.R.; Baxter, L.L.; Bryers, R.W.; Jenkins, B.M.; Oden, L.L. (1996). Boiler deposits from firing biomass fuels. *Biomass and Bioenergy*; **10**:125-

138.

Nielsen, H.P.; Frandsen, F.; Dam-Johansen, K.; Baxter, L. (2000). The implications of chlorine-associated corrosion on the operation of biomass-fired boilers. *Process in Energy and Combustion Science*; **26**(3): 283-298.

Salmenoja, K.; Mäkelä, K.; Hupa, M.; Backman, R. (1996). Superheater corrosion in environments containing potassium and chlorine. *Journal of the Institute of Energy*; **69**:155-162.

Sudol, S (2005). Peat Fuel - A Clean Solution to Northwestern Ontario's Energy Crisis. INORD Commentary. *http://inord.laurentian.ca/commentaries.htm.* (accessed on May 2010).

Theis, M.; Skrifvars, B.J.; Hupa, M.; Tran, H. (2006a). Fouling tendency of ash resulting from burning mixtures of biofuels. Part 1: Deposition rates. *Fuel*; **85**(7-8):1125-1130.

Theis, M., Skrifvars, B.J., Zevenhoven, M., Hupa, M. and Tran, H. (2006b), Fouling tendency of ash resulting from burning mixtures of biofuels. Part 2: Deposit chemistry. *Fuel*; **85**(14-15):1992-2001.

Theis, M.; Skrifvars, B.J.; Zevenhoven, M.; Hupa, M.; Tran, H. (2006c). Fouling tendency of ash resulting from burning mixtures of biofuels. Part 3: Influence of probe surface temperature. *Fuel*; **85**(14-15): 2002-2011.

World Energy Council (WEC) (2004). Survey of energy resources. *http://www.worldenergy.org/documents/ser2004.pdf* (accessed on October 2010)**.**

Xie, Y.; Xie, W.; Pan, W.P.; Riga, A. (2000). Characterization of the ash deposits from AFBC system using thermal techniques. *Thermochim Acta*; **357**:231–238.

CHAPTER 9. CONCLUSIONS AND RECOMMENDATIONS

9.1. Conclusions

In this thesis, fly ash deposition behaviours during the co-firing of a woody biomass, white pine pellets or a Canadian peat (pellets) with a local coal (crushed lignite) and the gasification of white pine sawdust and crushed peat were comprehensively studied in a pilot-scale fluidized-bed reactor. A custom-designed air-cooled probe was installed in the freeboard of the fluidized bed to simulate a heat transfer surface. By comparing ash deposition rates and characterizing the collected ash deposits from the surface of the probe using different analytical methods (i.e. XRF, XRD, IC, SEM, etc.), effects of different parameters on ash deposition during the co-firing/combustion and the gasification were investigated to help identifying favourable operational conditions to minimize the fly ash deposition on the heat transfer surface. The tested operating parameters included fuel type, blending ratio, moisture content, the ratio of air to fuel, and sulphur addition for combustion/co-combustion of biomass/peat with coal, as well as fuel type, bed material, and equivalence ratio for gasification of white pine sawdust and crushed peat.

As expected, co-firing of the lignite and the wood pellets (with a much lower ash-content than the lignite) resulted in a decreased absolute rate of ash deposition. However, co-firing of woody biomass and lignite coal did not significantly increase the ash deposition tendency in terms of the values of RD_A, and more interestingly, co-firing of the fuel blend of 50% lignite-50% white pine pellets produced a lower RD_A. Co-combustion of three-fuel blend at 20%lignite-40%peat-40%pine resulted in the lowest deposition rate and the least deposition tendency among all the combustion tests with

various mixed fuels or individual fuels.

Moisture contents in feedstock played a positive role in retarding the ash deposition for all of the individual fuels and the fuel blends tested. The effects of air-to-fuel ratio on ash deposition depended on the fuel type. Adding sulphur into the fuel of coal or peat could effectively decrease the chloride deposition in the ash deposits via sulphation. The sulphur addition could also reduce the ash deposition rate for the combustion of lignite, while it slightly increased the ash deposition rate for the peat fuel.

A higher chlorine concentration in the feed would generally result in a higher tendency of ash deposition. For instance, combustion of 100% peat pellet showed a much higher tendency of ash deposition than combustion of the lignite alone. Nevertheless, co-firing of the lignite-peat blends with 50% peat resulted in lower tendency of ash deposition.

The experimental results of air-blown gasification of white pine sawdust and crushed peat demonstrated that among the four bed materials (olivine, limestone, iron ore, and dolomite), the use of olivine resulted in the lowest ash deposition rate < 1.0 $gm^{-2}h^{-1}$, compared with ~ 16 $gm^{-2}h^{-1}$ for limestone in the gasification of pine sawdust at an equivalence ratio (ER) of 0.35. The superb performance of olivine in retarding ash deposition could be accounted for by its outstanding thermal stability and mechanical strength. The other three bed materials, in particular limestone, were fragile during the fluidized bed gasification, and the fractured fines from the bed materials were found to deposit along with the fuel-ash on the heat transfer surface, leading to higher ash deposition rates. The ash deposition rates in the air-blown gasification process also strongly depended on the ER and the fuel type.

Mathematical models were developed to analyze the ash and chlorine deposition behavior based on the experimental data from co-firing peat with lignite coal. The developed equations in this study can not only describe the dependence of the deposition rate and the ash chlorine content on the fraction of peat, but can also determine suitable range of the peat fraction for smooth operations, which would be useful for co-firing other fuel blends.

9.2. Recommendations for future work

Fly ash deposition rates and mechanisms in co-firing of various fuels or fuel blends in fluidized beds are dependent on a large matrix of operating parameters including fuel type, fuel properties and compositions, combustion conditions, bed materials, etc. Future work is thus needed to achieve a deeper and more comprehensive understanding of fly ash deposition mechanism, and to develop effective techniques to minimize or retard the ash deposition on heat transfer surfaces. The following lists some future work suggested by the author:

(1) **Fusion tests of ash deposits collected from the co-combustion/gasification tests**:

As discussed previously, the melting points of compounds in ash deposits would strongly influence the tendency of ash deposition and fouling/slagging in co-firing of biomass/peat with coal. There is limited information concerning the fusion temperatures of various deposits obtained from co-firing of various fuel blends, although the fusion temperature of some individual ash compounds are available.

(2) **Technologies for monitoring and for tracing chlorine-containing species** (i.e. KCl, Cl_2, HCl, etc.): Simple and highly effective approaches to sample and analyze the above chlorine-containing species need to be developed.

(3) **Full scale tests**: A series of full scale tests were scheduled in this project. Unfortunately, the tests had to be abandoned due to the availability of the testing facility (a pulverized coal boiler at a local power generating station operated by OPG). However, long-term operation of co-firing in a full-scale unit would be extremely beneficial for investigation of ash deposition behaviour, and the associated problems with fouling/slagging and corrosion of the heat transfer units inside a co-firing boiler.

APPENDIX A1. COMBUSTION/CO-COMBUSTION TEST PLAN

Run #	Fuel or fuel blend (on thermal input base)					A/F Ratio (-)	Moisture	S addition (wt%)
	CL	PP	WPP	CP	WPS			
1	100%	0%	0%	0%	0%	1.4	As Received	0
2	0%	0%	0%	100%	0%	1.4	As Received	0
3	0%	100%	0%	0%	0%	1.4	As Received	0
4	0%	0%	0%	0%	100%	1.4	As Received	0
5	0%	0%	100%	0%	0%	1.4	As Received	0
6	80%	20%	0%	0%	0%	1.4	As Received	0
7	80%	0%	20%	0%	0%	1.4	As Received	0
8	50%	50%	0%	0%	0%	1.4	As Received	0
9	50%	0%	50%	0%	0%	1.4	As Received	0
10	20%	80%	0%	0%	0%	1.4	As Received	0
11	20%	0%	80%	0%	0%	1.4	As Received	0
12	50%	25%	25%	0%	0%	1.4	As Received	0
13	20%	40%	40%	0%	0%	1.4	As Received	0
14	100%	0%	0%	0%	0%	1.6	As Received	0
15	0%	100%	0%	0%	0%	1.6	As Received	0
16	0%	0%	100%	0%	0%	1.6	As Received	0
17	50%	50%	0%	0%	0%	1.6	As Received	0
18	50%	0%	50%	0%	0%	1.6	As Received	0
19	100%	0%	0%	0%	0%	1.4	Oven Dried	0
20	0%	100%	0%	0%	0%	1.4	Oven Dried	0
21	0%	0%	100%	0%	0%	1.4	Oven Dried	0
22	50%	50%	0%	0%	0%	1.4	Oven Dried	0
23	50%	0%	50%	0%	0%	1.4	Oven Dried	0
24	100%	0%	0%	0%	0%	1.4	As Received	1
25	0%	100%	0%	0%	0%	1.4	As Received	1
26	0%	0%	100%	0%	0%	1.4	As Received	1
27	100%	0%	0%	0%	0%	1.4	As Received	5
28	0%	100%	0%	0%	0%	1.4	As Received	5
29	0%	0%	100%	0%	0%	1.4	As Received	5

APPENDIX A2. GASIFICATION TEST PLAN

Run #	Fuel	ER (-)	Bed material
1	WPS	0.2	Dolomite
2	WPS	0.2	Limestone
3	WPS	0.2	Olivine
4	WPS	0.2	Iron oxide
5	WPS	0.25	Dolomite
6	WPS	0.25	Limestone
7	WPS	0.25	Olivine
8	WPS	0.25	Iron oxide
9	WPS	0.3	Dolomite
10	WPS	0.3	Limestone
11	WPS	0.3	Olivine
12	WPS	0.3	Iron oxide
13	WPS	0.35	Dolomite
14	WPS	0.35	Limestone
15	WPS	0.35	Olivine
16	WPS	0.35	Iron oxide
17	WPS	0.4	Dolomite
18	WPS	0.4	Limestone
19	WPS	0.4	Olivine
20	WPS	0.4	Iron oxide
21	CP	0.2	Olivine
22	CP	0.25	Olivine
23	CP	0.3	Olivine
24	CP	0.35	Olivine

APPENDIX B1. PHOTOS OF FEED SYSTEM OF THE FLUIDIZED BED REACTOR

Overview:

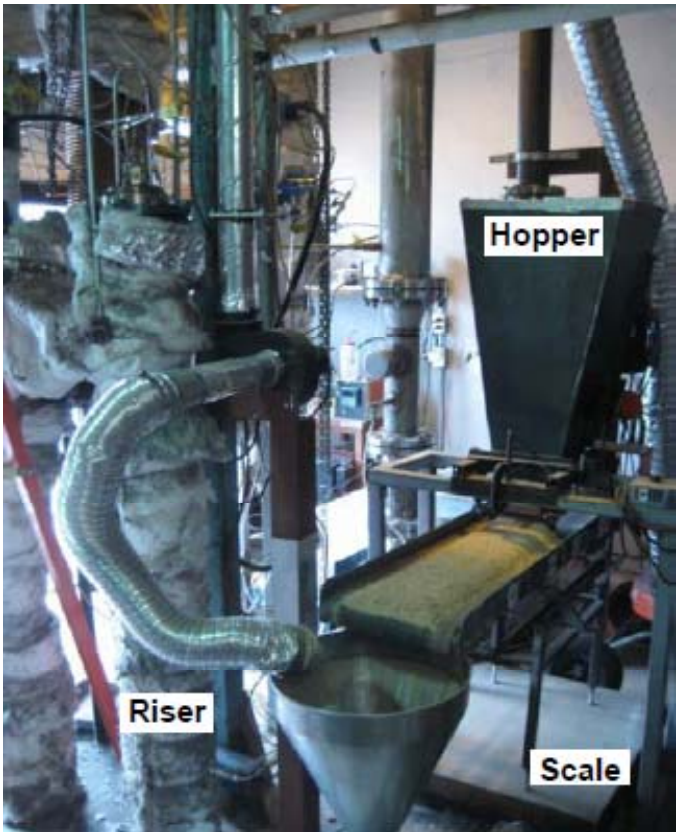

During Co-combustion:

APPENDIX B2. PHOTOS OF APPARATUS FOR FUEL PREPARATION

Electric grinder used for crushing peat:

Rotary dryer used for drying and crushing pine sawdust:

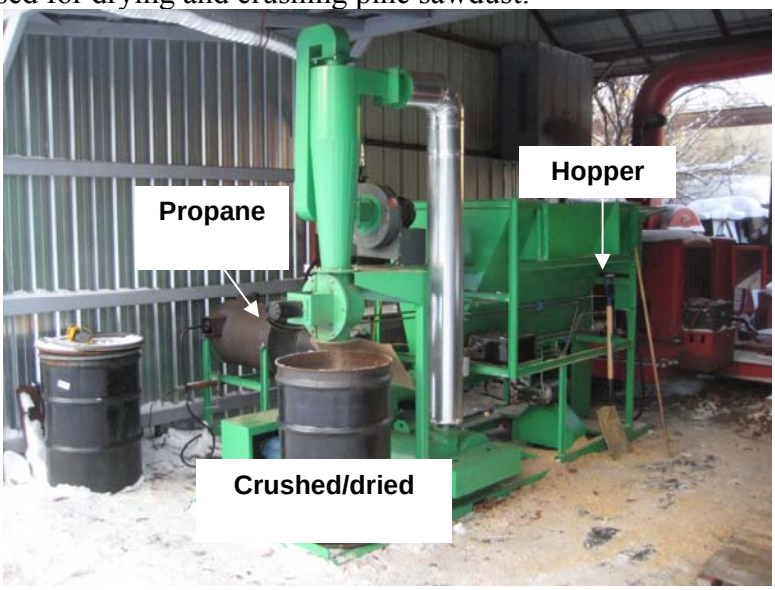

APPENDIX C1. ASH COMPOSITIONS OF FUEL/FUEL BLENDS EMPLOYED IN COMBUSTION TESTS

Unit: wt% dry base.

Run #	SiO_2	Al_2O_3	Fe_2O_3	TiO_2	P_2O_5	CaO	MgO	SO_3	Na_2O	K_2O
1	49.76	19.71	3.82	0.86	0.30	9.91	2.11	6.09	4.20	1.04
2	28.05	8.63	5.56	0.48	1.31	12.65	17.72	12.73	2.84	1.14
3	28.05	8.63	5.56	0.48	1.31	12.65	17.72	12.73	2.84	1.14
4	6.70	1.97	1.46	0.09	3.52	31.10	4.34	2.80	0.36	15.45
5	3.80	0.49	0.58	0.03	23.13	23.36	6.86	17.98	1.29	16.48
6	49.27	19.46	3.86	0.85	0.32	9.97	2.46	6.24	4.17	1.04
7	47.82	18.90	3.68	0.82	1.27	10.48	2.31	6.59	4.08	1.69
8	47.95	18.78	3.97	0.83	0.38	10.14	3.41	6.64	4.09	1.05
9	43.86	17.24	3.40	0.75	3.23	11.64	2.72	7.62	3.83	3.02
10	43.96	16.75	4.28	0.76	0.57	10.64	6.28	7.86	3.84	1.07
11	32.00	12.28	2.57	0.54	9.12	15.11	3.95	10.69	3.08	7.01
12	45.79	17.97	3.67	0.79	1.88	10.93	3.05	7.16	3.95	2.09
13	37.35	14.25	3.38	0.64	5.16	13.06	5.17	9.44	3.42	4.25
14	49.76	19.71	3.82	0.86	0.30	9.91	2.11	6.09	4.20	1.04
15	28.05	8.63	5.56	0.48	1.31	12.65	17.72	12.73	2.84	1.14
16	3.80	0.49	0.58	0.03	23.13	23.36	6.86	17.98	1.29	16.48
17	47.95	18.78	3.97	0.83	0.38	10.14	3.41	6.64	4.09	1.05
18	43.86	17.24	3.40	0.75	3.23	11.64	2.72	7.62	3.83	3.02
19	49.76	19.71	3.82	0.86	0.30	9.91	2.11	6.09	4.20	1.04
20	28.05	8.63	5.56	0.48	1.31	12.65	17.72	12.73	2.84	1.14
21	3.80	0.49	0.58	0.03	23.13	23.36	6.86	17.98	1.29	16.48
22	47.73	18.67	3.98	0.82	0.39	10.17	3.57	6.71	4.07	1.05
23	43.52	17.10	3.38	0.75	3.40	11.74	2.76	7.71	3.80	3.14
24	49.76	19.71	3.82	0.86	0.30	9.91	2.11	6.09	4.20	1.04
25	28.05	8.63	5.56	0.48	1.31	12.65	17.72	12.73	2.84	1.14
26	3.80	0.49	0.58	0.03	23.13	23.36	6.86	17.98	1.29	16.48
27	49.76	19.71	3.82	0.86	0.30	9.91	2.11	6.09	4.20	1.04
28	28.05	8.63	5.56	0.48	1.31	12.65	17.72	12.73	2.84	1.14
29	3.80	0.49	0.58	0.03	23.13	23.36	6.86	17.98	1.29	16.48

Note: the ash compositions of fuel blends used in all co-firing tests were calculated from the corresponding individual fuel ash compositions based on the moisture contents and the feed rate during the test.

APPENDIX C2. ASH DEPOSITION RATES DURING COMBUSTION TESTS

Effective surface area of the deposition probe: 0.09791 m^2

Run#	Weight (g)	Duration (h)	Absolute deposition rate (D_A) ($g\ m^{-2}\ h^{-1}$)	Relative deposition rate (RD_A) ($g\ m^{-2}\ h^{-1}$)
1	4.6214	5.00	9.4	9.4
R1-1*	3.7159	4.50	8.4	8.4
R1-2*	4.001	4.00	10.2	10.2
2	2.1021	7.13	3.0	33.1
3	2.2808	7.13	3.3	35.9
R3*	2.3147	7.00	3.4	37.2
4	0.3154	4.08	0.8	9.1
5	1.0078	6.58	1.6	11.5
6	4.8622	5.08	9.8	12.0
7	6.2078	6.53	9.7	12.3
8	2.9418	5.27	5.7	10.5
9	1.2666	4.13	3.1	5.7
10	2.7613	7.00	4.0	14.8
11	1.7982	6.28	2.9	10.1
12	3.6812	5.05	7.4	13.6
13	0.4071	2.53	1.6	6.0
14	3.0296	5.23	5.9	5.9
15	1.3503	6.62	2.1	22.9
17	0.4147	5.50	0.8	5.6
17	3.0088	5.17	5.9	10.9
18	1.7215	3.02	5.8	10.6
19	7.0748	5.57	13.0	13.0
20	1.8677	4.28	4.5	49.0
21	0.6188	2.27	2.8	20.4
22	3.9297	5.35	7.5	14.5
23	2.0803	2.95	7.2	13.4
24	4.4833	5.05	9.1	9.1
25	2.4051	4.55	5.4	59.4
26	3.4054	6.50	5.4	39.2
27	2.3451	2.95	8.1	8.1
28	1.9868	4.97	4.1	44.9
29	3.3312	4.93	6.9	50.6

*: repeat test.

APPENDIX C3. CHEMICAL COMPOSITIONS OF ASH DEPOSITS OBTAINED FROM COMBUSTION TESTS

Unit: wt% dry base.

Run #	SiO_2	Al_2O_3	Fe_2O_3	TiO_2	P_2O_5	CaO	MgO	SO_3	Na_2O	K_2O
1	38.01	15.36	7.41	0.65	0.47	12.14	9.23	5.25	4.56	0.68
R1*	31.72	12.80	9.05	0.43	0.61	10.82	9.53	5.70	4.94	0.83
2	36.58	9.09	20.47	0.42	0.26	5.95	14.01	4.70	3.07	0.87
3	34.63	8.02	10.80	0.40	0.53	8.17	18.24	6.26	3.60	1.44
R3*	31.38	4.19	17.89	0.16	0.53	5.94	16.46	4.08	1.71	1.07
4	37.35	7.65	16.76	0.35	0.25	5.20	18.66	1.40	3.34	1.06
5	29.62	4.31	25.41	0.17	0.37	8.82	18.44	2.54	1.70	1.12
6	32.39	17.71	7.72	0.73	0.80	18.59	4.86	5.15	5.23	0.68
7	35.25	18.29	8.35	0.77	0.61	16.68	3.63	5.32	5.50	0.60
8	30.89	15.25	8.94	0.64	0.78	17.10	7.41	6.04	4.86	1.20
9	35.65	16.94	7.04	0.67	3.30	12.82	4.22	4.89	4.42	3.20
10	29.02	12.93	7.02	0.59	0.81	14.66	8.34	8.31	5.45	1.56
11	28.93	12.56	6.24	0.52	6.57	13.77	5.44	6.65	3.54	4.57
12	28.04	14.80	7.63	0.62	2.48	16.49	4.53	6.44	5.24	1.94
13	27.85	12.38	3.48	0.50	5.61	12.71	4.51	6.34	3.56	4.07
14	38.47	17.62	7.53	0.77	0.58	15.41	6.27	4.68	4.63	0.57
15	29.31	5.22	24.09	0.24	0.41	5.75	18.02	5.86	3.06	1.48
16	31.27	4.26	27.64	0.20	0.20	3.54	20.95	3.09	2.00	0.67
17	13.46	2.66	7.00	0.11	11.90	13.40	9.90	9.84	2.45	8.27
18	29.79	15.75	9.39	0.65	0.81	17.68	6.11	6.21	5.43	1.01
19	36.99	18.57	5.50	0.73	3.28	14.95	3.96	4.8	4.37	2.96
20	32.39	18.43	7.51	0.79	0.77	19.88	4.47	4.66	4.96	0.42
21	32.01	8.40	16.31	0.39	0.53	8.42	14.48	5.29	4.25	1.28
22	14.73	2.02	18.17	0.08	9.94	13.68	11.81	8.46	1.75	6.68
23	32.83	16.67	6.83	0.71	0.66	17.10	5.73	6.14	5.30	0.57
24	35.66	18.07	4.04	0.74	3.74	14.53	3.42	5.04	4.73	2.65
25	33.09	17.19	7.35	0.73	0.64	16.88	3.95	6.58	5.30	0.57
26	30.80	7.21	13.41	0.33	0.54	8.02	15.91	6.37	3.06	1.00
27	9.56	2.38	4.41	0.12	16.07	11.91	6.95	9.82	5.55	9.10
28	42.06	19.87	4.25	0.81	0.36	11.67	2.81	4.15	4.03	0.61
29	51.56	23.15	3.87	0.94	0.20	8.10	2.78	2.38	3.75	0.80

*: repeat test.

APPENDIX C4. CHEMICAL COMPOSITIONS OF CYCLONE BOTTOM ASH OBTAINED FROM SOME* COMBUSTION TESTS

Unit: wt% dry base.

Run #	SiO_2	Al_2O_3	Fe_2O_3	TiO_2	P_2O_5	CaO	MgO	SO_3	Na_2O	K_2O
3	32.88	8.85	7.61	0.43	0.61	10.18	15.48	3.9	3.22	0.97
4	25.92	7.33	13.31	0.38	0.75	17.35	6	2.94	1.92	2.07
5	27.75	6.5	14.03	0.3	0.87	20.44	12.64	1.81	1.87	1.38
8	34.77	17.96	6.46	0.71	0.63	16.5	5.7	1.68	4.47	0.76
9	30.61	15.68	5.54	0.6	4.4	15.29	4.43	2.56	3.79	3.15
14	42.23	20.84	4.91	0.89	0.53	15.46	3.77	1.33	4.08	0.52
15	34.33	8.51	8.19	0.4	0.55	9.57	13.76	3.12	2.96	1.01
18	32.23	16.91	5.22	0.67	4.11	17.16	4.4	3.54	4.14	2.82
22	22.71	9.8	6.04	0.41	0.29	7.87	5.31	1.87	2.78	0.37
27	41.5	20.08	4.12	0.84	0.4	13.21	2.48	2.88	4.04	0.56

*: Because of limited experimental conditions, only a few cyclone bottom ash samples were selected to be analyzed for chemical compositions.

APPENDIX C5. MINERALOGICAL COMPOSITIONS OF ASH DEPOSITS OBTAINED FROM COMBUSTION TESTS

Run #	1	2	3	4	5	6	7	8	9	10	11	12	13	14	15
Chemical Compound	Percentage of Chemical Compound (wt. %)														
Åkermanite ($Ca_2MgSi_2O_7$)	0.9	1.9	2.4	0.1		2.9	5.5	7.6	3.4	4.4	2.3	5.2	2.9	2.4	5.5
Albite ($NaAlSi_3O_8$)				2.0											
Anhydrite ($CaSO_4$)	4.1	3.1	3.6	3.4	4.0	9.2	8.3	8.6	6.2	3.3		12.7	5.8	4.4	5.8
Anorthite ($CaAl_2Si_2O_8$)	1.5	1.7	3.0						4.2		4.0		4.1		5.0
Bredigite ($Ca_{14}Mg_2(SiO_4)_8$)														2.9	
Brownmillerite ($Ca_2Al_2Fe_2O_5$)	1.6					2.2	2.1	1.8	1.5	0.6	1.2	3.5	2.0	0.8	
Calcite ($CaCO_3$)				0.6					2.8		3.0	1.6	1.4		
Chromite ($FeCr_2O_4$)					1.8										
Dolomite ($CaMg(CO_3)_2$)	0.9			2.5					1.2						
Forsterite (Mg_2SiO_4)	5.8	3.4	14.8	18.0	6.4		6.1	8.8	2.6	2.0	3.8		4.7	6.4	11.6
Goethite (FeO(OH))	1.5			2.2											
Hauyne ($Na_6Ca_2Al_6Si_6O_{24}(SO_4)_2$)												0.9			
Hematitle (Fe_2O_3)	1.6	0.7	1.0	2.5	2.0	1.8	3.4	2.3	1.9	0.8	5.3	3.7	1.8	1.0	4.4
Lime (CaO)	0.3	0.1	0.4		0.4	0.9	0.9	1.3	0.7	0.2	17.3	0.8	1.0	0.4	
Magnesium Oxide (MgO)	1.3	0.8	2.6	1.5	0.5	1.5	2.2	3.8	0.9	1.1	1.0	1.8	0.8	1.8	3.8
Magnesioferrite Aluminian ($MgAl_{0.74}Fe_{1.26}O_4$)	1.1			1.8							0.9				
Magnesioferrite ($MgFe_2O_4$)						3.6	1.3	2.0		0.2					
Magnesium Chlorate Hydrate ($Mg(ClO_4)_2(H_2O)_6$)												3.1			
Magnetite (Fe_3O_4)															10.0
Mercallite ($KHSO_4$)												0.9			
Merwinite ($Ca_3Mg(SiO_4)_2$)						4.4		4.9		1.4					
Moticellite ($CaMgSiO_4$)		0.7													
Potassium Manganese Oxide ($K_3(MnO_4)_2$)				2.2											
Quartz (SiO_2)	7.6	4.3	4.2	5.9	2.7	8.8	10.3	7.6	8.9	2.4	13.0	8.2	10.3	8.3	7.1
Sodium Calcium Sulfate Hydrate ($Na_2Ca_5(SO_4)_6 \cdot 3H_2O$)									4.0		1.0		12.6	0.4	
Tychite ($Na_6Mg_2(CO_3)_4(SO_4)$)	1.4	0.9	1.0			4.2	1.1		0.6	0.3		6.2	1.8	0.9	1.7
Crystallinity (wt %)	**29.5**	**17.6**	**33.0**	**42.9**	**17.7**	**44.5**	**41.2**	**50.9**	**38.9**	**16.7**	**66.3**	**48.5**	**49.1**	**29.7**	**55.4**
Amorphous content (wt %)	**70.5**	**82.4**	**67.0**	**57.1**	**82.3**	**55.5**	**58.8**	**49.1**	**61.1**	**83.3**	**33.7**	**51.5**	**50.9**	**70.3**	**44.6**

Appendix C5. Cont'd

Run #	16	17	18	19	20	21	22	23	24	25	26	27	28	29
Chemical Compound	**Percentage of Chemical Compound (wt. %)**													
Åkermanite ($Ca_2MgSi_2O_7$)	0.9	5.0	6.4	4.7	5.5		12.7	2.0	7.7	3.6		5.6	2.0	6.2
Albite ($NaAlSi_3O_8$)					7.6					16.5				6.1
Anhydrite ($CaSO_4$)	5.0	5.9	2.0	5.2	3.8	11.1	13.2	14.6	16.0	8.0	4.2	8.4	8.1	7.3
Anorthite ($CaAl_2Si_2O_8$)						3.4					7.8		1.6	7.5
Brownmillerite ($Ca_2Al_2Fe_2O_5$)		1.4	2.8	1.4	1.9		4.9	6.4	11.9	1.6	1.7	5.9		
Calcite ($CaCO_3$)	0.6		1.7		2.6	0.6	1.3	1.3	1.8	1.7	5.7	1.9	0.5	2.7
Calcium phosphate sulfide ($Ca_{10}(PO_4)_6S$)	4.6												3.2	3.2
Chromite ($FeCr_2O_4$)						8.9								
Disodium Nickel Oxide ($Na_2(NiO_2)$)	0.5													
Dimagnesium Diphosphate ($Mg_2P_2O_7$)	1.1													
Dolomite ($CaMg(CO_3)_2$)	0.6		0.1		1.8	1.5		2.1	1.5	1.6	3.5		1.2	2.2
Forsterite (Mg_2SiO_4)	2.6	6.1			13.5	4.8	10.8			16.2	1.5			7.7
Goethite ($FeO(OH)$)							4.5						2.0	
Hauyne ($Na_6Ca_2Al_6Si_6O_{24}(SO_4)_2$)			1.3						3.9					
Hematitle (Fe_2O_3)	0.4	2.0	1.1	1.5	2.3	2.1	5.1	4.4	6.0	1.7	1.8	1.8	1.6	2.0
Iwakiite ($MnFe_2O_4$)	0.1													
Kalsilite ($KAlSiO_4$)													2.4	
Lime (CaO)	0.2	1.3	0.6	0.5	0.5	0.3	0.9	0.9	0.3	0.4	0.3		0.7	0.3
Magnesium Oxide (MgO)	0.3	2.5	0.8	1.0	2.4	1.2	2.9	1.4	4.0		1.3	3.3	1.4	2.1
Magnanese Diphosphate ($Mn_2P_2O_7$)	0.7													
Magnanese Phosphate ($Mn_3(PO_4)_2$)	3.2													
Magnesioferrite Aluminian ($MgAl_{0.74}Fe_{1.26}O_4$)	0.4				3.3					3.2			1.3	
Magnesioferrite ($MgFe_2O_4$)		1.5												0.8
Magnesium Chlorate Hydrate ($Mg(ClO_4)_2(H_2O)_6$)			3.9					6.8						
Mercallite ($KHSO_4$)			1.0		3.9			0.5	8.7	2.8	5.0		1.2	
Merwinite ($Ca_3Mg(SiO_4)_2$)		2.7		2.0										
Nepheline ($K_{1.35}Na_6(Al_8Si_8O_{32})$						3.4								
Pyrope ($Mg_3Al_2(SiO_4)_3$)						6.6							26.6	
Quartz (SiO_2)	0.8	6.4	9.4	6.9	8.5	0.4	15.1	13.2	17.9	10.9	1.1	23.8	5.8	2.6
Sodium Calcium Sulfate Hydrate ($Na_2Ca_5(SO_4)_6 \cdot 3H_2O$)				1.1										
Sodium Aluminum Silicate ($NaAlSiO_4$)					3.8				13.9	2.4		9.1		
Tychite ($Na_6Mg_2(CO_3)_4(SO_4)$)		1.5	0.9	1.2	1.5		7.1	3.1	2.5	1.0		1.9		
Crystallinity (wt %)	**22.0**	**36.5**	**31.9**	**26.6**	**62.7**	**42.9**	**78.6**	**58.2**	**96.2**	**74.4**	**34.1**	**67.9**	**71.0**	**51.9**
Amorphous content (wt %)	**78.0**	**63.5**	**68.1**	**73.4**	**37.3**	**57.1**	**21.4**	**41.8**	**3.8**	**25.6**	**65.9**	**32.1**	**29.0**	**48.1**

APPENDIX C6. CHLROINE AND SULPHATE CONCENTRATION IN DEPOSITS OBTAINED FROM COMBUSTION TESTS

Unit: µg/g dry base

Run#	Soluble Sulphate[1]	Soluble Chloride[1]	Total Chlorine[2]
1	60,000	N/D[3]	506
2	100,000	1445	1580
3	79,000	1616	1950
4	14,000	N/D[3]	448
5	28,000	409	397
6	38,000	1968	1660
7	42,000	544	389
8	53,000	2553	2240
9	65,000	N/D[3]	691
10	100,000	3943	4260
11	64,000	N/D[3]	2010
12	73,000	N/D[3]	2640
13	64,000	N/D[3]	3140
14	42,000	319	207
15	75,000	761	948
16	110,000	N/D[3]	2270
17	56,000	2523	2950
18	43,000	N/D[3]	383
19	28,000	441	314
20	68,000	N/D[3]	3120
21	93,000	N/D[3]	1280
22	48,000	N/D[3]	4060
23	47,000	N/D[3]	981
24	78,000	N/D[3]	403
25	81,000	N/D[3]	1590
26	110,000	N/D[3]	4670
27	53,000	N/D[3]	130
28	140,000	N/D[3]	980
29	140,000	N/D[3]	1730

[1]: by IC;
[2]:by Pyrohydrolysis;
[3]: not detectable

APPENDIX C7. TEMPERATURE PROFILES OF COMBUSTION TESTS

Unit: °C

Run #	Bed height (m)								
	0.2 (T1)	0.4 (T2)	0.8 (T3)	0.9 (T4)	1.2 (T5)	1.4 (T6)	1.5 (T7)	2.2 (T8)	3.0 (T9)
1	792±9	799±10	807±9	810±6	858±4	818±21	793±38	769±34	691±41
2	812±23	817±21	826±19	836±16	847±15	790±29	745±40	704±34	621±43
3	797±9	797±9	818±8	852±5	872±6	809±10	759±13	715±12	634±13
4	769±49	769±46	799±43	880±56	913±50	861±38	820±34	760±31	684±20
5	863±39	868±26	875±23	879±23	885±21	847±22	801±17	754±16	671±9
6	872±61	877±49	880±56	880±63	868±89	815±112	757±129	734±116	633±127
7	775±52	783±48	797±39	803±61	825±72	782±82	749±83	697±79	584±98
8	837±72	844±60	850±58	850±61	849±68	806±88	747±102	716±88	611±99
9	860±3	865±3	870±3	875±2	921±3	883±3	840±3	785±4	724±5
10	819±10	825±10	831±10	835±9	860±7	845±9	819±11	769±11	687±9
11	794±9	796±10	815±9	836±7	844±12	781±11	735±11	679±9	614±4
12	812±6	823±4	837±4	846±4	902±5	868±7	836±7	785±7	713±10
13	785±11	788±11	806±9	824±7	831±11	769±8	724±8	672±6	611±3
14	798±27	805±27	816±25	827±22	840±15	799±21	766±21	728±18	668±19
15	829±20	836±19	844±17	854±15	860±13	803±14	767±17	723±15	653±15
16	853±17	------	869±15	860±34	845±27	777±21	734±18	687±17	599±11
17	840±37	852±39	858±37	860±39	847±43	775±53	719±73	690±59	589±75
18	824±9	830±9	836±9	845±7	901±10	871±11	831±7	765±6	687±7
19	------	815±8	824±8	842±7	897±5	871±11	823±8	771±7	697±7
20	852±12	857±10	861±9	862±15	876±15	853±15	819±19	765±17	681±16
21	873±27	------	886±26	877±25	864±22	808±23	766±20	722±20	646±20
22	785±4	791±4	799±4	809±6	847±8	803±11	759±10	699±9	618±7
23	717±27	729±22	750±25	837±21	907±16	830±16	787±14	731±14	657±9
24	810±21	817±20	826±19	833±15	856±18	823±29	788±28	737±32	653±40
25	814±12	822±7	829±6	833±8	851±8	818±8	780±9	720±7	637±4
26	832±31	837±32	844±29	849±26	862±20	868±28	845±34	797±25	731±29
27	776±11	784±11	795±11	809±11	856±6	826±8	776±10	719±13	640±10
28	792±4	799±4	805±3	811±3	835±4	839±7	820±6	767±6	688±5
29	860±25	863±25	874±24	877±29	899±39	864±54	839±74	789±67	701±81

APPENDIX D1. OPERATIONAL PARAMETERS AND ASH DEPOSTION RATES DURING GASIFICATION TESTS

Effective surface area of the deposition probe: 0.1338 m^2

Run#	Feed rate (kg/h)	Total air flow rate (L/min)	Weight of deposit (g)	Duration (h)	Ash deposition rate (D_A) (g m^{-2} h^{-1})
1	20.7	290	1.4682	2.17	5.1
2	19.0	270	0.7098	2.12	0.2
3	20.4	290	0.0758	3.00	2.5
4	21.0	290	1.8725	3.00	4.7
5	16.6	290	0.9952	2.20	3.4
6	17.7	300	1.0333	2.17	3.6
7	16.4	290	0.0673	1.88	0.3
8	16.3	270	3.3537	3.77	6.7
9	13.9	290	0.9207	2.35	2.9
10	16.0	300	2.2247	3.23	5.1
R10*	16.0	300	1.7236	2.83	4.6
11	14.1	300	0.1705	1.57	0.8
12	16.0	315	1.5968	3.28	3.6
13	12.0	292	0.8014	2.12	2.8
14	15.0	370	4.6306	2.17	16.0
15	12.2	300	0.0910	4.25	0.2
16	12.2	290	0.6941	3.28	1.6
17	10.8	300	0.6278	2.13	2.2
18	15.0	400	4.0043	2.30	13.0
19	10.4	300	0.0474	2.00	0.18
R19*	10.4	300	0.0821	2.5	0.25
20	10.4	290	2.3566	3.38	5.2
21	17.4	290	3.2242	4.32	5.6
22	14.5	300	0.8204	2.00	3.1
23	12.0	300	09412	2.47	2.8
24	10.9	300	0.2777	2.38	0.9

*: repeat test

APPENDIX D2. CHEMICAL COMPOSITIONS OF ASH DEPOSITS AND SOME CYCLONE BOTTOM ASH OBTAINED FROM GASIFICATION TESTS

Unit: wt% dry base.

Run #	SiO_2	Al_2O_3	Fe_2O_3	TiO_2	P_2O_5	CaO	MgO	SO_3	Na_2O	K_2O	Loss on fusion
1	0.8	0.19	1	0.03	0.14	9.94	4.26	0.12	0.20	0.87	82.53
2	1.06	0.32	0.92	0.03	0.14	29.25	0.46	0.1	0.2	0.45	67.20
3	0.93	0.72	5.75	0.03	0.21	4.95	0.20	0.10	0.20	1.31	85.55
4	0.57	0.21	6.22	0.03	0.07	0.8	0.2	0.1	0.2	0.3	91.42
5	1.47	0.66	2.97	0.03	0.44	29.02	14.43	0.10	0.20	1.41	49.10
6	1.45	0.43	1.19	0.03	0.12	49.62	0.74	0.11	0.20	0.34	45.78
7	6.13	2.75	9.04	0.03	0.86	6.97	0.20	0.16	0.44	4.27	66.80
8	0.94	0.28	38.42	0.03	0.07	0.67	0.2	0.1	0.2	0.19	59.11
8B*	2.01	0.51	49.37	0.03	0.11	0.82	0.3	0.1	0.2	0.27	46.44
9	2.6	1.27	4.73	0.03	0.21	22.84	10.78	0.10	0.20	1.77	55.04
10	1.07	0.26	0.85	0.03	0.04	60.79	0.64	0.8	0.2	0.29	34.98
10B*	1.16	0.27	1.12	0.03	0.04	65	0.67	0.1	0.2	0.13	31.48
11	17.3	4.15	21.71	0.2	1.34	14.52	4.44	0.47	1.61	3.64	29.16
11B*	2.04	0.47	1.99	0.03	0.23	2.34	1.08	0.1	0.2	0.69	90.86
12	1.17	0.38	31.43	0.03	0.07	0.46	0.2	0.1	0.2	0.25	65.73
13	2.29	1.02	3.85	0.03	0.24	26.08	13.27	0.10	0.20	1.93	50.37
14	1.34	0.36	0.9	0.03	0.06	61.23	0.79	0.33	0.2	0.27	34.34
15	19.65	4.96	19.25	0.06	1.03	9.74	3.19	0.1	2.21	3.31	35.30
16	1.43	0.41	60.91	0.03	0.11	0.8	0.3	0.1	0.2	0.2	35.54
17	1.25	0.75	3.72	0.03	0.24	18.42	8.94	2.61	0.24	4.97	57.09
18	1.05	0.25	0.92	0.03	0.08	55.65	0.63	0.42	0.20	0.52	40.18
19	7.6	1.47	10.71	0.03	0.53	6.77	2.26	0.1	0.2	2.31	67.19
20	2.92	0.79	77.82	0.03	0.19	1.25	0.75	0.16	0.2	0.36	15.23
21	3.31	1.36	2.67	0.06	0.36	2.91	3.85	2.09	0.43	0.31	82.40
22	13.4	5	11.64	0.16	1.13	9.53	12.37	8.11	2.21	2.02	19.20
22B*	6.42	1.73	3.67	0.08	0.25	2.78	3.39	0.65	0.4	0.27	80.25
23	7.66	2.71	5.01	0.14	0.63	5.44	7.51	3.31	1.5	0.81	64.82
24	14.17	4.53	15.2	0.2	0.93	8.2	10.45	4.93	2.02	1.61	33.06

*: Cyclone bottom ash

APPENDIX D3. TEMPERATURE PROFILES OF GASIFICATION TESTS

Unit: °C

Run#	Bed height (m)				
	0.4 (T2)	1.2 (T5)	1.5 (T7)	2.2 (T8)	3.0 (T9)
1	705±20	581±20	544±37	542±41	522±50
2	763±8	644±19	612±16	601±15	551±14
3	759±9	548±24	528±24	524±27	501±31
4	729±15	572±12	529±9	524±9	495±11
5	783±7	610±11	582±14	578±16	546±18
6	748±16	685±9	671±6	640±6	600±11
7	803±12	578±26	558±29	554±29	528±29
8	898±15	483±22	454±26	448±27	426±32
9	839±47	637±19	597±26	590±28	557±34
10	750±3	703±17	720±18	686±19	652±26
11	862±24	571±27	559±29	555±32	531±35
12	883±25	621±26	562±25	557±25	518±22
13	860±47	718±27	641±15	634±16	591±18
14	741±14	768±23	770±18	735±15	680±7
15	855±10	826±24	747±25	732±24	660±14
16	882±10	636±14	578±12	571±12	521±10
17	835±24	798±20	703±13	691±11	641±7
18	686±40	752±31	730±35	726±40	638±55
19	830±38	837±17	784±17	768±18	692±14
20	920±13	753±27	658±13	646±12	589±12
21	737±13	658±20	581±16	569±15	526±14
22	853±14	768±15	686±19	672±20	617±19
23	843±14	726±16	642±11	630±9	575±6
24	850±9	850±17	767±19	750±19	685±19

CURRICULUM VITAE

Yuanyuan Shao

Education

Ph.D. Chemical Engineering (April / 2011)
the University of Western Ontario, London, Ontario, Canada
Thesis topic: Investigation of ash deposition during co-firing biomass/peat with coal in a pilot-scale fluidized-bed reactor

M.E.Sc. Environmental Engineering (August / 2007)
Lakehead University, Thunder Bay, Ontario, Canada
Thesis topic: Removal of phamaceutically active compounds from water systems by freeze concentration

B.E.Sc. Civil Engineering (July / 2004)
Institute of Civil Engineering and Architecture, Beijing, China
Thesis topic: Design of a water plant in Madao central business district

Experience

Research Assistant 2008-2011
Department of Chemical and Biochemical Engineering, the University of Western Ontario, London, ON., Canada

Investigating ash deposition during biomass and coal co-firing/gasification, collaborative project with Ontario Power Gerenation, CanmetENERGY - Ottawa, Superior Thermowood and Peat Resources Ltd. Project budget: $1 million.

- ✦ Investigated the ash deposition behaviors during co-combustion of a woody biomass and lignite coal in a fluidized bed;
- ✦ Investigated the ash deposition behaviors during co-combustion of peat and lignite coal in a fluidized bed;
- ✦ Investigated the ash deposition behaviors during co-combustion of fuel blends of biomass, peat and lignite in a fluidized bed;
- ✦ Investigated the ash deposition behaviors during fluidized-bed air-blown

gasification of a woody biomass and peat.

Teaching Assistant 2005-2011
Department of Chemical and Biochemical Engineering, the University of Western Ontario, London, ON., Canada

- ✦ Assisted with six undergraduate courses and one graduate course: Soil mechanics, Steel design, Open channel flow, Mechanics of solids, Unit operation III-Particulate operations, Stage operation, and Advanced high velocity fluidization technology;
- ✦ Gave course tutorials in class and prepared assignments;
- ✦ Graded and provided feedback with assignments.

Research Assistant 2005-2008
Department of Environmental Engineering, Lakehead University, Thunder bay, ON., Canada
Studying on removal of phamaceutically active compounds (PhACs) from water systems by freeze concentration.

- ✦ Evaluated the potential of unidirectional downward freeze concentration process for removing PhACs;
- ✦ Investigated the effect of different factors such initial drug concentration, freezing temperature and freezing level on the treatment efficiency.

Chemical Engineer 2004-2005
Termites Controlling Center, Jingdezhen, Jangxi, China

- ✦ Chemical preparation for termite controlling

Publications

Y. Shao, C. Xu, J. Zhu, F. Preto, J. Wang, G. Tourigny, C. Badour and H. Li: Ash deposition during co-firing biomass and coal in a fluidized-bed combustor. *Energy Fuels* 2010, 24(9): 4681-4688. (Chapter 4 of this thesis)

Y. Shao, J. Wang, C. Xu, J. Zhu, F. Preto, G. Tourigny, C. Badour and H. Li: An experimental and modeling study of ash deposition behavior for co-firing peat with lignite. *Applied Energy* 2011, 88: 2635-2640. (Chapter 8 of this thesis)

Y. Shao, J. Zhu, F. Preto, G. Tourigny, J. Wang, C. Badour, H. Li and C. Xu: Characterizations of deposited ash during co-firing of white pine and lignite in fluidized bed combustor. In: Proceedings of the 20th international conference on fluidized bed combustion-2009, Xian, China, 2010, Part 7: 1041-1047, DOI: 10.1007/978-3-642-02682-9_162.

Y. Shao, J. Zhu, F. Preto, G. Tourigny, J. Wang, C. Badour, H. Li, and C. Xu :

Characterizations of deposited ash during co-firing of peat and lignite in fluidized bed combustor. In Proc. IASTED International Conference Environmental Management and Engineering (EME 2009), Banff, Canada, July 7-8, 2009.

Y. Shao, C. Xu, F. Preto, G. Tourigny, H. Li, J. Wang and J. Zhu: Ash deposition in co-firing biomass/peat and coal in fluidized bed. In: Proceeding of the 8th world congress of chemical engineering (WCCE8)-2009, Montreal, Canada.

Y. Shao, C. Xu, J. Zhu, F. Preto, J. Wang, G. Tourigny, C. Badour and H. Li: Ash and chlorine deposition during co-combustion of lignite and a chlorine-rich Canadian peat in a fluidized bed - Effects of blending ratio, moisture content and sulfur addition. Submitted to *Fuel* in January 2011. (Chapter 5 of this thesis)

Y. Shao, C. Xu, J. Zhu, F. Preto, J. Wang, Hanning Li and C. Badour: Ash deposition in co-firing mixtures of peat, woody biomass and lignite in a pilot-scale fluidized-bed reactor. Submitted to *Energy Fuels* in February 2011. (Chapter 6 of this thesis)

Y. Shao, C. Xu, J. Zhu, F. Preto, J. Wang, and S. Hurley: Ash deposition in air-blown gasification of peat and woody biomass in a fluidized-bed gasifier. Submitted to *Biomass & Bioenergy* in March 2011. (Chapter 7 of this thesis)

Course Works

Environmental chemistry, Advanced topics analytical chemistry, Physiochemical treatment process, Biological treatment processes, Mathematical methods in engineering, Biochemical engineering, Advance high velocity fluidization technology, Green energy and engineering, Transport processes, Water analytical chemistry, Water quality engineering, water resource protection and utilizing, water treatment technologies, design of wastewater treatment plant

Awards

Ross and Jean Clark Scholarship, 2011

Western Engineering Graduate Scholarship, 2008-2011

Bombardier Inc. Transportation Equipment Group Lakehead University Anniversary Graduate Scholarships, 2005